bcn: 405294

LIFE CYCLE SYNCHRONISATION TO ENVIRONMENTAL PERIODICITIES: THE INFLUENCE OF STAGE SPECIFIC DEVELOPMENT

by

Eric Paul Mario Grist

Submitted for the Degree of
Doctor of Philosophy
in the
Department of Statistics and Modelling Science

November 1994

University of Strathclyde Glasgow, Scotland.

The copyright of this thesis belongs to the author under the terms of the United Kingdom Copyright Acts as qualified by University of Strathclyde Regulation 3.49. Due acknowledgement must always be made of the use of any material contained in, or derived from, this thesis.

To Mum and Dad

A plausible impossibility is always preferable to an unconvincing possibility- Aristotle

ACKNOWLEDGEMENTS

This work was funded by a studentship from the Science and Engineering Research Council.

I first and foremost thank Wilson Lamb for invaluable discussions on the wonders of dynamical systems and an enviably clear exposition on the circle map.

I have been extremely lucky to have shared time in the STAMS Department with excellent room companions Rosa Capobianco, Na-eem Rehman, Tong Ling, Stephen Tobia, Tim Mcgeever, and Helen Dobby. My time in Glasgow has also been immeasurably enhanced by memorable musical abstractions not too numerous to mention. For these I must thank Carl Ewens, Robert Smith and Duncan Davison. For always inspirational conversation and simply being there I thank Shirley McClure, Colin Wolff, Glyn Turner, Andrew Paine, Maria Kateri, and Tom Mills.

Great appreciation for unerring advice around potential computer hazards is expressed towards David Middleton and Stephen Tobia. Bill Gurney who was alotted supervisor has been a keen science and model enthusiast. Departmental secretaries Alison Mitchell and Lynn Westwood have been consistently helpful.

I am indebted to Roy Veitch, Xuerong Mao and George Gettinby for pleasantly insightful conversations. Finally I thank Phil Crowley, Werner Topp and Mike Heath for providing vital biological perspective.

ABSTRACT

In the natural environment many organisms demonstrate the ability to synchronise their life cycle to periodic environmental variations. Previous studies have shown that life histories consisting of a contiguous series of stages all with density independent development rates exhibiting the *same* dependence on time cannot synchronise to a periodic environmental variation. The same studies established that both dormancy and quiescence at specific points in the life cycle could produce strong synchronising effects.

In this thesis I examine a very general strategic model of a two-stage life-cycle, each stage having a density independent development rate with a characteristic periodic time-dependence. I develop a concise circle map representation between the emergences of successive generations. The two stage circle map which relates these emergences is composed from two simple rotations and an interphase map which represents the relationship between the physiological times for the two life-history stages. I explore synchronisation behaviour of the life cycle model in terms of the qualitative dynamics that correspond to the iterative dynamic behaviour of the associated two stage circle map.

I derive a series of analytic results relating the behaviour of systems whose interphase maps are interrelated and give analytic conditions for a broad class of two-stage circle maps to have a fixed point (that is for the systems they describe to reach the critical life-history stage at the same point in each environmental cycle). Finally I report the results of numerical investigations of the relationship between the biological characteristics of the development functions and the fine-scale details of the locking behaviour of the systems they define. I illustrate the practical implications of these findings by examining results obtained when the model is parameterised with data for two diverse organisms, namely a beetle *Catops nigricans* and a micro-organism *phytoplankton*.

TABLE OF CONTENTS

CHAPTER 0:	text page
INTRODUCTION	
0.0 Introduction	2
0.1 Biological synchrony	4
0.2 A brief history of timers	7
0.3 Development in a constant environment	10
0.4 Development in a changing environment	15
0.5 Overview of thesis	20
CHAPTER 1:	
A LIFE CYCLE IN A SEASONALLY VARYING ENVIRONS	MENT
Catops Nigricans	
1.0 Introduction	22
1.1 Biology of Catops Nigricans	23
1.2 A life cycle model of Catops Nigricans	28
1.3 Simulation results	37
1.4 A two stage model	43
1.5 Discussion	46
CHAPTER 2:	
PHYSIOLOGICAL TIME	
2.0 Introduction	49
2.1 Simplifying the Analysis: Physiological Time	51
2.2 Incorporating physiological time into a circle map description	54
2.3 The one stage life cycle	57
CHAPTER 3:	
CIRCLE MAPS	
3.0 Introduction	61
3.1 Basic definitions	62
3.2 Iterative dynamics	64
3.3 Circle maps	69
3.4 Some further theorems	72
CHAPTER 4:	ADIEC
CIRCLE MAPS ARISING FROM TWO STAGE LIFE HISTO	
4.0 Introduction	76
4.1 Synchronisation through specialised dormancy	78
4.2 A general two stage model	83
4.3 The Interphase Map	87
4.4 Generic interphase map shape: two frequent situations	91
4.5 Discussion	94

CHAPTER 5:	N. A. DO
GENERAL PROPERTIES OF TWO STAGE CIRCLE 5.0 Introduction	96
5.1 Interphase map transformations	90 98
5.2 The behaviour portrait	102
5.3 Conditions for synchronisation	102
5.4 Numerical investigations of Case 1 and Case 2	110
5.5 Discussion	113
CHAPTER 6:	
AN INVESTIGATION OF THE SLIM CIRCLE MAP	MODEL
6.0 Introduction	115
6.1 Biological interpretation	116
6.2 The SLIM circle map	118
6.3 Conditions for synchronisation	122
6.4 The SLIM behaviour portrait	127
6.5 Trails investigation	134
6.6 Discussion	138
CHAPTER 7:	
THE GENERAL EFFECT OF INTERPHASE MAP SI	HAPE ON
SYNCHRONISATION	
7.0 Introduction	140
7.1 TLIM and THLIM	141
7.2 Development function and interphase map shape	147
7.3 Closeness to the leading 45° diagonal	151
7.4 Practical biological implications	154
7.5 Discussion	159
CHAPTER 8:	
DISCUSSION	160
REFERENCES	166
APPENDICES	179

CHAPTER 0 INTRODUCTION

0.0 INTRODUCTION

The most persistent cycle in nature is the diurnal light cycle which is accompanied by a slightly out of phase temperature cycle. It is hard to imagine how cells in the course of their evolution could have ignored this physical relationship and the limitations it imposed' (James 1964)

Almost all organisms exist in environments which exhibit predictable variations in quality. Evidence abounds in the real world of organisms that can at least on average, predict the timing of periods of both favourable and unfavourable conditions with considerable accuracy because the relevant factors show variation which has a very strong periodic component. These natural periodicities result from the inexorable periodic motions of the earth about its own axis or the sun, or even the moon about the earth. They can also come from more unexpected sources, such as variations in the rate of addition of nutrient to a commercial yeast or bacterial culture arising from organisational or experimental regimen. Populations in such periodically varying environments frequently exhibit dramatic changes in the relative abundance of individuals in different life-history stages at frequencies which are clearly harmonically related to that of the environmental variation. These changes often show every sign of being synchronised to the environmental periodicity in the sense that key biological events occur at the same point (or points) in the environmental cycle.

The advantages to an organism of synchronising its life-cycle to those of its conspecifics include increasing survival by predator satiation and (in sexually reproducing organisms) enhancing the probability of finding a suitable mate. Although synchronisation to the life-cycle of con-specifics does not logically imply synchronisation to a periodic environment it is clear that if a population of identical organisms synchronise tightly to an environmental periodicity then they are by definition synchronised to one another. Moreover, the benefits of synchronisation to con-specifics accrue only where the population of such conspecifics is large (such as emergence synchrony induced by pheromones in locusts (Mordue et al 1980)) whereas the benefits of synchronisation to the environment (and the penalties of failure to achieve that synchrony) continue to operate even when the population contains very few individuals.

Although mechanisms have been proposed which produce such synchrony by operating at the population level (see for example Hoppensteadt & Keller 1976), I suggest that the most general class of mechanisms operates by controlling the development rate of the individual organism. In this thesis I seek to elucidate the necessary characteristics of a broad class of such mechanisms which can lead to synchronisation of an individual life-cycle to periodic environmental variation. I examine the conditions under which an organism whose development rate is a periodic function of time can achieve synchronisation to that periodicity or to a harmonic or sub-harmonic of it.

I shall shortly give an outline of the two main classes of synchronisation mechanisms that have been hypothesised but prefer to first present a diverse selection of reported examples, both natural and induced, of biological synchrony.

0.1 BIOLOGICAL SYNCHRONY

Biological (as opposed to formal) synchrony is defined (less strictly) to be a high degree of concurrence (rather than exact simultineity) of a population in the engagement of a particular activity (Zeuthen 1964). Although laboratory experiments to induce synchrony in mass cultures go back to at least Angerer (1936), I surprisingly find that not until Zeuthen (1964) are the topics of induced and natural synchrony considered together in the same volume. Perhaps this stems from the large scale chanelling of resources in the singular quest for the hypothesised (but still unfound) autonomous biological clock (e.g. Edmunds 1976, Winfree 1986).

Natural Synchrony

At the most fundamental level, mitotic synchrony (division of nuclei) within the cell has long been documented in the embryos of a wide range of taxa including slime moulds (Lister & Lister 1925), amoebae (Kudo 1947), sea urchins (Agrell 1956), Euglenineae (Leedale 1959, Cook & James 1960) and amphibians (Agrell 1964). The natural life cycle synchrony of cell division (from mother to two daughter cells) was first reported at micro-organism level in 1905 by Gough for the dinoflagellate Ceratium and subsequently in the individual cells of larger animals (Carleton 1934, Halberg et al 1958). In the case of Ceratium such natural synchrony of division was later confirmed in the laboratory to be so precise as to occur only at night around 3.30 A.M. (Braarud & Pappas 1951, Sweeney & Hastings 1958). Shortly after this, 'natural phasing' of cell division was observed in a variety of algae such as the genus Chlamydomonas (Bernstein 1960) and thereafter in several others (Sweeney & Hastings 1962). Ongoing research has continued to show that synchronous behaviour among such simple organisms is indeed widespread (Heath 1988).

Life cycle synchrony of more complex (multi-cellular) organisms is well documented in arthropods through observations of the emergence of adults. One of the most dramatic examples of this phenomenon is the regular appearance of adults of the various USA cicadas which in some species takes place at intervals of up to every 17 years (Simon 1979). A related pattern of behaviour is shown by many odonate species (damselflies and dragonflies) which have life cycle lengths in the range three to seven years. Although adults of these species appear in most years they do so only at a small number of highly predictable

times (Corbet 1957, Lutz 1968, Norling 1984c, Crowley et al 1987). Amongst those synchronous arthropods with sub-annual life cycle lengths are locusts (Mordue et al 1980), beetles (Engler 1982, Topp 1990, Tasch & Topp 1991), moths (Common 1954, Nagase & Masaki 1991, Topp & Kirsten 1991), midges (Brust 1991) and spiders (Downes 1988, Tanaka 1992). Examples of organisms showing a fixed number of years per generation with key events occurring at predictable times of year are also common among herbaceous plants (Courtney 1968).

In the case of insects the combined morphological factors of small size, poikilothermy and poor insulation necessarily maintain their body temperature close to that of the environment (Mordue et al 1980). The benefits to such an individual of synchronising its life cycle to a periodic environment are therefore obvious. It can ensure that the only life history stages exposed to periods of highly adverse conditions (winter cold, summer heat or drought) are those specially adapted to survive them and it can ensure that the offspring which carry its hope of genetic survival will be produced at a time giving maximum chance of survival to maturity.

Induced Synchrony

Experiments to artificially induce synchrony boomed in the 1950's when realisation dawned that what is determined for a synchronised culture of cells pertains as a reliable first approximation to the individual cell (Zeuthen 1964). Studies conducted on such synchronised mass populations of micro-organisms have two clear practical advantages. Firstly they enable representative samples to be withdrawn without disturbing the cyclic chain of events under scrutiny. Secondly they permit sophisticated structural studies and chemical analyses to be carried out which cannot be performed on a single or few individual cells.

Earlier experiments with micro-organisms established that synchrony could be induced by a diverse range of periodic regimen. Angerer (1936) put it emphatically 'any treatment which alters the growth rate of a culture may be a potential synchronising one'. Apart from the natural occurring environmental periodicities of daylight and temperature, successfully applied regimen have included periodic treatments of nutrient increase or mechanical agitation (Angerer 1936), starvation (Sylven et al 1959) and even irradiation with X-rays (Spoerl & Looney 1959). Famous populations of organisms succumbing to such

inductive synchronisation treatments included algae such as *Chlorella* (Tamiya et al 1953), dinoflagellates such as *Gonyaulux* (Sweeney & Hastings 1958), amoebae (Angerer 1936, James 1959), yeasts (Sylven et al 1959, Spoerl & Looney 1959), and ciliate protozoa such as *Tetrahymena* (Zeuthen 1964).

The fact that synchronous behaviour could be induced in cell populations by external treatments sparked much excitement into speculation of potential underlying mechanisms. Intuitively it is clear what effect a synchronising mechanism must induce in the population for synchronisation to be achieved. James and Zeuthen have provided eloquent summary statements:

"Successful experimental induction of division synchrony requires that a growing culture be subjected to an experimental treatment which will either advance or retard some of the cells in their duplication cycle with respect to the remainder" (James 1964).

"Synchronisation depends on the establishment of conditions which will reduce the rate of preparation along one or a few channels, primarily the change in rate depending on stage of division such that individuals closest to division are most retarded those furthest away are least retarded" (Zeuthen 1964).

However, it is much less obvious (and still unresolved) what the underlying mechanism(s) actually are. Postulated synchronisation mechanisms, although not necessarily mutually exclusive, fall into two main classes according to their proposed undelying *timer*. These proposed timers by their very definition, as we shall now see, are necessarily mutually exclusive.

0.2 A BRIEF HISTORY OF TIMERS

The broad class of proposed biological timers divides into two distinct subgroups according to the category of timer mechanism hypothesized to underly the biological process.

(a) Autonomous Clock Hypothesis

The most obvious hypothesized timer is an autonomous biological clock located inside the organism which is subject to entrainment by external periodicity (Edmunds 1976). Time information is postulated to be generated intrinsically from within the organism and interaction with the external environment merely serves to adjust the biological process so that it remains 'in sync'.

A frequently cited observation put forward as evidence for the existence of an autonomous biological clock is that of the circadien rhythm observed in many insect species (Brown 1976, Mordue et al 1980). Such a rhythm is displayed in the perochial 'cockroach in the actograph' experiment through locomotor activity which recurs in a regular daily pattern. The persistence of this rhythm when the insect is kept under constant light-proof conditions away from a zeitgeber (transmitter of temporal information) has been the single definitive result interpreted to demand the requirement for a private endogeneous timer (Brown 1976).

Significantly, a circadien rhythmn has never been found to exactly match external (solar) time but rather 'free runs' or 'drifts' relative to it. This implies that the rhythmn recurs only at intervals of slightly more (or less, depending on the species) than 24 hours. Indeed, the term circadien was first coined by Halberg (1959) to emphasise the *approximate* character (*circa*- about, dien -a day) of the observed biological rhythmn.

Supporters of the autonomous clock have argued that because the duration of the drift is stable and largely resistant to the level of constant temperature ($Q_{10} = 1$), the drift must correspond with the period of oscillation of the postulated internal clock. They deduce that the presence of the external zeitgeber merely acts to entrain the postulated inate timer of the organism to that of the periodic environment. Perversely the conclusion is drawn that the observed drift gives further support to the hypothesis that the timer is in the organism rather than in

the environment. I prefer to interpret this empirical observation more objectively. In the insightful words of Brown (1976), '... the experiment merely demonstrates that whereas biological rhythmns can become circadien it is only hypothesis that the clocks are too'.

In the insect literature the autonomous clock hypothesis has recently fallen into disfavour and has been entirely abandoned in the context of explaining diapause because of observed 'gradual changes in diapause intensity' (Hodek 1983). The greatest argument against the existence of an autonomous clock is the simple fact that despite many years of searching not even a single component has yet been discovered (Palmer 1976, John Tyson personal communication SIAM conference San Diego 1994).

(b) Non-autonomous Clock Hypothesis

The second main hypothesis postulates that time interval information is received from an external source (such as the sun) and is then transformed into time information by the organism. Supporters of the non-autonomous clock hypothesis advocate that the periodic motions of the earth, moon and sun relative to each other provide a continual time reference frame which is mediated to the organism through the biological effect of the environmental periodicities that they engender. This is such a broad definition that it could holistically embrace all other proposed timers. In a sense the non-autonomous clock hypothesis can thus be regarded as the alternate hypothesis to the autonomous clock (either the proposed timer is dependent on the environment or it is not).

There is an argument that the above historically-adhered-to classification is an over-simplification of the types of timer mechanism that may exist. Even where the proposed timer is (supposedly) autonomous, we have seen that some interaction with the environment (entrainment) is necessary to keep perfect time. Further, there is no requirement that proposed timers be mutually exclusive.

Perhaps a more appropriate classification would be in terms of the 'plasticity' of the internal response exhibited to the environment. The autonomous clock timer could then be classified as a rigid type of internal response in which the organism could only keep correct time under a very *narrow* range of external (environmental) periodicity (e.g. 24 hour). The non-autonomous timer response would imply a more plastic response whereby the organism could maintain

appropriate timing throughout a much broader range of environmental periodicities.

In this thesis I explore the synchronous prospects for a mechanism which operates through an internal stage specific development response exhibited to an external periodic forcing. Rate of progression through the life-cycle, whilst proceeding at constant speed in constant conditions, responds to the periodic forcing in such a way as to induce synchrony between the life-cycle and the environment. Such a mechanism would be placed under the historical non-autonomous clock 'camp' banner. As a final preliminary, I now provide a quintessential review of biological development.

0. 3 DEVELOPMENT IN A CONSTANT ENVIRONMENT

Biological development of an organism is the resultant of an immense number of chemical and physical reactions (Johnson & Lewin 1946, Wigglesworth 1972, Sharpe & de Michele 1977). It involves processes of growth and differentiation which ultimately result in the organism passing from one condition to another. In many interesting situations (which I seek to investigate), such a transition occurs between two or more clearly definable states which are exhibited as a contiguous sequence of discrete successive *stages*. Typical examples of such 'stage specificity' are to be seen at the cellular level in cellular divisions (Mitchison 1971), in the progress from one instar to the next in arthropods (Logan et al 1976) and in the appearance of buds in flowers (Overcash & Campbell 1955). In section 0.5 I shall outline a generic model which can encompass this entire broad class of situations.

Let us make the reasonable assumption that development within any stage proceeds continuously at a constant rate under constant environmental conditions. Assuming a development index is possible for the organism (see section 0.4 below) a simple measure of *development rate* can be encapsulated by a 'development velocity' defined in terms of a goal quantity of development required to complete the stage (measured on the development index) divided by the time taken to traverse it (Wigglesworth 1972). If development velocity is charted throughout a complete range of different (but constant) environmental conditions, the stage development rate can be set up as a continuous function of the varying parameter(s).

Since the rate of all chemical reactions is dependent on temperature it follows that the rate of progress of most physiological processes bears a strong relationship with this parameter. It is therefore unsurprising that most historical studies have seeked to establish development rate as a function of *temperature*. There have been two main classes of attempts by which past authors have sought to achieve this, namely empirical or theoretical. I now briefly review the more prominent of these.

(a) Empirical derivations

The insect literature overflows with empirical formulations of development rate derived by holding a particular species under a range of constant laboratory temperature regimes and then fitting a curve to the acquired data. The earliest attempts at deriving development rate as a function of temperature were made with the implicit assumption that development increases in a linear fashion (de Candolle 1855, Sanderson 1910, Blunck 1914, Krogh 1914). In all these studies development rate g was presumed to be related to temperature T by

$$g(T) = k(T - a) \tag{0.1}$$

where k and a are constants. The value of the constant a is referred to as the 'development threshold'. Although the relationship of equation (0.1) holds for some organisms over the main range of naturally encountered temperatures (Williams & Wratten 1987) and most apparently for the insect orders Lepidoptera and Diptera (Peairs 1927, Hughes 1970) it generally becomes increasingly inaccurate as temperatures become more extreme (Mordue et al 1980). Many later authors attempted to improve upon this by deriving better empirical descriptions both within the fields of insect (Zwolfer 1934, Davidson 1942) and plant ecology (Leitch 1916, Shelford 1929, Barton-Wright 1933).

Most notable amongst these studies is Davidson (1942) who in a now famous paper employed the Verhurst logistic curve

$$g(T) = \frac{k}{1 + e^{(a-bT)}}$$
 (0.2)

where k, a and b are constants, to accurately describe the development of eggs of the human body louse. According to Wigglesworth (1972), this single curve affords a faithful representation for 85-90% of the complete temperature range over which development can occur in many insects and has since been applied in a more general context to other animals (Andrewartha & Birch 1954). However, the effects of

retardation may still be inadequately taken into account at higher temperatures (Davidson 1942 on Ludwig & Cable (1933) *Drosophilia* data).

Observing this deficiency, Pradhan (1946) went on to suggest the new formula

$$g(T) = ke^{-a(T_0 - T)^2}$$
 (0.3)

where k, a and T₀ are constants, whose graph deviates strongly from linearity at both lower and higher extreme temperatures. He demonstrated that this functional relationship accurately depicts the development rates through the egg and larval stages of 3 species of insect taken from different orders, most noteworthily the desert locust *Schistocerca gregaria* (Orthoptera) using data taken from Hussain & Ahmad (1936).

(b) Theoretical derivations

More ambitiously, there have been attempts at deriving alleged general descriptions of development rate by appealing to some theoretical principle extracted from the physical sciences. Such attempts are characterised by the author outlining the virtues of the chosen principle which (it is claimed) necessarily underlies the whole development process. Famous amongst such descriptions are the catenary curves of Janisch (1938) extracted from dynamics theory. Although these curves accurately depict the development of muscid flies (Larsen & Thomson 1940), they frequently give much poorer estimates at the lower range of developmental temperatures (Messenger & Fitters 1959, Messenger 1964).

In general the more simpler the theoretical relationship, the more limited the temperature range over which it holds (Nielsen & Evans 1960). Nevertheless some authors have still favoured simple relationships such as the Eyring equation taken from physical chemistry (Eyring & Stern 1939) or the exponential rule of Van't Hoff and Arrhenius (for chemical reactions)

$$g(T) = Ak^{T} (0.4)$$

where A and k are constants, as good general descriptions of metabolism (Palmer 1976).

A popular recent variation on the theoretical theme is the 'thermodynamic model' of Sharpe & de Michele (1977). This model blends the early high temperature enzymatic descriptions of Johnson & Lewis (1946) with similar at low temperature by Hultin (1955) through a linear relationship over the intermediate temperature range (their equation 17). The graph of this function gives rise to the most widely accepted generic relationship between development rate and temperature namely that of an S-shaped curve as shown in Diagram 0.1 (Mordue et al 1980).

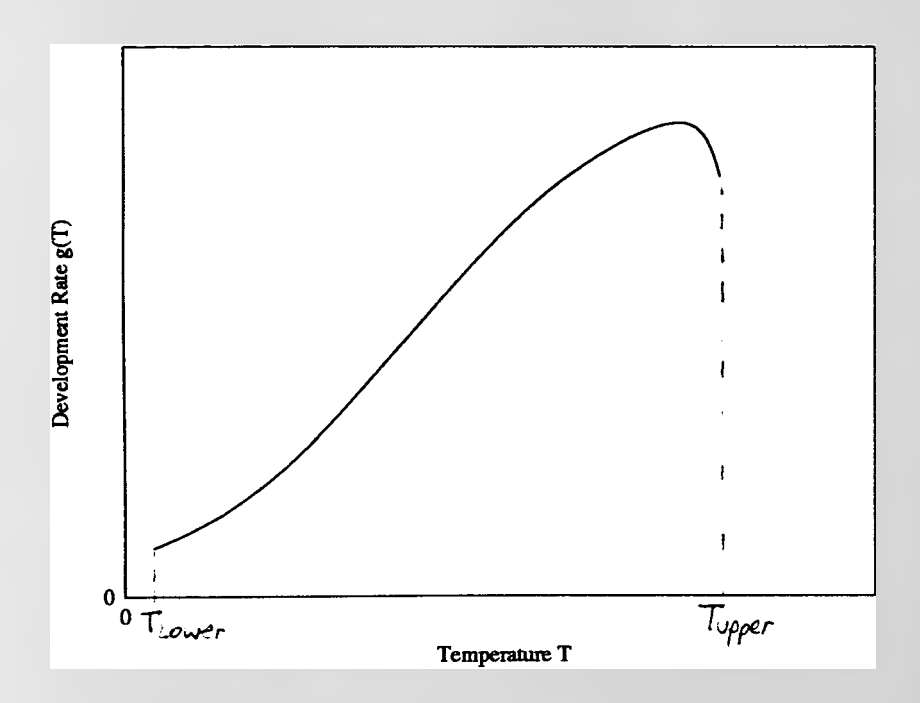


DIAGRAM 0.1. The general relationship between biological development rate and temperature (Mordue et al 1980). Beyond the ends of the plot (above temperature T_{lower}) or below temperature T_{lower}) the organism dies.

Other recent authors have continued to add to this already vast body of literature. Eubank (1973) introduced parabolic functions, Parker & Pardue (1974) increased the empirical catalogue, Stinner et al (1974) modified a sigmoid curve first introduced by Crozier in 1926 to exhibit a more impressive dip at higher temperatures. Logan et al (1976) applied the method of matched asymptotic expansions in a boundary layer context taken from the physical sciences (Lin & Segel 1974) to derive a two-part development rate function which, for the first time, was asymmetrical about the peak value.

I summarise all of the above with wise words of Wigglesworth (1972), "... whereas particular curves can be made to fit particular cases, no description is of sufficiently general application to be regarded as embodying any rational principle".

0.4 DEVELOPMENT IN A CHANGING ENVIRONMENT

My main interest lies in investigating situations where the organism is exposed to a periodically varying environment. How valid are the above descriptions when the same organism is exposed to a changing environment? There is no logical reason to expect that each of the many processes constituting development will necessarily exhibit the same *rate* of response to a given change of environmental parameter. By a continuation of this argument, there is no logical reason for development rate (the resultant rate of all such processes) to follow the same relationship under time-varying conditions as that obtained when the conditions are held constant. Thus, a question of central importance is whether the functional relationship between development rate and environmental parameter(s) obtained under constant conditions does indeed still hold when the parameters vary with time. Unsurprisingly, the precise answer is that this depends upon both the organism and the parameters being varied (Cloudsley-Thompson 1953, Wigglesworth 1972).

In the case of temperature, it is well known that changes can have a stimulating or retarding effect on development beyond the functional relationship obtained under constant conditions (Parker 1929, Powsner 1935, Precht et al 1973). That temperature fluctuations can accelerate development has been established by past studies in the germination and bud break of plants (Overcash & Campbell 1955, Kramer 1958, Hellmers & Sundahl 1959) and some species of insects (Parker 1929, Cloudsely-Thompson 1953, Clarke 1967, Remmert & Wunderling 1970). On the other hand, it has been equally well established that for a range of taxa as diverse as bedbugs (Johnson 1940,1942) and flies (Ludwig & Cable 1933, Vogt et al 1990) to amphibian embryos (Khan 1965) no such developmental stimulation occurs.

Throughout this thesis I make the simplifying assumption that the functional relationship exhibited between development rate and environmental parameter(s) under constant conditions is maintained when the parameter(s) change with time. Even though such a description may not aways be entirely accurate, I take the view (by

appeal to Occam's razor) that it is unrivalled in terms of general compactness and cogency.

Thermal Summation

Thermal summation originates from first attempts to assess the duration of development of an organism situated in a changing temperature. Historically, the technique first appeared in the insect literature with the implicit assumption that development rate is a linear function of temperature (de Candolle 1855) as in equation (0.1). For such a model, the product of degrees above the zero development threshold with development duration is of constant value (proof: If g(T) = k(T-a) so that the excess temperature x = T - a then the product of excess temperature and development time is $x(\frac{1}{b}) = \frac{1}{k} = \text{constant}$). This gives rise to the simple hypothesis that a fixed number of 'degree-days' must be required for the organism to complete its development (applied by Blunck (1914) in his studies on *Dytiscus* water beetles). A further piecewise linear extension of the approach to cover situations where development is non-linear was outlined by Sanderson (1910).

Development Index

The concept of degree-days ultimately relies upon the assumption that development of the organism proceeds cumulatively in a (linear) quantifiable way. A natural continuation of the idea is to move to a more general development description defined in terms of an abstract scale referred to as a *development index* (e.g Pradhan 1946). To do this requires the almost hidden assumption that, in the first place, development of the organism is expressable cumulatively as a function of time only.

Assuming this to be so, development *rate* is determined first (as a function of time) by appealing to the relationship established under constant conditions between development time and an influential environmental parameter such as temperature (e.g. Pradhan 1946). This necessitates use of the earlier assumption that the same relationship (established under constant conditions) holds when conditions are changing. What are the benefits of this approach?

The great merit of obtaining development rate as a function of time only is that physiological progress (development) can then be dealt with in an analogous fashion to a distance travelled (Stinner et al 1974, Logan et al 1976). Essentially development then corresponds to the area under the development velocity vs time graph. I shall show in Chapter 2 that this in turn allows a tremendously simpler model formulation in terms of a measure that I shall refer to as *physiological time*.

A Generic Life Cycle Model

Any complex life cycle can be regarded as a combination of several successive simpler component mechanisms (Danks 1991). For many organisms the successive transitions that occur in the life cycle are so rapid in relation to the duration of the life history that the intermediate state can be justifiably considered as a component *stage* of the life history (Mitchison 1971, Wigglesworth 1972). In such cases the main characterising feature of the life cycle is a contiguous sequence of separate 'differentially sensitive' stages (Palmer 1976). I seek to construct a simple life cycle model which incorporates this quintessential feature.

Usher (1976) has proposed excellent guidelines for any model which purports to describe a biological process. These specify that it must (a) encompass some biological feeling, (b) give a satisfactory fit to the process it describes, (c) be sufficiently general to describe a wide range of similar processes, (d) be tractable.

Following these, I suggest that the simplest generic model of such a life cycle is one composed of a contiguous sequence of discrete stages each of which has an associated continuous density independent time-varying development rate function. The only restriction which I shall place on the nature of these development rate functions is that all are periodic with the same repeat period. I make one further simplifying assumption, namely that there exists a finite point in time at which a given generation disappears and the next one appears (which necessitates the implicit assumption that reproduction occurs over a sufficiently short period that it can be considered as a point event in time). Completion of each generation is then analagous to the 'tick' of the underlying timer mechanism.

At first sight the assumption of such an instantaneous transition might seem unrealistic because of the likelihood of a blurring caused through individual non-homogeneity. However, the model is well suited to explosive reproducers such as 'big bang' insects (Roff 1990) (e.g. *Catops nigricans* of Chapter 1) and the general multitude of cases of cell division which have been outlined earlier in section 0.1 (e.g. Spudich & Sager 1980). It has also been argued that such a description is appropriate for organisms with a more protracted reproductive period provided that mortality during the period when emergence occurs is high (so that only those individuals which emerge within a narrow time interval survive to reproduce) (Roff 1990).

Because I wish to conduct an in-depth exploration of stage specificity, in this thesis I shall exclude any effects that may result from stochasticity produced by environmental noise or individual heterogeneity. In due course we shall see that such a model satisfies all of the Usher guidelines.

Observe now that this generic model, although simple, permits investigation of the entire class of situations in which each stage in the life cycle 'exhibits' a different developmental response that is, where

- (a) a different internal (biotic) development response takes place within each developmental stage, or
- (b) a different external (abiotic) environmental forcing function affects each stage of development such as when the organism has different developmental stages in different media (e,g dragonflies), or
- (c) a combination of both (a) and (b) occurs in the life history.

In this thesis I shift our main focus to the simplest such model with the minimal set of necessary characteristics, namely one in which the life-history consists of two stages. I do this primarily because I seek to investigate the extent to which life cycle synchrony can be influenced by stage specificity *per se*. I use this simplest model to explore (at minimum cost to intractability) the general synchronous implications of exhibiting a stage-specific developmental response in a periodically varying environment.

Support for the realistic worth of even such a simple model can easily be found. The observations of Spudich and Sager (1980) on *chlamydomonas* and Heath & Spencer (1985) on a number of marine algae are consistent with this picture. Gurney et al (1992, 1994) have shown that two special cases of this type of mechanism predict dynamic behaviour similar to that observed in many odonate populations (see section 4.1).

0.5 OVERVIEW OF THESIS

I commence with a detailed case study performed with a stage specific model of the univoltine European beetle *Catops nigricans* parameterised with data obtained by Topp (1990). I demonstrate that the model formulation not only gives realistic synchronisation results but also that equally valid results are obtained by collapsing the model into a simpler appropriate two stage description.

Realising that future analytic tractability could easily be lost, the concept of *physiological time* is introduced early in the next Chapter. Immediately, I demonstrate the potency of this description by constructing a straightforward formal proof (of the observation by Gurney et al 1992) that no *physiologically unstructured* population whose development rate depends only on time can ever achieve synchrony.

In Chapter 3 I dig into dynamical systems literature to extract a foundational block of theory which will later serve as fundamental throughout the thesis. Utilising this, I set up a general two stage model in Chapter 4 and together with the broad analysis performed in Chapter 5 uncover a powerful repertoire of general properties. These are summarised by a selection of compact new Theorems together with novel relationships between *interphase map* and *behaviour portrait*.

In Chapter 6 I take a 'time out' from the general model to explore a simpler linearised version which enables higher-ordered locking behaviour to be more thoroughly investigated. The analysis of this model provides insight into other (though biologically less interesting) forms of dynamic behaviour that can occur such as neutral stability.

I return to the general model in Chapter 7 and show a selection of surveys via sequences of behaviour portraits. These demonstrate how the *shape* of the interphase map largely determines synchronisation behaviour. Important practical biological implications are mentioned in the final section. In particular, the *Catops nigricans* model is re-examined in the light of its associated behaviour portrait. A concluding discussion which includes an outline of possible future avenues of research is covered in Chapter 8.

CHAPTER 1

A LIFE CYCLE IN A SEASONALLY VARYING ENVIRONMENT

Catops Nigricans

'[Coleoptera] provide excellent illustrations and test cases for almost every general evolutionary principle, and future study of the group may well lead to the formulation of new generalisations'. R.A. Crowson (1981).

1.0 INTRODUCTION

The small European beetle Catops Nigricans (Catops for brevity) displays remarkable univoltine seasonal synchronicity in times of adult emergence and oviposition. A central quest of this detailed case study is to determine whether such a phenomenon can arise purely through a stage specific developmental response to periodic environmental variations. Although other abiotic development factors such as humidity may be important (Evans 1975), I make the assumption that their developmental effects are negligible. For the purposes of this investigation, Catops shall essentially be reduced as near as possible to a mere bag of chemicals.

In line with the assumptions of section 0.4, I shall construct a stage specific life cycle model of *Catops* which utilises the complete development data presented in a study by Topp (1990). Seasonal environmental variations of temperature and photoperiod shall be represented by sinusoidal driver functions (of time) thereby defining stage specific *annual* development rates for each stage throughout the year. This 'default' model shall give the best possible representation of *Catops* together with its immediate external abiotic environment. I shall use this model to investigate the synchronising effect of periodic environmental variations of temperature and light on the adult eclosion and oviposition times of an arbritrary initial cohort, over several generations. Can the observed real life synchronisation of the *Catops* life cycle be wholly attributed to a stage specific developmental response to known periodic variations of temperature and photoperiod?

1.1 BIOLOGY OF CATOPS NIGRICANS

Natural History

Somewhat unusually for an insect of temperate latitudes, the life cycle of *Catops Nigricans* (Coleoptera: Leoididae: Catopinae: Spence 1813) begins with oviposition in the autumn. Larval development then proceeds throughout the winter months before the newly formed immature adult beetle emerges from the pupa stage in the following spring. A period of diapause during the summer months (referred to as aestivation) typical of Catopinae (Engler 1982) delays development of female reproductive organs. Maturation and oviposition finally take place in the autumn, to complete the univoltine life history. The reproductive period is relatively brief in comparison to the length of the complete life history so that *Catops* is a 'big bang' insect (section 0.4) and exhibits this through briefly semelparous reproduction (Topp 1990).

Catops leads a secretive existence. As a typical member of the Catops genus at 5.5 to 6.5mm long (Jeannel 1936), it is to be found as a general forager in the litter layer of European forests, with northern limits on its distribution ranging from Iceland and Scotland through to northern Norway and Finland (Topp 1990). The species was classified as eucoenic in a survey by Israelson (1971) since it was so rarely to be met with outside of the burrows of small mammals. By no accounts does it ever venture upwards beyond the litter layer level (Topp and Engler 1980). The question as to how far it ventures below ground is less easily answered and most ecological (as opposed to biological) information on Catops appears to be purely anecdotal (Topp 1993, personal communication). Catops does enter soil layers of up to 25 cm during adult diapause and should be able to permanently live in the burrows of small mammals (Topp 1990). Research by Topp in the same study also showed that as far as temperature measurements are concerned, an adequate permanent habitat is certainly to be found in mole nests. Indeed, Casale (1975) unhesitatingly links the home of a close relative Catops Nigriclavis with such places. It would therefore appear that Catops is very partial to subterranean life and this is not entirely surprising given that other members of the Catopinae with a more southerly European distribution (such as some in the genus Choleva) are exclusively cave-dwellers (Deleurance-Glacon 1963)

Life Cycle

Like most species of beetles, *Catops* commences life as an egg and then passes passes through 3 distinct larval instars labelled L1, L2, L3 and finally a pupa stage before

emerging as an adult. At the time of emergence into the world as an adult (eclosion) the young *Catops* is immature. According to Topp (1990) the delay between adult emergence and maturation, as measured by the period between eclosion and deposition of eggs (oviposition), lasts between 97 and 212 days. The duration of this relatively long delay (symptomatic of diapause) is referred to as diapause intensity. Diapause actually corresponds to a slowing down of internal metabolic processes and surfaces most visibly as a retardation of development. The occurrence of adult diapause within the insect life cycle is certainly well known (Hodek, Pener & Orshan 1983) and frequently has a retarding effect (as it does for *Catops*) on the *female* reproductive organs (Beck 1980, Danilevskii 1965). I choose to consider the period of adult diapause as a 6th stage of development which follows immediately after the pupa stage. I shall refer to this convenient 6th stage as the Immature Adult (IA) stage.

Topp's (1990) Laboratory Data

Catops is easily reared in the laboratory and is ideal for 'generation' studies because of the ease with which it can be bred (Topp and Engler 1980). Larval development is temperature dependent (typically $Q_{10}=2$ to 3) and maturation of the ovaries in the adult female also depends upon photoperiod (Engler 1982). Topp (1990) recorded complete data on the development times of each of the distinct 5 pre-adult stages, egg to pupa inclusive, when Koln beetles were kept under regulated laboratory conditions of temperature and light (Topp 1990). These data consist of the mean durations of each pre-adult stage under controlled regimes of either Short Day (SD) or Long Day (LD) photoperiod conditions, held under a range of constant temperatures. SD data refers to data that were obtained for individuals exposed to shorter periods of light throughout development in the ratio 8:16 hours light:dark (or photophase: scotophase) per day. Similarly, LD data refers to data obtained in which light:dark was regulated at 16:8 hours per day. The chosen photoperiod regimes, SD and LD respectively, correspond to minimal (mid-winter) and maximal (mid-summer) periods of daylight at Koln latitudes.

All beetles were reared from eggs inside incubators in which temperature was maintained at a constant level. The chosen constant temperatures started at 5 C and increased in steps of 5 C up to 25C. For both photoperiod regimes (SD and LD) the mean time taken for each pre-adult stage to complete development where death did not occur was recorded. Under either regime, when temperatures were held at 20 C and 25 C, Topp found that individuals died during larval instars L2 and L1 respectively (consequently there is no data for the later stages L3 and pupa at these

temperatures). Topp's data showed that only development of the L3 instar was greatly affected by photoperiod.

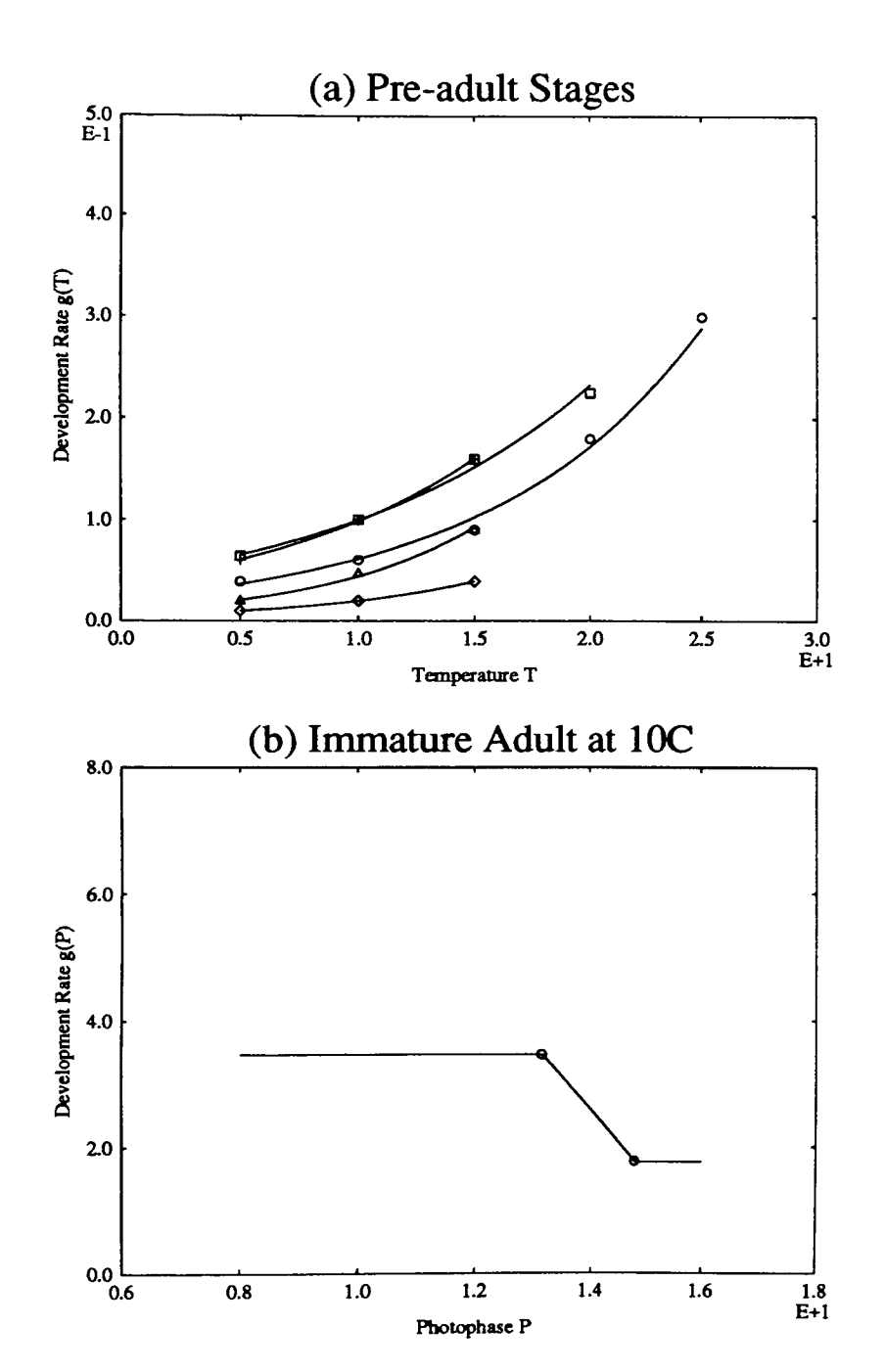


DIAGRAM 1.1 Rates of development per Topp's 1990 Laboratory Data
(a) Short Day regime, Key: O Egg, □ L1 stage, + L2 stage, ◊ L3 stage, △ Pupa.
(b) Immature Adult at 10 C

Diagram 1.1(a) shows data and plots of development rate v temperature for each of the pre-adult stages under the SD photoperiod regime. Plots of functions are constrained within the threshold temperatures of each stage. Thus for temperatures outside these ranges, development rates are strictly given by extrapolation. Only within the temperature range of 5-15C are no such extrapolations required for all stages.

The effect of increased photophase on instar L3 in the LD regime is shown in Diagram 1.2(a) by an upward shift in the development rate curve. On other pre-adult stages, Topp found this effect to be negligible. Thus, I reasonably define LD data as that set of data made up of LD data points for stage L3 and only SD data points otherwise.

For the Immature Adult stage, data on the female development time, referred to as 'diapause intensity', was available for a range of photophases held at a single temperature value of 10C. Topp's diapause data suggests that diapause intensity suddenly increases dramatically at a critical photophase Lcrit of approximately 13.2 hours and levels off at a photophase Rcrit of approximately 14.8 hours. For daily photophases of durations either side of these values, diapause intensity remains at a fairly constant plateau level. *Catops* therefore exhibits 'short day' insect development (Type II diapause response (Beck 1980)) since its development is enhanced (i.e. diapause duration reduced) by shorter periods of photophase. Diagram 1.1(b) shows the relationship between development rate (taken to be 1/diapause intensity) and photophase.

Less detailed data under the LD regime was also presented for diapause intensity at a constant temperature of 15C. Taken together with the former, the data suggests that the *Catops* diapause mechanism is dependent on both temperature and photoperiod as shown in Diagram 1.2(b). Such a temperature-compensatory effect is frequently found in the diapause of many species of insects (Beck 1980, Mordue et al 1980).

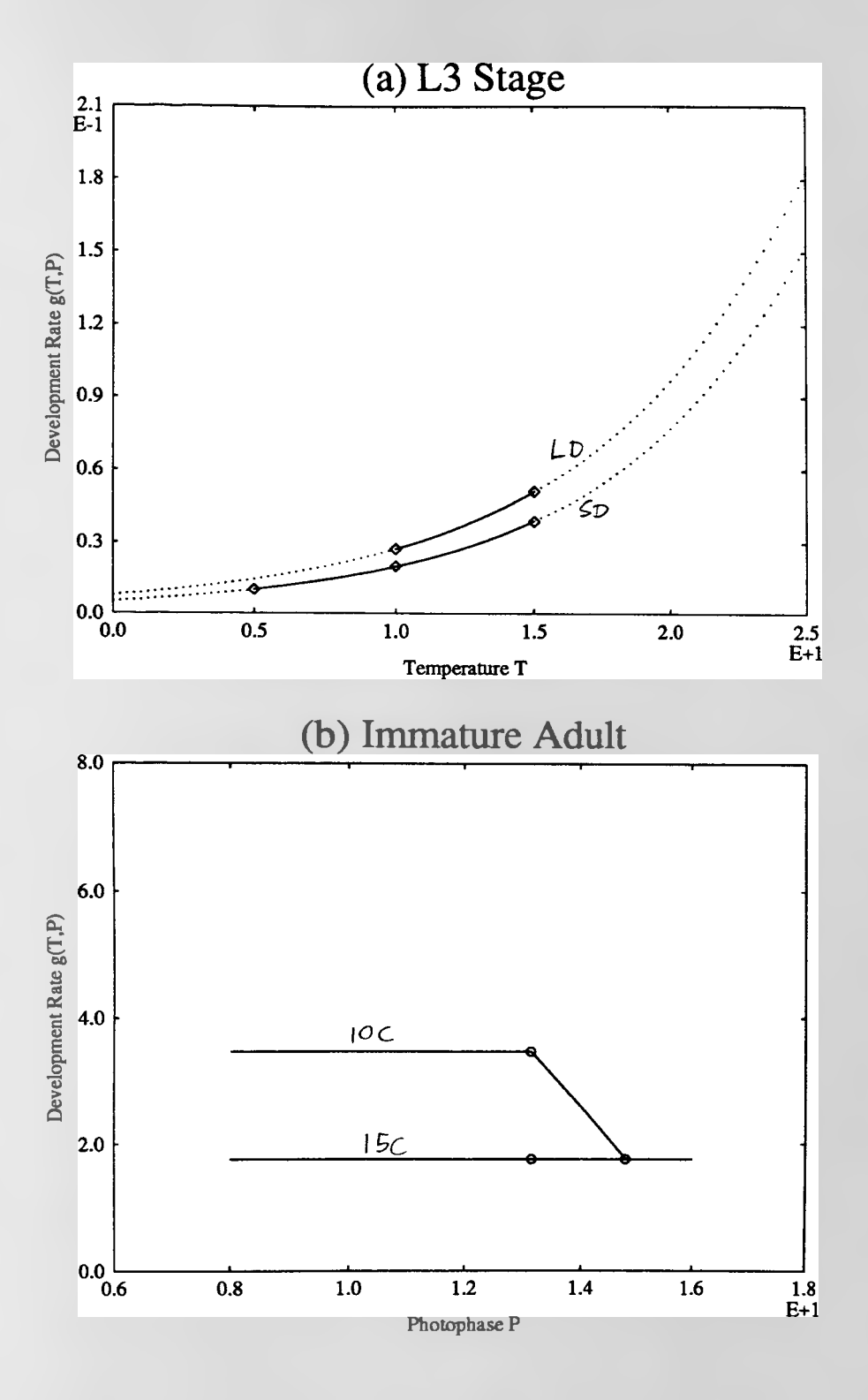


DIAGRAM 1.2 Effect of (a) photophase on L3 stage and (b) temperature on Immature Adult

1.2 A LIFE CYCLE MODEL OF CATOPS NIGRICANS

Environment

Meteorological records of the monthly mean air temperatures in the Koln locality over a 20 year period were obtained by Topp (1990) and these were found to periodically vary in a sinusoidal manner between an annual minimum of Tmin=2C at the end of January and an annual maximum of Tmax=21C in mid-July. I can thus choose to simulate the annual variation of air temperature T as a function of time t by

$$T(t) = T_0 - T_1 \cos k (t - T \sinh t)$$
 (1.1)

where Tshift is a one month time lag which displaces troughs and peaks by one month from the beginnings and centres of the years, with T_0 , T_1 and k suitable constants.

Annual variations of daily total photophase P at Koln latitudes also vary sinusoidally, between a minimum of Pmin=8 hours on 21st December and a maximum of Pmax=16 hours on 21st June, so that I can choose

$$P(t) = P_0 - P_1 \cos kt$$
 (1.2)

with P_0 and P_1 suitable fixed constants.

Since Catops prefers life below ground in its natural habitat, I must explore the implications of subterranean development by considering the effect of ground attenuation of surface temperature variation (Moon 1983, Gordon et al 1989). Suppose the surface temperature T_s oscillates in a sinusoidal manner about a mean surface temperature T_0 according to

$$T_s = T_0 - T_1 \cos kt \tag{1.3}$$

where T_1 is the amplitude, $k = 2\pi$ / P, and P is the period of the oscillation. Standard textbooks [e.g. Ingersoll et al 1948] show that the vertical heat flux (G) in the ground and the vertical temperature gradient $\frac{\partial T}{\partial Z}$ are related by

$$G = -k_s \frac{\partial T}{\partial Z} \tag{1.4}$$

where k_s is the thermal conductivity of the soil.

A reasonable approximation to temperature variation T_z at a depth z below the surface can be found by solving equation (1.4) for the simplest possible situation, namely that of constant k_s . In this case, the temperature variation below ground also turns out to be sinusoidal but with the surface amplitude exponentially damped as a function of the depth z so that

$$T_z = T_0 - T_1 e^{-\alpha z} Cos(kt - \alpha z)$$
 (1.5)

where

$$\alpha = \sqrt{\frac{\pi \rho c}{P k_s}}$$
, $\rho = \text{soil density}$, $c = \text{specific heat of soil}$. The parameter $\beta = \frac{k_s}{\rho c}$ is

known as the thermal diffusivity of the soil so I shall write $\alpha = \sqrt{\frac{\pi}{P\beta}}$. At a depth z below the soil surface the *amplitude* (range) of variation is therefore $T_1e^{-\alpha z}$.

The extent to which *Catops* regulates its own internal developmental processes by reacting to external stimuli (for example, burrowing deeper to avoid 'unpleasant' temperatures) is not known. This kind of behavioural non-homogeneity frequently occurs in many fields of animal ecology (Precht et al 1973, Grist 1994). I make the (usual) simplifying assumption that the organism does not significantly self-regulate its abiotic environment.

Model Definitions

I define development rate in time honoured fashion by reference to a Development Index based on temperature T (e.g Pradhan 1946 see Chapter 0), and defined on a continuous scale ranging from 0 at the start to 1 at the completion of the stage. The development rate with all abiotic conditions held constant is then taken to be given by development rate = 1 / development Time

For each pre-adult stage i = Egg to Pupa, I shall define the development rate as a continuous function g_i to fit Topp's data by

$$g_i = g_i(T)$$
 for i=Egg, L1, L2, Pupa, (1.6a)

$$g_i = g_i(T,P)$$
 for i=L3 (1.6b)

with g_i determined by regression. I carried out linear and loglinear regressions to obtain the g_i of best fit. Table 1 shows that loglinear regressions gave the better fits for all pre-adult stages and in particular for the obviously non-linear Egg stage.

Pre-imaginal Stage	R ² -Adjusted %	
	Loglinear Reg.	Linear Reg.
Egg	98.7	85.9
L1	99.3	97.3
L2	99.9	97.4
L3	100.0	93.8
Pupa	98.8	96.6

TABLE 1.

Comparison of quality of fit of linear and loglinear regression lines to Topp's 1990 pre-adult SD data.

I thus define development rate by the exponential function

$$g_i = g_i(T) = w_i e^{z_i T}$$
 for i=Egg, L1, L2, Pupa (1.7)

with w_i , z_i , the respective stage specific coefficients obtained by loglinear regression of SD data (that is as obtained from the linear regression lines $y_i(T) = \text{Ln}[g_i(T)] = \text{Ln}(w_i) + z_i T$ in the loglinear plane) and T(t) as in equation (1.1).

For stage L3, I construct a dynamic photoperiod-compensated version of equation (1.7) such that the development rate is now defined by

$$g_{L3} = g_{L3}(T, P) = w_{L3}(P)e^{z_{L3}(P)T}$$
 (1.8)

where $w_{L3}(P)$, $z_{L3}(P)$ are functions of photophase P obtained by loglinear regressions and T(t), P(t) are the driver functions given in equations (1.1) and (1.2) respectively. That the loglinear relationship is maintained when coefficients w_{L3} , z_{L3} are sinusoidally driven is a straightforward proof.

For the Immature Adult stage I treat diapause intensity in the same manner as preadult development so that under fixed abiotic conditions g_{IA} is defined as g_{IA} = diapause development rate=1/(diapause intensity). Thus, to reflect the dependence of diapause intensity on both temperature and photophase

$$g_{IA} = g_{IA} (T,P) \tag{1.9}$$

I fitted a piecewise linear function to Topp's diapause data as illustrated in Diagram 1.1(b). I modelled the temperature-compensatory effect in accordance with Topp's data so that the altitude of the leftmost 'plateau' decreases with increasing temperature as shown in Diagram 1.2(b). For T outside the range of temperature interpolation ($10C \le T \le 15C$), a 10C SD diapause ceiling value and a 15C LD diapause floor value were imposed in the Default Model (see 1.3 Structural Stability for other variants). The rightmost plateau was made temperature independent, reflecting the fact that at photophases above Rcrit, diapause development was found to be insignificantly affected by temperature variation. For photophases between Lcrit and Rcrit, diapause development rate was defined by interpolating photophase between the two plateau levels. Hence

$$g_{IA}(T,P) = \begin{cases} SD \text{ diapause rate} & T \leq 10 & 8 \leq P \leq L \text{crit} \\ mT + c & 10 < T \leq 15 \end{cases}$$

$$LD \text{ diapause rate} & 15 < T & (1.10)$$

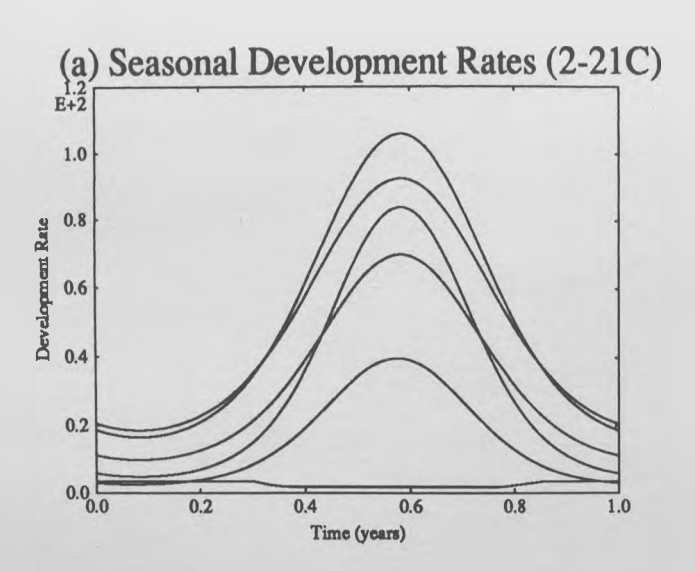
$$n(T)P + D(T) & L \text{crit} \leq P \leq R \text{crit} \\ LD \text{ diapause rate} & R \text{crit} \leq P < 16 \end{cases}$$

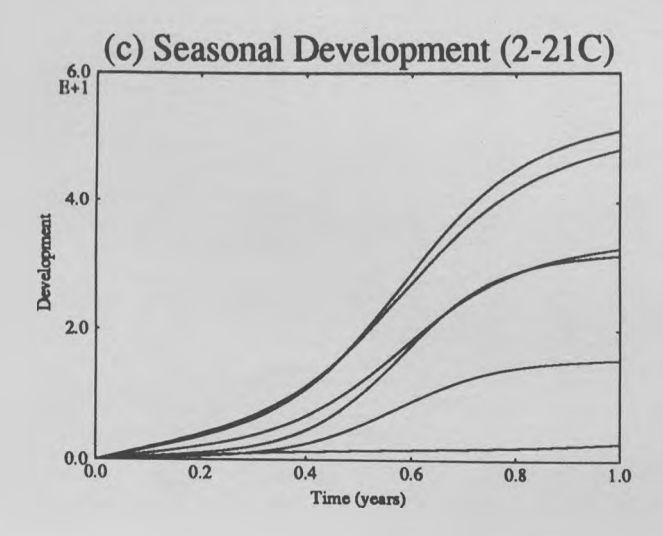
where m, c are constants and n(T), D(T) are linear functions of T. In the absence of enough data, I make two assumptions here, namely that:

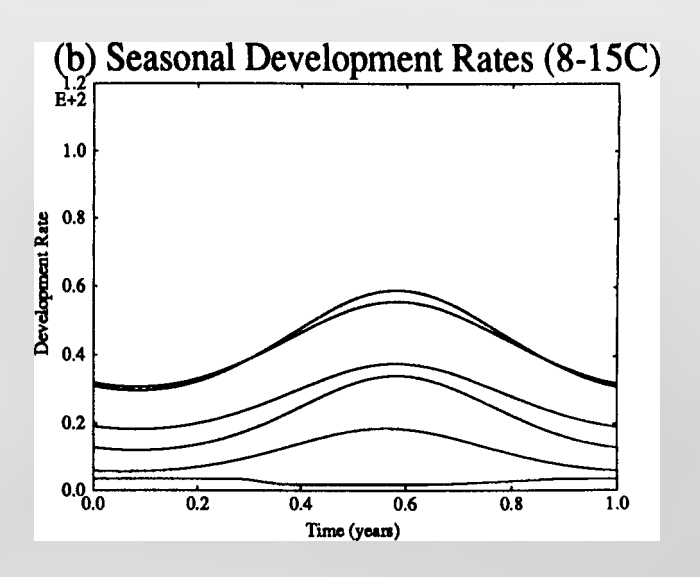
- (1) the form of this function always has left and right segments connected by a central joining line and
- (2) Lcrit and Rcrit critical photophases remain the same at any temperature that is, are temperature independent.

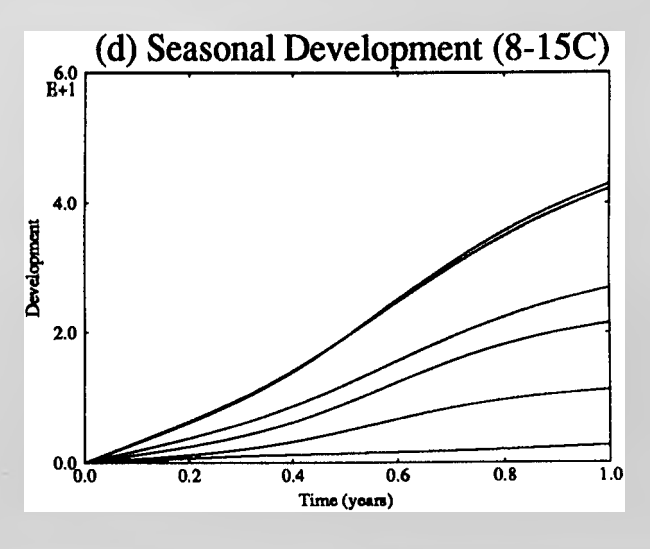
Diagram 1.3 shows plots of *periodic* (seasonal) development rates $S_i(t)$ for all stages i = Egg to Immature Adult, as functions of time of year t. The periodic development is shown in the frame below for the same temperature variations (1.3(c) and (d)). I notice that the general effect of an increase in annual temperature variation is to

DIAGRAM 1.3









accentuate both the peaks and the troughs of the periodic development rates for all stages.

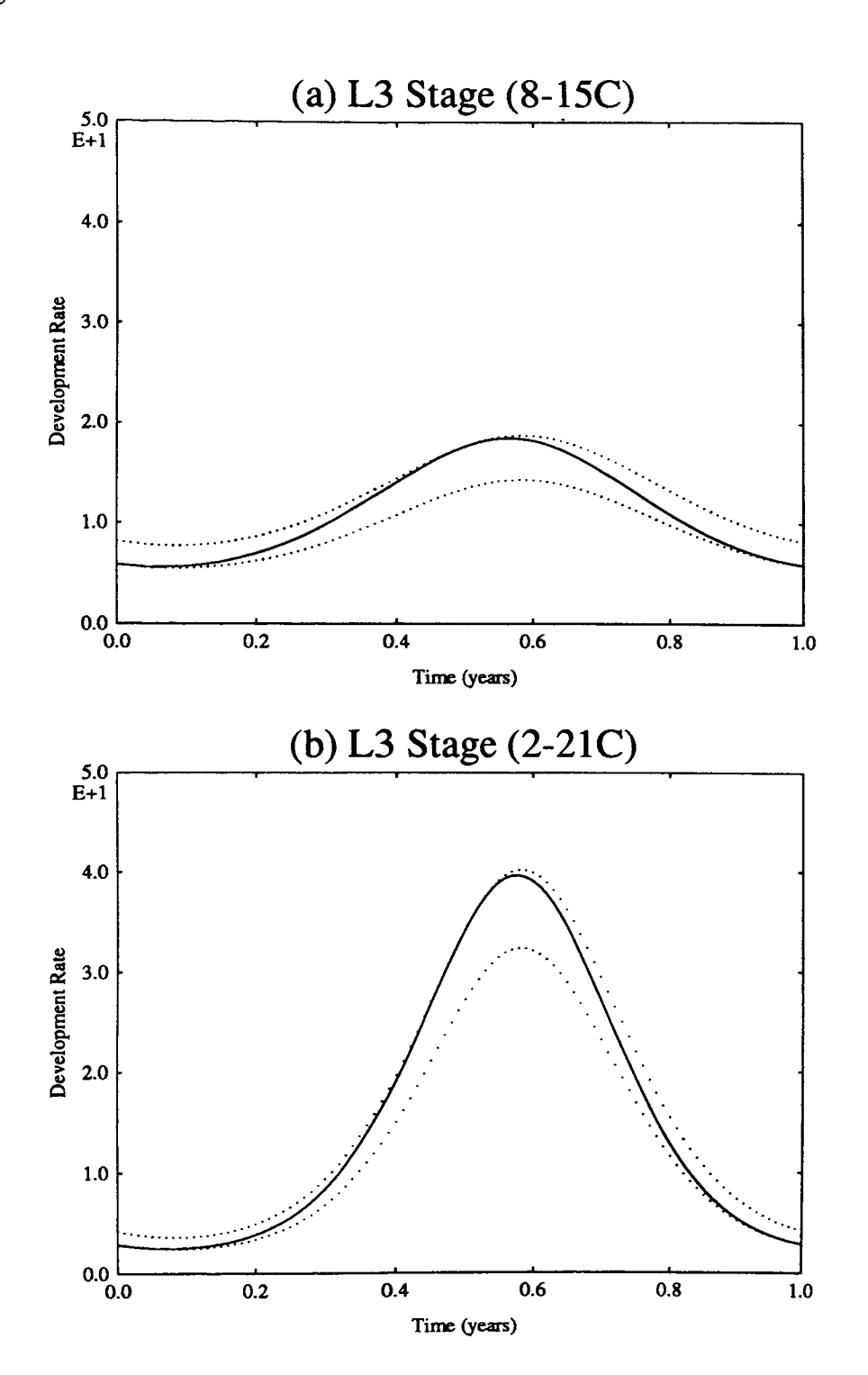


DIAGRAM 1.4 Effect of Short day/Long day photophase on L3 stage for annual temperature variations of (a) 8-15C (b) 2-21C

The photoperiod-compensatory mechanism embodied within the L3 stage causes a slight skewness of annual development rate when plotted as a function of time of year and this is shown in Diagram 1.4. I observe that this plot necessarily touches the SD and LD curves at the times when Pmin and Pmax occur, namely at the year ends and centre respectively.

The temperature-compensatory mechanism included within the Immature Adult stage has a more pronounced effect which can seen in Diagram 1.5. This time, the one month lag of temperature behind photoperiod causes the observed skewness which becomes more pronounced as the range of temperature variation is *decreased*.

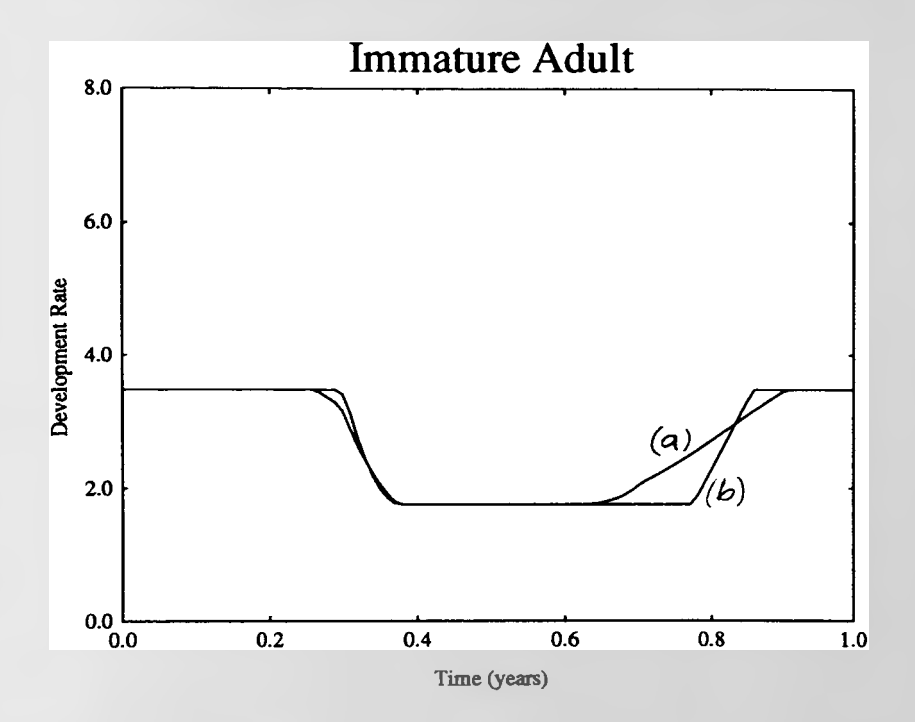


DIAGRAM 1.5 Effect of Short day/Long day photophase on Immature Adult for annual temperature variations of (a) 8-15C and (b) 2-21C.

Stage Specificity

I now formulate a simple model of *Catops* in which the complete life cycle consists of 6 discrete developmental stages, namely Egg, L1, L2, L3, Pupa and IA stages. I make the assumption that at the end of each stage, promotion to the next stage occurs instantaneously. By the brief semelparity of *Catops* I make the assumption that

reproduction occurs instantaneously and only once in the life cycle, after the completion of the Immature Adult stage (Topp 1990). Diagram 1.6 shows the stage specific life cycle structure.

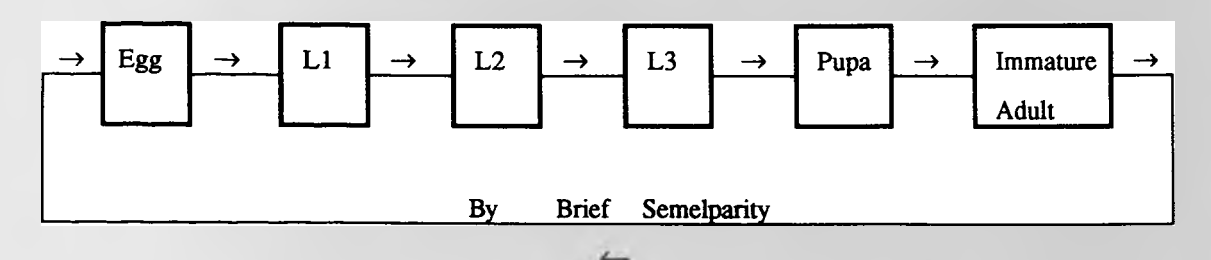


DIAGRAM 1.6 Schematic illustration of the Catops Life Cycle Model

For stage i=Egg to Immature Adult, let t_{Ri} denote the time at which an individual enters the stage and let x_i denote the stage duration so that promotion from the stage occurs at time $t_{Pi} = t_{Ri} + x_i$. By definition of development index

$$1 = \int_{t_{R_i}}^{t_{R_i}} S_i(t) dt = \int_{t_{R_i}}^{t_{R_i} + x_i} S_i(t) dt$$
(1.11)

Let $G_i(t) = \int S_i(t) dt$ with $G_i(0) = 0$ so that $G_i(t)$ (shown in Diagram 1.3 (c) and (d)) corresponds to the area under the graph of $S_i(t)$. Hence

$$1 = G_{i}(t_{Ri} + x_{i}) - G_{i}(t_{Ri})$$
 (1.12)

must be solved to find x_i . Since $S_i(t)$ is not analytically integrable for the g_i functions employed here, I used straightforward numerical integration techniques (Appendix A1.2) to calculate x_i . The life cycle duration L of a given individual is then simply given by the sum of all the separate stage durations x_i for i = Egg to Immature Adult.

I carefully note that in general, x_i is not a fixed time interval since the duration of any stage i is dependent on the time of year t at which the stage is commenced. So $x_i = x_i$ (t) and

$$L = L(t) = \sum_{i=egg}^{1A} x_i(t)$$
 (1.13)

For a given individual, let t_R (= t_{REgg}) be the time of recruitment to the life cycle and let t_M (= t_{MIA}) be the time of maturation. Then clearly

$$t_{M} = t_{R} + L(t_{R}) \qquad (1.14)$$

I prefer to think of the life cycle model in terms of a 'black box'. This black box is sensitive only to temperature and photoperiod and is continually exposed to the seasonal variations imposed by the temperature and driver functions T(t) and P(t) respectively. After the input of an initial time of year t_R (oviposition), 6 successive modes of internal response occur, each of which corresponds to a discrete stage of development. Whilst in each mode, a corresponding internal development rate (dependent only on time t) is utilised to calculate how long the black box remains in that particular mode. The total time taken for the black box to pass through all 6 modes is then added to the initial input time to produce an output time t_M .

Reproduction

I can think of the the black box as being an egg at the input time which thereafter develops through stages L1, L2, L3, Pupa, followed by the Immature Adult stage. For any input time, a single output time is eventually produced, which corresponds to the respective time of maturation of the Immature Adult. By brief semelparity, oviposition can be reasonably approximated as occuring at that same point in time. Thus, each time of maturation t_{Mn} of generation n is re-entered in a cycle as a time of recruitment $t_{R(n+1)}$ (= t_{Mn}) to generation n+1. The times of maturation/ recruitment of progeny stemming from any initial recruit (its lineage), can thus be calculated for several successive generations.

I extend the notation of equation (1.14) to encompass the nth generation of any lineage so that

$$t_{Mn} = t_{Rn} + L(t_{Rn})$$
 (1.15)

and since by brief semelparity

$$t_{M_n} = t_{R(n+1)}$$
 (or $t_{R_n} = t_{M(n-1)}$) (1.16)

successive times of maturation are given by

$$t_{Mn} = t_{M(n-1)} + L(t_{M(n-1)})$$
 (1.17)

Hence for any lineage the times of recruitment to all subsequent generations are determined solely by the time of recruitment of the first (ancestor) individual. I construct a simple algorithm to calculate all times of recruitment in successive generations up to a final generation $N \ge 2$ by combining equations (1.15) and (1.17).

Algorithm for times of recruitment

- (1) For generation n = 1: $t_{M1} = t_{R1} + L(t_{R1})$; (1 iteration)
- (2) For generations n=2 to N: REPEAT for n=2 to N, $t_{Mn}=t_{M(n-1)}+L(t_{M(n-1)})$

(N-1 iterations)

1.3 SIMULATION RESULTS

I carried out simulation studies to investigate the effect of annual temperature variation on the synchronisation of recruitment times. Synchronisation behaviour was conveniently illustrated by the use of Line Plot diagrams (Tasch and Topp 1991). For clarity, these were constructed by joining together the algorithmically calculated times of recruitment to successive generations (points) with straight lines. The 'trajectory' obtained thus represented the lineage which stemmed from the initial ancestor individual. Ground damping of surface air temperature variation was also taken into account for a variety of soil types. For each soil type a 'critical depth' was calculated, below which the effect of damping would be too great for 1 lock synchronisation to occur in the model.

All simulations were performed with an arbritrary initial cohort consisting of 27 individuals spaced equally at fortnightly intervals throughout the starting year. This initial cohort was then exposed to sinusoidal variations of temperature and photophase over a period of several seasonal cycles, keeping variation of temperature and photophase the same within each cycle. The lineage stemming from each individual (by semelparity only one such lineage could arise from each individual) was then plotted as a single trajectory line together with the complete set of all such trajectories stemming from all other individuals in the cohort. The resulting diagram, referred to as a Line Plot diagram, then clearly showed up any synchronisation behaviour by the convergence of these lines.

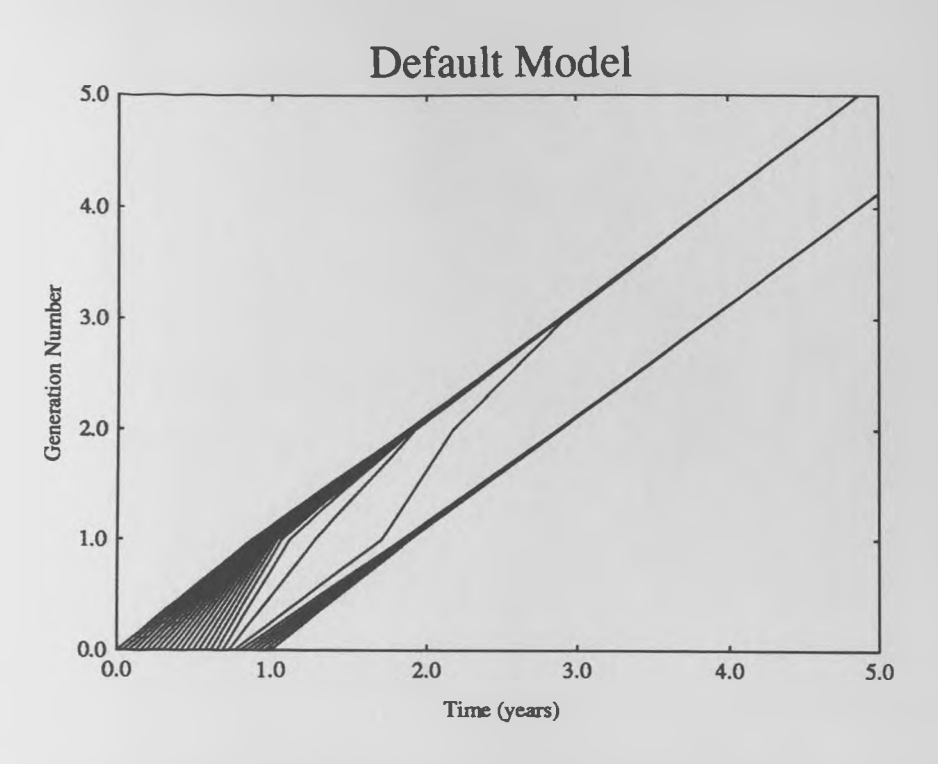
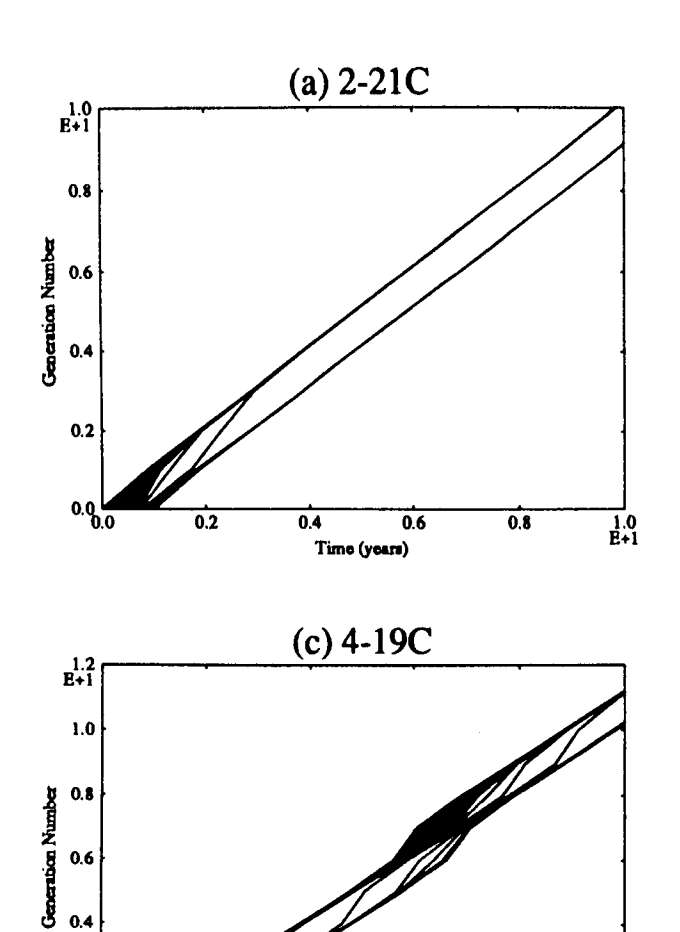


DIAGRAM 1.7 Synchronisation of lineages in the Default Model at 2-21C annual temperature variation.

Diagram 1.7 shows that when the annual temperature variation was fixed at 2-21C, rapid synchronisation to a 1 lock took place and the initial cohort was split into 2 distinct cohorts, each with successive recruitments separated by an interval of exactly 1 year. The synchronising effect of narrower variations in annual temperature (keeping the annual mean temperature fixed at 11.5C) is shown in Table 2 and by Line Plot diagrams in Diagram 1.8. Diagram 1.8(c) sharply illustrates that any initial tendency towards synchronisation (convergence of lineages) does not necessarily imply that synchronisation must ultimately occur.

DIAGRAM 1.8



0.2

0.2

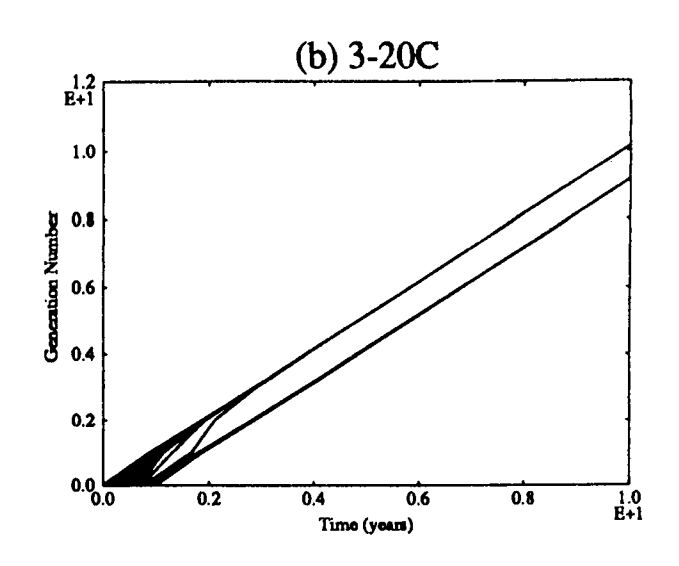
0.4

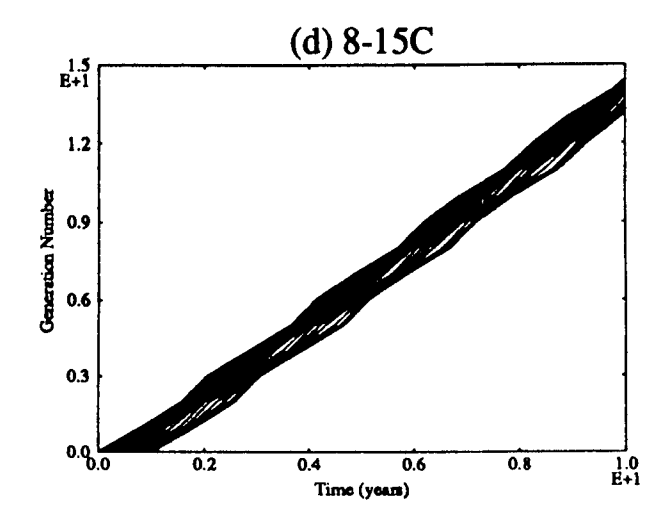
Time (years)

0.6

0.8

1.0 E+1





Anual Temperature variation (C)	Synchronisation behaviour	Diagram 1.8
11.5 ± 9.5 (2-21)	1 Lock	(a)
11.5 ± 8.5 (3-20)	1 Lock	(b)
11.5 ± 7.5 (4-19)	No Lock	(c)
11.5 ± 3.5 (8-15)	No Lock	(d)

TABLE 2

Behaviour of Default Model About 11.5C Annual Mean Temperature

Observe that for an annual temperature variation of less than ± 8.5 C (3-20C) no 1 lock occurs so that this particular range of variation can be considered as a minimum required to achieve 1 lock synchronisation. At what depth Z_{crit} below the ground surface does this critical minimum annual variation occur?

From section (1.3) I recall that temperature variation below ground is dependent on the thermal diffusivity β of the soil in question. If this parameter is assumed constant and the value is known for a particular soil type then by inspection of equation (1.5) $T_{1\text{Mim}} = T_1 e^{-\alpha Z_{\text{crit}}}$ so that

$$Z_{crit} = -\frac{1}{\alpha} Ln \left[\frac{T_{1Min}}{T_{1}} \right]$$
 (1.18)

where T_{1Min} is the minimum annual amplitude of variation required for a 1 Lock to occur. From Table 2 $T_{1Min} = 8.5C$ [8.5 = (20-3)/2] (note that the mean temperature value at any depth below ground always remains equal to the mean surface temperature (van Wijk and de Vries 1963)).

Table 3 shows the calculated critical soil depth $Z_{\rm crit}$ obtained from equation (1.18) for constant $k_{\rm S}$, for various soil types. I observe that damping to within the minimum annual temperature range of 3 - 20C (required for a 1 Lock) is impossible until a depth of at least 12cm below the surface is reached (in peat soil). With the proviso that *Catops* remains within the uppermost ground layers, this suggests that an annual air temperature variation of 2 - 21 C would only just be adequate to produce subterranean *Catops* synchronisation. A subterranean life would also ensure a more stable abiotic environment because the *daily* variation in temperature would be greatly reduced. Such daily variations are subject to a much greater percentage reduction than annual variations even at very shallow soil depths (van Wijk and de Vries 1963). The

reduction in daily environmental 'stress' that results from venturing downwards could possibly explain the observed preference for deeper soil layers during diapause.

SOIL TYPE	*Thermal Diffusivity β (cm ² s ⁻¹)	$\dagger \alpha = \sqrt{\frac{\pi}{P\beta}}$	Critical Soil Depth Z _{Crit} (cm)
Clay Soil - Dry	0.0018	0.0074	15
-Wet	0.005	0.0045	25
Sandy Soil - Dry	0.0024	0.0064	17
-Wet	0.0074	0.0036	30
Peat Soil (~ Same, Dry or Wet)	0.001	0.0095	12

^{*} from van Wijk and de Vries (1963). † where P is the period of oscillation taken to be 1 year here.

TABLE 3

Critical Soil Depth Z_{crit} at which annual surface temperature variation of 2-21C is damped to 3-20C. Thermal conductivity $k_{\rm S}$, assumed constant for each soil type.

Structural Stability

How does the range of annual temperature affect synchronisation behaviour as the mean annual temperature is varied? Fixing the annual mean temperature at a variety of values, I performed simulations to find the minimum range of annual temperature variation required for 1 lock synchronisation to occur. The results of simulation studies are shown in Table 4.

I observe from these that as the annual mean temperature increases, the required range of variation about that mean to achieve 1 lock synchronisation also increases. Interestingly, this property runs counter to the earth's climatic temperature trend as degrees of latitude are decreased. It could hint at the potential existence of an associated minimum latitude, below which no 1 lock syncronisation for this species is possible. Alternatively Catops may have evolved a mechanism to compensate for the effects of different latitudes (e.g Conover & Present 1990)

Simulations were also performed using different but equally plausible L3 stage and Immature Adult developmental responses. Results demonstrate that the pronounced quiescence effect of photoperiod on the L3 stage (relative to the other pre-adult stages) only slightly affects the synchronisation behaviour of the model.

(a) I first investigated the effect of *relative* displacment between T(t) and P(t) on synchronisation behaviour.

Variant 1

Temperature was *not* shifted relative to photophase. Hence Tmin and Tmax were made to occur at the end of December and mid-June respectively.

Variant 2

Photoperiod was *also* shifted by one month. Hence (unnaturally) Pmin and Pmax as well as Tmin and Tmax were made to occur at the end of January and mid-July.

Neither of the above variations made any difference to simulation results.

(b) Secondly, I investigated the potential significance of the photoperiod-compensatory mechanism in the L3 stage and the temperature-compensatory mechanism in the Immature Adult.

Variant 3

The L3 stage development rate was defined solely as a function of temperature (independent of photophase) at either SD or LD rates respectively. Results at SD rates were the same as those with the Default Model but no 1 lock occurred at 2-21C annual temperature variation when the L3 stage development rate was parameterised with LD values.

Variant 4

Some other temperature-compensated responses were incorporated in the Immature Adult development for temperatures outside the interpolation range of $10C \le T \le 15C$.

Response 1.

For $T \le 10C$ NO ceiling was imposed

For $T \ge 15C$ a floor was imposed.

Response 2.

For $T \le 10C$ a 'rebound' occurred at 10C 'off' of the 10C ceiling. The rebound 'hits' the 15C floor when T = 5C and continues to 'sink' for T < 5C nearly reaching a 0 diapause rate at T=0C. (NB: not defined for T < 0C.)

For $T \ge 15C$ a floor was imposed.

Neither of these alterations in development response made any difference to simulation results.

Thus it turns out that only an alteration to L3 stage developmental response (Variant 3) had any noticeable effect on the synchronisation behaviour of the Default Model.

ANNUAL MEAN	REQUIRED ANNUAL	VARIATION	
TEMP (C)	TEMP VARIATION	ABOUT ANNUAL	
	(C)	MEAN (C)	
14	2-26	± 12	
13	3-23	± 10	
12	3-21	± 9	
11.5	3-20	± 8.5	
11	3-19	± 8	
10	3-17	± 7	
9	3-15	± 6	
8	3-13	± 5	

TABLE 4
Minimum Annual Temperature Variation required for 1 Lock synchronisation to occur in the *Catops* Default Model for decreasing annual mean temperatures (to nearest C).

Preliminary Conclusions

The intricacies modelled in terms of the choice of possible *Catops* developmental responses for the L3 and Immature Adult stages had only a marginal effect on synchronisation behaviour. This was clearly seen in terms of the consistency of simulation outcomes for a selection of different diapause responses incorporated within the Immature Adult stage. In fact, provided that the *duration* of diapause was at least 183 days, synchronisation to a univoltine life cycle still occurred even when diapause development rate was simply held constant. From this, I infer that the main synchronising influence produced by diapause (and also of the L3 stage quiescence) takes effect by prolonging the total life cycle duration. The acute sparsity of data quantifying the precise effects of photoperiod on the development of the two photosensitive stages therefore turns out to be largely inconsequential.

1.4 A TWO STAGE MODEL

The first five (pre-adult) developmental stages of the Default Model follow a similar seasonal development pattern which is reflected by the single solitary peak shape of all the graphs shown in Diagram 1.3 ((a) and (b)). I carried out a simple reparameterisation to obtain the average seasonal development rate taken over all these stages and thus collapse them into a single 'pseudo' pre-adult developmental stage. The most different Immature Adult stage was kept unchanged. Thus, I constructed a two stage model composed of a single stage with the same Gaussian seasonal form as any original pre-adult stage and a second Immature Adult stage as defined in the Default Model.

Diagram 1.9 shows the graphs of the seasonal development rates of both these stages. (The graph of the pre-adult stage achieves a much lower altitude than any of the original pre-adult stages because all of these stages were calibrated to achieve a development index of 1 before moving on to the next stage.) Extensive simulation studies with the two stage model demonstrated that all the quantitative and qualitative dynamics of the Default Model were preserved.

Table 5 compares the synchronised times-of-year for oviposition or eclosion and time duration for diapause. Results between the default and two stage models were virtually indistinguishable.

	Date of oviposition	Date of eclosion	Diapause duration
Real Life Average	6th May	11th October	158 days
(Per Topp 1990)			
Default Model	25th April	1st November	190 days
Two Stage Model	22nd April	30th October	191 days

TABLE 5

Comparison of synchronised times of key Catops life-cycle events with those of results from simulations at 2-21C

Diagram 1.10 confirms by comparison of Line Plot diagrams, that the synchronisation behaviour of each model is identical.

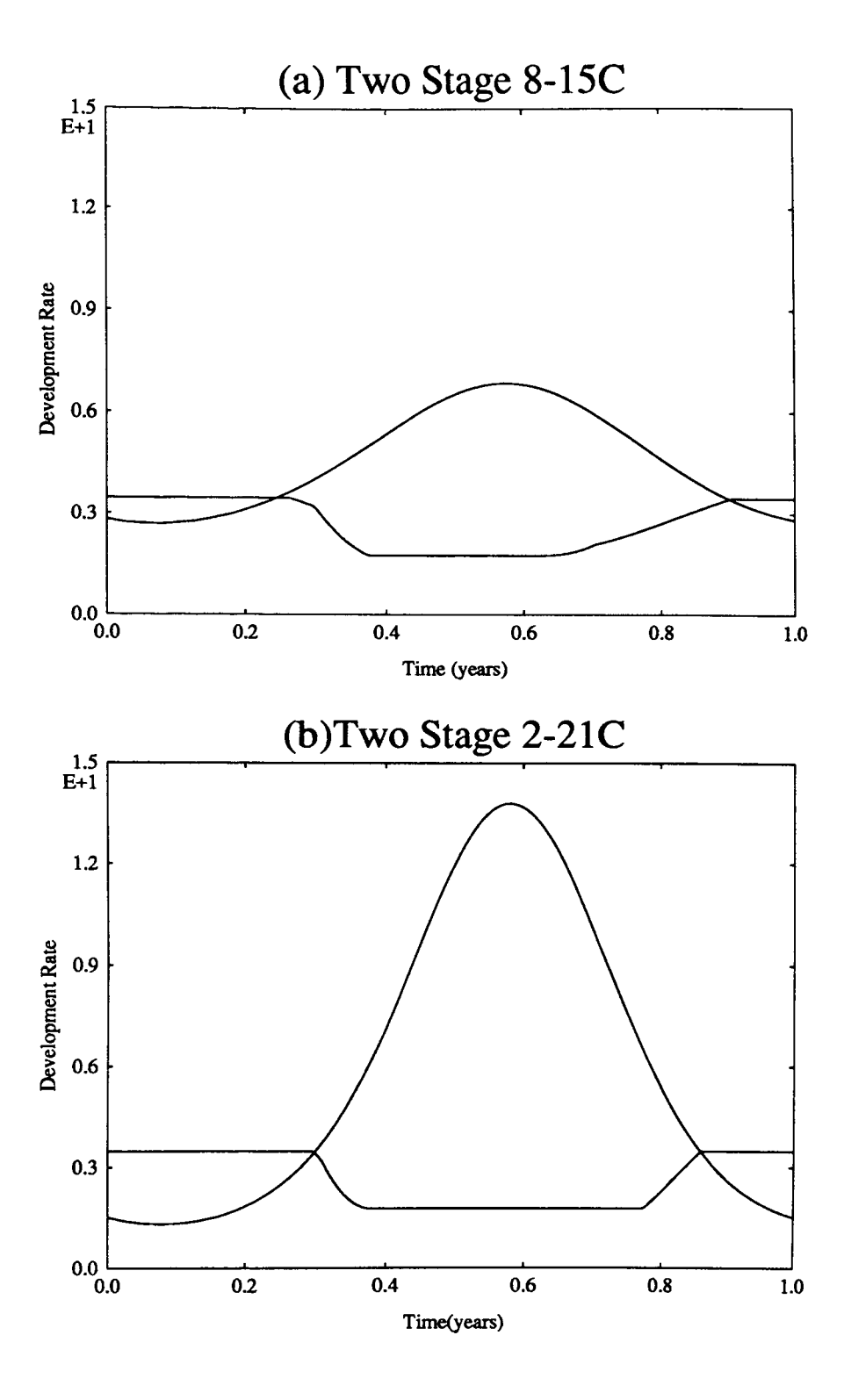


DIAGRAM 1.9 Development rates of the pre-adult and immature adult stages of the two stage model at (a) 8-15C (b) 2-21C.

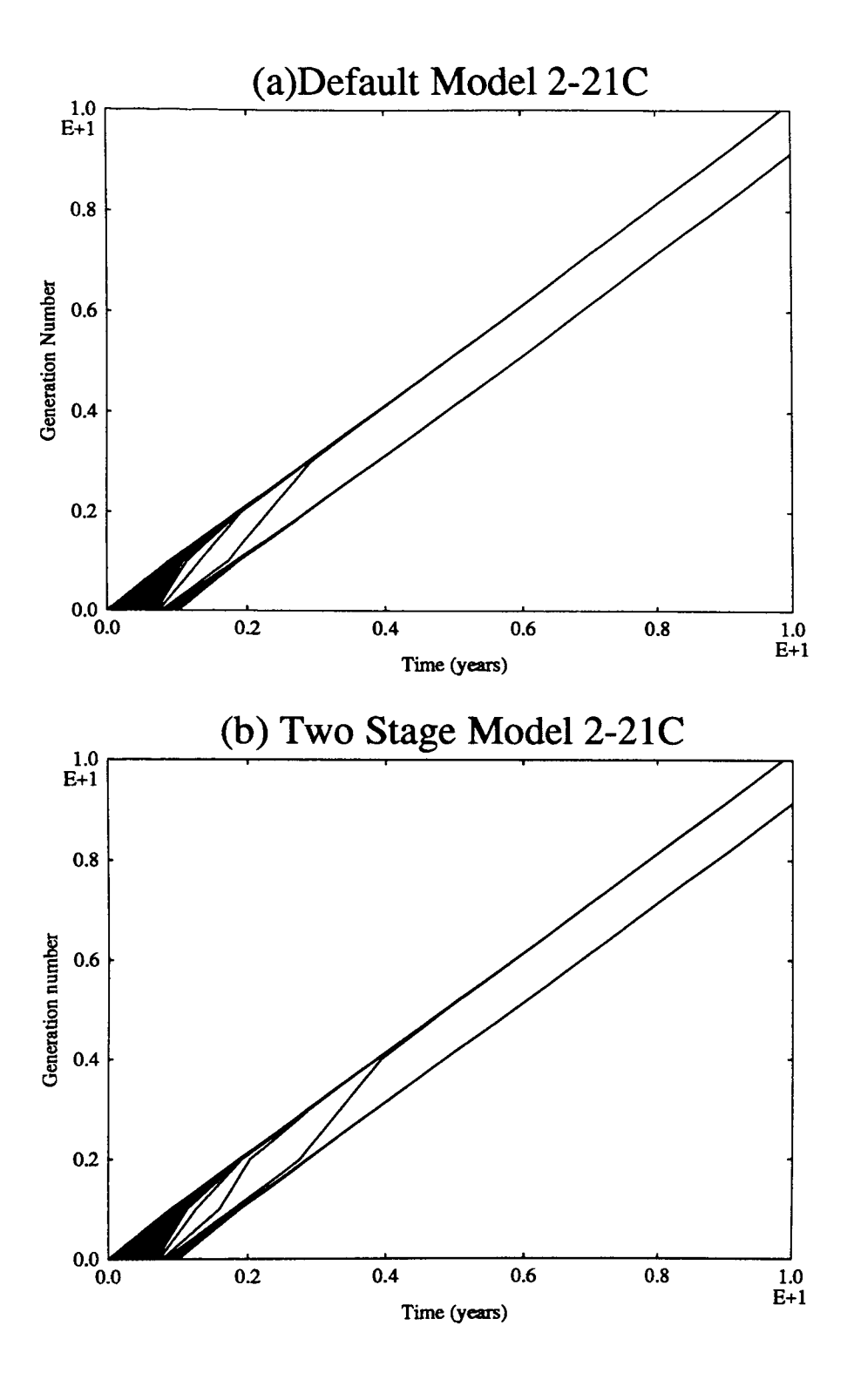


DIAGRAM 1.10 Comparison of simulation results with annual temperature variation of 2-21C (a) Default Model (b) Two Stage Model

1.5 DISCUSSION

The Default Model synchronises to a univoltine life cycle as an autumnal breeder for an annual temperature variation of 2-21C in the same way as *Catops* does in the Koln locality. Although this fact is singularly impressive and still holds even when a modest subterrranean existence is allowed for, it becomes less so in the light of how easily it fails to happen. When annual temperature variation narrows by any more than ± 1 C, no synchronisation occurs (Table 2, and Diagram 1.8).

The overall sparsity of data, in any event, automatically ensures that sweeping inferences about *Catops per se* are not sensibly possible. This is particularly true in respect of stage specific threshold temperature values that were laboratory-measured in constant conditions. The ability of an individual in a given stage to survive a life-threatening temperature depends not only on the temperature value but also on the length of time that it has to be endured (Precht et al 1973). It is well known that insects can survive both higher and lower lethal temperatures under a variable temperature regime than under constant temperatures (Headlee 1914, Messenger & Flitters 1959). Indeed, Watt (1968) has suggested five major factors that influence mortality at extreme temperatures:

- (1) the lethal temperature
- (2) temperature prior to exposure
- (3) length of exposure to the non-lethal temperature
- (4) length of exposure to the lethal temperature
- (5) time taken to change from non-lethal to lethal temperature

Since life-threatening temperatures do not occur to *Catops* until the range 5-15C is exceeded (per Topp's data), I reasonably infer that for an annual surface temperature variation of 2-21C such temperatures will (if at all) be encountered only for very short durations. In the *Catops* model, I therefore reasonably make the assumption that they are not lethal and that death does not occur.

The model also demonstrates that early convergence of lineages does not necessarily imply ultimate life cycle synchronisation, since divergence of lineages may still occur before the former is achieved. Hence a preliminary overview of data which indicates that times of adult oviposition (or emergence) converge together over one generation cannot justifiably allow a leap to the conclusion made by some authors (Topp 1990,

Tasch and Topp 1991) that synchronisation *must* occur. Lineages must be projected forward over several generations before the long term synchronisation behaviour can be inferred from any data set.

In summary, two central key points emerge from this empirical case study. Firstly, the *Catops* Default Model establishes that a purely stage specific developmental response within a periodically varying environment does indeed provide a mechanism by which life cycle synchronisation can occur. Secondly, the case study shows that the seasonal pattern of development (shape of the graph) of separate developmental stages is important in the sense that synchronisation behaviour is dependent on *how* different these actually are. The two stage model demonstrated (by way of alterations to the amplitude of periodic variation) that the more pronounced this difference is, the stronger the synchronising effect. Simultaneously, this parameter-sparse version of *Catops* pleasingly established that the qualitative dynamic behaviour of the Default Model could still be retained within a minimal two stage representation simply by collapsing all of the (similar) pre-adult stages into one, whilst keeping the (most different) Immature Adult stage unaltered.

In the next chapter, I shall show that a one stage model cannot synchronise to any external periodic variation. Prompted by the encouraging results of the reparameterised two stage *Catops* model, I now have reasonable grounds to commence a trail of investigation into the simplest (minimal) stage specific life cycle model that can synchronise, namely that consisting of only two stages.

CHAPTER 2 PHYSIOLOGICAL TIME

2.0 INTRODUCTION

Before proceeding further, I first ask whether a more translucent way of analysing synchronisation behaviour is possible. The question arises, because of the rapidity with which calculations performed in real time descend into intractability. This intractableness stems from the dependence of stage duration on the real time at which recruitment to the stage occurs. Stage duration, other than where it is equal to an integer multiple of the environmental repeat cycle, is generally not a fixed quantity, but rather has an upper and lower bound which differ increasingly as the periodic environmental variation becomes more extreme. A corollary to this, is that equal periods of real time do not generally produce equal increments in development. This simple fact is a major source of extraneous complications in any analysis conducted in real time.

It turns out that many of the analytic unpleasantries can be alleviated by characterizing development status by reference to *physiological* age. Such a paradigm shift of emphasis is well established in insect studies, where the point reached on the road to complete development is frequently more important than the (real) time taken to get there (Hughes 1970, Stinner et al 1974, Logan et al 1976, Berry et al 1977). Thus, the fact that all members of a cohort have attained a given physical attribute (for example are all able to bite) is biologically more pertinent than the fact that they are all the same (real time) age but have not (Hughes 1970, Kunz et al 1976, Berry et al 1977, Palmer et al 1981, Moon 1983, Huryn & Wallace 1986, Vogt et al 1990). Provided that times in either measure are interchangeable, I can choose to perform analyses in physiological time that are directly interpretable in real time. In this way, I shall by-pass much of the otherwise more protracted analytic tedium.

In this chapter, I focus on how a *physiological time* scale can be set up in the context of a single stage, as a preliminary to dealing with the multi-stage situation. The new scale is derived directly in terms of the proportion of development required to traverse each developmental stage. Since I am primarily concerned with the timing of events within the repeat cycle, I slightly modify the scale to define a relative physiological time, referred to as *phase*. Immediately, I gather the reward of a simple *circle map* relationship between the points of recruitment to and promotion from the stage. The approach serves as a foundation for the two-stage situation and shall be extended in Chapter 4.

I briefly consider the simple situation where the entire life cycle model consists of only one stage. That such a model cannot synchronise to a periodic environment is easily proven and instructively demonstrates the benefit of conducting analyses in the physiological time scale.

2.1 SIMPLIFYING THE ANALYSIS: PHYSIOLOGICAL TIME

I consider the progress of an organism through a single life history stage in which the (strictly positive) development rate g is dependent only on time. To represent the underlying regularity to which synchronisation may be possible (that is seasonal or daily cycle) I regard g(x) as strictly periodic with period T.

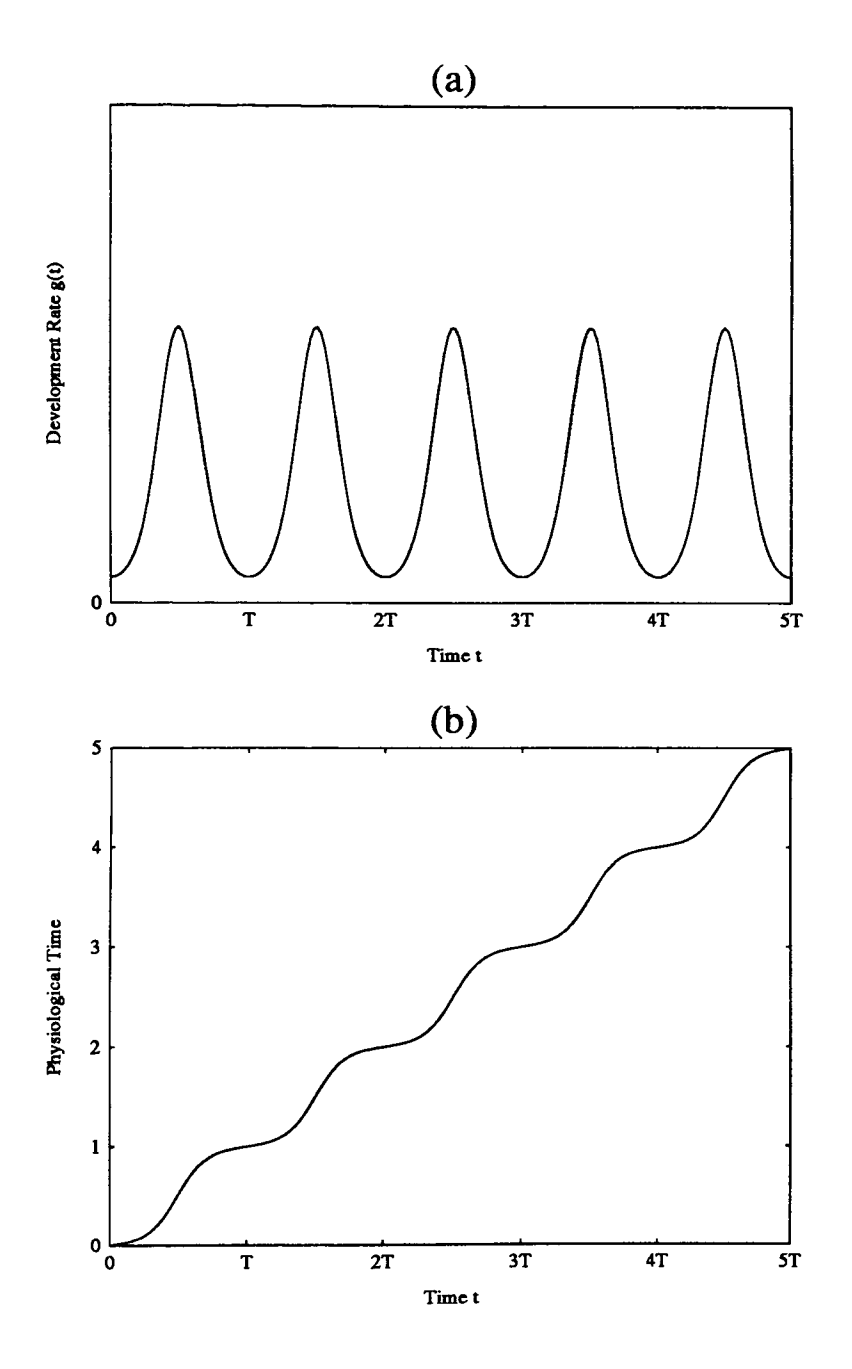


DIAGRAM 2.1 Typical Graphs. (a) Development Rate g(t) (b) respective Physiological Time $\varphi(t)$

Diagram 2.1(a) shows the graph of a typical development response, in which the development rate peaks at the midpoint of the environmental repeat cycle. The key to simplification is to set up a new scale in which stage duration is measured in terms of physiological development rather than real time. Such an approach is akin to the method of thermal summation (section 0.4) in the sense that developmental progress is measured directly in terms of the achievement of a fixed goal quantity of some appropriate measure (previously a number of degree-days). Indeed, I must still make the same underlying biological assumptions, namely that development is quantifiable in the first place and that it acts cumulatively with the passage of time. With all of this in mind, I carefully define a cumulative development function

$$C(t) = \int_{0}^{t} g(x)dx$$
 (2.1)

C(T) is then the total development, measured in terms of the appropriate development index, achieveable during a single environmental repeat cycle. I define a dimensionless new measure $\phi(t)$ which I shall henceforth refer to as *physiological time* (itself a function of time) by

$$\phi(t) = \frac{C(t)}{C(T)} \tag{2.2}$$

so that $\phi(t)$ is the total stage development achieved by time t as a fraction of C(T). Observe that since the development rate is strictly positive, $\phi(t)$ must be a monotonically increasing function. Because of the normalisation by C(T), the physiological time scale conveniently achieves integer values at the turn of every repeat cycle. Diagram 2.1(b) shows the respective graph of $\phi(t)$ for the periodic development rate shown in Diagram 2.1(a). We shall see in the next Chapter that physiological time is in fact the *lift* of phase (Definition 3.12).

Physiological time satisfies the quest for a new scale in which equal intervals within the scale produce equal increments in development. I show this easily. Let γ be a fixed 'period' of physiological time. Then

$$\gamma = \phi(t_2) - \phi(t_1) \text{ for a pair of real times } t_1, t_2 \text{ with } t_2 > t_1,$$

$$= \frac{1}{C(T)} \left(\int_0^{t_2} g(x) dx - \int_0^{t_1} g(x) dx \right) = \frac{1}{C(T)} \int_{t_1}^{t_2} g(x) dx$$

$$\therefore \int_{t_1}^{t_2} g(x) dx = \gamma C(T)$$
 (2.3)

Equation (2.3) tells us that the development increment occurring in physiological time interval γ is dependent only on γ and T. Since both of these are fixed, it follows that

equal 'periods' of physiological time produce equal increments in development

which, paradoxically, implies that the development rate of a stage expressed in terms of its own physiological time is always constant.

2.2 INCORPORATING PHYSIOLOGICAL TIME INTO A CIRCLE MAP DESCRIPTION

I am principally interested in the positioning of key events within the repeat-cycle so I shall naturally define a relative physiological time θ , hereafter known as *phase* (Gurney et al 1992), by

$$\theta(t) \equiv \phi(t)^* \equiv \phi(t) \bmod 1 \tag{2.4}$$

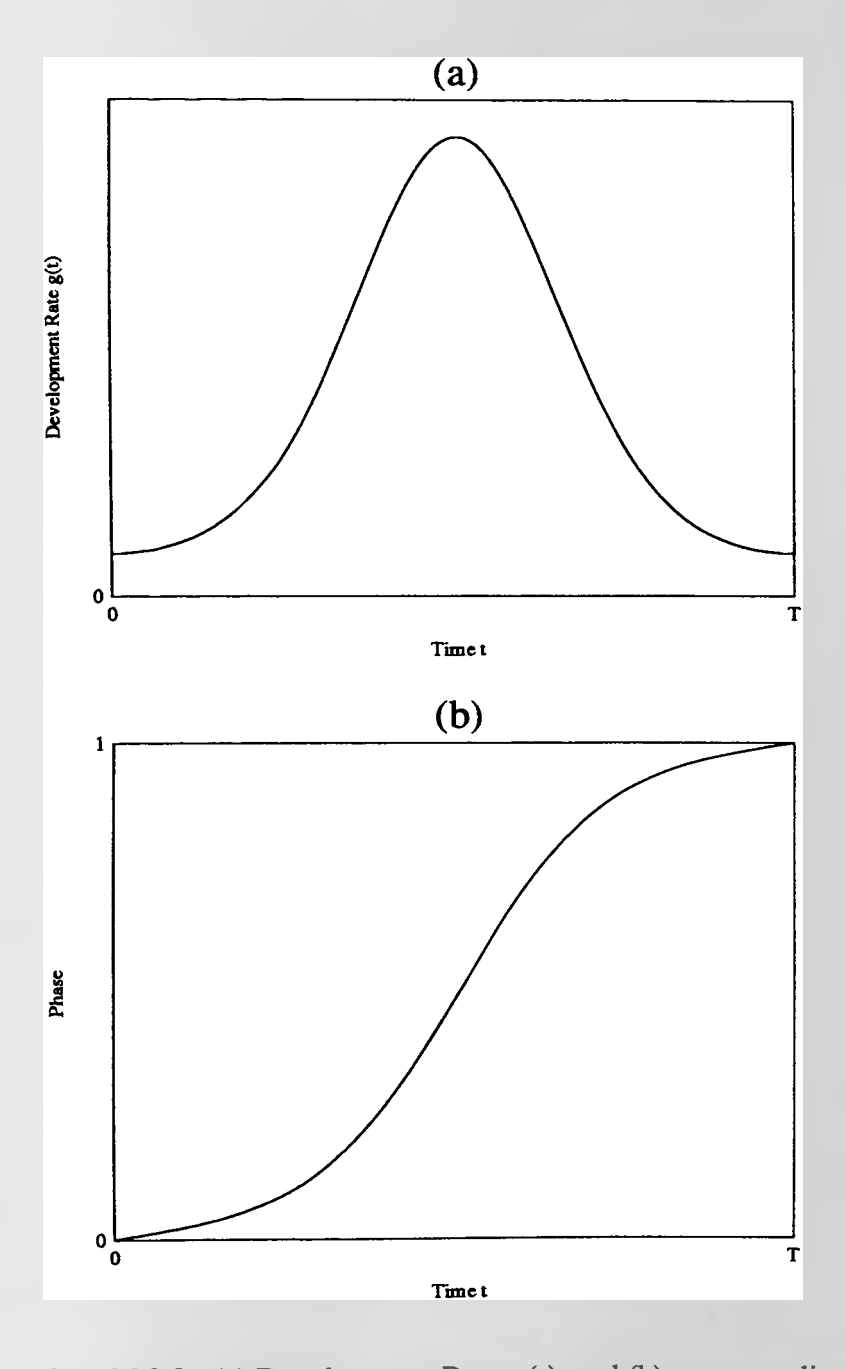
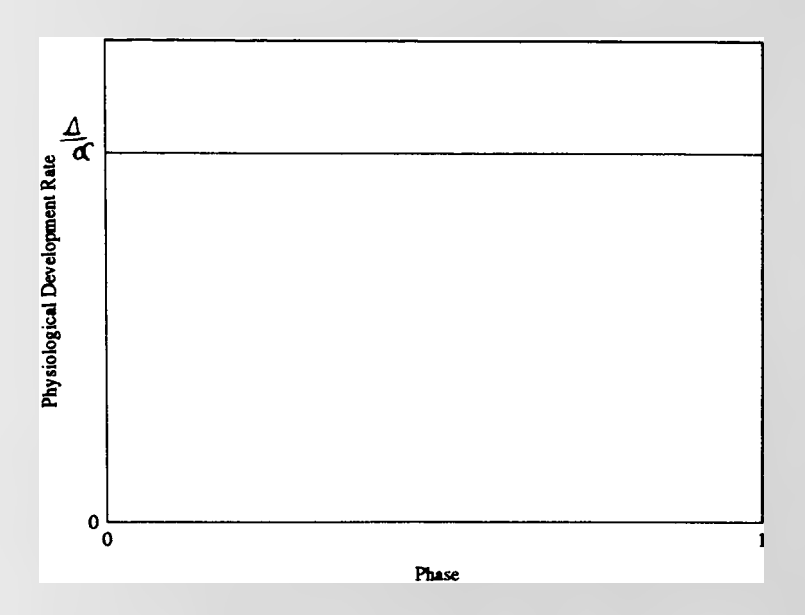


DIAGRAM 2.2 (a) Development Rate g(t) and (b) corresponding plot of Phase $\theta(t)$

Since equal intervals of physiological time represent equal development increments, the passage of an individual through the developmental stage can now be described very compactly in terms of phase. If the total development required to transit the stage is Δ and t_r , t_p are the real times of recruitment and promotion respectively, then the stage physiological time required is given by

$$\alpha \equiv \phi(t_p) - \phi(t_r) = \frac{1}{C(T)} \left[C(t_p) - C(t_r) \right] = \frac{\Delta}{C(T)}$$
 (2.5)

Development on the physiological or phase time scale therefore always occurs at the constant rate $\Delta / \alpha = C(T)$



Continuing with this powerful theme, I define an operator

$$R_{\alpha}(x) \equiv (x+\alpha)^* \equiv (x+\alpha) \mod 1 \tag{2.6}$$

and observe that an individual recruited to the stage at phase θ_n must complete its passage through the stage at phase θ_{n+1} given by

$$\theta_{n+1} = R_{\alpha}(\theta_n) \tag{2.7}$$

Equation (2.7) defines one of the simplest examples of a *circle map* relationship (Chillingworth 1976). Any circle map can be thought of as a map between points on

the circumference of a circle. However, I can still construct a Euclidean' plot of R_{α} in the plane and find that this simply consists of two straight 45° lines displaced from the leading 45° diagonal as shown in Diagram 2.3.

Although frequently useful, such a plot fails to convey the true topology of a circle map, in the same way that a world map is unable to display the true curved nature of the globe. Thus, no discontinuity occurs where the plot moves 'beyond' an edge of the unit square to 'reappear' on the opposite side. This is nicely exemplified by the plot of R_{α} in which the two 'separate' lines are not disconnected, but really form part of the same single continuous entity.

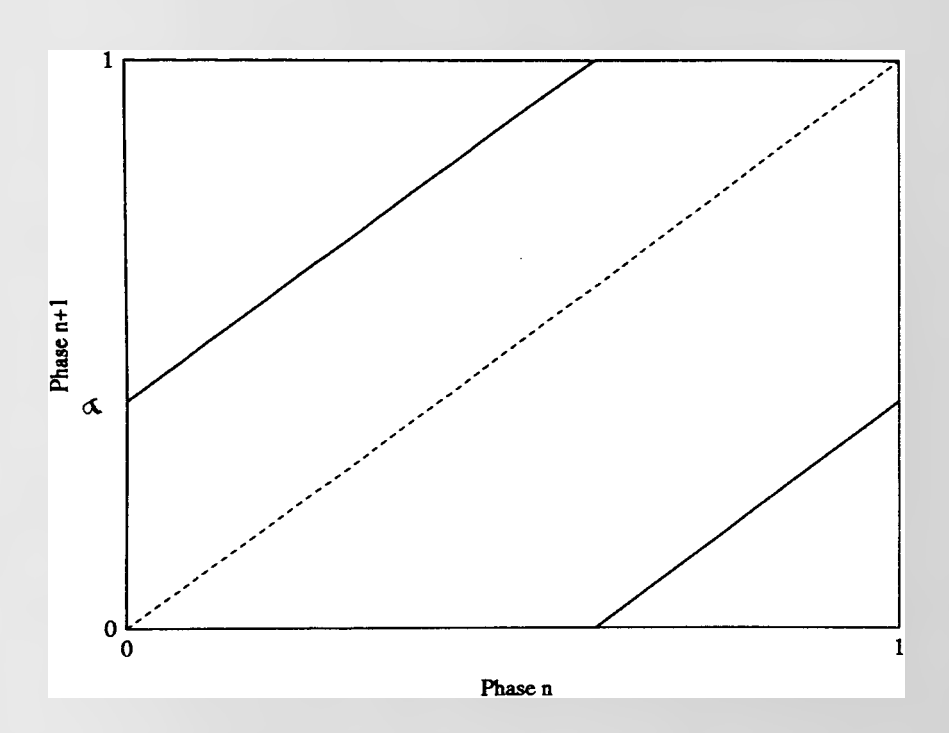


DIAGRAM 2.3 (Euclidean) Plot of the circle map $\theta_{n+1} = R_{\alpha}(\theta_n)$

2.3 THE ONE STAGE LIFE CYCLE

Consider a life cycle that is made up of only one stage. Assume that emergence followed by recruitment to successive generations occurs immediately, at the same point in the environmental repeat cycle (as where the newly emerging individual or its progeny immediately re-enter). Repeated iteration of the circle map R_{α} in equation (2.7) then corresponds to a one stage life cycle model of these successive emergences. Traditionally, the effect of such iterations is shown in the plot by a path which spiderly 'cobwebs' along inbetween touching the plot and the leading 45° diagonal (e.g Bak 1986).

I prefer to think of this iterative effect in its true non-Euclidean context. Each iteration of the map R_{α} has the simple effect of rotating all points in the circle by an angular displacement of α about its centre and is thus referred to as a 'pure' rotation. Realising this, I can easily prove the observation of Gurney et al (1992) that for a life cycle consisting of a single developmental stage driven by a single environmental forcing function, no synchronisation to that function is possible.

If α is irrational then $m\alpha$ cannot be an integer for any integer m, so that for any phase θ

$$R_{\alpha}^{m}(\theta) = (\theta + m\alpha) \mod 1 \neq \theta \tag{2.8}$$

which immediately proves that no synchronisation is possible. In fact, it turns out that in this case lineages (orbits) are 'space-filling' or 'dense' (Arnold 1973) so that all values of phase will be approached arbritrarily close by repeated iteration of any initial phase.

Alternatively, if α is rational I can write that $\alpha=p/q$ for some relatively prime integers p,q and so

$$R_{\alpha}^{q}(\theta) = (\theta + p) \mod 1 = \theta \tag{2.9}$$

so that any starting phase will repeatedly visit itself after every q iterations (the orbit of any phase is therefore a q-cycle). However, since all points on the circumference of the circle are rotated uniformly, no contraction takes place over any segment (arc) which in turn implies that no stable phase attractor exists to which lineages stemming

from a variety of initial phases might converge. Hence in this case no synchronisation is possible either. This completes the proof.

Gurney et al (1992) also showed that the above result can be extended to a model composed of any number of contiguous life-history stages provided that each stage exhibits the same development response to the environmental forcing function. Intuitively, this powerful result is unsurprising because in such a situation each stage merely acts to produce a single fixed displacement in physiological time. Passage through the entire life cycle can therefore only produce a similar fixed displacement (consisting of the sum of all the separate stage displacements) in an analagous manner to the single stage model. Thus, the synchronisation of such a multi-stage life cycle to the environmental repeat cycle is impossible.

This is easily proved more formally by induction. Suppose the organism has a total of Z stages in the life history each with a corresponding stage specific physiological duration of α_i , for j = 1 to Z. For ease of notation I shall denote

$$S_{z} \equiv \sum_{i=1}^{z} \alpha_{i}$$
 (2.10)

I must show that if the life cycle is commenced at phase θ_n then it is completed at phase θ_{n+Z} where

$$\theta_{n+Z} = R_{sz}(\theta_n) \tag{2.11}$$

If equation (2.11) is true for some k (< Z), that is

$$\theta_{n+k} = R_{s_k}(\theta_n) \tag{2.12}$$

then

$$\begin{aligned} \theta_{(n+k)+1} &= R_{\alpha_{k+1}}(\theta_{n+k}) \\ &= R_{\alpha_{k+1}} \left(R_{S_k}(\theta_n) \right) \\ &= R_{(\alpha_{k+1}+S_k)}(\theta_n) \\ &= R_{S_{k+1}}(\theta_n) \end{aligned}$$

so that equation (2.11) is also true for k+1 thereby completing the inductive step. Clearly, equation (2.12) holds for k=1 therefore equation (2.11) is true for all k=1 to Z and the proof is completed.

Because of the inherent periodicity imposed by the environmental forcing function, the *circle map* representation of the chosen phase formulation between recruitment and promotion is a natural one. I shall now take a whole chapter interlude to expand upon this and other central concepts from dynamical systems theory. In Chapter 4 I shall return to the physiological time description and extend the current formulation to encompass a general two stage model.

CHAPTER 3 CIRCLE MAPS

3.0 INTRODUCTION

I am led to investigate the dynamics that result from a system governed by the first order difference equation

$$\mathbf{x}_{i+1} = \mathbf{f}(\mathbf{x}_i) \ \mathbf{i} \in \mathbf{Z} \text{ or } \mathbf{N} \tag{3.1}$$

where f is a map between successive states x_i, x_{i+1} which take values in some state or phase space. There is much theory on such a one dimensional dynamical system (Collet & Eckman 1980, Preston 1983, de Melo & van Strien 1992) and in particular for when the state space is a topological space (Dugundji 1965).

Fortunately, many interesting situations can be modelled when the arena for dynamics takes the form of some human envisageable structure such as the surface of a sphere (S^2) , torus, or indeed circumference of a circle (S^1) (Bak 1986, Parker & Chua 1987, Schaffer 1988, Courtemanche et al 1989, Gurney et al 1992, 1994). All of these particular topological spaces are examples of differentiable manifolds (Matsushima 1972, Arrowsmith & Place 1990). Because of the cyclic nature of the phenomena being modelled, I shall mainly focus on the situation in which the state space setting is S^1 . In this case, the map f is referred to as a *circle map*.

Clearly, the general theory of maps on a differentiable manifold must also apply to the more specialised scenario of a circle map. I must introduce some concepts taken from the broader theory before moving on to the more special situation of the circle map scenario. The single most important concept is that of topological conjugacy. If two maps are topologically conjugate then the number and character of any attractors the two maps may possess must be the same and hence all the qualitative features of their orbits (in particular the existence and repeat lengths of stable cycles) must also be the same.

Much of this chapter will form the subtext of discussion for later chapters. I begin by introducing some basic definitions.

3.1 BASIC DEFINITIONS

Let X and Y be sets.

Definition 3.0

A map f is a correspondence that associates to each element $x \in X$ an element $f(x) \in Y$.

Definition 3.1

f is a one-to-one map from X into Y iff for any two distinct elements $x, y \in X$, $f(x) \neq f(y)$, that is f(x) and f(y) are also distinct.

Definition 3.2

f is an onto map from X onto Y iff $\forall y \in Y, \exists x \in X \text{ such that } f(x) = y$

A one-to-one and onto map is often referred to as a bijection.

Now let X and Y be topological spaces that is sets for which topologies are defined (Dugundji 1965).

Definition 3.3

f is a homeomorphism from X onto Y iff

- 1. f is a one-to-one and onto map from X to Y and
- 2. f and f^{-1} are both continuous $[f^{-1}]$ is the map from Y to X defined by $f^{-1}(y) = x$ if y = f(x)

Differentiable Manifold

A diffferentiable manifold is the natural setting for dynamics (Arrowsmith & Place 1990). Roughly speaking, a differentiable manifold M is a topological space which has the extra property that every point x has a neighbourhood for which it is possible to define a differentiable function between any two sets of points in the neighbourhood. A precise definition can be found in Matsushima (1972). The most important property of differentiable manifolds is that such spaces always have local euclidean properties, which implies that the concept of differentiability can be meaningfully extended to any global function defined on the whole manifold M.

A particularly well-behaved map that can be defined between two differentiable manifolds is a diffeomorphism.

Definition 3.4

Let M and N be differentiable manifolds. f is a diffeomorphism from M onto N iff

- 1. f is a one-to-one and onto map from M to N and
- 2. f and f⁻¹ are both differentiable at all points of M and N respectively.

Diffeomorphisms are logically classified according to the number of times n that they are differentiable and referred to as being of type C^n . Thus, a homeomorphism is a C^0 -diffeomorphism. In general the resulting iterative dynamics become increasingly well-behaved as $n \rightarrow \infty$ (Smale 1967).

3.2 ITERATIVE DYNAMICS

Although the iteration of maps has a long history going back as far as the Babylonians and Ancient Greeks when calculating calendric cycles (Neugebauer 1969,1975, Fowler 1990) a more deeper understanding of the dynamics that they lead to only began with Poincare last century (de Melo & van Strien 1992). Today the general theory of the dynamics that result from iterating one dimensional maps is well developed (Arnold 1988, Smale 1965, 1967, Collet & Eckman 1980, Preston 1983, de Melo & van Strien 1992). Although such dynamics can be extremely complicated, they can be described completely in a topological sense (de Melo & van Strien 1992, Akin 1993). There are two main aspects which we should always like to enquire about when iterating any map.

Topological aspect. What are the attractors, which maps are dynamically equivalent, and which are structurally stable?

Ergodic aspect. What is the 'dynamic behaviour' of the sequence of iterates?

Henceforth I shall focus soley on the differentiable manifold setting even though some of the subsequent definitions can also be adequately defined for other spaces. I immediately clarify a frequent source of confusion that occurs in the use of the word 'iterate' within the language of dynamical systems. An iterate of f is a map f^n , $n \in N$ in its own right defined by f^0 = identity map, $f^1 = f$, $f^n = f(f^{n-1}) = f'$ n times', whereas an iterate of a point $x \in M$ is the point given by $f^n(x)$. Further, if f is invertible as when a homeomorphism, then I can define the map $f^{-n} \equiv (f^{-1})^n$, $n \in N$ because in this case $f^n(f^{-1})^n = f^0$. If f is non-invertible the best that can be done is to define f^{-n} such that $f^{-n}(y) = \{x: f^n(x) = y\}$, $n \in N$.

The set of iterates of a point $x \in M$ under f form a sequence which I shall henceforth term an orbit.

Definition 3.5
An orbit
$$O_f(x)$$
 of a point $x \in M$ is defined as the set $O_f(x) \equiv \{f^n(x): n \in Z\}$

Thus, $O_f(x)$ consists of the sequence of distinct points generated from x by successive iterations of f. I also choose to name some special points.

Definition 3.6
A point
$$x^* \in M$$
 is a fixed point of f iff $f^m(x^*) = x^* \forall m \in Z$

Definition 3.7

A point $x \in M$ is a periodic point of f iff $f^q(x^*) = x^*$ for some integer q > 1

The least value of q which satisfies this definition is referred to as the *period* of x^* . A fixed point is therefore a periodic point with a period of one. It follows that a fixed point is completely unaffected by the repeated operation of f whereas a periodic point recurs every q iterations. Clearly, any periodic point x^* of f with period q is a fixed point of f^q .

q-cycle $O_f^q(x^*)$

The orbit of any periodic point x^* with period q must consist of exactly q distinct points (otherwise its period would not be q). I shall henceforth refer to such an orbit as a q-cycle $Q = O_f^q(x^*)$. In the situation where the map f is a homeomorphism, some very simple but powerful properties pertain to the orbits that arise. I demonstrate two of the most important by way of two short theorems.

Theorem 3.0

The elements of a q-cycle Q belong to no other p-cycle P where $p\neq q$ (alternatively, the members of any two cycles form disjoint sets).

Proof

Suppose for some $x_j^* \in Q$ that $x_j^* \in P$. Then $f^p(x_j^*) = x_j^*$ and clearly I need only consider p > q. But $f^q(x_j^*) = x_j^*$ and therefore $f^{(p-q)}(x_j^*) = f^{(p-q)}(f^q(x_j^*)) = x_j^*$ which contradicts the fact that x_i^* has period p [since (p-q) < p].

Theorem 3.1

Each element of a q-cycle Q is also a periodic point of f with period q.

Proof

Let
$$x_j^* = f^j(x_0^*) \in Q = O_f^q(x_0^*)$$
 for some periodic point x_0^* .
Then $f^q(x_i^*) = f^q(f^j(x_0^*)) = f^j(f^q(x_0^*)) = f^j(x_0^*) = x_j^*$.

Topological Conjugacy

How can the 'same dynamic behaviour' be defined between two maps f and g? The most natural way is to define an equivalence relation between the two maps which has the property that corresponding sequences of iterates are the same up to a coordinate change. Two such maps are then said to be *topologically conjugate*.

Definition 3.8

Two continuous maps f, g: $M \rightarrow M$ are topologically conjugate iff \exists a homeomorphism h: $M \rightarrow M$ such that hf = gh (or $g = hfh^{-1}$)

Notice that f and g are not required to be differentiable (Devaney 1986, de Melo & van Strien 1992) so that for example, they could be homeomorphisms. The map h must be a homeomorphism however, to ensure that orbits of f and g behave in a similar manner. Thus $\mathbf{x}_{n+1} = \mathbf{f}(\mathbf{x}_n)$ and $\mathbf{y}_{n+1} = \mathbf{g}(\mathbf{y}_n)$ are then identical up to a coordinate change so that $\mathbf{hf}^n(\mathbf{x}_n) = \mathbf{g}^n \mathbf{h}(\mathbf{x}_n)$ and h takes orbits of f into orbits of g. I prove this by induction.

Theorem 3.2

Let f, g: $M \rightarrow M$ be continuous maps and let h: $M \rightarrow M$ be a homeomorphism such that hf = gh (or $g = hfh^{-1}$). If $\{x_n\}$ is the orbit produced by the map f starting from an initial value x_0 and $\{y_n\}$ is the orbit produced by the map g starting from a related value $y_0 = h(x_0)$, then $\forall n \ge 1$ and $\forall x_0 \in M$

$$y_n = h(x_n) \tag{3.2}$$

Proof.

If it is true for some integer $k \ge 1$ and $x \in M$ that

$$g^{k}(x) = h f^{k} h^{-1}(x)$$
 (3.3)

then

$$g^{k+1}(x) = g(g^{k}(x))$$

$$= g(h f^{k} h^{-1}(x))$$

$$= h f h^{-1}(h f^{k} h^{-1}(x))$$

$$= h f^{k+1} h^{-1}(x)$$
(3.4)

By definition of g, equation (3.3) is true for k=1, so, by induction we have that equation (3.3) holds for all integer $k \ge 1$. But $y_n = g^n(y_0)$ and $y_0 = h(x_0)$, so

$$y_{n} = g^{n}(h(x_{0}))$$

$$= hf^{n}h^{-1}(h(x_{0})) \text{ by (3.4)}$$

$$= hf^{n}(x_{0})$$

$$= h(f^{n}(x_{0}))$$

$$= h(x_{n})$$
(3.5)

If I choose to relax the homeomorphic requirement that h be invertible then f and g are said to be *combinatorially equivalent*. In the case of maps f, g: $S^1 \rightarrow S^1$, combinatorial equivalence between them only ensures that each orbit of f occurs in S^1 in the same order as the corresponding orbit of g (de Melo & van Strien 1992). Whereas two maps that are combinatorially equivalent may share many dynamical properties (van Strien 1991), the stronger requirement of topological conjugacy ensures that all the qualitative features of orbits and in particular the existence and repeat lengths of stable cycles must be the same. If topological conjugacy is to be established between f and g then the map h must always be shown to be a homeomorphism.

Stability

I introduce some standard definitions to describe the ergodicity of points in the neighbourhood of any fixed or periodic points. Although other types of stability such as 'semi-stable' or 'one-sided stable' can also be defined (Devaney 1986) three types of stability in the style of Liapunov will suffice for our purposes.

Definition 3.9

A periodic point x^* is *stable* iff for every neighbourhood N of x^* \exists a neighbourhood $N' \subset N$ of x^* such that if $x \in N'$ then $f^m(x^*) \in N$ for all m > 0.

Definition 3.10

A periodic point x* is unstable iff it is not stable.

Definition 3.11

A periodic point x^* is asymptotically stable iff x^* is stable and $\lim_{m\to\infty} f^m(x) = x^*$ for all x in some neighbourhood of x^* .

Periodic points that are stable but not asymptotically so, shall henceforth be referred to as neutrally stable.

Stability of a q-cycle $O_f^q(x^*)$

When both f and f^{-1} are also differentiable at all points in M (and therefore diffeomorphisms) it turns out that $Df^k(x^*)$ takes the same value for any x^* in the q-cycle. Surprisingly, many authors quote this powerful property without proof (e.g. Collet & Eckman 1980, Sandefur 1990). I give a general proof using induction.

Theorem 3.3

 $\mathrm{Df}^{\,q}(x_j^*)$ takes the same value $\forall \ x_j^* \in \mathrm{O}_f^q(x_j^*)$

Proof

By the chain rule of differentiation

$$\begin{split} Df^{\,q}(x) &= D\Big[f\Big(f^{\,q-1}(x)\Big)\Big] = Df\Big(f^{\,q-1}(x)\Big).Df^{\,q-1}(x) = Df\Big(f^{\,q-1}(x)\Big).D\Big[f\Big(f^{\,q-2}(x)\Big)\Big] \\ &= Df\Big(f^{\,q-1}(x)\Big).Df\Big(f^{\,q-2}(x)\Big)Df^{\,q-2}(x) \\ &= \prod_{i=1}^q Df\Big(f^{\,q-i}(x)\Big) \ \ \text{with} \ \ f^{\,0}(x) = x \end{split}$$

Suppose $Df^{q}(x_{k}^{*}) = c$ for some $1 \le k \le q$. Then

$$\begin{split} Df^{q}(x_{k+1}^{*}) &= \prod_{i=1}^{q} Df \Big(f^{q-i}(x_{k+1}^{*}) \Big) = \prod_{i=1}^{q} Df \Big(f^{q-i} \Big[f(x_{k}^{*}) \Big] \Big) = \prod_{i=1}^{q} Df \Big(f^{q-i+1}(x_{k}^{*}) \Big) \\ &= \prod_{i=0}^{q-1} Df \Big(f^{q-i}(x_{k}^{*}) \Big) \\ &= \prod_{i=1}^{q} Df \Big(f^{q-i}(x_{k}^{*}) \Big) \text{ because } f^{q-0}(x_{k}^{*}) = f^{q}(x_{k}^{*}) \\ &= Df^{q}(x_{k}^{*}) = c \text{ also, completing the inductive step.} \end{split}$$

The result establishes that it is meaningful to refer to the stability of a q-cycle in terms of the stability of any individual member.

3.3 CIRCLE MAPS

I now consider the special situation in which the differentiable manifold M is the circumference of a circle S^1 . Any map $f: S^1 \to S^1$ is referred to as a *circle map*.

The setting is not to be confused with the topologically entirely different situation of a map of the interval. Whereas both settings are one-dimensional (only one variable is needed to specify the position of any point) the outcome of the iterative dynamics that result from each situation may be different.

However, a useful representation of a circle map can be made in the plane by plotting f in time honoured fashion as a function of x in the closed real interval I. Such a plot will reveal key properties such as whether f is invertible or not. If f(x) 'doubles back' producing a kink this immediately tells us that f is non-invertible and that the iterative dynamics are likely to be chaotic (non-invertibility is a necessary ingredient for chaos e.g. Baker & Gollub 1990).

Let us now assume that f is a homeomorphism. In this case, the graph of f(x) will either be monotone increasing or decreasing depending on whether f is respectively orientation-preserving or orientation-reversing. How do the interval dynamics of the graph of f(x) compare with the dynamics of the homeomorphism f? I sketch a straightforward argument to show that they will in general be different.

Consider first the graph of f(x). Let $x \in I$ and suppose first that f(x) is monotone increasing. If f(x) > x then by induction $f^{n}(x) > f^{n-1}(x)$ so that the sequence $\{f^{n}(x)\}$ is monotone increasing and must converge to some limit $y = \sup\{f^{n}(x)\}$. By the continuity of f(x),

$$f(y) = f\left(\lim_{n \to \infty} f^{n}(x)\right) = \lim_{n \to \infty} f^{n+1}(x) = y$$
(3.6)

so that $f^n(x)$ must therefore converge to a fixed point y. A parallel argument holds if f(x) < x. Thus every orbit $O_f(x)$ converges to a fixed point of f(x). Alternatively, if f(x) is monotone decreasing then $f^2(x)$ is monotone increasing. A simple modification of the above argument this time shows that either every orbit converges to a periodic point of period 2 or to a fixed point. Thus the dynamics of a monotone increasing or decreasing map of the interval are very simple.

Now consider the homeomorphism f. There are two cases possible depending on whether f has a periodic point or not.

If f has a periodic point then it turns out that all orbits must converge to a periodic point. The argument follows logically from the above by considering f^k (where k is the period) as a map $f^k(x)$ of the interval for each of the k segments of S^1 situated between periodic points. If f is orientation-preserving then so is f^k and $f^k(x)$ is monotone increasing so all orbits converge to one of the k periodic points. If f is orientation-reversing then f^2 is orientation-preserving and a slightly more subtle argument this time shows that all orbits either converge to the corresponding 2-cycle or to one of a possible two fixed points (de Melo & van Strien 1992).

If f does not have a periodic point the situation is more complicated but in all cases the resulting dynamics are combinatorially equivalent to a pure rotation of the circle by a Poincare Theorem.

A more realistic representation of f can be made by continuing the graph of f(x) beyond the unit square. Moving diagonally away from the origin, f(x) then perpetually repeats itself within each unit square situated on the leading 45° diagonal. The plot obtained is a graph of a function $\overline{f}: R \to R$ termed the *lift* of f (Devaney 1986, Arrowsmith & Place 1990).

Definition 3.12

$$\overline{f}: R \to R$$
 is a *lift* of f onto R iff \overline{f} is continuous and $(\overline{f}(x))^* = f(x^*)$

The graph of the lift \bar{f} not only enables periodic or fixed points of f to be easily identified by their location on the 45° diagonal but also serves to give a compact classic definition of the *rotation* (or *winding*) number $\rho(f)$ associated with any circle map.

Definition 3.13

Let $f \colon S^1 \to S^1$ be a homeomorphism. The rotation number $\rho(f)$ is defined by

$$\rho(f) \equiv \lim_{n \to \infty} \left(\frac{\bar{f}^n(x) - x}{n} \right)$$
 (3.7)

Observe that $\rho(f)$ is independent of x and is the single most important topological invariant that can be associated with any circle map (Devaney 1986, de Melo & van Strien 1992).

Poincare (1885) established that when $f:S^1 \to S^1$ is a homeomorphism, iterative dynamic behaviour of f is completely determined by whether $\rho(f)$ is rational or irrational. I quote two powerful theorems due to Poincare. Readable proofs are given in de Melo & van Strien (1992).

Theorem 3.4 $\rho(f)$ is rational if and only if f has periodic points.

Theorem 3.5 If $\rho(f)$ is irrational (so f has no periodic points) then f is *combinatorially* equivalent to a pure rotation R with the same rotation number.

Combined with the earlier observation that all orbits converge towards periodic points it follows from Theorem 3.4 that whenever $\rho(f)$ is rational all orbits asymptotically converge to q-cycles. I exemplify this by returning to the situation of Chapter 2 equation (2.6) where f is the pure rotation $R_{\alpha}(x) = (x + \alpha)^{*}$. The lift \overline{R}_{α} of R_{α} is then simply given by $\overline{R}_{\alpha}(x) = x + \alpha$ so that $\overline{R}_{\alpha}^{n}(x) = x + n\alpha$ and

$$\rho(R_{\alpha}) = \lim_{n \to \infty} \left(\frac{(x + n\alpha) - x}{n} \right) = \alpha$$
 (3.8)

Hence in this case the periodicity of R_{α} is directly determined by whether α is rational or irrational, a fact that we already know about from Chapter 2 (section 2.3). In general, if $\rho(f)$ is irrational there is no concise general description of the dynamics that can occur. In the special case where f is at least twice-differentiable (a C^2 -diffeomorphism) the dynamics are always topologically conjugate (by a Denjoy Theorem) to a pure rotation with irrational rotation number and thus quasi-periodic. $\rho(f)$ is frequently difficult to evaluate so that empirical methods of determining dynamic behaviour, as we shall see later, may be quicker in practice.

3.4 SOME FURTHER THEOREMS

Let $f: M \rightarrow M$ be a diffeomorphism.

Theorem 3.6

If Q is a stable (unstable) q-cycle of f then it is an unstable (stable) q-cycle of f -1

Proof.

Let $Df^{q}(x)$ denote the derivative of $f^{q}(x)$ and let $x^* \in Q$.

$$f^{q}(x^{*}) = x^{*} \iff f^{-q}(x^{*}) = f^{-q}(f^{q}(x^{*})) = x^{*} \iff (f^{-1})^{q}(x^{*}) = x^{*}$$

 $\therefore x^{*}$ a q-periodic point under $f \iff x^{*}$ a q-periodic point under f^{-1}

I use the following standard numerical analysis result

Iff
$$|Df^{q}(x^{*})| > 1$$
 then Q is stable, (3.9a)

By Theorem 3.3, $Df^{q}(x^{*})$ takes the same value $\forall x^{*} \in Q$ so that it makes sense to refer to the stability of Q in terms of the stability of a particular $x^* \in Q$.

Further, since $f^{-q}(x)$ is a reflection of $f^{q}(x)$ in the leading 45° diagonal, the gradients of $f^{q}(x)$ and $f^{q}(x)$ at x^{*} are related by their reciprocals so that

$$\left| Df^{q}(x^{*}) \right| = \frac{1}{\left| Df^{-q}(x^{*}) \right|}$$
 (3.10)

Thus

$$\begin{aligned} \left| Df^{q}(\mathbf{x}^{*}) \right| > 1 &\Leftrightarrow \left| Df^{-q}(\mathbf{x}^{*}) \right| < 1 \\ \left| Df^{q}(\mathbf{x}^{*}) \right| < 1 &\Leftrightarrow \left| Df^{-q}(\mathbf{x}^{*}) \right| > 1 \end{aligned}$$
(3.11a)

$$\left| \mathrm{Df}^{\,\mathrm{q}}(\mathbf{x}^{\,\star}) \right| < 1 \iff \left| \mathrm{Df}^{\,\mathrm{-q}}(\mathbf{x}^{\,\star}) \right| > 1 \tag{3.11b}$$

and hence by inequalities (3.9),

Q stable (unstable) under $f \Leftrightarrow K$ unstable (stable) under f^{-1} .

Theorem 3,7

Let U be the set of all cycles of f and let U' be the set of all cycles of f⁻¹. Then

$$U = U'$$

Proof.

I divide the proof into 2 parts.

(i) Let S and S' consist of the sets of all periodic points of f and f^{-1} respectively. Then

$$S = S'$$

Proof

Let $x^* \in S$ be a periodic point of f with period n. Thus

$$f^{n}(x^{*}) = x^{*} \Leftrightarrow f^{-n}(f^{n}(x^{*})) = f^{-n}(x^{*}) \Leftrightarrow x^{*} = f^{-n}(x^{*})$$
 (3.12)

so that x^* is also a periodic point of f^{-1} with period n and $x^* \in S'$.

(ii) I must still show that all cycles produced under f are the same as those produced under f^{-1} . Since by Theorem 3.0, all cycles form disjoint sets it suffices to show that:

If Q is a q-cycle of f then Q is also a q-cycle of f^{-1} .

Proof.

Since Q is a q-cycle I can write that

$$Q = \left\{ x_0^*, x_1^*, \dots, x_{q-1}^* \right\} \text{ for } q \ge 1, \tag{3.13}$$

where each x_i^* is distinct and where

$$x_{i}^{*} = f^{q}(x_{i}^{*}) \text{ and } x_{(i+1) \text{ mod } n}^{*} = f(x_{i}^{*}) \quad \forall x_{i}^{*} \in Q$$
 (3.14)

But $\forall x_i^* \in Q$,

$$f^{-q}(x_i^*) = f^{-q}(f^q(x_i^*)) = x_i^*$$
 (3.15)

and also

$$f^{-1}(\mathbf{x}_{i}^{*}) = f^{-1}(f^{q}(\mathbf{x}_{i}^{*}))$$

$$= f^{q-1}(\mathbf{x}_{i}^{*})$$

$$= f^{q-1}(f(\mathbf{x}_{(i-1) \bmod k}^{*}))$$

$$= f^{q}(\mathbf{x}_{(i-1) \bmod k}^{*})$$

$$= \mathbf{x}_{(i-1) \bmod k}^{*}$$
(3.16)
(3.17)
(3.18)
(3.19)

Hence Q is also a q-cycle of f^{-1} , which orbits in the reverse direction. This completes the proof of Theorem 3.7.

CHAPTER 4

CIRCLE MAPS ARISING FROM TWO STAGE LIFE HISTORIES

4.0 INTRODUCTION

In Chapter 2, I proved that synchronisation to a periodic environment is impossible for a life cycle composed from stages which all exhibit the same developmental response. Faced with such a breathtaking negative, I argue that the route to positive analytical enlightenment begins with the life cycle of simplest physiological structure, namely that composed from only two stages. This is the simplest stage specific scheme which can contrast different (biotic) responses to continuous (abiotic) factors. Any stage specific life cycle must be composed of a repeated sequence of this basic couplet. I conjecture that an intimate understanding of the two stage situation is a necessary and vital preliminary to an understanding of the synchronising effects produced by stage specificity. In this Chapter, equipped with the armoury of dynamical systems theory from Chapter 3, I resume the trail of investigation into the fundamental (minimal) two stage model.

Previous investigations with specialised stage specific models of odonata species have demonstrated that synchronisation of emergences can be induced in a periodic environment by incorporating seasonal dormancy mechanisms (Gurney et al 1992, 1994). Although I shall review these mechanisms, I really wish to elucidate whether a more general mechanism can produce similar results. Without these abstract models, I therefore seek to establish the existence of a general minimum requirement for synchronisation to occur.

To achieve this, I must commence from a more general set of assumptions. The Catops investigation of Chapter 1 hints that a multi-stage life cycle can be regarded in terms of an appropriate (much simpler) two stage affair. The work of Heath & Spencer (1985) makes it clear that the key element which leads to synchronisation of phytoplankton life-cycles is the existence of two distinguishable stages in the life-cycle each with a different (characteristic) response to environmental variation. In section 4.2, I formulate a very general strategic model of an organism with a two-stage life-cycle each stage having a density independent development rate with a characteristic (periodic) time-dependence. The only restriction that I shall place on the nature of these development rate functions is that both are periodic with the same repeat period.

I develop a compact representation of this model in terms of a circle map composed from two simple rotations and the "interphase map" representing the relationship between the physiological times for the two life-history stages. The interphase map

enables the phase of either stage to be obtained in terms of the phase of the other. Crucially, this implies that any point in the entire life cycle can be expressed in terms of any chosen stage phase. I arrive at a parameter sparse description which uses only two dimensionless parameters corresponding to the physiological durations of each stage, namely α and β .

For a more general n-stage life history where n > 1, the same approach can be applied repeatedly to yield (n-1) interphase maps between each of the other (n-1) stages thus permitting any stage specific life cycle to be described in terms of a single stage-phase.

4.1 SYNCHRONISATION THROUGH SPECIALISED DORMANCY

That seasonal dormancy contributes towards life cycle synchronisation is well known across a wide range of taxa for both plants (Courtney 1968, Harper 1977, Lacey 1986) and animals (Common 1954, Corbet 1957, Cohen 1967, Norling 1984a,b,c, Taylor 1980, Topp 1984,1990, Denlinger 1986, Tauber et al 1986, Gruner & Sauer 1988, Wipking 1988, Zaslavski 1988, Tasch & Topp 1991).

In this section, I briefly review two specialised dormancy mechanisms incorporated in stage specific models investigated by Gurney et al (1992, 1994). Both mechanisms were postulated from detailed biological studies carried out on odonata (dragonflies) located in temperate climes (Corbet 1957, Norling 1984a,b,c). Odonata are of tropical origin and have evolved dormancy mechanisms to survive more temperate (and seasonally periodic) environments (Norling 1984c, Corbet 1957, 1980). The adults are unquestionably the least suited of all stages to survive winter (Norling 1984c). In view of this, it is unsurprising that such dormancy is found to occur exclusively in the aquatic pre-adult stages.

Previous simulations using complex damselfly models (Crowley et al 1987) have indicated that for such organisms the non-linearities which regulate population numbers have only a weak effect on the *timing* of emergence and reproduction. By these studies, the most significant environmental factor affecting emergence timing was found to be fluctuations in temperature. Observing this, Gurney et al (1992,1994) constructed models that were driven only by a single temperature driver function. Neither of these models addresses the important question of how development in different environmental mediums (in a single life cycle) may affect synchronisation of emergences. In this respect, both models are surprisingly artificial.

The Corbet Model

Corbet (1957) proposed a stage specific 'overwintering' mechanism through which odonata in temperate climes such as Britain may achieve synchronisation of emergence. Species located in such environments frequently have life-cycles of a duration greater than one year and so must pass through at least one winter in a preadult (larval) stage.

Corbet postulated the existence of a special reversible dormancy (quiescence) which could occur in all stages throughout the 'stressful' winter period. He suggested that

the field-observed increasing sequence of lower temperature thresholds (in successive development stages) implied the existence of a stage specific quiescence (SSQ). Such a mechanism ensures that individuals in earlier stages of development start or resume development sooner in the following spring than those in more advanced stages. Corbet hypothesised that in a strongly seasonal environment the SSQ mechanism contributes towards synchronisation by producing a temporal convergence of developmental trajectories. Clearly, the potential for synchronisation through such a mechanism is self-evident.

Gurney et al (1994) constructed a stage specific model to test the hypothesis that SSQ alone may synchronise life cycles. The model incorporated a simple representation of the SSQ mechanism and closely resembled the development data obtained by Lutz (1968) for a North American damselfly. They found that such a mechanism produces a 'quiescence lens' which acts to 'condense' developmental trajectories stemming from those stages that remain dormant during the winter period. Thus, repeated passage through the quiescence lens of developmental trajectories that emanate from successive generations can (in turn) produce the temporal convergence of lineages that leads to synchronisation of emergence. Diagram 4.1(a) shows a circle map plot of the Corbet model (Gurney et al 1994). Observe that the effect of the SSQ mechanism is to produce a segment that deviates away from 45°.

The Norling Model

Unlike Corbet (1957), Norling (1984a,b,c) in his studies on the Scandinavian odonata observed that several species exhibited the special dormant state of *facultative diapause* over the winter period. Facultative (as opposed to obligatory) diapause differs in two main respects from quiescence. Firstly, it is induced by environmental signals before the onset of adverse conditions and secondly, once entered such dormancy is not easily reversed (Danilevskii 1965, Saunders 1982, Hodek et al 1983).

Norling proposed a simple mechanism by which odonata exhibiting facultative diapause may achieve synchronisation of emergence. He postulated the existence of a critical stage and a critical time of year (CST) during development, at which entry to diapause is determined (or not). Individuals reaching the critical stage before the critical time of year continue their development to maturity, whereas those that reach the critical stage after the critical time, enter diapause and suspend development until the following spring. Photoperiod is much the most reliable cue for insects (Danilevskii 1965, Beck 1980, Mordue et al 1980, Corbet 1989, Tanaka 1992) and in

line with this, Norling believed that diapause was induced by a critical photoperiod associated with the critical time of year (Norling 1984a,b,c).

Gurney et al (1992) demonstrated that a very simple two stage model of a briefly semelparous organism based on the Norling CST mechanism always synchronised to a periodic variation in environment or to some harmonic or subharmonic of the variation. The life cycle was represented by two contiguous stages, A (first) and B (second). Any individual that reached the critical size (arbritrarily chosen to occur at the end of the A stage) before the pre-determined critical time of year, continued development through the B stage. Any individuals that reached the critical size after the critical time of year immediately entered diapause and recommenced development (in the B stage) at the start of the next year. Either way, reproduction occurred instantaneously at the time of emergence from the B stage and progeny were assumed to immediately re-enter the life-cycle. The CST mechanism therefore gives rise to a selective period of delay (situated between the critical time of year and the year end) through which lineages stemming from individuals failing to reach the critical size 'accumulate' at the year end. Thus, the emergences of all successive generations stemming from these individuals are thereafter perfectly synchronised. Diagram 4.1(b) shows a circle map plot of the Norling model (Gurney et al 1994). The CST mechanism produces a horizontal segment corresponding to the period of delay.

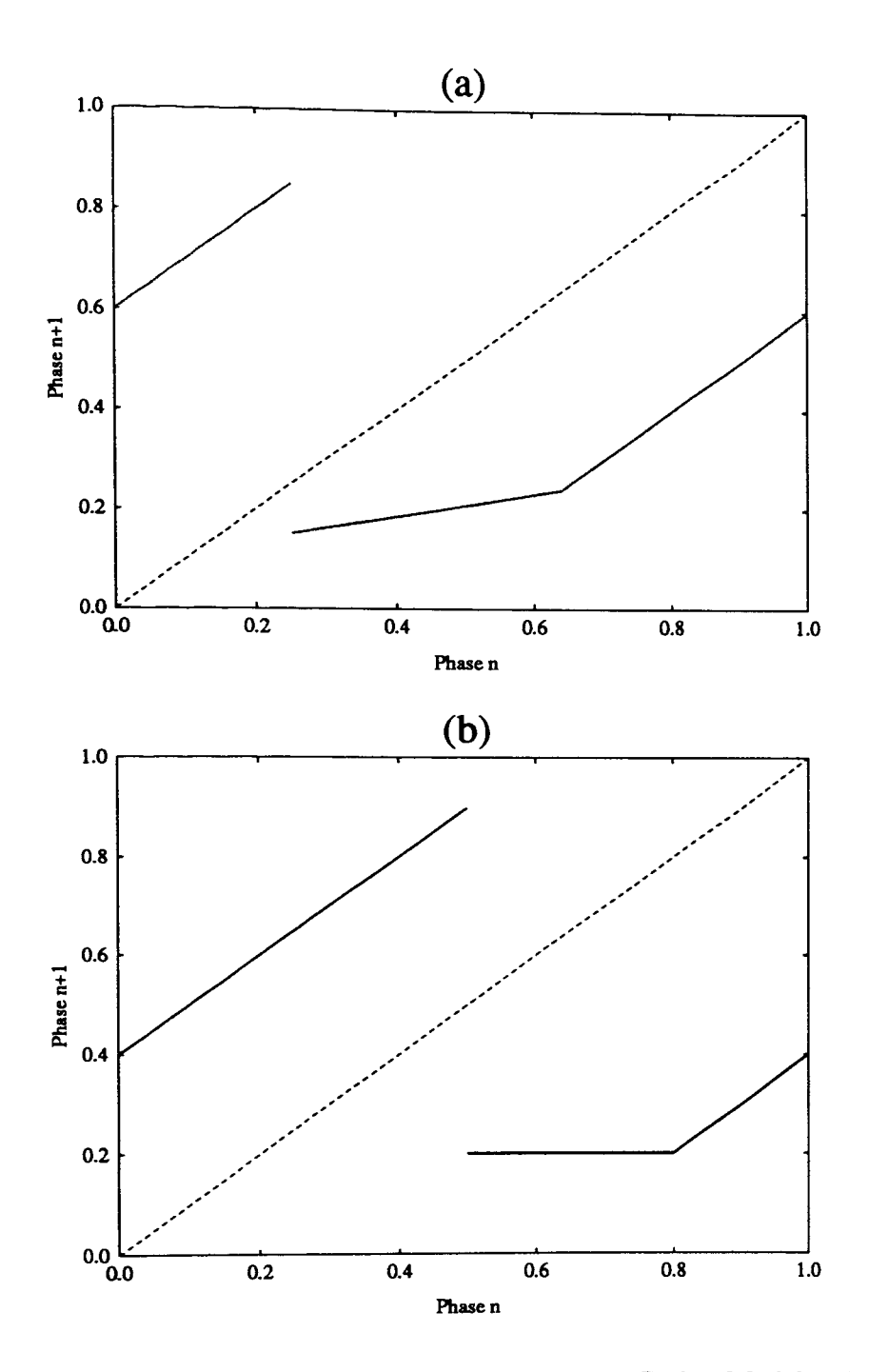


DIAGRAM 4.1. Typical circle map plots of (a) the Corbet Model and (b) the Norling Model (Gurney et al 1994,1992)

An obvious but severe limitation of both the Corbet and Norling mechanisms is that they are abstractions which may resemble relatively few of the diverse natural means by which organisms achieve life cycle synchronisation. In nature, hybrid mechanisms abound which combine features of both, such as the 'eudiapause' described by Muller

(1970) where diapause is terminated by quiescence, the increasing stage thresholds for quiescence that follow after the spring emergence from diapause in arctic chironomids (Danks and Oliver 1972) or the characteristic quiescence to be found in late winter after diapause has ended in many typical temperate insect species (Danks 1987). All of these would require separate treatments.

The most general two stage life cycle which would encompass all such permutations (and more) is that where, quite simply, each stage exhibits a *different* development response. The way forward is by formulating a more general model. I shall now formulate such a model.

4.2 A GENERAL TWO STAGE MODEL

I consider an organism whose life-cycle is composed of two contiguous stages A and B which occur in that chronological order and in each of which the development rate (g_A, g_B) is dependent only on time t. In all interesting cases, these development rate functions will represent reactions to different combinations of environmental variables and will thus have different time dependence. I make the assumption that instantaneous promotion to the B stage occurs at the end of the A stage. As with the one stage model, to represent the underlying regularity to which synchronisation may be possible (that is a seasonal or daily cycle) I regard each function as strictly periodic with period T.

I define a cumulative development function for each stage i by

$$C_{i}(t) \equiv \int_{0}^{t} g_{i}(x) dx \qquad i \in \{A,B\}$$
 (4.1)

and hence stage-specific physiological times

$$\phi_{i}(t) \equiv \left\lceil \frac{C_{i}(t)}{C_{i}(T)} \right\rceil \qquad i \in \{A,B\}$$
 (4.2)

Here $\phi_i(t)$ represents the total stage i development achieved by time t as a fraction of the total development achievable in that stage during a single environmental repeat cycle. For each stage, I naturally define a stage-specific relative physiological time, hereafter known as *stage-i phase*, by

$$\theta_i(t) \equiv \phi_i(t)^* \equiv \phi_i(t) \mod 1$$
 $i \in \{A,B\}.$ (4.3)

Because of the 'normalisation' of equation (4.2), these phases match each other at real times t=mT (m integer) that is, at each turn of the year. Observe also that each stage-i physiological time $\phi_i(t)$ is a lift of its own phase $\theta_i(t)$ (Chapter 3 Definition 3).

From Chapter 2, I recall that an individual recruited to stage A at an A-stage phase θ_A^r must complete its passage through the stage at an A-stage phase θ_A^p given by

$$\theta_{\mathbf{A}}^{\mathbf{p}} = \mathbf{R}_{\alpha}(\theta_{\mathbf{A}}^{\mathbf{r}}) \tag{4.4a}$$

where R_{α} is a simple rotation, and α is the A stage physiological time duration of the A stage. An exactly parallel treatment shows that if β is the B-stage physiological time required to traverse the stage B then, in terms of that stage's own physiological time, the phases of recruitment θ_B^r and completion θ_B^p are related by

$$\theta_{\rm B}^{\rm p} = R_{\rm \beta}(\theta_{\rm B}^{\rm r}) \tag{4.4b}$$

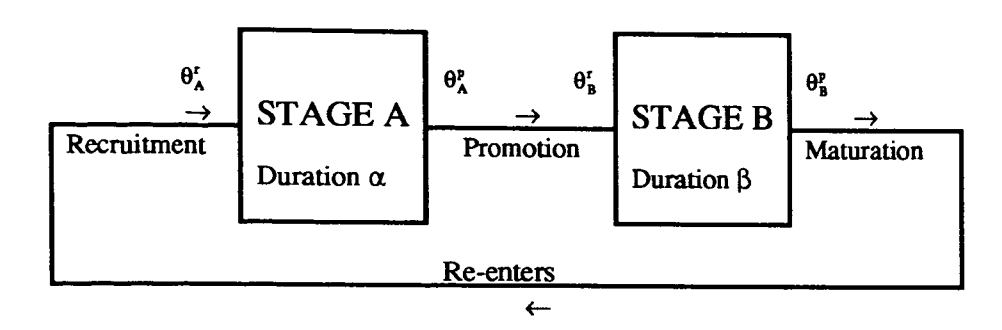


DIAGRAM 4.2 Representation of the General Two-Stage Life Cycle Model operating in physiological time

Although equations (4.4) show that passage through either stage is simple when considered in its own physiological time, if I am to consider the *whole* life-cycle I need to work with a single measure of time. How can the single stage phase description of Chapter 2 be extended to an organism whose life history is made up of two stages?

I solve this by performing a 'conversion' between the stage-i phases θ_i . To achieve this, I require two maps f_{AB} and f_{BA} which map A-stage phase θ_A into the 'equivalent' B-stage phase θ_B and vice-versa. I define these maps in the natural way, namely so that any point in either stage-phase is mapped to its image point (in the other phase) via its correspondance with *real* time t.

Definition 4.1

The forward interphase map $f_{AB}: S^1 \to S^1$ which takes $\theta_A \to \theta_B$ and reverse interphase map $f_{BA}: S^1 \to S^1$ which takes $\theta_B \to \theta_A$ are defined respectively by

$$f_{AB}(\theta_A(t)) \equiv \theta_B(t)$$
 (4.5a)

$$f_{RA}(\theta_R(t)) \equiv \theta_A(t).$$
 (4.5b)

The existence of both f_{AB} and f_{BA} (in a well-defined mathematical sense) is dependent on the nature of the relationship between each phase $\theta_i(t)$ and real time t that is, as revealed by the *shapes* of the associated pair of phase plots $\theta_i(t)$ vs t for i=A and B. I shall return to the important question on the circumstances under which these maps exist in section 4.3.

Equipped with such maps, I can easily derive the relation between the phases of recruitment (to) and promotion (from) the life cycle in terms of either stage phase. Without loss of generality I shall choose to describe the entire life-cycle in terms of Astage phase.

Since I make the assumption that passage between the stages occurs instantaneously, promotion from the A stage to the B stage corresponds with recruitment to the B stage so that

$$\theta_{B}^{r} = f_{AB}(\theta_{A}^{p})$$

$$= f_{AB}[R_{\alpha}(\theta_{A}^{r})] \quad \text{by (4.4a),}$$

$$= f_{AB}R_{\alpha}(\theta_{A}^{r}) \qquad (4.6)$$

In a similar fashion, I deduce that an individual who is recruited into stage A at an A-stage phase θ_A^r will *complete* its passage through stage B (and therefore emerge) at an A-stage phase θ_A^E given by

$$\begin{aligned} \theta_{A}^{E} &= f_{BA}(\theta_{B}^{p}) \\ &= f_{BA}R_{\beta}(\theta_{B}^{r}) \quad \text{by (4.4b),} \\ &= f_{BA}R_{\beta}(f_{AB}R_{\alpha}(\theta_{A}^{r})) \quad \text{by (4.6)} \end{aligned}$$

For compactness I write this expression as

$$\theta_{AE} = F_{\alpha,\beta}(\theta_{AR}) \tag{4.7a}$$

where the map $F_{\alpha,\beta}$ is defined by

$$F_{\alpha\beta} \equiv f_{BA} R_{\beta} f_{AB} R_{\alpha}. \tag{4.7b}$$

I now assume that when an individual reaches the end of stage B it, or its progeny, immediately re-enter stage A. Such a description would apply as a reasonable approximation to a 'big bang' insect (see Chapter 0) such as the briefly semelparous Catops Nigricans (Topp 1990) of Chapter 1, where the end of stage B would

represent emergence as a mature adult and the beginning of stage A would represent oviposition. It would apply exactly to successive divisions of a cell-line reproducing by binary fission, where the end of stage B would represent the instant of division, after which both two daughter cells would immediately re-start the cell cycle at the beginning of stage A. Classic examples of such a life cycle are to be found in the complete cell cycle of several species of phytoplankton (Sweeney & Hastings 1958, Bernstein 1960, Spudich & Sager 1980, Heath & Spencer 1985, Heath 1988).

Denoting the value of A stage phase at the n^{th} entry to stage A by θ_n , the relation between the phases at recruitment of generations n and n+1 is then

$$\theta_{n+1} = F_{\alpha,\beta}(\theta_n). \tag{4.8}$$

Since the phase θ_n is topologically a position on the circle S^1 , I shall refer to the map $F_{\alpha,\beta}$ as a two-stage circle map. Thus, the two-stage circle map $F_{\alpha,\beta}$ gives the phase at which recruitment to generation n+1 occurs in terms of the phase of recruitment to generation n, expressed soley in terms of the A stage phase.

4.3 THE INTERPHASE MAP

I primarily seek to investigate synchronisation between the life-cycle of successive "generations" and the underlying periodicity of the environmental variation. Such synchronisation is indicated by the existence of stable, fixed or periodic points of the circle map $F_{\alpha,\beta}$. The maps (R_{α}, R_{β}) representing passage through each individual stage in its own physiological time (see equations (4.4)) are pure rotations and so cannot play any significant role in creating such points. The critical properties of the two-stage circle map are thus determined by the relationship between the two phases that is by the properties of the forward and reverse *interphase maps* f_{AB} and f_{BA} . Do both of these necessarily exist?

Notice first that equations (4.1) to (4.3) show that both stage-specific phases must be zero at t=mT and must tend to 1^- as t \rightarrow mT⁻ (integer m). The Euclidean plot of $f_{AB}(x)$ (or $f_{BA}(x)$) vs x thus always passes through the origin, and approaches arbitrarily close to (1,1). I return to the question on the existence of such maps by considering a critical pathological example.

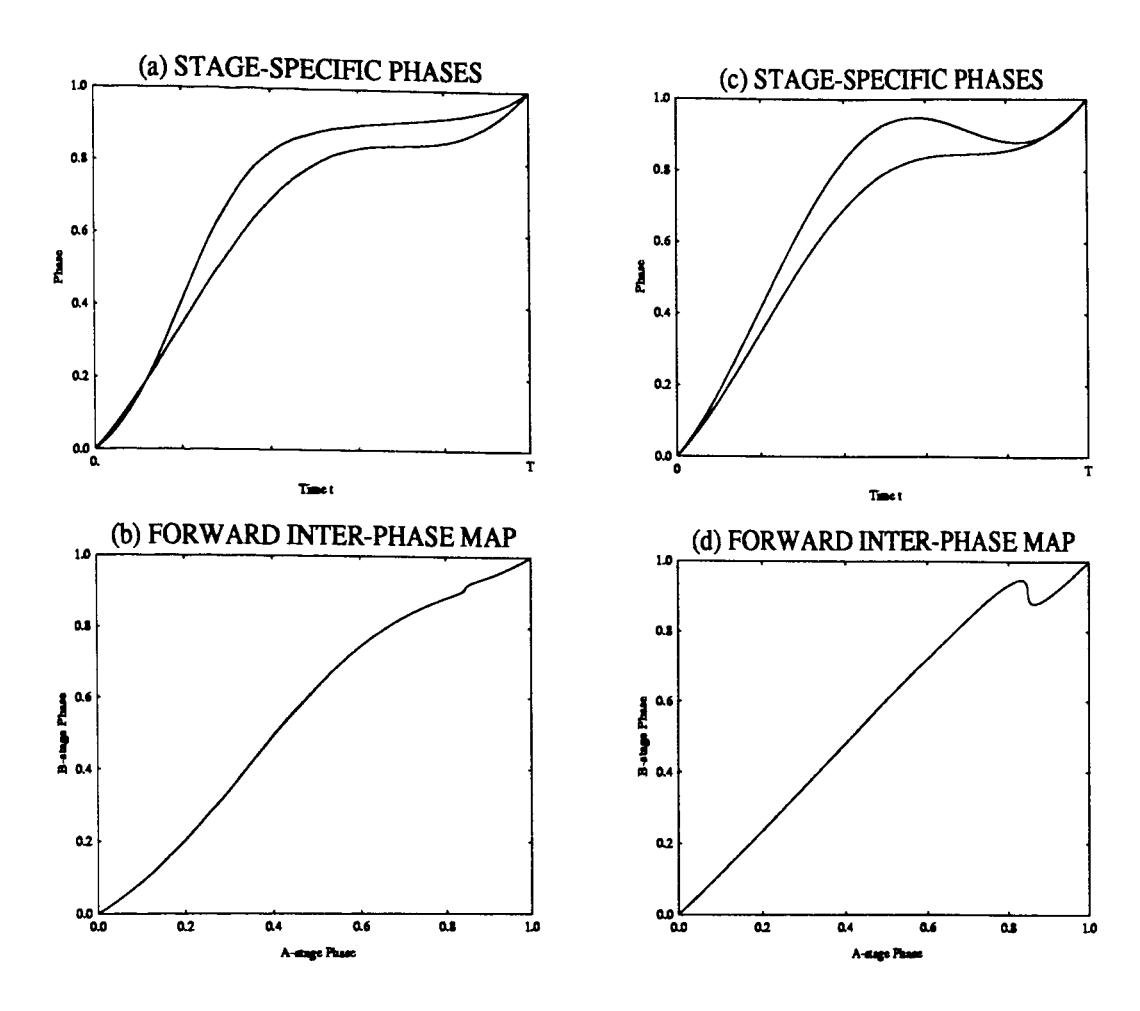


DIAGRAM 4.3 Relationships between stage phases and forward interphase map f_{AB} Sequence (a to b) plots where both stages are diffeomorphisms, (c tod) where B-stage phase is not.

Diagram 4.3 shows two situations represented by pairs of phase plots (a) and (c) respectively. For clarity, θ_A is the same diffeomorphism in both situations.

In the first situation shown in 4.3(a), θ_B is also a diffeomorphism. The forward or reverse interphase map (4.3(b)) is thus well-defined and is a diffeomorphism. However, in the second situation (4.3(c)) the phase plot of $\theta_B(t)$ vs t reveals a 'kink' produced by θ_B doubling back on itself. This kink is passed on to the corresponding forward interphase map f_{AB} and surfaces in the plot of $f_{AB}(\theta_A)$ vs θ_A (4.3(d)). Thus, the forward interphase map f_{AB} is non-invertible and the reverse interphase map f_{BA} does not exist.

The kink problem will occur whenever a development rate goes below zero. Such a problem can be avoided by making the biologically reasonable assumption that

development is irreversible. This ensures that development rate either proceeds forward at a strictly positive rate or at worse reaches zero.

If development rate falls to zero (other than at the origin) the corresponding interphase map is no longer single-valued and consequently is not a homeomorphism. Thus, if a zero development rate occurs in the model, theoretical complications arise. Fortunately these complications are of hypothetical interest only, since an organism's development rate can be *effectively* zero (arbritarily small) without actually reaching zero (beyond the accuracy of any measuring device) in the real world.

If the development rate functions g_A and g_B are both strictly positive and bounded above then both stage-specific phases are continuous monotone increasing functions of time. This in turn implies that the forward interphase map f_{AB} must be a continuous monotone increasing function of A-stage phase, and is therefore a homeomorphism. The reverse interphase map f_{BA} is just its inverse so that $f_{AB}f_{BA}(x)=x$ is assured for all x. A plot of $f_{BA}(x)$ vs x is thus a reflection of the plot of $f_{AB}(x)$ vs x in the leading 45° diagonal. I shall refer to such interphase maps as continuous interphase maps.

I observe further that development rate functions g_A and g_B need only be continuous to ensure that the forward interphase map is everywhere differentiable. Thus, where both development rate functions are also continuous the (forward or reverse) interphase map is everywhere differentiable, and is a diffeomorphism. I refer to interphase maps in this class as differentiable interphase maps. I neatly produce a definition which summarises this.

Definition 4.2 A continuous (differentiable) interphase map is a strictly increasing homeomeorphism (diffeomorphism) on S^1 which satisfies f(0)=0 [and f(1)=1 in the plot].

Henceforth in the remainder of this Chapter and throughout Chapter 5, I shall focus on the important broad class of biologically feasible life cycles whose development rate functions are strictly positive, finite and continuous. For compactness I shall denote the forward interphase map f_{AB} simply by f and the reverse interphase map f_{BA} by f^{-1} . The two-stage circle map $F_{\alpha,\beta}$ defined in equation (4.7b) then becomes

$$F_{\alpha\beta} = f^{-1}R_{\beta}fR_{\alpha}. \tag{4.10}$$

Since f and f^{-1} are continuous and monotone increasing the associated two-stage circle map $F_{\alpha\beta}$ has the same property and is thus a homeomorphism. Similarly, if f and f^{-1} are differentiable then $F_{\alpha\beta}$ still retains the same property and is a diffeomorphism. I summarise this in a definition.

Definition 4.3 A continuous (differentiable) two stage circle map is a strictly increasing homeomeorphism (diffeomorphism) on S¹ composed from a continuous (differentiable) interphase map.

Notice that because $F_{\alpha,\beta}$ is (at worst) a homeomorphism, $F_{\alpha,\beta}^{-1}$ exists and thus $F_{\alpha,\beta}$ is always invertible. Since non-invertibility is a necessary condition for chaos (e.g. see Arnold 1973) no chaos can occur in the system described in equation (4.8) whenever $F_{\alpha,\beta}$ is the beast of Definition 4.3.

I easily show that the extension of the physiological time formulation to two stages is consistent with the previous (one stage) theoretical framework. Suppose that stages A and B exhibit the same developmental response. This implies that $\theta_A = \theta_B$ so that the plot of the interphase map is simply the leading 45° diagonal. Hence $f(x) = f^{-1}(x) = x$ so that

$$F_{\alpha\beta} = f^{-1}R_{\beta}fR_{\alpha} = R_{\beta}R_{\alpha} = R_{\beta+\alpha}$$
(4.11)

which corresponds to two consecutive rotations. Thus, in this case the two stage model behaves as a one stage model and no synchronisation occurs (Chapter 2).

4.4 GENERIC INTERPHASE MAP SHAPE: TWO FREQUENT SITUATIONS

In this section I shall illustrate how generic shape of the interphase map can be related to a biological context. I restrict our consideration to a frequent life cycle situation, namely that in which the development rate functions g_A and g_B have a single maximum within the repeat period T.

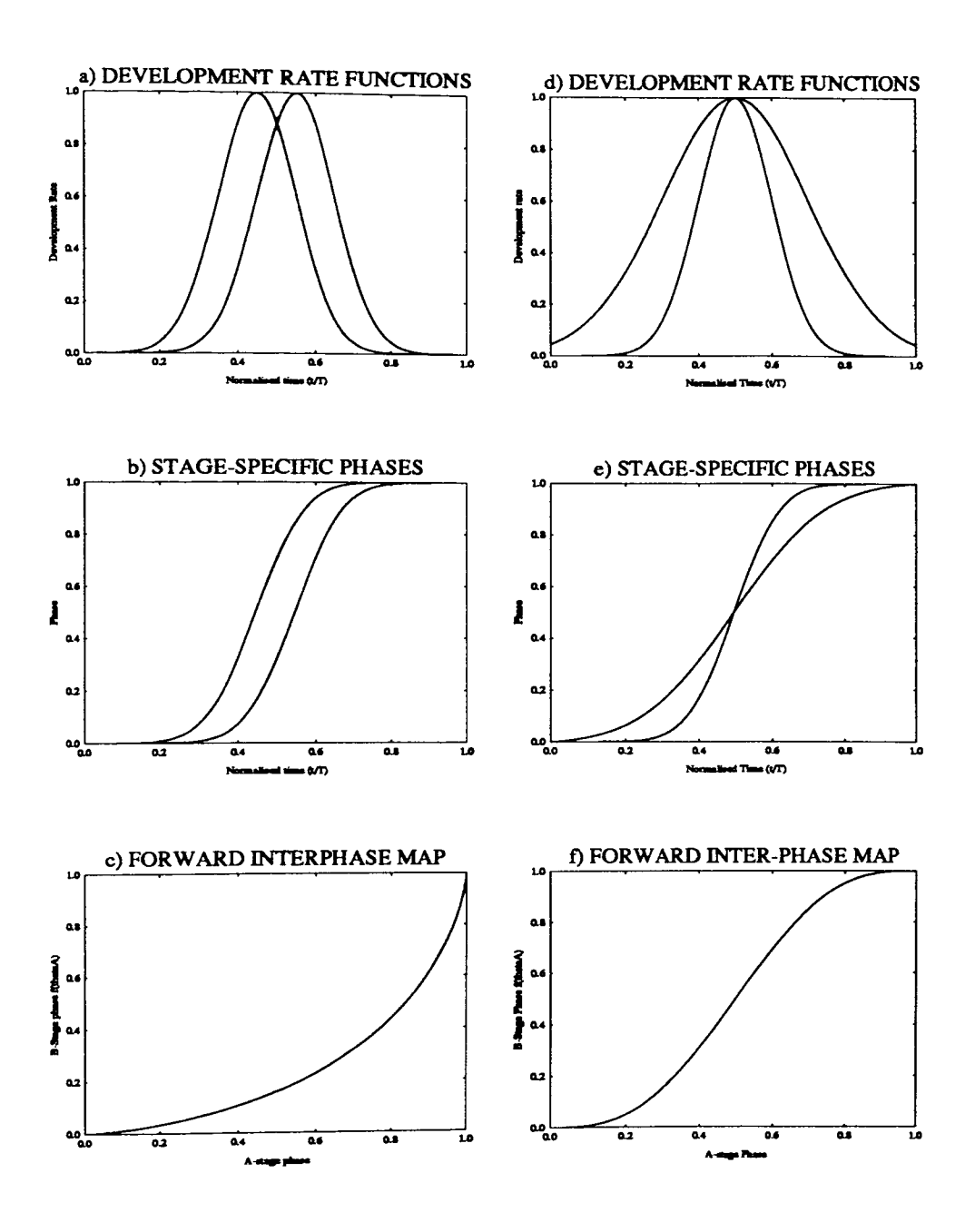


DIAGRAM 4.4 Patterns of development. (a and d) Development rates with respective plots of (b and e) Phase and (c and f) Interphase maps.

In such cases the forward interphase map f (that is, f_{AB}) has only a small repertoire of possible shapes, which are illustrated in Diagram 4.4. Development rate functions are shown in normalised form for convenience (the altitude of development rate functions has no effect on interphase map shape because of the normalisation of the cumulative development functions in equation (4.1), but note that the values of α and β are dependent on altitude).

Diagram 4.4 sequence (a) to (c) shows the behaviour of a life cycle with equal width Gaussian development rate functions (s.d.=0.1T) with a lag between stage-A and stage-B development peaks equal to one standard deviation. Sequence (d) to (f) shows the behaviour of a life cycle with two Gaussian development functions both peaking at the same point but with the stage-A development function having twice the width of the stage-B function. In both sequences the first frame ((a) and (d)) shows the development rates as a function of time, the second frame ((b) and (e)) shows the two stage specific phases as a function of time, and the third frame ((c) and (f)) shows the forward interphase map. I shall categorise these patterns of development as two generic cases.

Case 1 (lag between development rate functions)

Stage A development takes place earlier in the repeat period than stage B development (as in 4.4(a)). This implies that the A-stage phase leads the B-stage phase at all times (4.4(b)) and the forward interphase map is a monotone increasing, strictly concave function (4.4(c)).

Case 2 (different length of growing season)

The timing of the maximum development is much the same for both stages, but the A-stage is capable of rapid development over a larger part of the repeat time than the B-stage (as in 4.4(d)). This implies that the A-stage phase leads the B-stage phase in the early part of the cycle but lags it in the later part (4.4(e)). In this case the forward interphase map adopts a characteristic S-shape (4.4(f)).

In both cases, $g_i(t)$ is a Gaussian function truncated at 0 and 1 thereby ensuring that strict continuity is maintained in the periodic form. In Case 1 the lag of the B stage (a horizontal shift parallel to the x-axis) may imply that the ratio of the gradients of the stage specific phase $d\theta_B/d\theta_A$ at the point $0 \in S^1$ tend to different values from below and above thus producing a non-differentiable point. In other words, although the

resulting interphase map must still be continuous and differentiable for 0 < x < 1, we are no longer guaranteed that

$$\lim_{x\to 0^+} \left(\frac{g_B(x)}{g_A(x)}\right) = \lim_{x\to 1^-} \left(\frac{g_B(x)}{g_A(x)}\right),$$

so it may contain a non-differentiable point at x=0. In this case I refer to it as an interior differentiable interphase map.

Diagram 4.5 shows the corresponding two-stage circle map plots for each pattern of development. Observe that the plots differ significantly from those associated with the Corbet and Norling models in that they are made up of nonlinear (curved) sections.

Other than curvature, the plots of $F_{\alpha,\beta}$ for Case 1 and Case 2 have some notable features imputed by the interphase map f and its inverse f^{-1} .

In Case 1 the non-differentiable point at x=0 in f (discontinuity in Df) is subject to displacements ('modulo 1 translations'- see Definition 5.1) of 1- α * horizontally and β * vertically by the pure rotations R_{α} and R_{β} and corresponds to the point P_1 in Diagram 4.5(a). Similarly, the non-differentiable point at x=0 in f $^{-1}$ is carried through to $F_{\alpha,\beta}$ so that it appears at the point P_2 . The steepness of the section P_2P_1 actually results from the parameter choice of α and β used in the plot.

In Case 2 the interphase map has no non-differentiable points but the gradient of f is zero at x=0 thus implying that the gradient of f^{-1} achieves infinity at x=0. This appears at the point P_3 in the plot, displacement away from x=0 again being due to the rotations R_{α} and R_{β} within the composite map $F_{\alpha,\beta}$.

It is essential to the subsequent analysis that I distinguish between two-stage circle maps containing linear segments parallel to the leading 45° diagonal and those without such features. It is clear from equation (4.10) that such linear segments in the circle map can only arise as a consequence of linear 45° segments in the interphase map. These in turn must indicate that the development rate functions have equal values over intervals (rather than at a finite set of points). I shall refer to the class of continuous two-stage circle maps which excludes those containing 45° line segments as continuous non-diagonal two-stage circle maps.

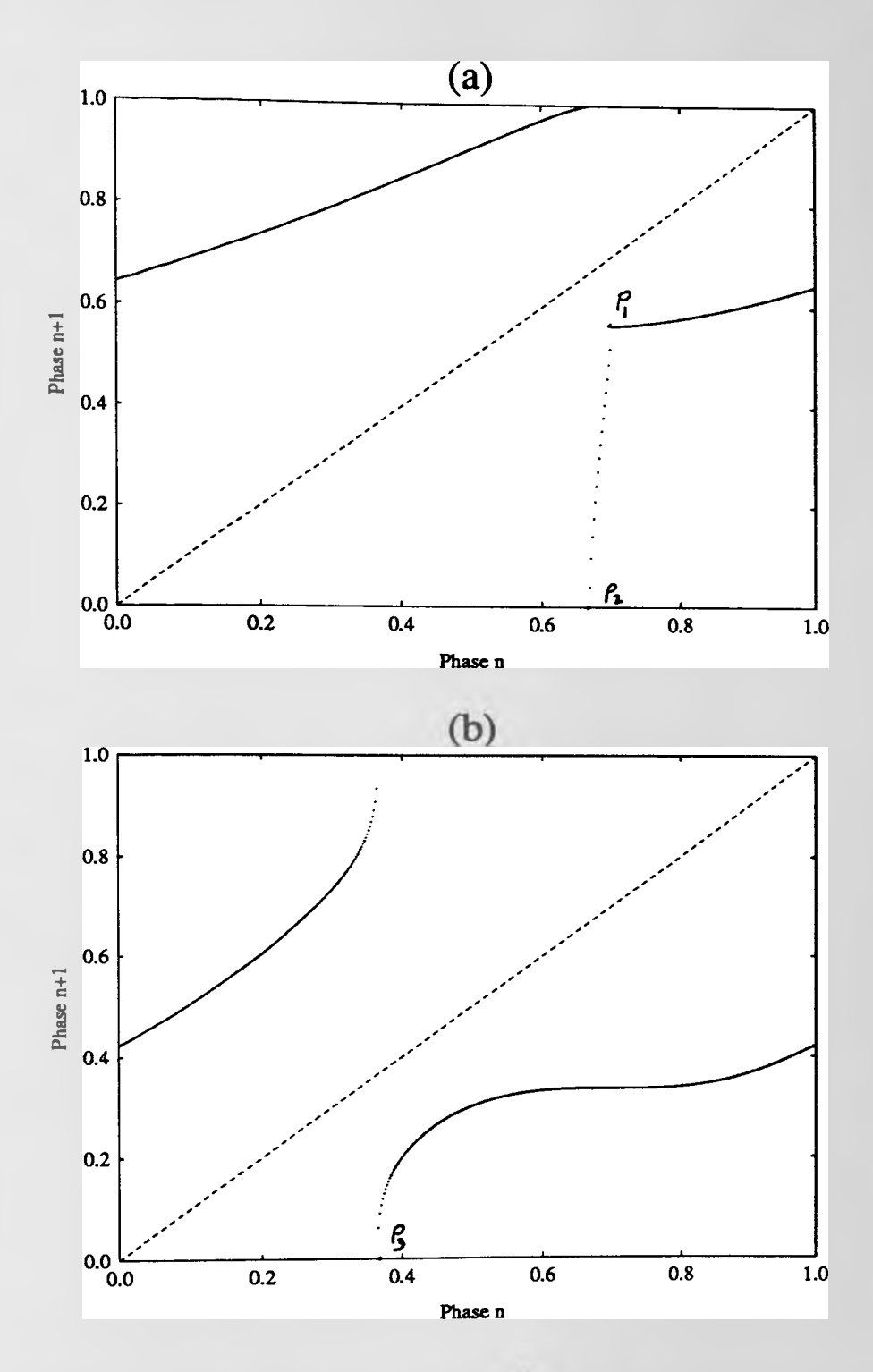


DIAGRAM 4.5. Plots of two-stage circle map $F_{\alpha\beta}$ corresponding to Diagram 4.4 (a) first pattern of development [sequence 4.4(a to d)] (b) second pattern of development [sequence 4.4(d to f)]

4.5 DISCUSSION

At the core of the general two stage model formulation lies the interphase map. This homeomorphism provides an elegant means of encapsulating the relationship between the two stage phases. Furthermore, it enables a concise circle map description of the general two stage model to be obtained in physiological time.

The shape of the interphase map gives a simple visual measure by which the stage difference in developmental response (the stage specificity) can be immediately assessed. Paradoxically, it gives a continuous perspective on the extent of discontinuity present in the development process. I now know that where no such discontinuity exists, no synchronisation is possible (cf section 4.3) That stage specificity is vitally important in determining synchronisation behaviour is thus readily apparent.

Although I have indicated that the multi-stage way ahead is clear, I shall not attempt to expand the current description beyond two stages. I also argue that chaos has no biologically meaningful role to play in the current formulation because this can only occur if development proceeds 'backwards'. Neither of these considerations are covered in this thesis in an attempt to keep the system as simple as possible and to study the key synchronising effects of stage specificity in isolation.

Instead, I prefer to focus on the key role that the interphase map plays in determining the dynamic outcome of the system. In the next chapter, I will show that interphase map shape (and in particular its deviation from the leading 45° diagonal) largely determines the synchronisation properties of the general two stage model.

CHAPTER 5 GENERAL PROPERTIES OF TWO STAGE CIRCLE MAPS

5.0 INTRODUCTION

I shall conduct an in-depth investigation of the key role that the interphase map f plays in determining the synchronisation behaviour of the general two stage model. I gain initial insight into the importance of interphase map shape by conducting explorations through simple transformations T(f) of the interphase map. By establishing topological conjugacy between $F_{\alpha,\beta}$ and $G_{\alpha,\beta}$ (composed from interphase map $g \equiv T(f)$), I show that the dynamic behaviour of $F_{\alpha,\beta}$ is invariant to certain transformations of the interphase map from which it is composed. For simplicity, I choose to focus on those transformations which result in a simple visual geometric effect (such as a reflection) of the plot of f on the plane. I compactly summarise the fruits of these explorations in the form of a collection of respective Theorems for each transformation $g \equiv T(f)$ investigated. These Theorems later prove invaluable in developing a more general understanding of the synchronisation behaviour of $F_{\alpha,\beta}$.

More profoundly, I ask about the general synchronisation behaviour of $F_{\alpha\beta}$. When do the orbits of $F_{\alpha\beta}$ form (asymptotically) stable q-cycles? As with any circle map, the dynamic behaviour of $F_{\alpha\beta}$ is dependent on its shape and configuration which (in the case of a two stage circle map) is dependent on the shape of the interphase map f from which it is composed and the values of the parameters α and β . Because $F_{\alpha\beta}$ is a circle homeomorphism, I already know from section 3.3 that stable q-cycles must exist if $F_{\alpha\beta}$ has any periodic points. Thus the question posed at the start of the paragraph simplifies to asking under what conditions periodic points of $F_{\alpha\beta}$ necessarily exist. I provide a fast general answer to this question by a numerical approach which generates a behaviour portrait. This picture also concisely shows the general robustness of any two stage circle map model.

The most visually spectacular property of the behaviour portrait is its twofold rotational symmetry about its centre point. In Theorem 5.5 I prove the powerful result that when $F_{\alpha\beta}$ is a diffeomorphism (which it will be if the development rate functions g_A and g_B are strictly positive and continuous) the number of stable q-cycles that occur must equal the number of unstable q-cycles. Because it turns out that only one such *stable* cycle ever occurs, the general rotational symmetry property of $F_{\alpha\beta}$ follows as an easy corollary and thus holds for any differentiable two-stage circle map.

I initially began algebraic explorations by seeking general analytic conditions for a general q lock to occur that is, conditions to be satisfied for repeated iteration of the

map $F_{\alpha\beta}$ to eventually yield a stable q-cycle of recruitment phases. I derived such analytic 1 lock conditions in the two broad classes of situations where the plot of f has either of the two generic shapes outlined in the previous section (4.4). Beyond a 1 lock, these workings rapidly deterioate into gruelling intractability.

In section 5.4 I carry out some numerical investigations via the behaviour portrait into the specific pair of patterns of development where the development rate functions are shaped like truncated Normal distributions (Case 1 and Case 2 of section 4.4). For both situations, I construct a sequence of behaviour portraits which immediately illustrate the strong action of stage specificity as a general locking agent. These sequences demonstrate the depth of insight into synchronisation behaviour that can be gathered from a simply visual survey of the behaviour portrait.

5.1 INTERPHASE MAP TRANSFORMATIONS

I now ask what happens to the qualitative nature of the orbits produced by iterating a two-stage circle-map $F_{\alpha\beta}$ when certain transformations are applied to the interphase map f from which it is composed. The key to all but one of the following proofs is topological conjugacy (see 3.2). Recall from Definition 3.8 that to prove two circle maps F and G are dynamically equivalent I need only show that they are topologically conjugate that is, \exists a homeomorphism $h: S^1 \to S^1$ such that $G = hFh^{-1}$.

In all the theorems that follow the interphase map f need only be a homeomorphism h :S $^1 \rightarrow S^1$. Observe first that the pure rotation map R_{γ} has the general property that

$$R_{\gamma}^{-1}(x) = R_{-\gamma}(x) = (x - \gamma)^* = (x + (1 - \gamma))^* = R_{1-\gamma}(x)$$
 (5.1)

and that for any map composed of homeomorphisms F,G, $(FG)^{-1} = G^{-1}F^{-1}$.

Theorem 5.1

Let f and g be circle homeomorphisms related by $g(x) \equiv f(R_{\delta}(x))$. If $F_{\alpha\beta}$ and $G_{\alpha\beta}$ are continuous two-stage circle maps composed from f and g respectively according to equation (4.10), then they are topologically conjugate.

$$\begin{aligned} &\textit{Proof} \\ &G_{\alpha,\beta} = (fR_{\delta})^{-1}R_{\beta}(fR_{\delta})R_{\alpha} = R_{-\delta}f^{-1}R_{\beta}fR_{\alpha}R_{\delta} = R_{-\delta}F_{\alpha,\beta}(R_{-\delta})^{-1} \end{aligned}$$

Theorem 5.2

Let f and g be circle homeomorphisms related by $g(x) \equiv R_{\delta}(f(x))$. If $F_{\alpha\beta}$ and $G_{\alpha\beta}$ are continuous two-stage circle maps composed from f and g respectively according to equation (4.10), then $F_{\alpha\beta} = G_{\alpha\beta}$.

$$\begin{aligned} & \textit{Proof} \\ & G_{\alpha\beta} = (R_{\delta}f)^{-1}R_{\beta}(R_{\delta}f)R_{\alpha} = f^{-1}R_{-\delta}R_{\beta}R_{\delta}fR_{\alpha} = f^{-1}R_{\beta}fR_{\alpha} = F_{\alpha\beta} \end{aligned}$$

Theorem 5.3

Let f and g be circle homeomorphisms, with $g = f^{-1}$. If $F_{\alpha\beta}$ and $G_{\alpha\beta}$ are continuous two-stage circle maps composed from f and g respectively according to equation (4.10), then $G_{\alpha\beta}$ and $F_{\beta\alpha}$ are topologically conjugate.

$$\begin{aligned} & \textit{Proof} \\ & G_{\alpha,\beta} = f R_{\beta} f^{-1} R_{\alpha} = R_{\alpha}^{-1} f(f^{-1} R_{\alpha} f R_{\beta}) f^{-1} R_{\alpha} = (R_{\alpha}^{-1} f) F_{\beta,\alpha} (R_{\alpha}^{-1} f)^{-1} \end{aligned}$$

Theorem 5.4

Let f and g be circle homeomorphisms with $g(x)\equiv 1-f(1-x)$. If $F_{\alpha,\beta}$ and $G_{\alpha,\beta}$ are continuous two-stage circle maps composed from f and g respectively according to equation (4.10), then $G_{\alpha,\beta}$ and $F_{1-\alpha,1-\beta}$ are topologically conjugate.

Proof

I choose h to be the (monotone decreasing) circle homeomorphism defined by

$$h(x) = (1-x) \tag{5.2}$$

so that g=hfh. I note $h^{-1}=h$ and $hR\gamma h^{-1}=R_{-\gamma}$.

Now
$$G_{\alpha,\beta} = (hfh)^{-1}R_{\beta}(hfh)R_{\alpha} = hf^{-1}hR_{\beta}hfhR_{\alpha}$$
 but $h(h(x))=x$ so

$$G_{\alpha,\beta} = h(f^{-1}hR_{\beta}hfhR_{\alpha}h)h = h(f^{-1}R_{-\beta}fR_{-\alpha})h = h(f^{-1}R_{1-\beta}fR_{1-\alpha})h$$

and thus
$$G_{\alpha,\beta}=h(F_{1-\alpha,1-\beta})h=h(F_{1-\alpha,1-\beta})h^{-1}$$

Theorems 5.1 and 5.2 demonstrate that the qualitative dynamics of a continuous two-stage circle-map $F_{\alpha,\beta}$ are unchanged if I alter the associated interphase map in such a way that the plot of f(x) vs x is translated (modulo 1) parallel to either the x or the f(x) axis. I introduce the concept of a mod 1 translation.

Definition 5.1

Let (x,y) be a point in the unit square and let (x',y') be the image of (x,y) under a translation in the usual geometric sense. The image of (x,y) under a translation modulo l is defined as the point $((x')^*, (y')^*)$.

Thus a translation modulo 1 is the same as a translation in the usual geometric sense when both x' and y' are less than 1, but otherwise has the property that any points of a curve that are translated 'off' a given edge of the unit square 'reappear' at the opposite edge. Such points then continue being translated in the same direction as previously. In simple terms this means that the image graph of any curve under a translation modulo 1 will in general be a permutation of the original, consisting of a rearrangement of certain segments. Diagram 5.1 shows the effect of a translation modulo 1 parallel to the x axis, on the plot of an S shaped interphase map.

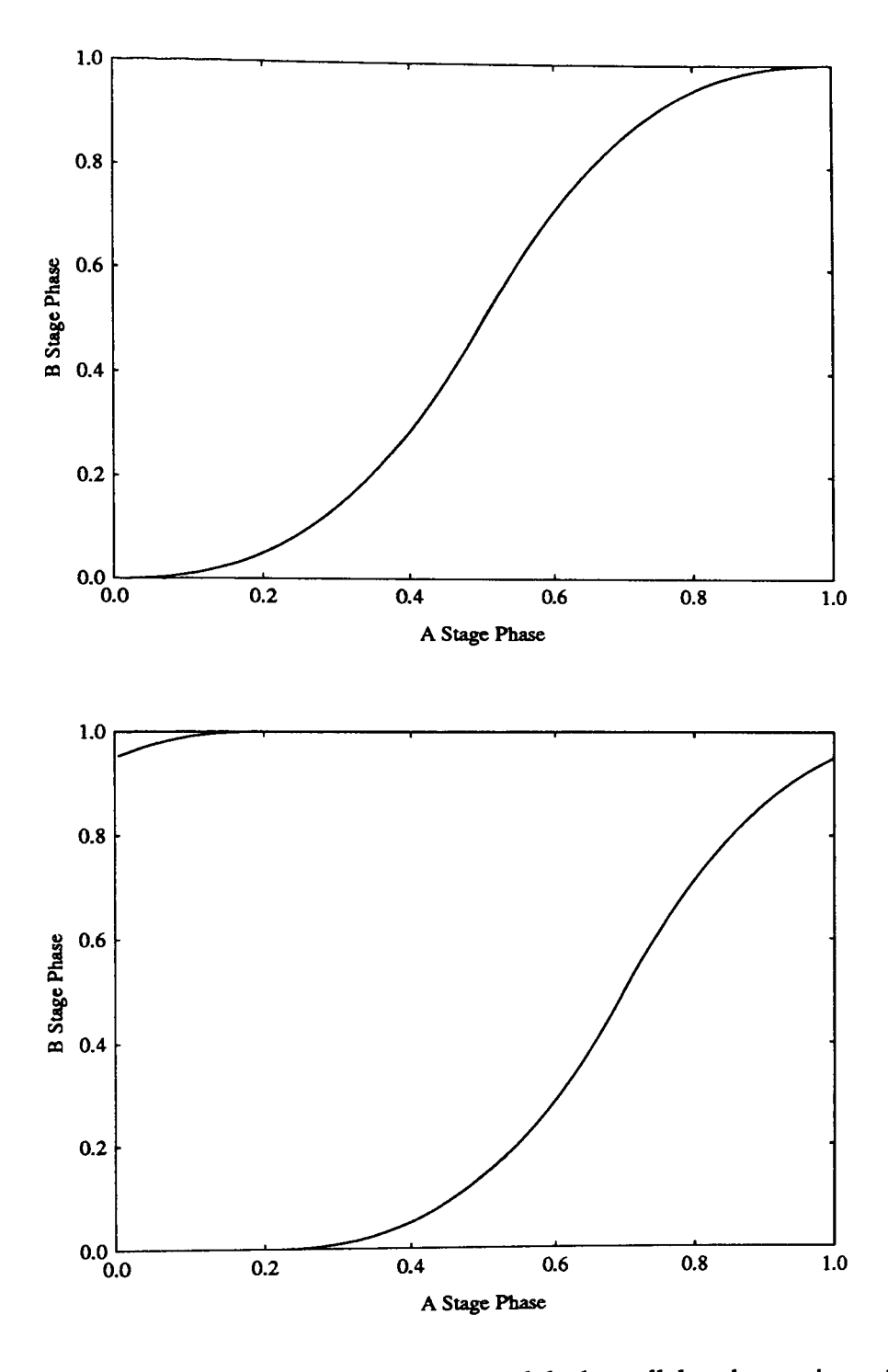


DIAGRAM 5.1 The effect of a translation modulo 1 parallel to the x axis on the plot of an interphase map.

In fact Theorem 5.2 goes further and shows that a pure rotation transformation T (where $T \equiv R_{\gamma}(f)$) applied to the interphase map f has no effect on the resulting iterative dynamic behaviour of $F_{\alpha\beta}$.

Theorem 5.3 shows that if the interphase map f from which $F_{\alpha\beta}$ is composed is interchanged with its own inverse (so that the plot of f is reflected in the leading 45° diagonal) the dynamic behaviour of $F_{\alpha\beta}$ is equivalent to that when the parameters α and β are simply interchanged. Theorem 5.4 shows that a transformation of the interphase map resulting in the plot of mapped phase against original phase being rotated 180° about the point (½,½) is equivalent to changing the parameters α and β to 1- α and 1- β respectively. For two special classes of interphase map shape, these last two theorems also give insight into how the parameters α and β may be interchanged without affecting the dynamic behaviour of $F_{\alpha\beta}$.

I next enquire about the sensitivity of $F_{\alpha\beta}$ composed from a general interphase map, to changes in value of the parameters α and β .

5.2 THE BEHAVIOUR PORTRAIT

Since $F_{\alpha\beta}$ is a circle homeomorphism, one way of establishing when synchronisation occurs (periodic points exist) would be to determine whether the associated rotation number is rational or irrational (see 3.3. on how this was done for the pure rotation map R_{α}). However, algebraic evaluation of this limit can be extremely protracted. Instead, I prefer a faster numerical approach which, as we shall see, has the bonus of generating a visual feel for the overall robustness of the model.

Extensive simulation studies show that all the maps with which I shall be concerned, possess at most one stable cycle for each set of parameter values. A central tool in my investigation of the generic properties of such maps is the *behaviour portrait*. This is a picture on the (α,β) -plane, constructed with any ancilliary parameters held constant, in which (to a pre-determined resolution) each point is marked with a colour characteristic of the repeat-length of the cycle implied by the attractor, or by a null marker if no attractor exists. The behaviour portrait of $F_{\alpha,\beta}$ therefore shows the complete range of dynamic behaviour of $F_{\alpha,\beta}$ in terms of stable cycles or otherwise. At the same time it shows the general sensitivity of $F_{\alpha,\beta}$ to changes in value of the parameters α^* and β^* and therefore gives extensive insight into robustness. It follows from the definition of the rotation operator (equation (2.6)) that the behaviour of the map $F_{\alpha,\beta}$ depends only on the values of α and β modulo 1 (hereafter denoted by α^* and β^*). Thus the behaviour portrait replicates itself in every complete adjacent unit square situated on the (α,β) -plane.

I can calculate good approximations to behaviour portraits very efficiently using a straightforward numerical approach, by first dividing up the unit square into small squares of finite width termed 'pixels'. The position of each pixel is then used to complete the definition of the circle map which is then iterated (to an accuracy of 1 part in 10⁵) until either a stable q-cycle is found, or if this does not occur, until a predefined number (10⁴) of iterations are performed. If a stable q-cycle is found then an appropriate colour dependent on the value of q is used to illuminate the pixel. For brevity I shall refer to q, which actually represents the number of generations between each stationary phase, as the lock number. If no such stable q-cycle is found the pixel is left unilluminated and therefore appears black in the behaviour portrait. Several examples are shown in Portraits 1 to 3 below. I shall now seek to identify generic properties of the behaviour portrait.

By Theorem 5.4, I observe first that a transformation of the interphase map f which results in the plot of f(x) vs x being rotated 180° about (1/2,1/2) is equivalent to interchanging the parameters $\alpha \rightarrow (1-\alpha)$, $\beta \rightarrow (1-\beta)$. Thus, such a transformation of f effects an equivalent rotation of the behaviour portrait.

Where the plot of f(x) vs x is invariant against such rotation (e.g. Diagram 4.4f) this has the corollary that the behaviour portrait for the associated two-stage circle map must have two-fold rotational symmetry about $(\frac{1}{2},\frac{1}{2})$.

Corollary to Theorem 5.4

If the plot of the interphase map f has rotational symmetry of 2 about $(\frac{1}{2},\frac{1}{2})$ (that is $f(1-x)=1-f(x) \ \forall \ x$) then its associated behaviour portrait P also has rotational symmetry of 2 about its centre point $(\frac{1}{2},\frac{1}{2})$.

Proof

Let the transformation T(f) of the interphase map f be defined by T(f(1-x)) = 1 - f(x). If f(1-x) = 1 - f(x) then

$$T(f(x)) = 1 - f(1-x) = 1 - (1-f(x)) = f(x)$$

so that f is invariant under T which implies that the behaviour portraits P of f and P' of g=T(f) are identical. But by Theorem 5.4, T(f) effects a half turn rotation of the behaviour portrait of f about its centre point $(\frac{1}{2},\frac{1}{2})$. Hence P has a rotational symmetry of 2 about its centre point $(\frac{1}{2},\frac{1}{2})$.

Remarkably, it turns out that rotational symmetry is not restricted to the special case described above. I shall now show that the behaviour portraits yielded by all continuous non-diagonal two-stage circle maps $F_{\alpha,\beta}$ with stable cycles only of order q for each value of the parameters must have two-fold rotational symmetry about the point (½,½). I shall first prove that $F_{1-\alpha,1-\beta}$ has the same number of stable q-cycles as $F_{\alpha,\beta}$ and for this I require two Lemmas. Lemma 5.1 is encompassed by the result of Theorem 3.6 (Chapter3) for q-cycles but I give a separate more compact version here for a q-periodic point.

Lemma 5.1

If x^* is a stable (unstable) *q-periodic point* of a continuous non-diagonal two-stage circle map $F_{\alpha,\beta}$ then it is an unstable (stable) *q-periodic* point of $F_{\alpha,\beta}^{-1}$.

Proof

$$F^{\mathsf{q}}_{\alpha,\beta}(x^{^{\bullet}}) = x^{^{\bullet}} \quad \Longleftrightarrow \quad F^{\mathsf{-q}}_{\alpha,\beta}(x^{^{\bullet}}) = F^{\mathsf{-q}}_{\alpha,\beta}\Big(F^{\mathsf{q}}_{\alpha,\beta}\big(x^{^{\bullet}}\big)\Big) = x^{^{\bullet}} \quad \Longleftrightarrow \quad \left(F^{\mathsf{-1}}_{\alpha,\beta}\right)^{\mathsf{q}}(x^{^{\bullet}}) = x^{^{\bullet}}$$

 x^* a q-periodic point under $F_{\alpha\beta} \Leftrightarrow x^*$ a q-periodic point under $F_{\alpha\beta}^{-1}$

Since the stability of the point x^* is defined $F_{\alpha,\beta}$ and $F_{\alpha,\beta}^{-1}$ must be differentiable at x^* .

Hence $F_{\alpha,\beta}^q$ and $F_{\alpha,\beta}^{-q}$ are differentiable at x^* and so

$$DF_{\alpha\beta}^{q}(x^{*}) < 1 \iff DF_{\alpha\beta}^{-q}(x^{*}) > 1$$

 \therefore x* stable (unstable) under $F_{\alpha,\beta} \Leftrightarrow$ x* unstable (stable) under $F_{\alpha,\beta}^{-1}$

Lemma 5.2

The continuous two-stage circle maps $F_{1-\alpha,1-\beta}^{-1}$ and $F_{\alpha,\beta}^{-1}$ are topologically conjugate.

Proof

$$\begin{split} F_{l-\alpha,l-\beta} &= f^{-1} R_{1-\beta} f R_{1-\alpha} = f^{-1} R_{-\beta} f R_{-\alpha} \\ \text{and} \qquad F_{\alpha,\beta}^{-1} &= \left(f^{-1} R_{\beta} f R_{\alpha} \right)^{-1} = R_{-\alpha} f^{-1} R_{-\beta} f \\ &\therefore \qquad \qquad R_{\alpha} (F_{\alpha,\beta}^{-1}) (R_{\alpha})^{-1} = R_{\alpha} (F_{\alpha,\beta}^{-1}) R_{-\alpha} = f^{-1} R_{-\beta} f R_{-\alpha} = F_{l-\alpha,l-\beta} \end{split}$$

Theorem 5.5

Let $F_{\alpha,\beta}$ be a *continuous non-diagonal* two-stage circle map. $F_{\alpha,\beta}$ and $F_{1-\alpha,1-\beta}$ have the *same number* of stable q-cycles.

Proof

Since $F^q_{\alpha,\beta}$ is everywhere differentiable it must cross the leading 45° diagonal an even number of times, each pair of crossings corresponding to one stable and one unstable q-periodic point of $F_{\alpha,\beta}$

The first line in Lemma 5.1 above shows that $F_{\alpha,\beta}$ and $F_{\alpha,\beta}^{-1}$ have the same set of q-periodic points [revealed in the plots of interphase maps by the fact that $\left(F_{\alpha,\beta}^{-1}\right)^q$ is the reflection of $F_{\alpha,\beta}^q$ in the leading 45° diagonal].

By Lemma 5.1 any stable q-periodic point of $F_{\alpha,\beta}$ must be an unstable q-periodic point of $F_{\alpha,\beta}^{-1}$ and vice versa. Hence $F_{\alpha,\beta}$ and $F_{\alpha,\beta}^{-1}$ must have the same number of stable q-cycles.

Since by Lemma 5.2, $F_{\alpha,\beta}^{-1}$ and $F_{1-\alpha,1-\beta}$ are topologically conjugate they each have the same number of stable q-cycles and hence $F_{\alpha,\beta}$ has the same number of stable q-cycles as $F_{1-\alpha,1-\beta}$.

Theorem 5.5 tells us that for any continuous non-diagonal two-stage circle map, substitution of the parameters α and β respectively with $1-\alpha$ and $1-\beta$, leaves the number of stable q-cycles unaffected. If there are only stable cycles of order q (in fact empirical studies show that only one stable cycle occurs) it immediately follows that

Corollary to Theorem 5.5 (general rotational symmetry of the behaviour portrait) The behaviour portrait of any continuous non-diagonal two stage circle map is always rotationally symmetric about its central point $(\frac{1}{2}, \frac{1}{2})$.

The above Corollary is stated in terms of a theoretical behaviour portrait. In practice the behaviour portrait is constructed using a numerical procedure so that the finescale detail can only be as precise as the rounding accuracy implemented within the procedure. The chosen procedure operates with sequences of iterations. Starting with an initial point located at the centre point of the pixel, an initial run of 10 iterations is made in which each member of the sequence is checked to the specified accuracy (1 part in 105) with the value of the initial point. If no member is found to be equal with the initial point, a second run is commenced, this time starting with the last value of the previous sequence. The same checking procedure is re-performed with the second sequence for a run of up to 20 iterations and the whole process is repeated, run lengths of consecutive sequences being doubled until either a repeat is found or the maximum number of iterations (104) is exceeded (in which case a 'no lock' is registered and the pixel is illuminated in black). Optimal accuracies in terms of minimising the calculation time without loss of resolution of visual detail were empirically found to be those stated above. Greater calculative precision beyond these levels served neither to enhance the finer resolution of the zones outside the lock regions nor their overall form (the resolution is, in any case, limited by the actual minimum size of the pixel).

Locks were formally (and correctly) detected in both the 'near graze' and 'actual graze' situations where the plot of $F^q_{\alpha,\beta}$ crossed and touched with the leading 45° diagonal even where the two-stage circle map was not Morse-Smale (that is, a diffeomorphism with rational rotation number [and hence periodic points by Theorem 3.4] with $\left|Df^q(x^*)\right| \neq 1$ where x^* is a periodic point of prime order q (Devaney 1986)) (see 'Bifurcations' on page 109 and Sketch 1(a) and (b) respectively). Whenever a 'gap' (e.g Sketch 1(c)) occurs, I find that the chosen levels of accuracy for the behaviour portrait are still correct beyond the visual resolution of the corresponding plot of $F^q_{\alpha,\beta}$ for a given parameter pair (α,β) .

5.3 CONDITIONS FOR SYNCHRONISATION

Observe that because two-stage circle-map $F_{\alpha,\beta}$ is a circle homeomorphism, I need only show that a periodic point exists to establish that all orbits must converge asymptotically towards periodic points and thus that synchronisation to a q-cycle must eventually occur (e.g de Melo & van Strien 1992 or see Section 3.3).

If $F_{\alpha,\beta}$ has a stable *fixed* point (i.e. only one periodic point) then the orbits produced by iterating it tend towards a state in which each generation of a particular lineage is replaced by its successor at the same point in the environmental cycle. If $F_{\alpha,\beta}$ has a stable q-periodic point then the orbits tend towards a stable cycle in which the changeover between generations takes place at the same phase every q generations. The existence of this form of attractor (a stable q-cycle) is indicated by the q^{th} iterate of the map $(F_{\alpha,\beta}^q)$ possessing a group of q (distinct) stable periodic points, each of which is a solution of $\theta = F_{\alpha,\beta}^q(\theta)$ and represents the phase at which one generation gives way to its successor. When $F_{\alpha,\beta}$ and hence $F_{\alpha,\beta}^q$ are strictly increasing non-diagonal homeomorphisms, each stable periodic point must be accompanied by a companion unstable periodic point. Thus if $F_{\alpha,\beta}$ exhibits m q-cycles the defining equation $\theta = F_{\alpha,\beta}^q(\theta)$ must have exactly 2mq solutions.

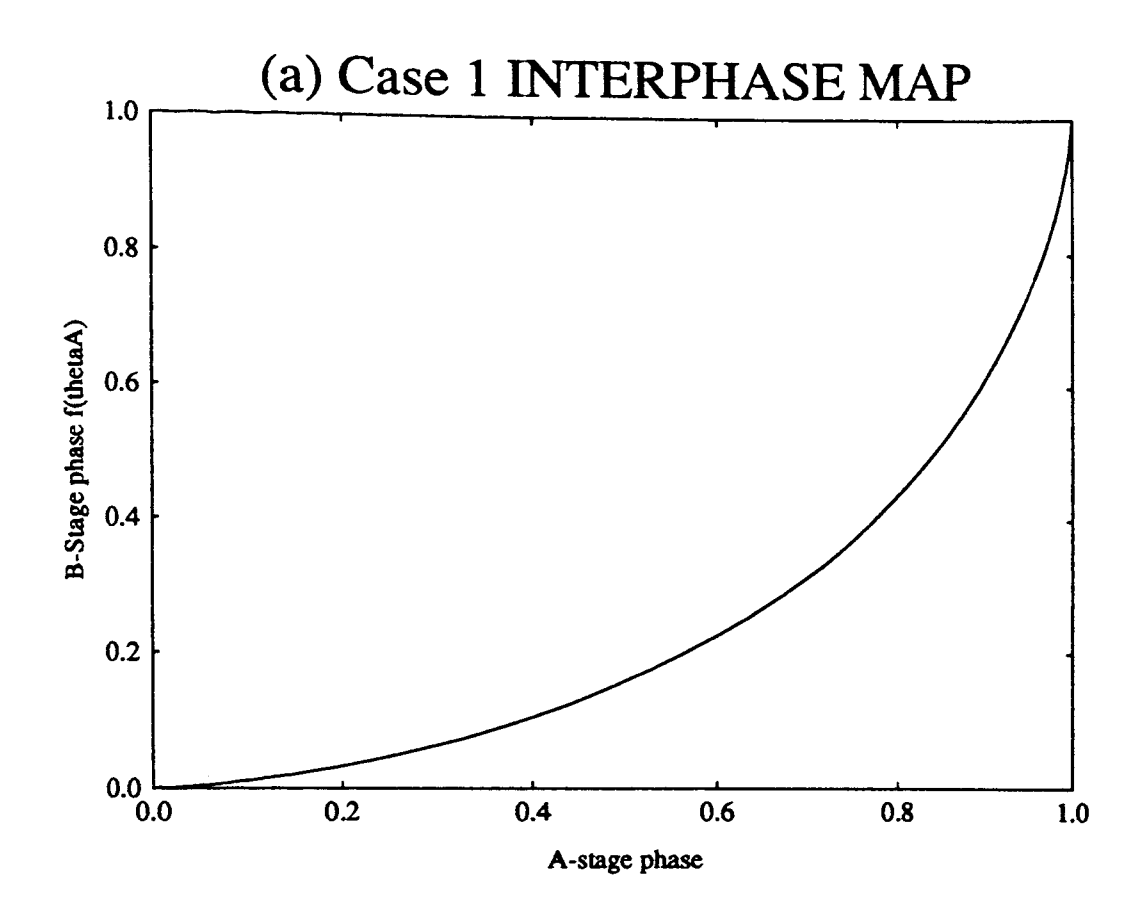
In line with empirical observations, I henceforth assume that any particular instance of a class of maps $F_{\alpha,\beta}$ derived from a given interphase map f has at most only a single stable q-cycle (m=1). I shall characterise the properties of that instance by the lock-number (the number of periodic points in that single stable q-cycle). Under what conditions does $F_{\alpha,\beta}$ have such periodic points that is, $\exists \theta^*$ such that $\theta^* = F_{\alpha,\beta}^q(\theta^*)$?

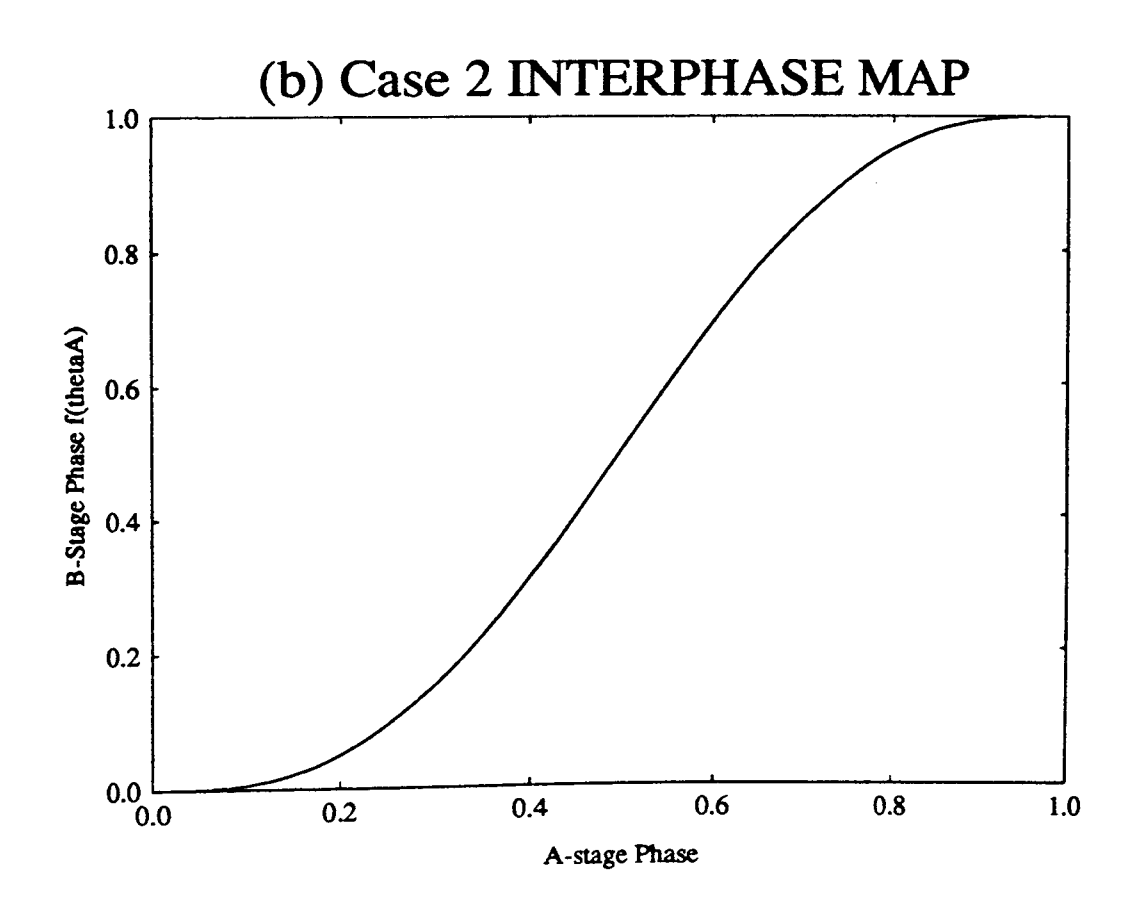
Case 1 and Case 2 generic patterns of development revisited

I now state two theorems which give necessary and sufficient conditions on the stage durations α and β in order for two-stage circle maps derived from the two broad classes of interphase map corresponding to Case 1 and Case 2 in section 4.4 to have a stable one-lock (that is a stable *fixed* point (periodic point of period 1)). The plots of the interphase maps for each Case are shown in Diagrams 5.2(a) and (b) respectively. The proof of these theorems is given in the Appendix A5.1.

Let $F_{\alpha,\beta}$ be a two-stage circle map composed from f according to equation 4.10.

Diagram 5.2





Theorem 5.6 (Case 1)

Let f be an interior differentiable interphase map satisfying Df >0 and D²f >0 \forall x. $F_{\alpha,\beta}$ has a stable fixed point iff

$$1 - f(\alpha^*) > \beta^* > f(1 - \alpha^*)$$
 (5.3)

Theorem 5.7 (Case 2)

Let f be a differentiable interphase map satisfying $f(1-x)=1-f(x) \ \forall \ x$; $Df(x)>0 \ \forall \ x$; $D^2f(x)>0$, $0 \le x < \frac{1}{2}$; $D^2f(\frac{1}{2})=0$; $D^2f(x)<0$, $\frac{1}{2}< x < 1$. $F_{\alpha,\beta}$ has a stable fixed point iff

$$1 - 2f(\alpha^*/2) > \beta^* > 2f((1 - \alpha^*)/2)$$
 (5.4)

Theorem 5.6 gives the condition for a one-lock in any two-stage circle map derived from an interphase map which is strictly increasing and strictly concave (i.e. has positive curvature and lies below the leading 45° diagonal). Diagram 4.4 (sequence (a) to (c)) shows that this interphase map shape results from a simple lag between the season of peak development rate for the B-stage and that for the A-stage. The converse biological situation, in which A-stage development lags B-stage development, will produce an interphase map which is strictly increasing and strictly convex. Any such interphase map can be changed into one to which Theorem 5.6 applies by reflection in the 45° diagonal. It is a corollary of Theorem 5.6 that the one-lock condition for such a map is simply inequality (5.3) with the inequalities reversed.

Corollary to Theorem 5.6

If $D^2 f < 0 \forall x$ in Theorem 5.6 then $F_{\alpha\beta}$ has a stable fixed point iff

$$1 - f(\alpha^*) < \beta^* < f(1 - \alpha^*)$$
 (5.5)

Proof

By Theorem 5.3, interchanging f with f $^{-1}$ and substituting α and β with β and α respectively in inequality (5.3) leaves the dynamic behaviour of $F_{\alpha,\beta}$ unaltered.

Now $D^2f < 0 \Leftrightarrow D^2f^{-1} > 0$ so that by Theorem 5.6

$$1-f^{-1}(\beta^*) > \alpha^* > f^{-1}(1-\beta^*)$$

$$\vdots \qquad 1-\alpha^* > f^{-1}(\beta^*) \text{ and } f(\alpha^*) > 1-\beta^*$$

$$\Leftrightarrow f(1-\alpha^*) > \beta^* > 1-f(\alpha^*)$$
or
$$1-f(\alpha^*) < \beta^* < f(1-\alpha^*)$$

Theorem 5.7 gives the one-lock condition for a two-stage circle map derived from an interphase map which is a symmetrical, initially concave S-shape (i.e. the interphase map is rotationally symmetrical about (½,½), lies below the leading diagonal for 0≤x<½, crosses the diagonal at x=½ and lies above the diagonal for ½<x<1). This interphase map shape arises when B-stage development occurs over a more restricted portion of the environmental repeat cycle than A-stage development, but peak development rates occur at more or less the same time as shown in Diagram 4.4 sequence (d) to (f). Clearly, the converse situation, in which A-stage development is possible for only a brief part of the cycle, and B-stage development for a more extended period, can be represented by inverting the generic interphase map. This again leads to a one-lock condition identical to that of Theorem 5.7 with the inequalities reversed.

Corollary to Theorem 5.7

If $D^2f(x)<0$, $0 \le x < \frac{1}{2}$; $D^2f(\frac{1}{2})=0$; $D^2f(x)>0 \frac{1}{2}< x < 1$ in Theorem 5.7 then $F_{\alpha,\beta}$ has a stable fixed point iff

$$1 - 2f(\alpha^*/2) < \beta^* < 2f((1 - \alpha^*)/2)$$
 (5.6)

Proof

By Theorem 5.3, interchanging f with f^{-1} and substituting α and β with β and α respectively in inequality (5.4) leaves the dynamic behaviour of $F_{\alpha\beta}$ unaltered.

Now $D^2f < (>)0 \Leftrightarrow D^2f^{-1} > (<)0$ so that by Theorem 5.7

$$1 - 2f^{-1}\left(\frac{\beta^{*}}{2}\right) > \alpha^{*} > f^{-1}\left(\frac{1 - \beta^{*}}{2}\right)$$

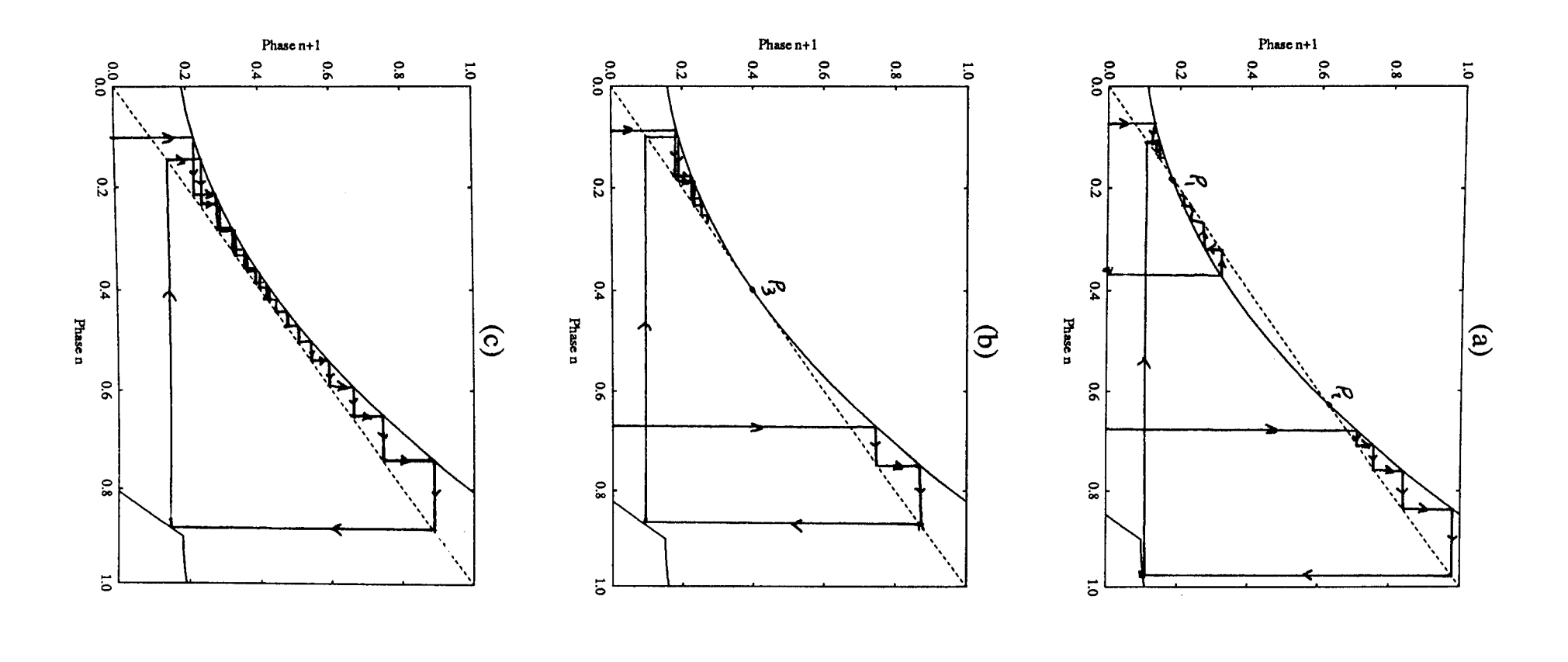
$$\Leftrightarrow 2f\left(\frac{1 - \alpha^{*}}{2}\right) > \beta^{*} \text{ and } f\left(\frac{\alpha^{*}}{2}\right) > \left(\frac{1 - \beta^{*}}{2}\right)$$
or
$$1 - 2f\left(\frac{\alpha^{*}}{2}\right) < \beta^{*} < 2f\left(\frac{1 - \alpha^{*}}{2}\right)$$

I note that both the regions of one-lock defined by inequalities (5.3) and (5.4) display the rotational symmetry about (½,½) implied by Theorem 5.5, for if I write $h(\alpha^*) = 1 - f(\alpha^*)$ in the LHS of (5.3) then the RHS

$$f(1-\alpha^*) = 1 - (1-f(1-\alpha^*)) = 1 - h(1-\alpha^*)$$

which proves that the one lock boundary in the lower part of the behaviour portrait is the rotational image of the upper boundary. By a similar argument, the same is true for (5.4).

Sketch 1



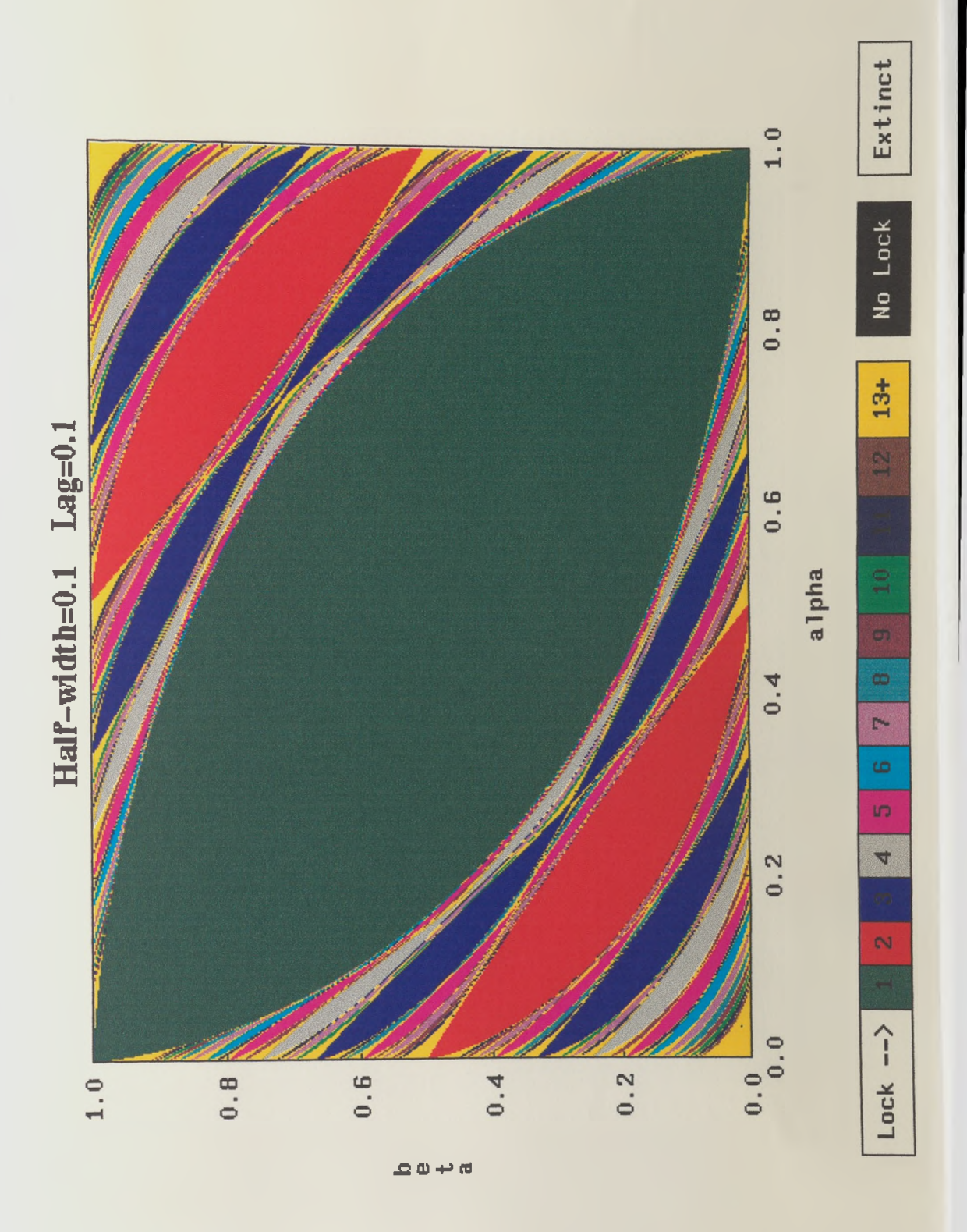
I note furthermore that the width of the region which each inequality defines is determined in a general sense by the non-linearity of the interphase map. In particular, if the interphase map becomes the 45° diagonal, (that is A-stage and B-stage physiological times become identical) the one-lock region formally disappears. However, if I extend Theorems 5.6 and 5.7 to include neutrally stable fixed points (by allowing equality in inequalities (5.3) and (5.4)) then the identity interphase map causes the "non-unstable one-lock" region to collapse to the line $\beta^*=1-\alpha^*$, which is the condition for a neutrally stable fixed point in a single stage model with stage length $\alpha^*+\beta^*$.

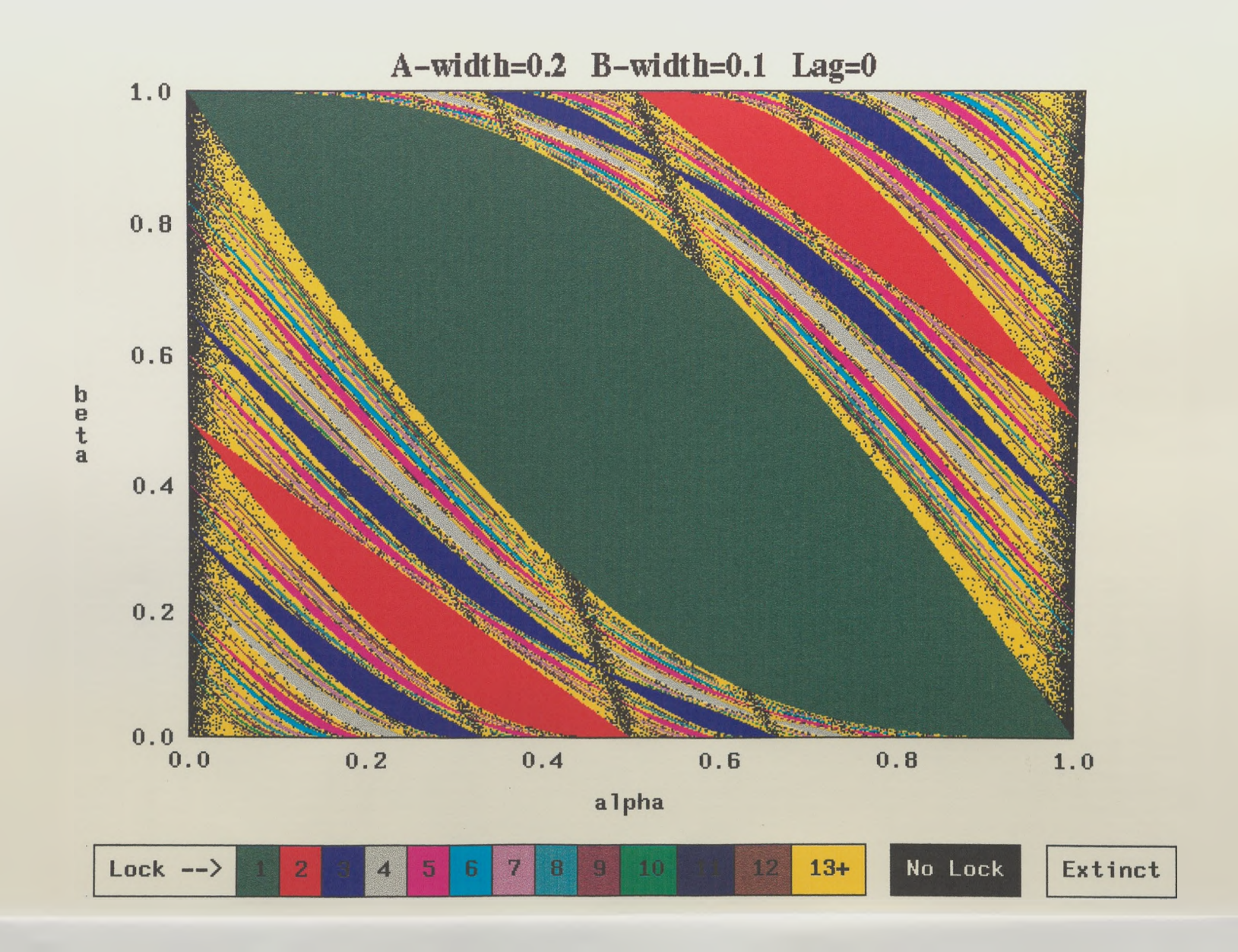
Bifurcations

Where bifurcations occur that is, where the dynamics change suddenly for small changes in the values of α^* and β^* (near the boundaries of lock regions), the distinction between (biologically less interesting) higher ordered lock and no lock (yellow or black for colour choice of associated pixel) is dependent on the levels of calculative accuracy chosen. Such bifurcations correspond to the plot of $F^q_{\alpha,\beta}$ passing through a transition as α^* and β^* are varied in which a 'graze' of some part of the plot occurs with the leading 45° diagonal. Passage through such a transition is helpfully envisaged in three stages with the use of "cobwebs" as shown in the example of Sketch 1. Note that $F_{\alpha,\beta}$ is not Morse-Smale here (Devaney 1986).

In (a) P_1 is a stable (attracting) fixed point because $DF_{\alpha,\beta}(P_1)$ <1 and P_2 is an unstable (repelling) fixed point because $DF_{\alpha,\beta}(P_2)$ >1. A small change in the parameter β^* results in the two points P_1 and P_2 'fusing' together to form a plot which just grazes the leading 45° diagonal at the single point P_3 as shown in (b). Simple cobwebs starting with an initial point located on either side of P_3 easily show that it is stable from the left but unstable from the right. Effectively this is a stable point because the closed topology of the circle ensures that the trajectory eventually returns from the left and is ultimately attracted to P_3 . As β^* is changed by a further small increment, situation (c) occurs in which a gap appears in the plot between the curve and the leading 45° diagonal so that a low-ordered lock is no longer possible and the corresponding pixel is either illuminated in yellow (if a lock occurs within 105 iterations) or black (if not).

Portraits 1 Associated behaviour portraits of Diagram 5.2 (a) Case 1 for systems with both development rate functions having a standard deviation of 0.1T and a lag 0.1T (b) Case 2 for systems where both development rate functions are centered at 0.5T with the stage-A development rate function having a standard deviation of 0.1T and stage-B having a standard deviation of 0.2T.





5.4 NUMERICAL INVESTIGATIONS OF CASE 1 AND CASE 2

In the previous section I discussed necessary and sufficient conditions for the orbits generated by two-stage circle maps composed from a subset of possible interphase map shapes, to converge ultimately to a single fixed point. However, even for this sub-set I have been unable to derive equivalent results for more complex locking behaviour. Special forms of the interphase map sometimes make it possible to derive such conditions but the resulting expressions are seldom very illuminating. I shall now utilise the associated behaviour portrait to circumnavigate this analytic intractability

(a) CASE 1 (Lag between development functions)

I first reconsider the earlier case in which the stage A and stage B development rate functions are shaped like truncated Gaussians (Normal distributions), each with the same width, but with a time lag between the peaks. In the specific example illustrated earlier in Diagram 4.4(a) the standard deviation of each distribution is 10% of the environmental period, leading to significant growth over some 50% of the environmental cycle. When the stage B development rate peak lags the stage A peak the resulting interphase map is strictly concave as shown reproduced in Diagram 5.2(a). The converse situation (stage B leads stage A) would produce an interphase map whose plot is the reflection of Diagram 5.2(a) in the 45° diagonal. Theorem 5.3 shows that I do not need to study this case separately.

Although I cannot write down a closed form for the interphase map in this case, the range of β^* over which one-lock occurs can be obtained from Diagram 5.2(a) and Theorem 5.6 for any desired value of α^* , thus allowing me to confirm the accuracy of my computational method. Portrait 1(a) shows the behaviour portrait obtained for the interphase map of Diagram 5.2(a) which corresponds to a lag of 10% of the environmental cycle.

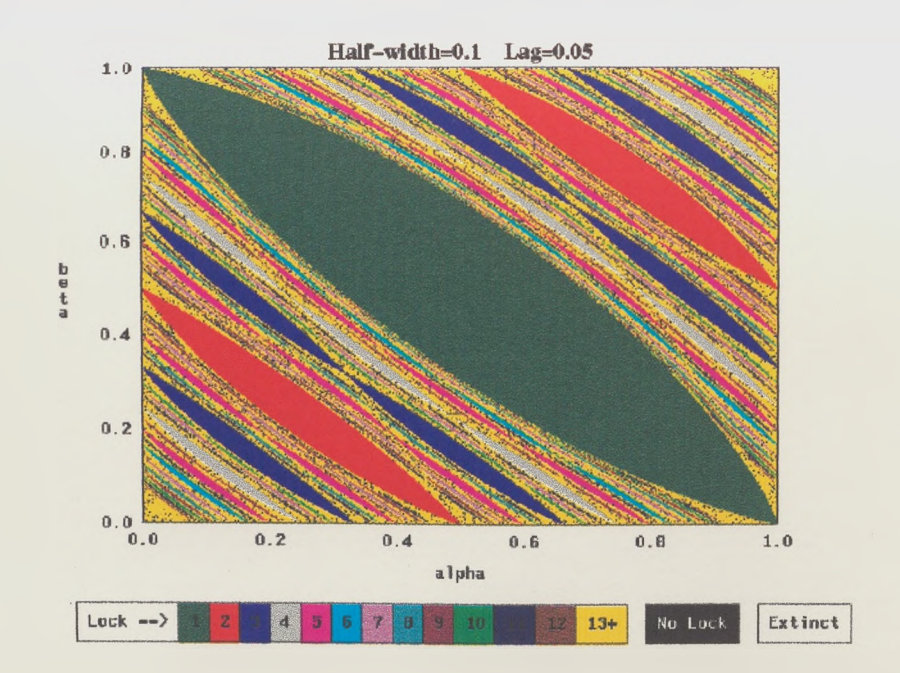
I observe first that the whole behaviour portrait shows the two-fold rotational symmetry required by Theorem 5.5, so I restrict further consideration to the triangle below the diagonal running from (0,1) to (1,0). Outside the one-lock region I see that virtually the whole of the remaining area is filled with colors indicating lock-numbers in the range 2-12, with the most significant regions being 2- and 3-locks. Only very small areas near the borders produce very complex locks (>12 iterations per cycle) and the only observable failures to detect an attractor occur on or very close to the boundaries of lock regions, where we expect neutral stability.

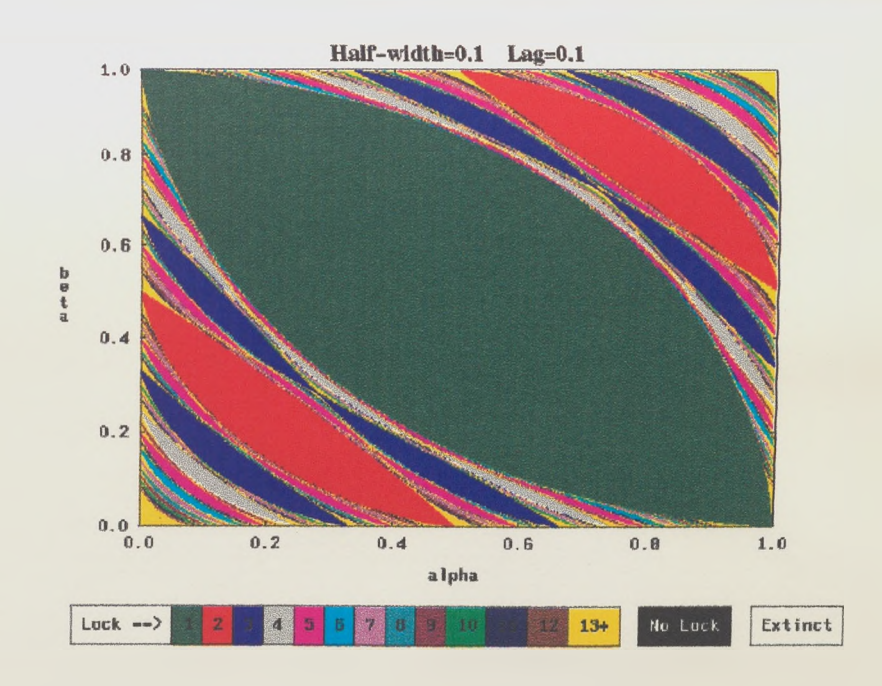
In Portraits 2 I show the variation of the behaviour portrait as the lag between two otherwise identical Gaussian development functions is varied. Portrait 2(b) shows the behaviour portrait first displayed in Portrait 1(a).

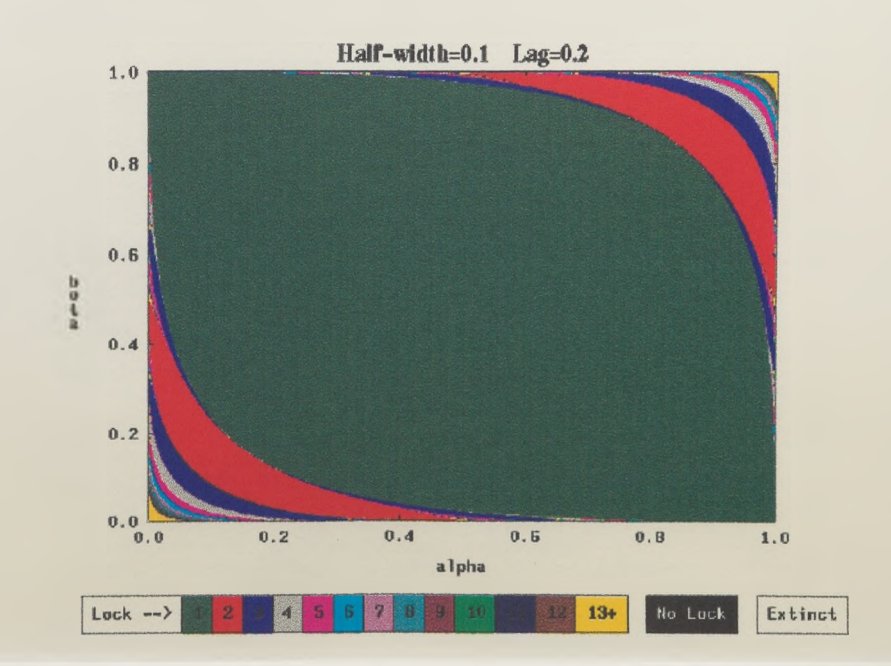
In Portraits 2(a) and (c) I show the result of respectively halving and doubling the lag. As I would expect, doubling the lag (and increasing the non-linearity of the interphase map) greatly increases the area over which one-locks occur. The remainder (<25%) of the (α,β) plane is mainly occupied with 2- and 3-locks. Halving the lag (Portrait 2(a)) causes the expected reduction in the area of the 1-, 2- and 3-lock regions, with a very significant proportion of the total area exhibiting complex locks with greater than 12 iterations. This reduction in the "strength" of the synchronisation is accompanied by the appearance of a significant concentration of points (marked in black) at which no repeat cycle can be detected. Since the two-stage circle maps discussed in this paper are all invertible and thus cannot produce chaos, this behaviour must indicate neutral stability, cycles longer than 10^3 or so points, or transients longer than 10^4 iterations. Detailed numerical investigation of a sub-set of these points indicates that they occur at or very close to points of neutral stability.

Finally I investigated the robustness of the results shown in Portraits 2. As I would expect from Theorem 1, lateral displacement of both growth peaks modulo T (equivalent to a change of the origin of timescale) has no effect on the behaviour portrait. Likewise, lateral displacement with simple truncation at zero and one (rather than a true modulo T displacement) has no detectable effect until intersection with the beginning or end of the environmental period begins to make a significant alteration in the overall shape of the development peaks. Lastly, I find that (again as one would expect) the nature of the behaviour portrait is dependent only on the ratio of the lag to the half-width rather than on the value of these two quantities separately.

Portraits 2 The effect of changes in development lag on a system with two equal-width Gaussian development rate functions. All frames show behaviour portraits for systems with both development functions having a standard deviation of 0.1T. Top left frame: lag = 0.05T, Top right frame: lag 0.1T, Bottom frame: lag 0.2T.







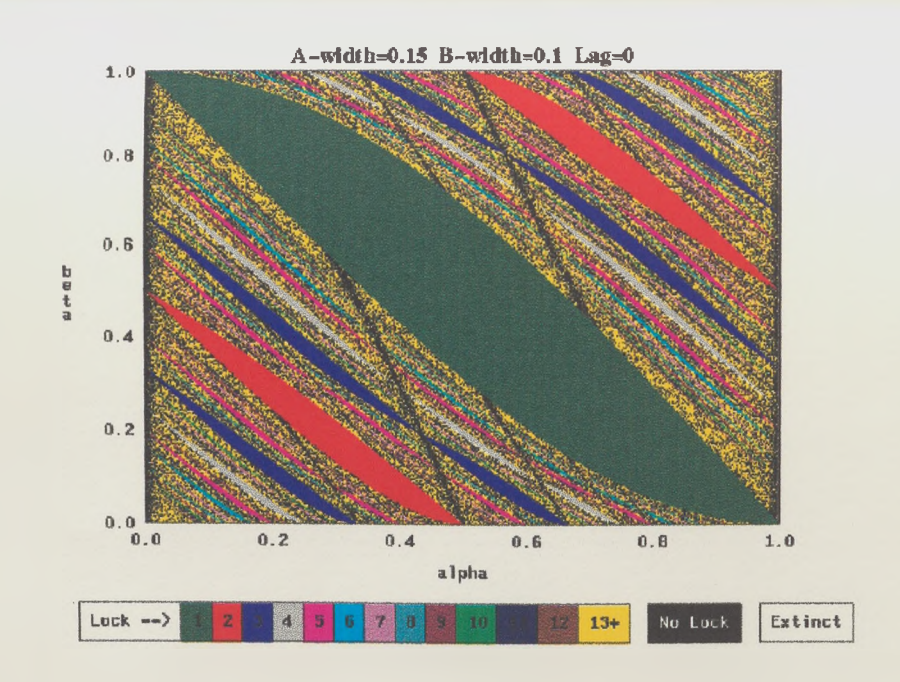
(b) CASE 2 (Differing length of growing season)

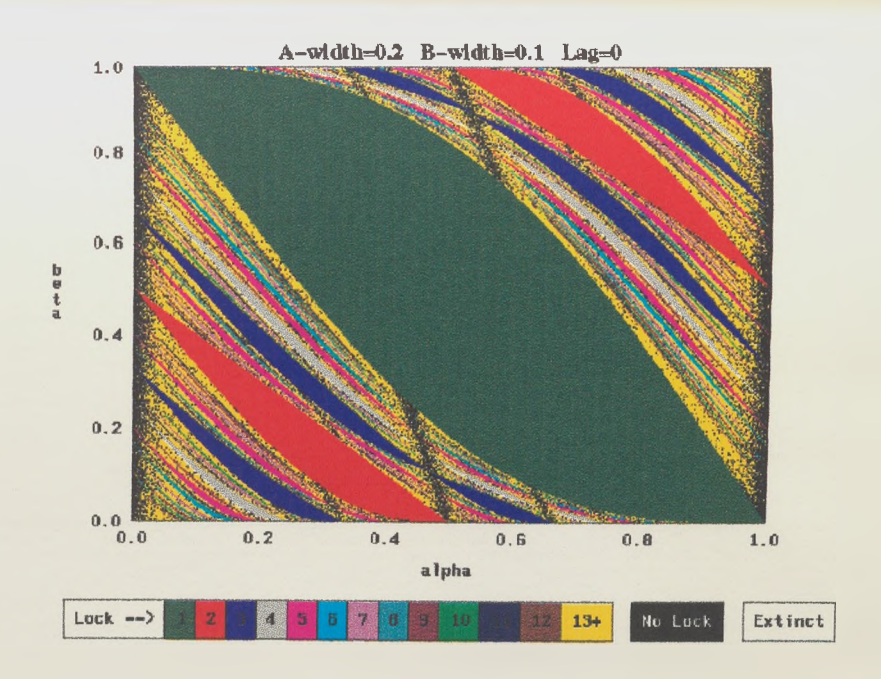
I next investigated the second biological situation illustrated earlier in Case 2 (Diagram 4.4(d)-(f)). Here the two development rate functions are still shaped like truncated Gaussians, but their peaks are at the same point, and they differ in width. In the situation illustrated, the B-stage development peak is narrower than that for the A-stage, leading to an intially concave, symmetrical S-shaped interphase map shown earlier in Diagram 4.4(f) (now reproduced in Diagram 5.2(b). Reversing the position, simply turns the interphase map into its own inverse. Theorem 5.3 again tells us that we need not investigate this possibility separately. Portrait 1(b) shows the behaviour portrait obtained for the interphase map shown in Diagram 5.2(b).

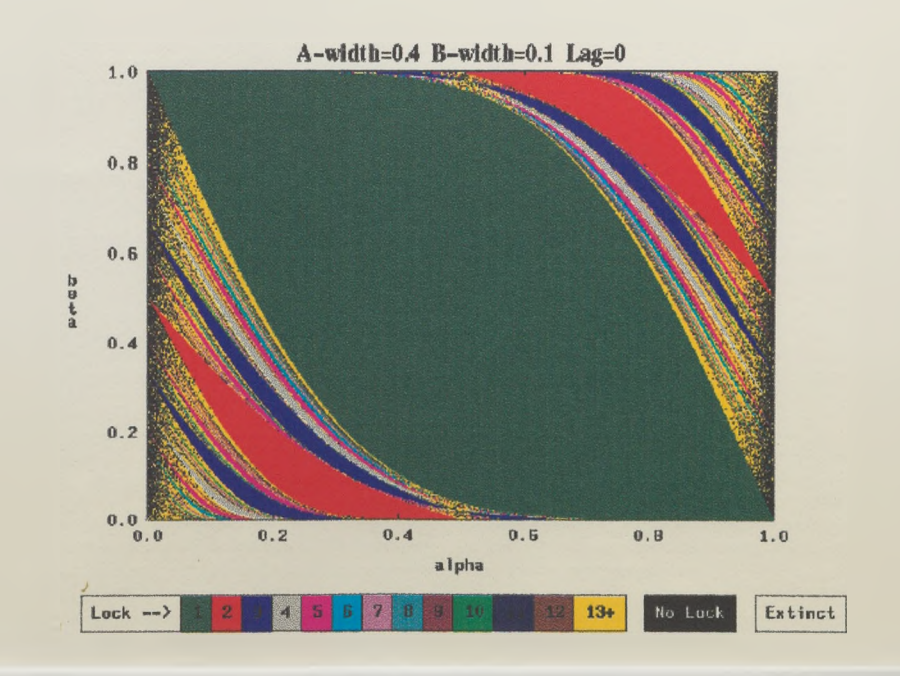
As we might expect from a comparison of Diagrams 5.2(a) and 5.2(b) the size of the one-lock region for this case is slightly smaller than the equivalent region in Portrait 1(a), with a somewhat greater reduction being evident in the areas of the 2-lock and 3-lock regions. However, the most noticeable difference between Portraits 1(a) and 1(b) is that the S-shaped interphase map gives rise to a noticeably greater area of complex locks, and shows a number of high concentrations of neutrally stable points, especially close to the α =0 and α =1 borders.

Portraits 3 shows the effect of varying the width of the A-stage growing season with the B-stage peak width held constant. Portrait 3(b) shows the behavour portrait first displayed in Portrait 1(b). Changes in the relative width of the two development peaks shown in Portraits 3(a) and 3(c) produce the expected changes in the strength of synchronisation, with increasing (decreasing) A-stage width increasing (decreasing) the area of the 1-, 2- and 3-lock regions. However, I notice that in all cases the ratio of the size of the multiple-lock regions to the size of the one-lock region is lower and the concentration of neutrally stable points is higher than that shown by circle-maps composed from a purely concave interphase map.

Portraits 3 The effect of changes in relative development function width on a system with two Gaussian development rate functions. All frames show behaviour portraits for systems with both development functions centered at 0.5T and with the stage-A development function having a standard deviation of 0.1T. Top left frame: s.d. A=0.15. Top right frame s.d. A=0.2, Bottom frame s.d. A=0.4.







5.5 DISCUSSION

Although the physiological time formulation has yielded a very concise model description, the dimensionless parameters α and β 'feel' inherently uncomfortable. This discomfort stems from the fact they do not easily translate into directly meaningful biological terms. In this chapter I have shown that the discomfort can nevertheless be alleviated by digesting a behaviour portrait which has the ubiquitous merit of displaying the full range of dynamic behaviour of $F_{\alpha\beta}$ as a single snapshot in the (α,β) -plane. The behaviour portrait grants us that desired biological feel in accordance with the Usher (1976) guidelines of Section 0.4. Each individual lock region clearly shows the values of α and β for which (asymptotically) stable cycles exist and hence when synchronization occurs in the model. I have conjectured that neutral stability only occurs on the boundaries of these regions.

Whereas the two stage circle maps $F_{\alpha,\beta}$ and its inverse $F_{\alpha,\beta}^{-1}$ must always have the same identical set of periodic points (because they are both continuous), when $F_{\alpha,\beta}$ is a diffeomorphism this entire set necessarily partitions into two equal size sets made up of stable and unstable periodic points respectively. Because only *one* stable cycle exists, the set of stable (unstable) periodic points collectively forms the stable (unstable) cycle and since $F_{\alpha,\beta}^{-1}$ is topologically conjugate to $F_{1-\alpha,1-\beta}$ this automatically implies that the behaviour portrait must be rotationally symmetric. I conjecture that this geometric property also extends to the more general situation in which $F_{\alpha,\beta}$ is a homeomorphism or the limiting case of one (that is when either of the development rate functions g_A or g_B are held at zero for a finite interval of real time). In the next chapter we shall see that this is indeed so for a particular two stage life cycle model composed from such an interphase map.

I still wish to investigate higher ordered locking behaviour more fully. Most of the analytic intractability that has been encountered so far, results from the nonlinearity of the interphase map. In classic fashion I shall first carry out a more complete investigation of higher ordered locking behaviour by appealling to the simpler situation in which the interphase map is reduced to a simple linear case.

CHAPTER 6

AN INVESTIGATION OF THE SLIM CIRCLE MAP MODEL

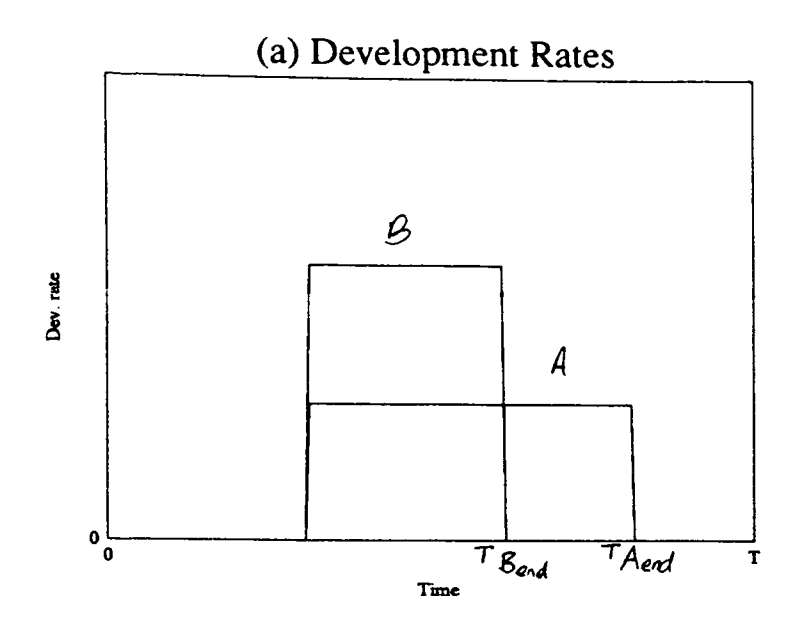
6.0 INTRODUCTION

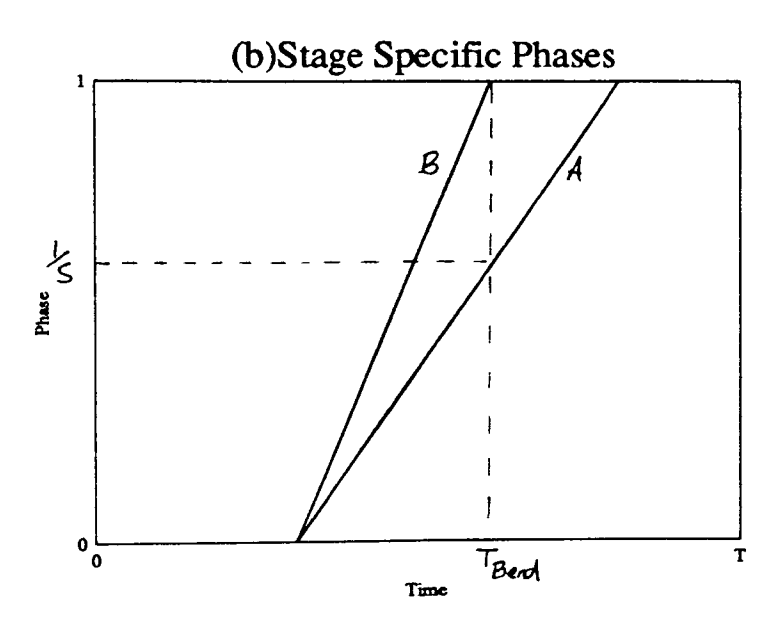
The numerical investigations of section 5.4 have revealed that the behaviour portrait in the (α,β) -plane is made up of separate lock regions together with areas or points of 'no lock' inbetween. The shape of the lock regions was found to be related to the shape of the interphase map. In two separate but broad classes of nonlinear interphase map, we have seen that the corresponding region for the simplest lock (a 1 lock), consists of the interior of a central zone situated between a pair of boundary conditions. I have proved that this whole zone corresponds to conditions which are expressable concisely in terms of the interphase map.

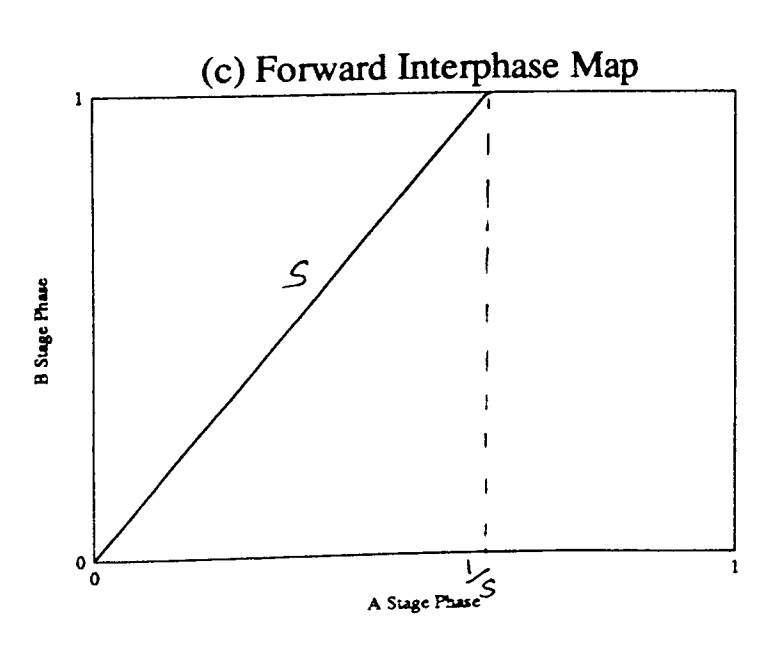
Although higher lock regions can be readily obtained by numerical procedures for any two stage circle map composed from a nonlinear interphase map, beyond a 1 lock their algebraic derivation rapidly becomes intractable. Progress in the analysis of higher ordered locking behaviour can be achieved without arduous algebraic tedium by focusing on the dynamics that result when the interphase map is reduced to a single straight line. However this necessitates a relaxation of the previously held (homeomorphic) requirement that zero development rate over a finite interval cannot occur. In this Chapter I investigate a circle map model which is composed from such an interphase map whose plot consists of a single straight line. Without loss of generality I choose the slope S >1 as shown in Diagram 6.1(c) and henceforth refer to the model as the SLIM (Single Line Interphase Map) circle map. I show that for this model, higher-order conditions and associated lock regions can be derived in straightforward algebraic terms. I also show that whole classes of itineraries correspond with separate regions of the associated behaviour portrait and these in turn give insight into the biological implications of various life cycle strategies.

Strictly speaking, the single line 'interphase map' is not an interphase map in the true sense (Chapter 4) since it is not single valued (one-to-one) throughout the entire unit phase circle. Consequently, neither it nor the SLIM circle map are invertible and (consequently also) neither of these maps are homeomorphisms. The SLIM circle map is therefore not a two stage circle map in the usual sense so that much of the theory developed over the past few chapters does not *automatically* apply. However, I circumnavigate most of these potential difficulties by viewing SLIM as the limiting case of a two piece linear homeomorphism TLIM (Two Line Interphase Map). I am then able to show that the SLIM circle map model still obeys the more salient properties of a continuous two stage circle map.

Diagram 6.1







6.1 BIOLOGICAL INTERPRETATION

An immediate benefit of reducing the interphase map to a straight line is the transparency with which the life cycle can be related to its constituent development rate functions. The SLIM circle map model corresponds to a life cycle in which the development rate in each stage takes the form of "top-hat" functions which match each other at the same point in the periodic cycle as illustrated in Diagram 6.1(a). Observe that altering the (strictly positive) height of the top hats would have no effect on the interphase map and also that only the ratio of their widths affects the slope S. Without loss of generality, I henceforth assume that the width of the A stage development function is the greater of the two stages which implies that the slope S of the *forward* interphase map (A→B) is greater than 1. Observe that in both stages development during the periodic cycle must either proceed at a fixed positive value or not at all (zero). This kind of developmental response is exhibited in the life cycles of many photosynthetic cells when exposed to alternating periods of light and dark (Nelson & Bland 1979, Spudich & Sager 1980).

Intuitively it is clear how life cycle synchronisation can be induced in a population of individuals that exhibit such a response to external periodic forcing. The key synchronising effect is produced by the *intervals* during which development rate is held at zero. These ensure that an individual's development is held back until a single point in time (the endpoint of the interval) is reached. A group of individuals recruited to a stage in such an interval are thus promoted from it simultaneously and lineages which stem from their progeny are thereafter perfectly synchronised. I observe that this can happen in two ways depending on whether the stage recruitment occurs in the A stage of B stage interval. Those individuals commencing their life cycle during the interval when A stage development rate is zero must wait until the start of the next environmental repeat cycle at which point they all begin their life cycles *together*. Alternatively, those individuals promoted out of the A stage during the interval when B stage development rate is zero, simultaneously restart development in the B stage, *together*. In both cases, emergences of all subsequent progeny are thereafter perfectly synchronised.

The intuitive argument of the above paragraph does not give the complete picture. In particular it is not clear whether synchronisation must (if at all) occur in all sequences or permutations of emergences. I do not know whether the progeny in every lineage must necessarily emerge within an interval of zero development and so eventually

become synchronised. Even where synchronisation does occur, I am unable to determine the repeat length of the respective cycle of emergences and have only a limited understanding of the overall qualitative or quantitative dynamics which may occur. In due course I shall address these aspects in the following analysis.

6.2 THE SLIM CIRCLE MAP

I compose the SLIM circle map $\tilde{F}_{\alpha,\beta}$ in usual two stage circle map fashion (by equation 4.10) from the SLIM map \tilde{f} together with an appropriate 'inverse' \tilde{f}^{-1} . I shall now establish an algebraic relationship between the phase emergences of successive generations.

Choosing to work in A-stage phase θ_A , I shall now derive an expression for the relationship between the emergences of successive generations at phases θ_{An} and $\theta_{A(n+1)}$

By definition of the SLIM circle map

$$\theta_{A(n+1)} = \tilde{F}_{\alpha,\beta}(\theta_{An}) \tag{6.0}$$

with

$$\tilde{\mathbf{F}}_{\alpha,\beta} = \tilde{\mathbf{f}}^{-1} \mathbf{R}_{\beta} \tilde{\mathbf{f}} \, \mathbf{R}_{\alpha} \tag{6.1}$$

and f defined by

$$\theta_{\rm B} \equiv \tilde{\mathbf{f}}(\theta_{\rm A}) = \begin{cases} S\theta_{\rm A} & 0 \le \theta_{\rm A} < \frac{1}{S} \\ 0 & \frac{1}{S} \le \theta_{\rm A} < 1 \end{cases} , \tag{6.2}$$

where S>1 is the gradient of the single line. I observe that \tilde{f} is not invertible because it is not one-to-one over the entire second segment $[\frac{1}{S},1)$ (all points in this part of the domain are contracted to a single point). Because this segment corresponds with that part of the environmental repeat cycle during which B stage development rate is held at zero, emergence from the life cycle into it is (in any event) not biologically possible. I shall henceforth refer to the segment $[\frac{1}{S},1)$ as the 'non-emergence' phase segment.

For the first segment $[0,\frac{1}{5})$ however, I can still define an 'inverse' map \tilde{f}^{-1} which will have the invertible property $\tilde{f}\,\tilde{f}^{-1}(x)=\tilde{f}^{-1}\tilde{f}(x)=x$, $\forall\,x\in[0,\frac{1}{5})$ by

$$\theta_{A} = \tilde{f}^{-1}(\theta_{B}) \equiv \frac{1}{S}\theta_{B}$$
 , $0 \le \theta_{B} < 1$ (6.3)

Substituting for \tilde{f} and \tilde{f}^{-1} in equation (6.1), I obtain the circle map

$$\theta_{A(n+1)} = \tilde{F}_{\alpha,\beta}(\theta_{An})$$

$$= \tilde{f}^{-1}R_{\beta}\tilde{f}R_{\alpha}(\theta_{An})$$

$$= \frac{1}{S} \left[\left(\beta + S(\theta_{An} + \alpha)^* \right)^* \right] \quad \text{for} \quad 0 \le (\theta_A + \alpha)^* < \frac{1}{S}$$

$$= \frac{\beta^*}{S} \qquad \text{for} \quad \frac{1}{S} \le (\theta_A + \alpha)^* \le 1$$

$$= \frac{\beta^*}{S} \qquad (6.5a)$$

But

$$(\beta + S(\theta_{An} + \alpha)^*)^* = (\beta^* + S(\theta_{An} + \alpha^*)^*)^*$$

$$= \beta^* + S(\theta_{An} + \alpha^*)^* \quad \text{for } (\theta_{An} + \alpha^*)^* < \frac{1 - \beta^*}{S}$$

$$= \beta^* + S(\theta_{An} + \alpha^*)^* - 1 \quad \text{for } (\theta_{An} + \alpha^*)^* \ge \frac{1 - \beta^*}{S}$$
(6.6b)
$$= \beta^* + S(\theta_{An} + \alpha^*)^* - 1 \quad \text{for } (\theta_{An} + \alpha^*)^* \ge \frac{1 - \beta^*}{S}$$
(6.6c)

so that equations (6.5) can be written as

$$\theta_{A(n+1)} = \frac{\beta^*}{S} + (\theta_{An} + \alpha)^* \qquad \text{for } 0 \le (\theta_{An} + \alpha^*)^* < \frac{1-\beta^*}{S} \qquad (6.7a)$$

$$= \frac{\beta^* - 1}{S} + (\theta_{An} + \alpha)^* \quad \text{for } \frac{1-\beta^*}{S} \le (\theta_{An} + \alpha^*)^* < \frac{1}{S} \qquad (6.7b)$$

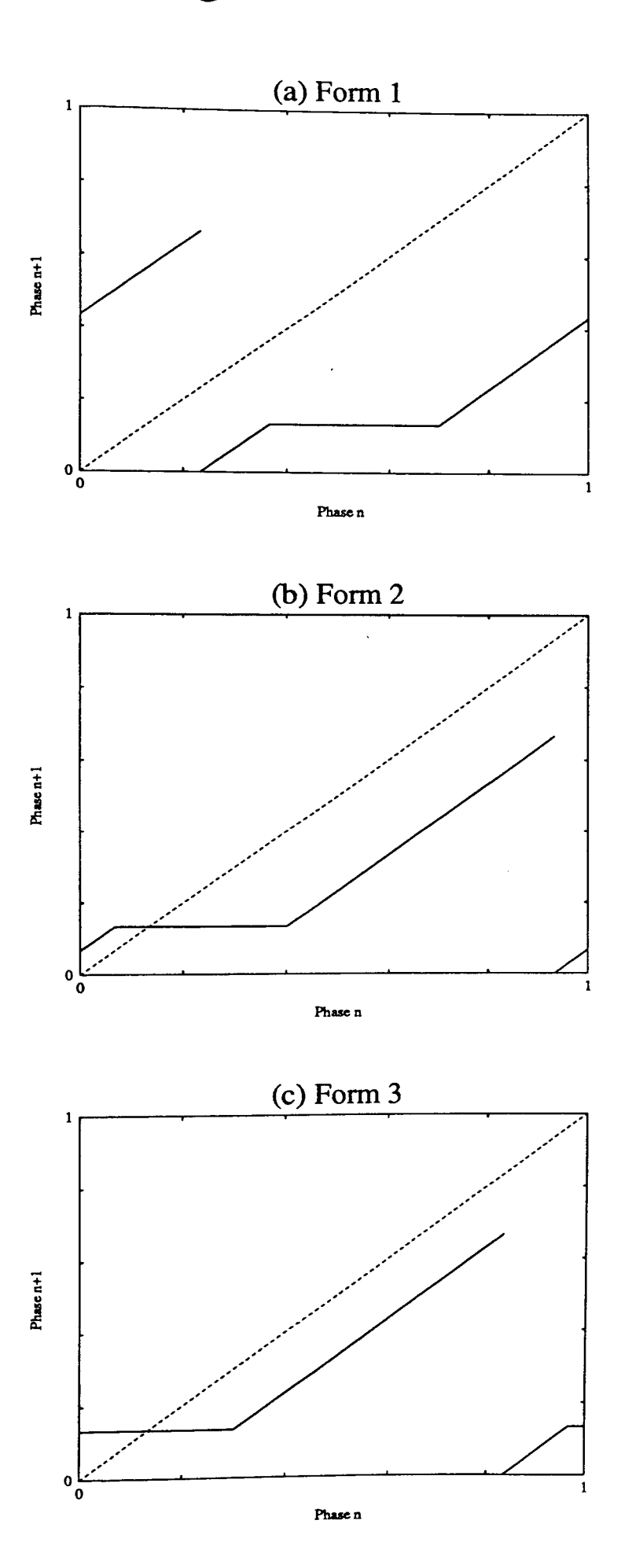
$$= \frac{\beta^*}{S} \qquad \qquad \text{for } \frac{1}{S} \le (\theta_{An} + \alpha^*)^* < 1 \qquad (6.7c)$$

Equations (6.7) show that the SLIM circle map has the virtuous feature of a single contractive segment in which contraction occurs to a single point (the phase $\frac{\beta^*}{S}$ in term 6.7(c)). We shall shortly see that it is this feature, together with the fact that over the rest of the domain $\tilde{F}_{\alpha,\beta}$ is neither contractive nor expansive, which permits tractable calculation of lock conditions up to a high order.

The plot of $\tilde{F}_{\alpha,\beta}$ consists of separate straight lines which are either slanted at an angle of exactly 45° when corresponding to equations (6.7a) or (6.7b) or horizontal when corresponding to equation (6.7c). I notice that equations (6.7) also imply that the precise configuration of these lines in the plot is dependent on the value of the parameter α^* . Diagram 6.2 shows the three generic plot configurations which I define in terms of the parameter $d \equiv \alpha^* + \frac{\beta^*}{s}$ (see Appendix A6.1) as Form 1 when $d < \frac{1}{s}$, Form 2 when $\frac{1}{s} < d < \frac{1+\beta^*}{s}$ or Form 3 when $\frac{1+\beta^*}{s} < d < 1+\frac{\beta^*}{s}$. I observe that the three Forms are topologically equivalent and are related by a simple modulo 1 translation by an amount α^* parallel to the x axis. If equality holds then an associated slanted 45° line in the plot lies exactly on the leading 45° diagonal. Complete synchronisation to a

(6.5b)

Diagram 6.2



q-cycle in this situation is therefore impossible since the circle map must have a neutrally stable segment.

Without loss of generality, I shall henceforth focus on the Form 1 configuration. This is characterised by a formation that consists of a single horizontal line attached between a leftmost and rightmost 45° line, together with a single disconnected 45° line situated at the far left as shown in Diagram 6.2(a) and featured in greater detail in Diagram 6.3 below.

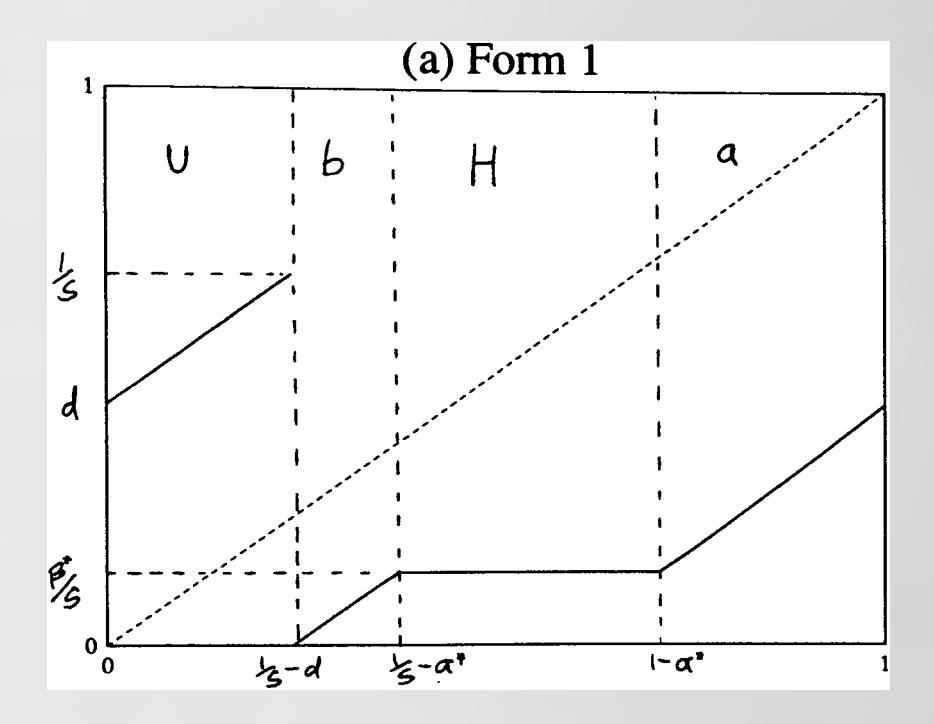


DIAGRAM 6.3 Plot of the SLIM FORM 1 circle map

Itinerary nomenclature

I divide the circle S^1 into the 4 segments associated with each of the 4 separate lines in the Form 1 plot, and label them as U, b, H, a, as shown in Diagram 6.3. The lineage produced from an initial recruitment phase by subsequent iterations of $\tilde{F}_{\alpha,\beta}$ can then be described by a sequence of letters with reference to the phase segment from which each successive generation is recruited. Such a sequence is referred to as an *itinerary* in the language of symbolic dynamics (e.g. Zheng 1989, 1991).

I base my nomenclature on the following life cycle features which characterise recruitment within each segment. For clarity I employ the term "year" to mean environmental repeat cycle.

- U Uninterrupted life cycle modulo 1 (uninterrupted if d < 1/S)
- b Life cycle passes through turn of year at least once in the B stage
- H Life cycle Held at zero development rate at the start of the B stage
- a Life cycle passes through turn of year at least once in the A stage

I see that *recruitment* of successive generations within the A stage (real time) interval in development is impossible because it is completely contained within the wider B stage (real time) interval (from which emergences from the life cycle are not possible). Thus the A stage interval is effectively redundant as a synchronising influence (unlike the B stage interval). I am therefore unsurprised that there is no phase segment in the SLIM circle map which corresponds to emergences in this (real time) interval (unlike segment H for the B stage).

I observe that a 1 lock cannot occur in the Form 1 configuration because segment H never intersects with the leading 45° diagonal in the plot. However, a 1 lock will occur in either of Forms 2 or 3 whenever $1-\alpha^* > \frac{\beta^*}{S}$ because H then cuts across the leading 45° diagonal. Thus $1-\alpha^* > \frac{\beta^*}{S} \Leftrightarrow d < 1$ is a necessary condition for a 1 lock (see equation (6.8)).

6.3 CONDITIONS FOR SYNCHRONISATION

I wish to find the long term ergodicity of $\tilde{F}_{\alpha,\beta}$ and thus determine the synchronisation behaviour of the lineage which stems from any initial recruit. To calculate lock conditions up to a high order, I make use of the fact the segment H is the sole contractive part of $\tilde{F}_{\alpha,\beta}$ and that such contraction occurs to a point

I first observe that the phase segment $H=(R_{-\alpha}(\frac{1}{S}),R_{-\alpha}(1))$ of the circle map has the same finite width $(1-\frac{1}{S})$ as the non-emergence segment $[\frac{1}{S},1)$ of the interphase map \tilde{f} . In plain english, as I would expect, the horizontal part of the circle map is directly related to the horizontal part of the interphase map. I see that because emergence from the life cycle into the 'non-emergence' phase segment is not possible, no sections of the circle map are above altitude 1/S.

Observe that any individual who commences its life cycle within segment H emerges at phase $\frac{\beta^*}{S}$. Thereafter, successive emergences of progeny from all lineages which pass through H are perfectly synchronised. Since a synchronising effect can *only* occur to those orbits which pass through H, any lineage which synchronises to a q-cycle must pass through (have an emergence phase within) this segment. Hence every stable q-cycle must have the emergence phase $\frac{\beta^*}{S}$ as a periodic point.

Because a q-cycle contains exactly q distinct points (section 3.2), successive emergences at $\frac{\beta^*}{S}$ must occur every q iterations (generations). Thus the itinerary produced by a q-cycle must also pass *through* H every q iterations. I shall use this property to deduce the complete itinerary of the q-cycle and to derive the corresponding conditions that must be satisfied. Although I shall give expressions for locks up to order 5, I only present calculations up to a 3 lock to save monotonous repetition.

Let us thus assume that an emergence occurs at phase $\frac{\beta^*}{S}$. I choose (arbitrarily) to label all itineraries with H as the first letter.

1 Lock conditions

Conditions for a 1 lock follow immediately from the observation that after emerging at $\frac{\beta}{S}$ the next generation must also emerge at $\frac{\beta}{S}$. Thus the associated itinerary must pass through segment H, which implies that the condition $\frac{1}{S} - \alpha^* < \frac{\beta^*}{S} < 1 - \alpha^*$ must be satisfied. For compactness I write this as

$$\frac{1}{S} < d < 1 \tag{6.8}$$

I see that this condition is consistent with the 1 lock conditions derived in the last Chapter (Theorem 5.6) and page 121 when the interphase map is strictly convex (Case1), for

$$1 - f(\alpha^*) < \beta^* < f(1 - \alpha^*)$$
 (6.9)

$$1 - S\alpha^* < \beta^* < S(1 - \alpha^*)$$

$$(6.10)$$

$$\therefore \frac{1}{S} < \alpha^* + \frac{\beta^*}{S} < 1 \tag{6.11}$$

I now introduce an intuitive general rule which all lineages (itineraries) must obey.

Itinerary Rule

If emergence from the life cycle occurs in a part of the plot situated below (above) the leading 45 'diagonal then the next generation must commence its life cycle at an earlier (later) phase than the previous one.

Thus it follows that all itineraries must steer left (right) after each emergence below (above) the leading 45° diagonal. In the case of the Form 1 configuration, the next emergence after phase $\frac{\beta^{\circ}}{s}$ must occur either in segments U or b situated to the left of segment H. Therefore all itineraries which synchronise to locks of order higher than one must pass through segment U at least once so as to return (steer right) back through H at the completion of the q-cycle. Returns back to H can only be accomplished when an emergence of the last generation in the repeat cycle occurs within either of the 'inward deflecting' segments U or a.

2 Lock conditions

(a) Form 1

I must first calculate those itineraries which return to segment H and emerge at phase $\frac{\beta^*}{S}$ after two further iterations. By the above, any candidate itinerary must pass through segment U in the next iteration to achieve this (passage through segment b would steer it left, away from segment H). Thus, only the itinerary HU can produce a 2 lock. The corresponding lock conditions can be deduced by observing that the itinerary must satisfy two separate criteria. Firstly, to return to H the total phase duration of itinerary HU must fall within the interval $(\frac{1}{S} - \alpha^*, 1 - \alpha^*)$ and thus the condition

$$(\frac{1}{S} - \alpha^*) < \frac{\beta^*}{S} + d < (1 - \alpha^*)$$

$$\Leftrightarrow \frac{1}{2S} < d < \frac{1}{2}$$
(6.12)

must be satisfied. Secondly to pass through segment U immediately after leaving segment H the condition

$$0 < \frac{\beta^*}{S} < \left(\frac{1}{S} - d\right)$$

$$\Rightarrow \qquad d < \frac{1 - \beta^*}{S}$$
(6.13)

must be satisfied. Hence conditions for a 2 lock are given by (6.12) and (6.13) together that is

$$\frac{1}{2S} < d < \frac{1}{2}$$
 and $d < \frac{1-\beta^*}{S}$ (6.14)

(b) Form 2 and Form 3

In these configurations (Diagram 6.2 (b) and (c)) the intuitive argument is complicated by the fact that section H may 'split' into two separate parts in the plot (strictly speaking 'straddle' across the leading 45° diagonal). I choose to calculate the possible lock itineraries algebraically (Appendix A6.2). By a parallel argument to the above I then obtain that the associated conditions for a 2 lock to occur are given by

$$\frac{1}{2} + \frac{1}{S} < d < 1 + \frac{1}{2S} \text{ and } 1 + \frac{1 - \beta^*}{S} < d$$
 (6.15)

(see Appendix A6.2).

3 Lock conditions

(a) Form 1

By the Itinerary Rule, I deduce that there are 3 itineraries which can re-emerge at phase $\frac{\beta^*}{s}$ after three further iterations. These are HUU, HbU, HUa. To save tedium I only present the calculation of associated lock conditions for itinerary HUU here,

preferring to show respective calculations for itineraries HbU and HUa in Appendix A6.3.

(i) Itinerary HUU

The total phase duration of itinerary HUU must satisfy

$$\left(\frac{1}{S} - \alpha^*\right) < \left(\frac{\beta^*}{S} + 2d\right) < (1 - \alpha^*)$$

$$\Leftrightarrow \frac{1}{3S} < d < \frac{1}{3}$$
(6.16)

Also, to pass through U consecutively after leaving segment H, the earlier inequality (6.13) together with the inequality

$$0 < \frac{\beta^*}{S} + d < \left(\frac{1}{S} - d\right)$$

$$\Rightarrow \qquad d < \frac{1 - \beta^*}{2S} \tag{6.17}$$

must be satisfied. Given that inequality (6.17) must hold, inequality (6.13) is redundant so that necessary and sufficient conditions for a 3 lock are inequalities (6.16) and (6.17) together namely

$$\frac{1}{3S} < d < \frac{1}{3}$$
 and $d < \frac{1-\beta^*}{2S}$ (6.18)

(ii) HbU (See Appendix A6.3 for calculation)

$$\frac{2}{3S} < d < \frac{1}{3} + \frac{1}{3S}$$
 and $\frac{1 - \beta^*}{S} < d < \frac{2 - \beta^*}{2S}$ (6.19)

(iii) HUa (see Appendix A6.3 for calculation)

$$\frac{1}{3} + \frac{1}{3S} < d < \frac{2}{3}$$
 and $d < \frac{1 - \beta^*}{S}$ (6.20)

(b) Form 2 and Form 3

By an exactly parallel treatment I obtain that a 3 lock also occurs when the conditions

$$\frac{2}{3} + \frac{1}{S} < d < 1 + \frac{2}{3S} \text{ and } 1 + \frac{2 - \beta^*}{2S} < d$$
or
$$\frac{2}{3} + \frac{2}{3S} < d < 1 + \frac{1}{3S} \text{ and } 1 + \frac{1 - \beta^*}{2S} < d < 1 + \frac{1 - \beta^*}{S}$$
or
$$\frac{1}{3} + \frac{1}{S} < d < \frac{2}{3} + \frac{2}{3S} \text{ and } 1 + \frac{1 - \beta^*}{S} < d$$
(6.21)
$$(6.22)$$

are satisfied.

Table 1 shows all the itineraries and associated lock conditions for the Form 1 SLIM circle map up to locks of order 5.

LOCK NUMBER	ITINERARY	CORRESPONDING A COMP CONTROL OF	
	TITILLANI	CORRESPONDING LOCK CONDITIONS	
		PARALLEL LINES	CROSS LINES
2	HU	$\frac{1}{2S} < d < \frac{1}{2}$	$d < \frac{1-\beta^*}{S}$
3	HUU	$\frac{1}{3S} < d < \frac{1}{3}$	$d < \frac{1-\beta^*}{2S}$
RIGHTMOST BLOCK	Г НЬ И	$\frac{2}{3S} < d < \frac{1}{3} + \frac{1}{3S}$	$\frac{1-\beta^*}{S} < d < \frac{2-\beta^*}{2S}$
	LHUa	$\frac{1}{3} + \frac{1}{3S} < d < \frac{2}{3}$	$d < \frac{1-\beta^*}{S}$
4	HUUU	$\frac{1}{4S} < d < \frac{1}{4}$	$d < \frac{1-\beta^*}{3S}$
RIGHTMOST BLOCK	HbbU	$\frac{3}{4S} < d < \frac{1}{4} + \frac{2}{4S}$	$\frac{2-\beta^{\bullet}}{2S} < d < \frac{3-\beta^{\bullet}}{3S}$
	HbUa	$\frac{1}{4} + \frac{2}{48} < d < \frac{2}{4} + \frac{1}{48}$	
	HUaa	$\frac{2}{4} + \frac{1}{48} < d < \frac{3}{4}$	$\frac{1-\beta^*}{S}d < \frac{2-\beta^*}{2S}$
			$d < \frac{1-\beta^*}{S}$
5	HUUUU	$\frac{1}{5S} < d < \frac{1}{S}$	$d < \frac{1-\beta^*}{4S}$
	HUbUU	$\frac{2}{5S} < d < \frac{1}{5} + \frac{1}{5S}$	$\frac{1-\beta^{\bullet}}{2S} < d < \frac{2-\beta^{\bullet}}{4S}$
	HUUaU	$\frac{1}{5} + \frac{1}{55} < d < \frac{2}{5}$	$d < \frac{1-\beta^{\circ}}{2S}$
	НьИьИ	$\frac{3}{5S} < d < \frac{1}{5} + \frac{2}{5S}$	$\frac{1-\beta^{\bullet}}{2S} < d < \frac{3-\beta^{\bullet}}{4S}$
	HUabU	$\frac{1}{5} + \frac{2}{55} < d < \frac{2}{5} + \frac{1}{55}$	$\frac{1}{3} + \frac{1-\beta^{\bullet}}{3S} d < \frac{1-\beta^{\bullet}}{S}$
	HUaUa		$\frac{3}{3} + \frac{3}{38} \cdot \alpha < \frac{3}{8}$
RIGHTMOST		$\frac{2}{5} + \frac{1}{55} < d < \frac{3}{5}$	$d < \frac{1}{3} + \frac{1-\beta^*}{3S}$
BLOCK	[HbbbU	$\frac{4}{5S} < d < \frac{1}{5} + \frac{3}{5S}$	3-8* , , 4-8*
	HbbUa	$\frac{1}{5} + \frac{3}{55} < d < \frac{2}{5} + \frac{2}{55}$	$\frac{3-\beta^2}{3S} < d < \frac{4-\beta^2}{4S}$
	HbUaa		$\frac{2-\beta^{\bullet}}{2S}d<\frac{3-\beta^{\bullet}}{3S}$
	HUaaa	$\frac{2}{5} + \frac{2}{58} < d < \frac{3}{5} + \frac{1}{58}$	$\frac{1-\beta^{\bullet}}{5}d < \frac{1}{3} + \frac{2-\beta^{\bullet}}{25}$
	LUaaa	$\frac{3}{5} + \frac{1}{55} < d < \frac{4}{5}$	
			$d < \frac{1-\beta}{s}$

TABLE 1 Lock conditions and associated itineraries up to lock number 5 for the Form 1 SLIM circle map.

6.4 THE SLIM BEHAVIOUR PORTRAIT

Diagram 6.4 shows plots of SLIM for a selection of increasing values of the slope parameter S. The associated behaviour portaits for each value are shown in Portraits 4. I observe that the SLIM behaviour portrait also has twofold rotational symmetry about its centre. By considering SLIM as the limiting case of a two-piece linear homeomorphism TLIM (Two Line Interphase Map), I will show in Chapter 7 (and Appendix 6.3) that I would indeed expect this generic property (of any two stage circle map) to be preserved.

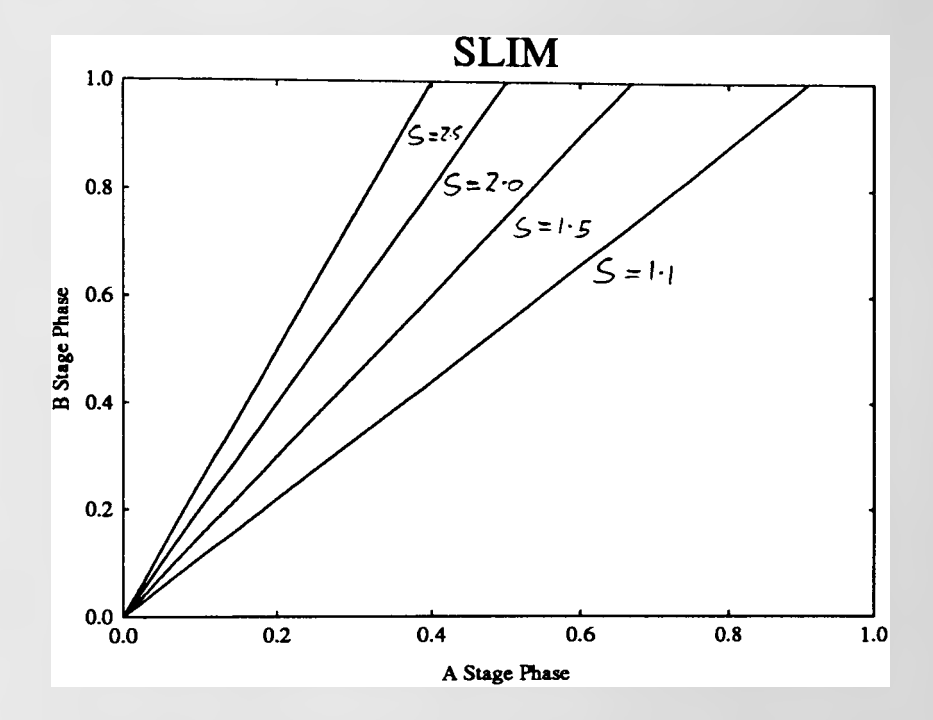
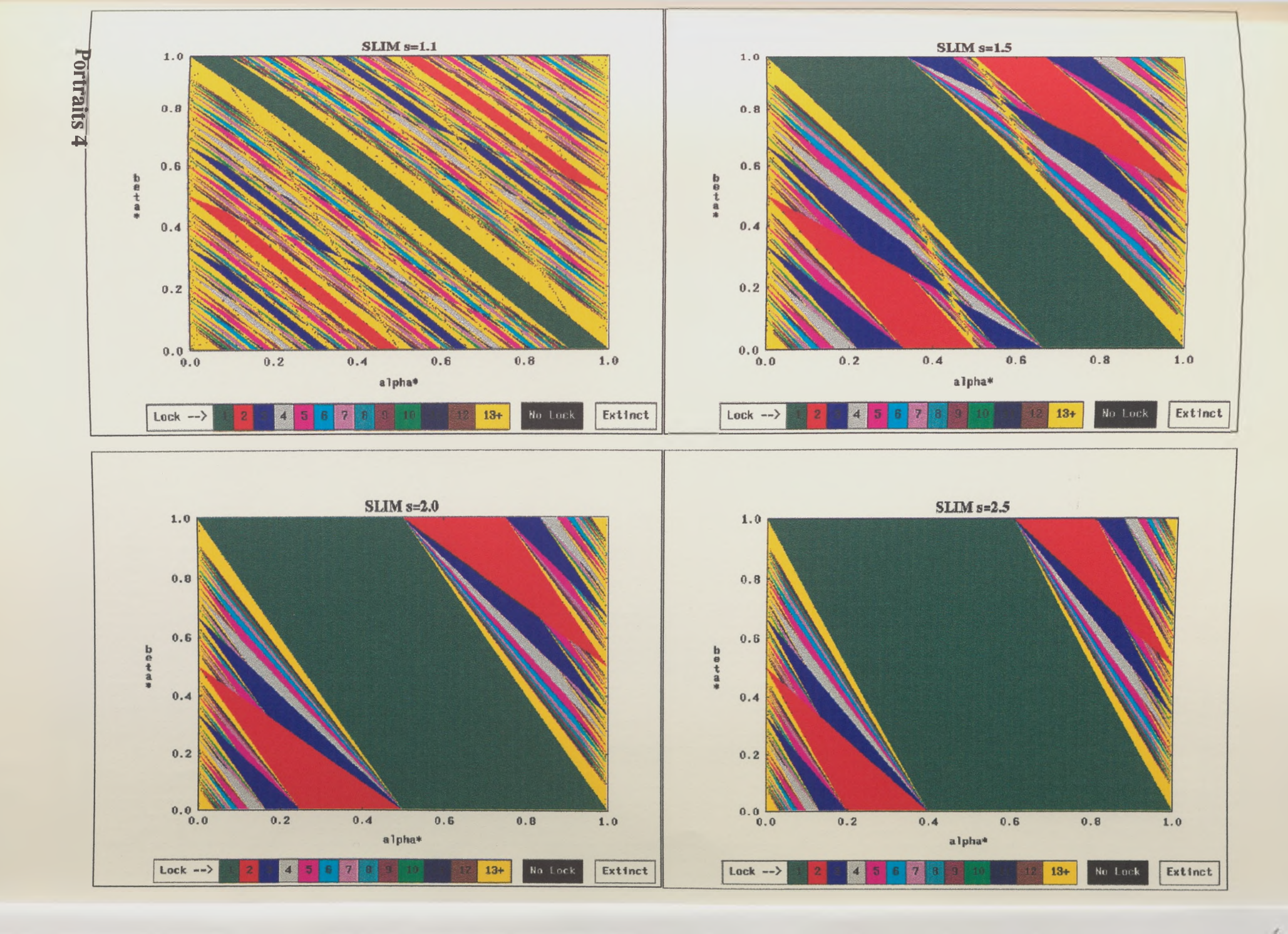


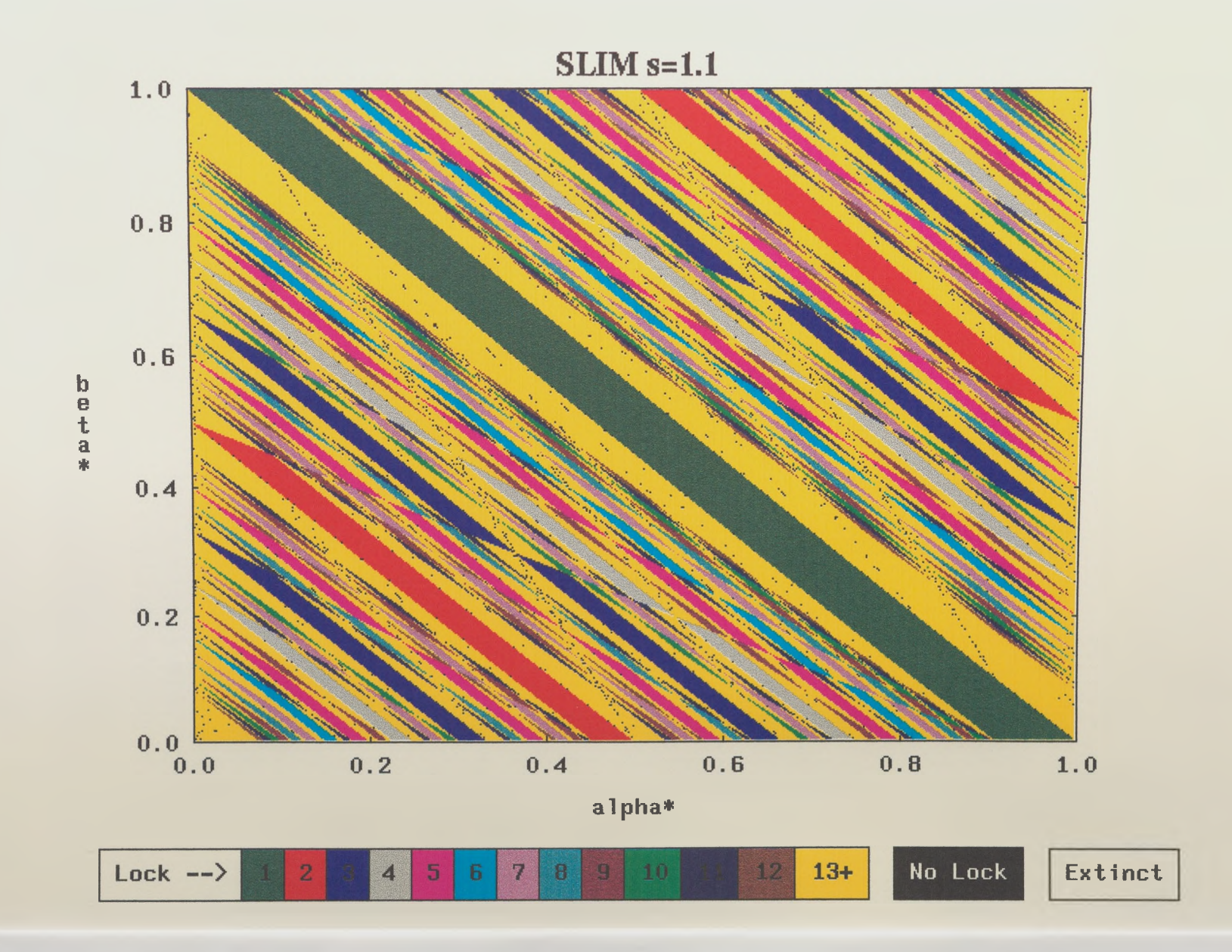
DIAGRAM 6.4 Plots of SLIM for increasing slope parameter S.

Since segment H has an interval width of $1-\frac{1}{S}$ it follows that as the slope S increases, this width must also increase $(1-\frac{1}{S}\to 1\text{ as }S\to +\infty)$. Thus the plot of the SLIM circle map must tend towards a single horizontal line which in turn implies that the 1 lock region of the SLIM behaviour portrait must ultimately expand to engulf the entire frame in the upper limit situation when SLIM reaches verticality. Portraits 4 confirm that the trend towards an entirely green behaviour portrait, does indeed occur as S increases in value.

Portraits 4 SLIM behaviour portraits associated with the above values of slope parameter S in Diagram 6.4

Portrait 5 Enlarged SLIM behaviour portrait associated with slope parameter S=1.1





Conversely, as $S \to 1$ the SLIM model must tend towards a state in which each stage phase is identical throughout the entire unit phase circle. This time H contracts towards zero width and the plot of the SLIM circle map tends towards the leading 45° diagonal. In the lower limit situation (when S=1), the model would be equivalent to the one-stage model of Chapter 2 in which no synchronisation is possible. Portraits 4 also confirm that as $S \to 1$ all lock regions diminish in area, a trend which if continued must result in all regions disappearing when S=1 is reached.

I observe that the 1 lock region of the behaviour portrait consists of a single central diagonal zone situated between the straight diagonal lines $d = \frac{1}{5}$ and d = 1. Each of the 3 circle map plot configurations defined earlier can be associated with 3 adjacent portions of the complete behaviour portrait. The Form 1 $(d < \frac{1}{5})$ configuration is associated with that portion which lies below the central 1 lock zone. The separate lock regions in this portion of the behaviour portrait correspond with itineraries which produce locks under the Form 1 configuration (as the parameters α^* and β^* are varied). For example the Form 1 3 lock conditions consist of 3 separate sets of expressions each of which corresponds to an itinerary HUU, HbU or HUa and an associated region in the behaviour portrait situated below the central zone. These are labelled up to lock number 4 on the behaviour portrait shown in Diagram 6.5.

Form $2\left(\frac{1}{S} < d < \frac{1+\beta^*}{S}\right)$ occurs within and above the central zone but to the left of the vertical line $\alpha^* = \frac{1}{S}$ whilst Form $3\left(\frac{1+\beta^*}{S} < d < 1 + \frac{\beta^*}{S}\right)$ occurs in the rightmost portion, namely that to the right of the line $\alpha^* = \frac{1}{S}$.

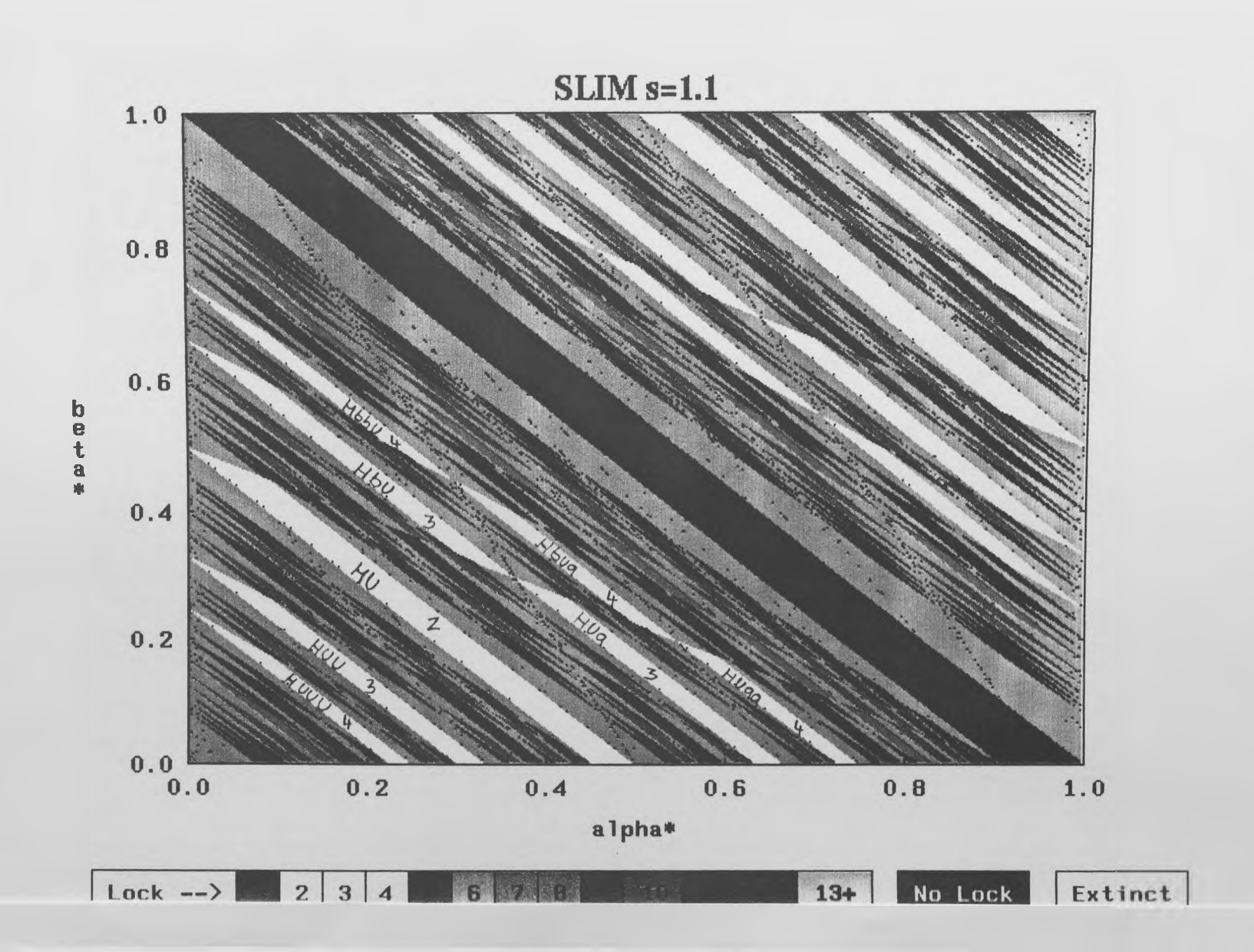
Relationship between Form 1 and (Form 2 and Form 3) lock conditions

Since the SLIM behaviour portrait has twofold rotational symmetry about its centre, those lock conditions for regions within the portion that lie *above* the 1 lock zone (that is those derived for Forms 2 and 3) are rotational half turn images of the Form 1 conditions situated *below*. The complete information content of the SLIM behaviour portrait is thus contained in the lower left portion (corresponding to the Form 1 circle map configuration) together with the central 1 lock zone. Hence all lock conditions associated with Forms 2 and 3 are in fact 'rotational half turn images' of Form 1 conditions and can therefore be obtained directly (without performing separate calculations) by making the substitutions

$$\alpha^* \to (\alpha^*)' = 1 - \alpha^*$$

$$\beta^* \to (\beta^*)' = 1 - \beta^*.$$
(6.24)

DIAGRAM 6.5



in the appropriate Form 1 expressions. I shall verify that the property holds for the 2 lock conditions associated with itinerary HU obtained earlier.

For itinerary HU

$$\frac{1}{2S} < d < \frac{1}{2} \rightarrow \frac{1}{2S} < (1 - \alpha^*) + \frac{(1 - \beta^*)}{S} < \frac{1}{2}$$
 (6.25)

and
$$d < \frac{1-\beta^*}{S}$$
 \rightarrow $(1-\alpha^*) + \frac{(1-\beta^*)}{S} < \frac{1-(1-\beta^*)}{S}$ (6.26)

Inequality (6.25) simplifies to

$$\alpha^* + \frac{\beta^*}{S} < 1 + \frac{1}{2S} \text{ and } \frac{1}{2} + \frac{1}{S} < \alpha^* + \frac{\beta^*}{S}$$

$$\Leftrightarrow \frac{1}{2} + \frac{1}{S} < d < 1 + \frac{1}{2S}$$
(6.27)

Inequality (6.26) simplifies to

$$1 + \frac{1}{S} < \alpha^* + \frac{\beta^*}{S} + \frac{\beta^*}{S}$$

$$\Leftrightarrow d > 1 + \frac{1 - \beta^*}{S}$$
(6.28)

Thus the image conditions are inequalities (6.27) and (6.28) together namely

$$\frac{1}{2} + \frac{1}{S} < d < 1 + \frac{1}{2S} \text{ and } d > 1 + \frac{1 - \beta^*}{S}$$
 (6.29)

in agreement with the Form 2 and Form 3 conditions for a 2 lock already derived (equation 6.15).

Lines of Neutral Stability

I have observed that neutral stability occurs when equality holds in the expressions for lock conditions and that such dynamic behaviour is associated with the black boundary lines of lock regions in the behaviour portrait. These boundaries are made up of straight lines which connect together to produce the bounded polygonal areas that I have called lock regions. $\bar{F}_{\alpha,\beta}$ fails to synchronise (not every orbit converges

(condenses) towards a q-cycle) when parameterised with any parameter pair (α^*, β^*) lying on such a boundary.

Examination of the SLIM behaviour portrait also reveals that these boundary lines fall into two categories. Namely, they are either parallel lines (which correspond to conditions of the form d=constant in the first column of Table 1) or alternatively, lines which cross them and which I shall refer to as 'cross lines' (which correspond to other conditions in the second column of Table 1). I observe that the cross lines emanate from some point situated on the α -axis and cut across the parallel lines producing a strip of lock region inbetween. For any given lock number, the associated lock regions in the behaviour portrait occur in connected blocks which span diagonally between the x and y axes.

Relationship of Lock Regions with The Farey Tree

Examination of Table 1 reveals a sequential pattern in the constants corresponding to parallel line boundaries of lock regions (conditions). I extract these rational constants and place them in rows of ascending magnitude characterised by outermost terms m/nS and m/n where m and n are integers (in which the denominator n is the associated lock number) to produce pyramids as shown in Table 2. Empirical studies show that the pattern continues to hold for an arbitrarily large lock number. Where such rows have outermost terms m/nS and m/n in which the integers m and n are NOT relatively prime (for example row 2 of lock number 4) they can be cancelled down to a similar pair with a *lower* associated lock number. This implies (because all the lock conditions are necessary and sufficient) that in such cases the parallel boundaries of the corresponding lock region must be *contained* within a region of lower lock number. Alternatively, where any overlap of a lock region occurs, low locking behaviour must dominate over high locking. Thus m and n must be relatively prime to ensure that the associated individual lock region(s) exist in their entirety.

Because the horizontal width (between the associated parallel boundaries) of any given lock region is dependent on the parameter S, a second necessary requirement for the region to exist in entirety is that S be small enough to ensure overlap with neighbouring regions does not occur. So how can the complete set of parallel boundary line coefficients be placed in ascending order of magnitude? I now introduce the Farey tree.

LOCK NUMBER	ROW	COEFFICIENTS d= CONSTANT OF PARALLEL LINES (BOUNDARY CONDITIONS)
2	n=1	$\frac{1}{2S}$ $\frac{1}{2}$
3	1	$\frac{1}{3S}$ $\frac{1}{3}$
	n=2	$\frac{2}{3S}$ $\frac{1}{3} + \frac{1}{3S}$ $\frac{2}{3}$
4	1	$\frac{1}{4S}$ $\frac{1}{4}$
	2	$\frac{2}{45} \frac{1}{4} + \frac{1}{45} \frac{2}{4}$ = $\frac{1}{25} \frac{1}{4} + \frac{1}{45} \frac{1}{2}$: parallels are within the
	n=3	$\frac{3}{4S} \frac{1}{4} + \frac{2}{4S} \frac{2}{4} + \frac{1}{4S} \frac{3}{4}$ 2 lock parallels.
5	1	1 5S 1 5
	2	$\frac{2}{5S}$ $\frac{1}{5} + \frac{1}{5S}$ $\frac{2}{5}$
	3	$\frac{3}{5S}$ $\frac{1}{5} + \frac{2}{5S}$ $\frac{2}{5} + \frac{1}{5S}$ $\frac{3}{5}$
	n=4	$\frac{4}{58} \frac{1}{5} + \frac{3}{58} \frac{2}{5} + \frac{2}{58} \frac{3}{5} + \frac{1}{58} \frac{4}{5}$
q	1	$\frac{1}{qS}$ $\frac{1}{q}$
	2	$\frac{2}{qS} \frac{1}{q} + \frac{1}{qS} \frac{2}{q}$
	3	$\frac{3}{qS} = \frac{1}{q} + \frac{2}{qS} = \frac{2}{q} + \frac{1}{qS} = \frac{3}{q}$
n=	q-1	
		$\frac{q-1}{qS}$ $\frac{1}{q} + \frac{q-2}{qS}$ $\frac{2}{q} + \frac{q-3}{qS}$ $\frac{3}{q} + \frac{q-4}{qS}$ $\frac{j}{q} + \frac{q-(j+1)}{qS}$ $\frac{q-1}{q}$

TABLE 2
Pattern of parallel lock condition coefficients for the Form1 SLIM Circle Map. n= level in Farey Tree. S= slope of SLIM.

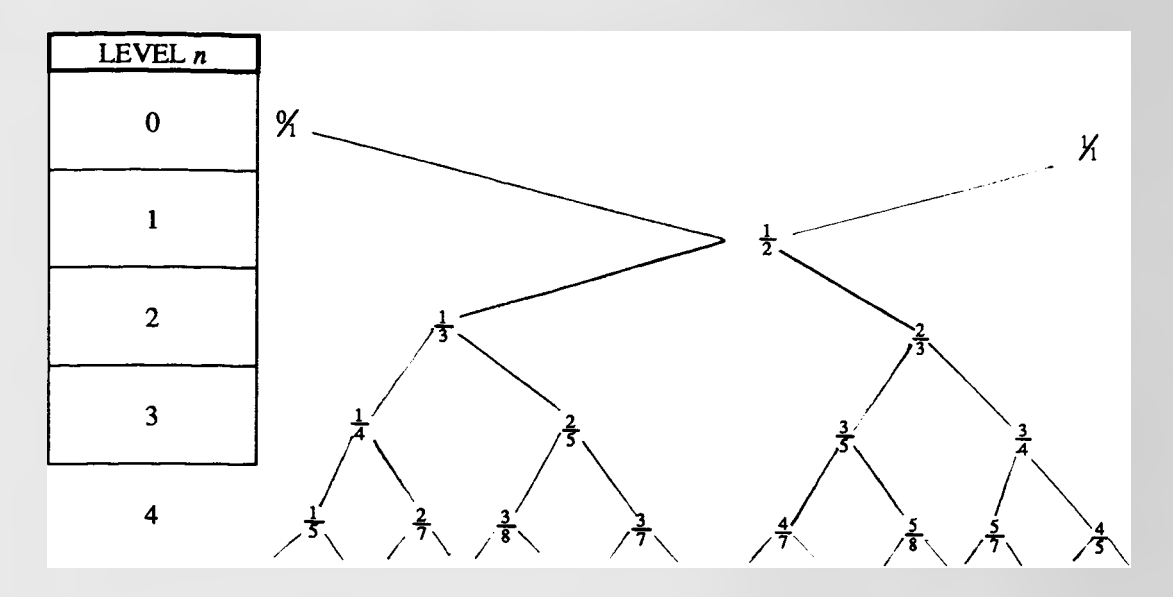


DIAGRAM 6.6 The Farey Tree (to Level 4)

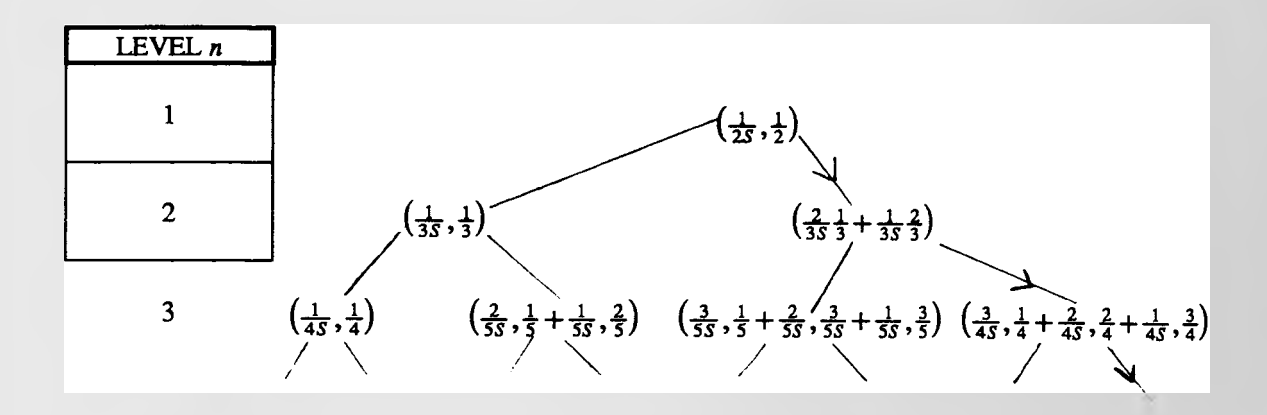


DIAGRAM 6.7 The SLIM Farey Tree (to Level 3). The last (rightmost) branch is arrowed \rightarrow .

The Farey tree is an orderly arrangement of rational numbers p/q where p and q are relatively prime integers (e.g. Kim & Ostlund 1989, Zheng 1989). The structure of the tree is imposed by taking the Farey sum of parent rationals p/q and p'/q' to produce the relatively prime daughter rational

$$\frac{p}{q} + \frac{p'}{q'} = \frac{p + p'}{q + q'}$$

located (in value) between the two parent rationals. Diagram 6.6 shows the Farey tree to level 4. For my purposes the Farey tree provides a means of placing the rational coefficients d=constant of parallel boundaries (as shown in Table 2) into ascending order. I show how a related structure, which I shall refer to as the SLIM Farey tree, can be constructed in Diagram 6.7.

The SLIM Farey tree tells us that the number of non-overlapping regions can be made arbitrarily large by choosing the parameter S to be small enough. For example, consider the set of parallel boundary coefficients $(\frac{2}{3S} - \frac{1}{5} + \frac{1}{3S} - \frac{2}{5})$ which occur at level 3 in Diagram 6.7 For the parallel boundaries associated with these coefficients to be outside the boundaries of the lock regions which correspond with the above levels (2 and 1) and thus to ensure that these regions do not overlap, the slope S must satisfy

$$\frac{\frac{1}{3} < \frac{2}{5S} \Leftrightarrow S < \frac{6}{5}}{\frac{2}{5} < \frac{1}{2S} \Leftrightarrow S < \frac{5}{4}} \Rightarrow S < \frac{6}{5}$$

A lock of order q has an associated pyramid of parallel coefficients with (q-1) rows the last of which appears at the nth level of the SLIM Farey tree. Thus I find that q-1=n. All lock regions of a given lock number q appear must appear in the behaviour portrait if S is small enough for the (q-1)th row of the SLIM Farey tree to be reached.

Without venturing further into mathematical niceties, I state another interesting property of the SLIM behaviour portrait obtained through empirical observation. The relationship between the number of lock regions in any block and the lock number of the block is given by

$$\frac{p}{q} = \frac{\text{Number of connected regions}}{\text{Lock number of the block}}$$

where p and q are relatively prime integers.

6.5 TRAILS INVESTIGATION

One of the most visually striking features of the SLIM behaviour portrait (and indeed all those thus far encountered) are the black clouds or 'blackness' that surface between the lock regions. Often these appear to form dark trails which traverse across the (α^*, β^*) plane as can be clearly seen in Portrait 5. Outwardly they have the appearance of vapour trails left in a bubble chamber by a charged particle. Their existence raises two main questions.

- (1) What dynamic behaviour corresponds to the 'no lock' black points which make up these clouds or trails?
- (2) Are the trails actually lines or are they composed from sequences of separate 'islands' or points that are situated on a line?

In answer to the first question I conjecture that only two types of dynamic behaviour can occur in the SLIM circle map, namely synchronisation (asymptotic stability) or neutral stability (but not quasi-periodicity). An intuitive sketch proof follows immediately from the observation that the configuration of any SLIM circle map plot is entirely composed from exactly 45° or exactly horizontal straight lines. Synchronisation occurs iff every orbit eventually passes through the contractive segment H. Synchronisation does not occur iff there exist orbits which *never* pass through H in which case they must continually pass through 45° segments. This can only happen if there exists at least one such segment which is displaced from the leading 45° diagonal by a rational number (otherwise if all the segments are displaced by an irrational amount, the orbit would eventually 'cobweb' its way of all such segments into the contractive segment H). In this case the orbit must eventually return back to the rationally displaced segment and the whole process repeats again producing neutrally stable dynamic behaviour.

In answer to the second question I note that empirical studies indicate that these trails always pass through the nodes of lock regions and this leads me to conjecture that they are entirely composed from them. To test this hypothesis I shall investigate the nodes produced by the intersections of a particular family of cross lines and parallels. Consider the family of cross lines which correspond to the conditions of the last (rightmost) block for every lock number that is, on choosing n as the level in the Slim Farey Tree, the conditions (see Table 1 right column)

$$d = \frac{(n-1)-\beta^*}{(n-1)S} \text{ for } n = 2, 3, 4, \dots$$
 (6.30)

which I write as

$$(n-1)\alpha^* + n\frac{\beta^*}{S} = \frac{n-1}{S}$$
 for $n = 1, 2, 3, 4, ...$ (6.31)

The family of cross lines 'fan out' from the point $(\frac{1}{5},0)$ in the Slim behaviour portrait.

(1) FIRST TRAIL OF FAMILY

First, consider the intersections of the family with parallels that correspond with coefficients situated 'one-in' from the left of the Slim Farey Tree at level n

$$d = \alpha^* + \frac{\beta^*}{S} = \frac{1}{n+1} + \frac{n-1}{(n+1)S} \text{ for } n = 1, 2, 3, \dots$$
 (6.32)

The nodes located at such intersections are therefore the solutions of the pairs of simultaneous equations in α^* and β^*

$$(n-1)\alpha^* + n\frac{\beta^*}{S} = \frac{n-1}{S}$$

$$\alpha^* + \frac{\beta^*}{S} = \frac{1}{n+1} + \frac{n-1}{(n+1)S}$$
 for $n = 1, 2, 3, ...$ (6.33)

I solved equation 6.33 and find that the solutions (α_n^*, β_n^*) for n = 1, 2, 3, ... are

$$\alpha_{n}^{*} = \frac{nS - n + 1}{(n+1)S}$$

$$\beta_{n}^{*} = \frac{(n-1)(2-S)}{(n+1)}$$
for $n = 1, 2, 3, ...$
(6.34)

In passing I observe that there exists a one-to-one correspondance between each node and level (a natural number) in the Farey tree so that the total number of nodes in the trail can only be countable. Denoting the kth node by (α_k^*, β_k^*) I see that the straight

line upon which any two successive nodes (α_k^*, β_k^*) , $(\alpha_{k+1}^*, \beta_{k+1}^*)$ lie has the equation $\beta^* = m\alpha^* + c$ where

$$m = \frac{\beta_{k+1}^* - \beta_k^*}{\alpha_{k+1}^* - \alpha_k^*}$$
 (6.35)

and

$$c = \beta_k^* - m\alpha_k^* \tag{6.36}$$

Solving equations (6.35) and (6.36) as a simultaneous pair in c and m I obtain after simplification that m=-2S and c=S so that the straight line which passes through any two successive nodes is given by

$$\beta^* = -2S\alpha^* + S = S(1 - 2\alpha^*)$$
 (6.37)

I observe that because equation (6.37) is independent of k the same straight line must pass through all successive pairs of nodes and hence all such nodes for n=1,2,3,... produce a trail which lies on a straight line.

(2) A FAMILY OF TRAILS

Now consider the family of intersections which are produced by intersections of cross lines with parallels that correspond with coefficients situated 'j - in' from the left of the Slim Farey Tree (for j = 1, 2, 3, ...) that is the parallel lines

$$d = \alpha^* + \frac{\beta^*}{S} = \frac{j}{n+1} + \frac{n-j}{(n+1)S} \text{ for } n = 1, 2, 3, ...$$

$$[n = q - 1 \text{ or } q = n + 1]$$
(6.38)

Nodes located at the intersection of the jth parallel line with the nth cross line are thus given by the solutions in α^* and β^* of the simultaneous equations

$$(n-1)\alpha^* + n\frac{\beta^*}{S} = \frac{n-1}{S}$$

$$\alpha^* + \frac{\beta^*}{S} = \frac{j}{n+1} + \frac{n-j}{(n+1)S}$$
for $n = 1, 2, 3, ...$ (6.39)

These solutions $(\alpha_{nj}^*, \beta_{nj}^*)$ for n = 1, 2, 3, ... and j = 1, 2, 3, ... after much tedium simplify to

$$\alpha_{nj}^* = \frac{((n+1)S - n)j + (1-S)j^2}{(n+1)S}$$

$$\beta_{nj}^* = \frac{(n-j)((1-S)j + 1)}{(n+1)}$$
for $n = 1, 2, 3, ..., j = 1, 2, 3, ..., (6.40)$

I happily observe with some relief that this agrees (as it must do) with equations (6.34) when j=1. Again, consider two successive nodes $(\alpha_{K_j}^*, \beta_{K_j}^*)(\alpha_{(K+1)_j}^*, \beta_{(K+1)_j}^*)$ this time located on the *j*th parallel line. After arduous algebra I find that the equation of the line which passes through these two consecutive nodes simplifies to

$$\beta^* = S\left(1 - \frac{(j+1)\alpha^*}{j}\right) \text{ for } j=1,2,3,...$$
 (6.44)

Since this expression is independent of k, the same line must pass through every such pair of nodes and hence all such nodes form a corresponding trail for each value of j which must lie on a straight line. The family of trails formed by all such nodes is therefore also a countable set of points (a countable set of sets containing at most a countable number of elements is at most countable e.g. see Kamke (1950)). Each trail in the family is therefore not a straight line but rather is made up of a set of 'islands' which are situated on a line as hypothesised.

This leads me to the further conjecture that the total number of nodes in the SLIM behaviour portrait is at most countable so there cannot really be any black regions but only particulate clouds. Since parallels are matched one-to-one to the Farey tree and each parallel has an associated block of countable terms it follows that the total number of parallels is at most countable (a countable set of sets containing at most a countable number of elements is at most countable). If the cross lines are also at most countable (as I believe they are) the truth of the conjecture follows.

6.6 DISCUSSION

The SLIM model demonstrates two important properties of the relationship between interphase map and behaviour portrait. Firstly, low locking behaviour dominates over high locking behaviour. Secondly this dominance becomes more acute as the slope S increases which in turn implies that as maximum deviation *away* from the leading 45° diagonal is increased, higher ordered locks become less prevalent. This property is reflected in the SLIM behaviour portrait by the expansion of low lock regions to the detriment of those of higher order. In the next Chapter I shall further explore the importance of these themes in the light of nonlinearity.

Whereas the SLIM behaviour portrait has the superficial appearance of a fractal it is not a true fractal because enclosed *regions* of all the same lock value (within which the global structure is no more) must exist for any S>1. Alternatively a true fractal structure could only exist for S=1 since by definition of a fractal structure, an arbitrarily small region must also have the same structure (Devaney 1990).

Because of its inherent linearity, SLIM is not a realistically shaped interphase map for the development response exhibited by most organisms. However the SLIM model can serve as a good approximation to the cell division cycle occuring in several species of marine phytoplankton (Heath & Spencer 1985). I shall show the closeness of the model by constructing associated behaviour portraits in Section 7.4

CHAPTER 7

THE GENERAL EFFECT OF INTERPHASE MAP SHAPE ON SYNCHRONIZATION

7.0 INTRODUCTION

In this Chapter I present the results of a selection of surveys which explore the general relationship between synchronisation behaviour of $F_{\alpha,\beta}$ and the interphase map from which it is composed. The mainly visual approach exploits the behaviour portrait as a tool for uncovering the relationship between interphase map shape and the dynamic behaviour of its corresponding class of two stage circle maps. In a variety of different scenarios, I demonstrate the effect of gradual changes in interphase map shape by examining the incumbent effect on the associated sequence of behaviour portraits. Impressed by the transparency of the SLIM model, I also choose to venture further into the more general top hat family of life cycle systems in which (more realistically) the top hat development rate functions need not be situated on a zero 'background' level.

I start by examining a simple (homeomorphic) two stage circle map composed from a two-piecewise lineate interphase map, TLIM. I deduce that this model is dynamically equivalent to a companion model composed from a three-piecewise lineate (lefthand Z shaped) interphase map THLIM. The influence of curvature in the interphase map is examined by gradually imposing rounded corners onto the THLIM shape. I see (as expected) that the resulting reduction in 'lineness' permeates through to the associated behaviour portrait. An unexpected outcome, which occurs concurrently, is that blackness becomes increasingly prevalent over regions of higher lock. This leads me to postulate that high order locks are more acutely affected by the close presence of portions of the interphase map to the leading 45° diagonal.

Motivated by the realisation that TLIM and THLIM are essentially the same thing, I endeavour to discover whether a similar transformation exists between their respective curved analogues, namely the Case 1 and Case 2 interphase maps. I (predictably) find that these are not essentially the same, Case 2 being equivalent to a non-strictly convex (or concave) shaped intermediate companion. However, the comparison also re-enforces the twin hypotheses that 'close presence of portions to' and 'maximum deviation from' the leading 45° diagonal are the major interphase map shape determinants of behaviour portrait design.

I exemplify the general results obtained with strategic models by showing their application to two diversely different real world organisms, namely the now familiar beetle *Catops* and an aquatic micro-organism, *phytoplankton*.

7.1 TLIM AND THLIM

TLIM

Consider a simple continuous Two Line Interphase Map (TLIM) defined by two parameters S_1 and S_2 (where $S_1 > 1$, $S_2 > 0$, $S_1 > S_2$) which respectively correspond to the slopes of the left and right lines of the TLIM plot, as shown in Diagram 7.1. In addition to being continuous and onto, TLIM (unlike SLIM) is a *one-to-one* map throughout the entire circle domain and thus is a homeomorphism. The interphase map transformation theorems derived in section 5.1 (other than Theorem 5.5) must hold for TLIM.

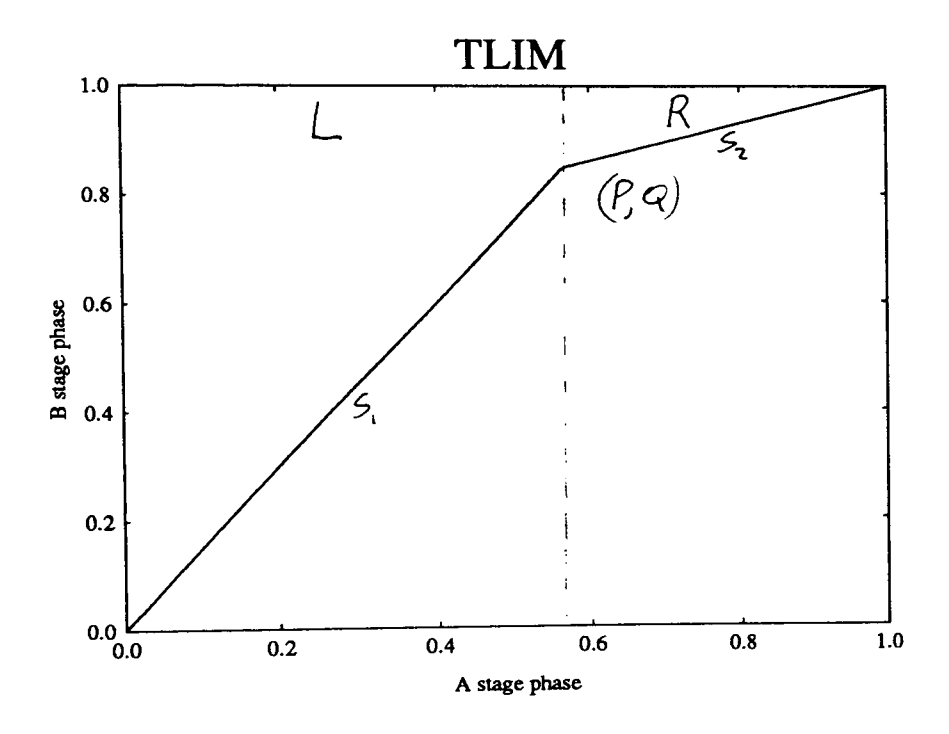


DIAGRAM 7.1 The TLIM interphase map

SLIM as a Limiting Case of TLIM

My main interest in TLIM is as a simple interphase map which (for small enough S_2) can be made arbitrarily close to SLIM. I illustrate this in Diagram 7.2 with a sequence of TLIM plots for diminishing slope S_2 where the horizontal displacement P is fixed. Clearly, SLIM is the limiting case of TLIM as the slope S_2 of the rightmost line falls to zero.

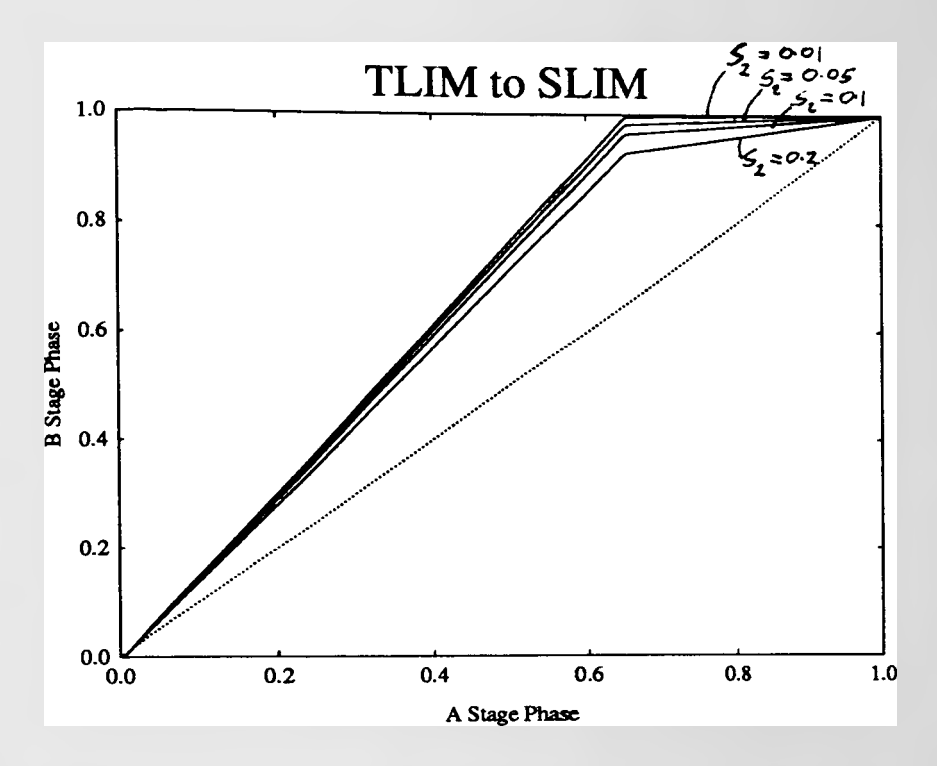


DIAGRAM 7.2 TLIM approaches SLIM

I also formally deduce that the SLIM circle map model is the limiting situation of the TLIM circle map (which I derive in a parallel manner to the SLIM circle map, in Appendix A7.1) which is

$$\theta_{n+1} = \begin{cases} \frac{\beta^*}{S_1} + (\theta_n + \alpha)^* & 0 \le (\theta_n + \alpha)^* < P - \frac{\beta^*}{S_1} \\ 1 + \frac{\beta^* - 1}{S_2} + \frac{S_1}{S_2} (\theta_n + \alpha)^* & P - \frac{\beta^*}{S_1} \le (\theta_n + \alpha)^* < \frac{1 - \beta^*}{S_1} \\ \frac{\beta^* - 1}{S_1} + (\theta_n + \alpha)^* & \frac{1 - \beta^*}{S_1} \le (\theta_n + \alpha)^* < P \end{cases}$$
(7.1b)
$$\frac{\beta^*}{S_2} + (\theta_n + \alpha)^* & P \le (\theta_n + \alpha)^* < 1 - \frac{\beta^*}{S_2} \end{cases}$$
(7.1d)
$$\frac{\beta^* - S_2}{S_1} + \frac{S_2}{S_1} (\theta_n + \alpha)^* & 1 - \frac{\beta^*}{S_2} \le (\theta_n + \alpha)^* < 1 - \frac{\beta^*}{S_2} + \frac{S_1}{S_2} P \end{cases}$$
(7.1e)
$$\frac{\beta^* - 1}{S_2} + (\theta_n + \alpha)^* & 1 - \frac{\beta^*}{S_2} + \frac{S_1}{S_2} P \le (\theta_n + \alpha)^* < 1$$
(7.1f)

by evaluating the limit of expressions (7.1) as $S_2 \to 0$ for fixed parameter P. I observe first that because $P = \frac{1 - S_2}{\overline{S}_1 - \overline{S}_2}$, $P \to \frac{1}{S_1}$ as $S_2 \to 0$. Dealing with each term of expressions (7.1) separately:

(7.1a) RHS inequality
$$\rightarrow 0 \le (\theta_n + \alpha)^* < \frac{1 - \beta^*}{S_1}$$

(7.1b) RHS inequality collapses to zero width and thus the LHS term vanishes

(7.1c) RHS inequality
$$\rightarrow \frac{1-\beta^*}{S_1} \le (\theta_n + \alpha)^* < \frac{1}{S_1}$$

(7.1d) RHS inequality collapses to zero width and thus the LHS term vanishes (7.1e) RHS inequality expands
$$\rightarrow \frac{1}{S_1} \le (\theta_n + \alpha)^* < 1$$

$$[1 - \frac{\beta^*}{S_2} + \frac{S_1}{S_2}P \rightarrow 1 + \frac{1 - \beta^*}{S_2} > 1]$$
and LHS term $\rightarrow \frac{\beta^*}{S_1}$

(7.1f) RHS inequality collapses to zero width, thus LHS term vanishes.

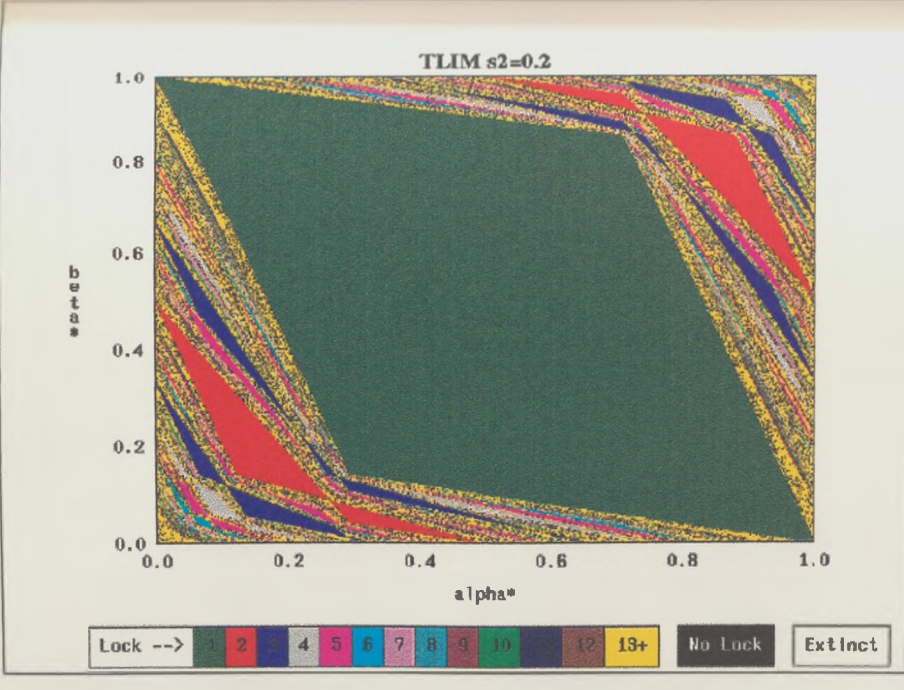
Hence only terms (7.1a) (7.1c) and (7.1e) will ultimately remain so that the limiting expression of the TLIM circle map is

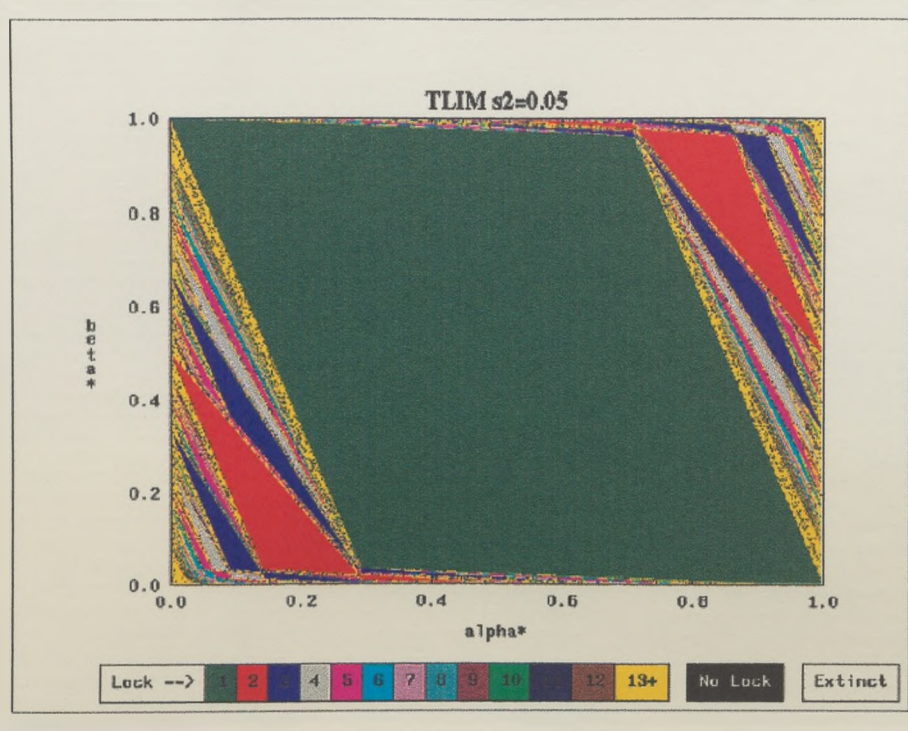
$$\theta_{n+1} = \begin{cases} \frac{\beta^*}{S_1} + (\theta_n + \alpha)^* & 0 \le (\theta_n + \alpha)^* < \frac{1 - \beta^*}{S_1} \\ \frac{\beta^* - 1}{S_1} + (\theta_n + \alpha)^* & \frac{1 - \beta^*}{S_1} \le (\theta_n + \alpha)^* < \frac{1}{S_1} \\ \frac{\beta^*}{S_1} & \frac{1}{S_1} \le (\theta_n + \alpha)^* < 1 \end{cases}$$
(7.2)

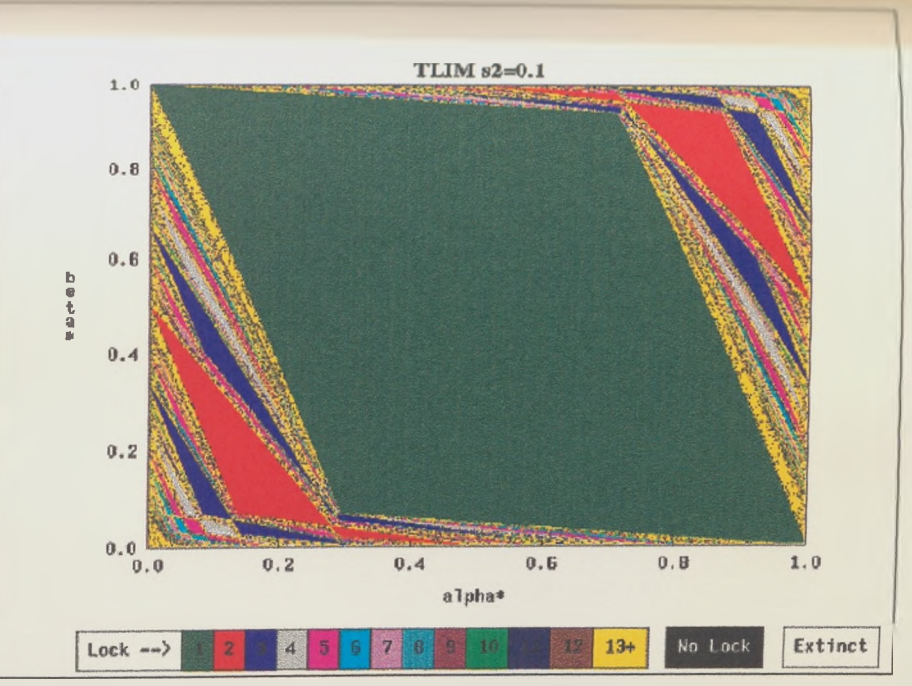
which (as I would expect) is none other than the SLIM circle map on taking $S_1 = S$ (equations 6.7).

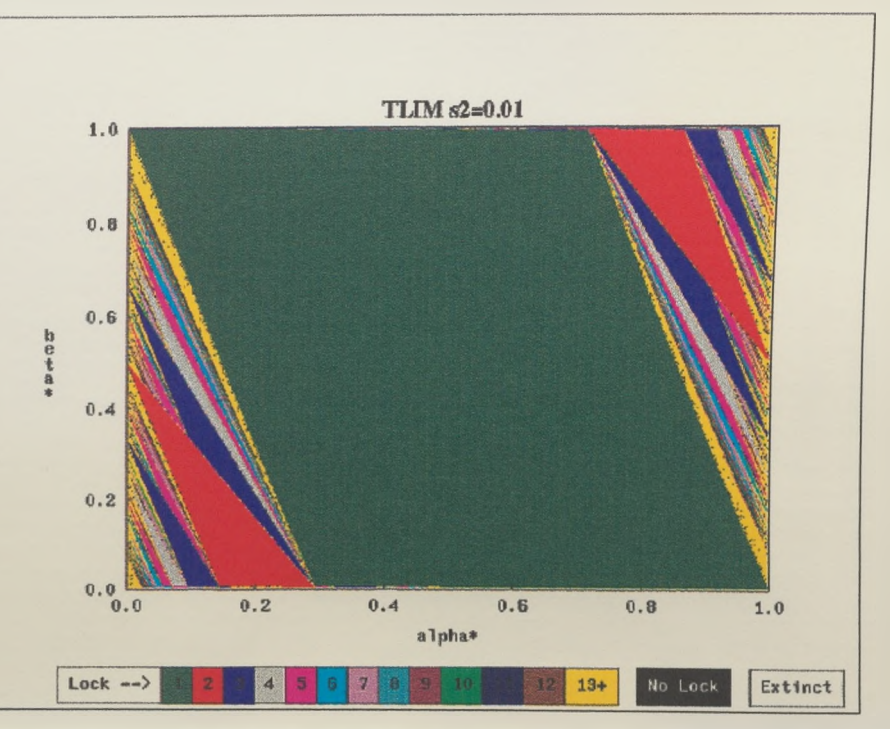
I show the accompanying sequence of associated behaviour portraits for the interphase map plots of Diagram 7.2 in Portraits 6. As expected, the TLIM behaviour portrait evolves towards the SLIM behaviour portrait. I see that the main effect of such a transition occurs by way of the dominating expansion of low numbered lock regions (1 and 2 in particular). In particular, the 1 lock quadrilateral expands towards the top and bottom edges to ultimately touch the top and bottom edges of the surrounding frame. I happily witness that twofold rotational symmetry of the whole behaviour portrait about the centre point $(\frac{1}{2}, \frac{1}{2})$ is maintained throughout this progression.

Portraits 6 Behaviour portraits associated with the TLIM plots of Diagram 7.2









TLIM =THLIM

I choose to transform TLIM by applying a translation modulo 1 parallel to the leading 45° diagonal so that its plot is transformed into a THree Line Interphase Map (THLIM) which has twofold rotational symmetry about the centre point $(\frac{1}{2}, \frac{1}{2})$ as shown in Diagram 7.3.

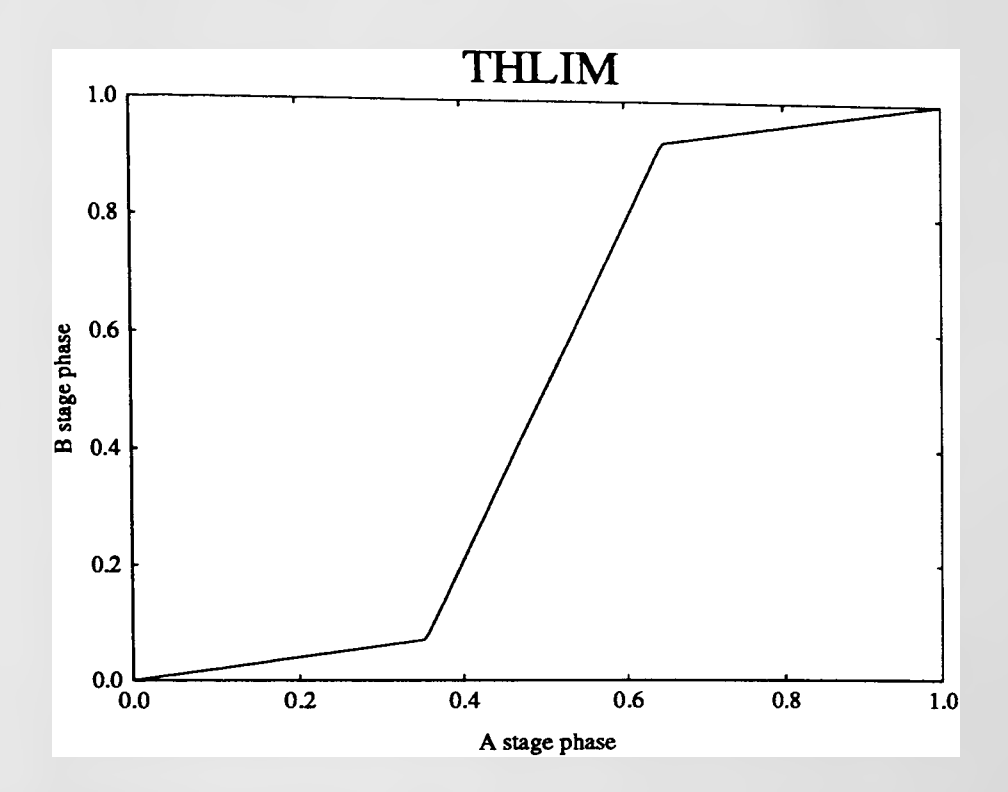


Diagram 7.3 The THLIM interphase map

Because TLIM is a homeomorphism, by Theorems 5.1 and 5.2 such a transformation has no effect on the dynamic behaviour of the TLIM two stage circle map. Hence I deduce that TLIM and companion THLIM behaviour portraits must be identical.

Since THLIM has twofold rotational symmetry about its centre point, it follows by the corollary to Theorem 5.4 that the THLIM behaviour portrait (and consequently the TLIM behaviour portrait also) must likewise have twofold rotational symmetry about the centre point $(\frac{1}{2}, \frac{1}{2})$. Thus even though TLIM and THLIM are not diffeomorphisms, the generic twofold rotational symmetry property established earlier for behaviour portraits derived from differentiable interphase maps, still holds for these special cases.

I make the observation that the shape of the separate plots of TLIM and THLIM resemble lineated versions of the interphase maps associated with Case 1 and Case 2 respectively (see Diagram 5.2). This leads me to ask whether there exists a translation modulo1 between the Case 1 and Case 2 interphase maps. I shall return to this question in due course in section 7.3..

7.2 DEVELOPMENT FUNCTION AND INTERPHASE MAP SHAPE

More Top Hats

We saw in Chapter 6 that SLIM corresponds to a life cycle resulting from a pair of top hat development rate functions situated on a zero background level which match each other at the leftmost upright edge. What are the development rate functions that underly TLIM and THLIM life cycles? Intuitively it is easy to see that the stage development rate functions g_A and g_B that give rise to the TLIM (and THLIM) model are still of top hat form but with the hat 'rims' elevated above the zero background level. Both TLIM and THLIM are members of the universal family of all interphase maps which result from development rate functions g_i of top-hat shape, that is

$$g_{i}(t) \equiv \begin{cases} 1.0 & T_{Mi} - T_{Wi} \le t \le T_{Mi} + T_{Wi} \\ \gamma_{Back} & \text{otherwise} \end{cases} \quad i \in \{A, B\}$$
 (7.3)

with peaks at T_{MA} and T_{MB} respectively and half-widths T_{WA} and T_{WB} respectively.

SLIM is a particular member of the special subfamily which consists of all interphase maps which result from top hats set on a zero background development rate (γ_{Back} =0). Although none of the theorems derived in Chapter 5 are strictly applicable to any member of this subfamily, such systems can be viewed as a limiting case of a series of systems to which Theorems 5.1 through to 5.7 do apply. In the same way that I have shown SLIM to be the limit situation of TLIM, their behaviour can be empirically confirmed to be an orderly limiting case of the appropriate non-zero background situation. My interest in setting γ_{Back} to zero (as previously for SLIM) is that the interphase map is then related to the parameters defining the development functions and hence to the biological context in a demonstrably clear way. Two further cases from the zero background subfamily are especially instructive.

When both development functions are identical in width $W\equiv 2T_{WA}=2T_{WB}$ but the B-stage peak lags the A-stage peak by a time $L\equiv T_{MB}-T_{MA}$, elementary algebra shows that the plots of the two stage specific phases are given as functions of normalised real time t by a part of the pair of straight lines

$$\theta_{i} = \left(\frac{t}{W} + \frac{1}{2} - \frac{T_{Mi}}{W}\right)^{*} \qquad i \in \{A, B\}$$
 (7.4)

Also, when

$$\begin{split} t &= T_{\text{MB}} - \frac{W}{2}, \ \theta_{\text{B}} = 0 \ \text{and} \ \theta_{\text{A}} = \frac{L}{W} \ , \\ t &= T_{\text{MA}} + \frac{W}{2}, \ \theta_{\text{A}} = 1 \ \text{and} \ \theta_{\text{B}} = 1 - \frac{L}{W} \end{split}$$

Thus the plot of the interphase map must pass through the points $(\frac{L}{W}, 0)$ and $(1, 1 - \frac{L}{W})$ which together with the fact that it is linear inbetween implies that

$$\theta_{B} = f(\theta_{A}) = \begin{cases} 0 & 0 \le \theta_{A} \le \frac{L}{W} \\ \theta_{A} - \frac{L}{W} & \frac{L}{W} < \theta_{A} < 1 \end{cases}$$
 (7.5)

Substituting this expression into inequality (5.3) given in Theorem 5.6, as my empirical studies indicate that I can safely do, then gives the one-lock condition as

$$1 - \alpha^* + \frac{L}{W} > \beta^* > 1 - \alpha^* - \frac{L}{W}$$
 (7.6)

I see immediately that the deviation of the interphase map from the leading 45° diagonal and the width of the one-lock region are both directly proportional to the ratio of the lag between the two development peaks to their (common) width. I note that when the lag is 30% of the development peak width, the one-lock region covers almost 50% of the total (α,β) plane.

For the second special case, namely where the two development functions have the same peak position but different half-widths, the two stage specific stages are given by parts of the pair of straight lines

$$\theta_{i} = \left(\frac{1}{2W_{i}}[t - T_{M}] + \frac{1}{2}\right)^{e} \qquad i \in \{A, B\}$$
 (7.7)

Also, when

$$\begin{split} t &= T_\text{M} - T_\text{WB} \,, \ \theta_\text{B} = 0 \ \text{and} \ \theta_\text{A} = \frac{1}{2} \Big(1 - \frac{T_\text{WB}}{T_\text{WA}} \Big), \\ t &= T_\text{M} + T_\text{WB} \,, \ \theta_\text{A} = 1 \ \text{and} \ \theta_\text{A} = \frac{1}{2} \Big(1 + \frac{T_\text{WB}}{T_\text{WA}} \Big) \end{split}$$

which this time imply that the interphase map f is given by

$$\theta_{\rm B} = f(\theta_{\rm A}) = \begin{cases} \frac{1}{2} + \left(\frac{T_{\rm WA}}{T_{\rm WB}}\right) \left(\theta_{\rm A} - \frac{1}{2}\right) & \frac{1}{2} \left(1 - \frac{T_{\rm WB}}{T_{\rm WA}}\right) < \theta_{\rm A} < \frac{1}{2} \left(1 + \frac{T_{\rm WB}}{T_{\rm WA}}\right) & \text{otherwise} \end{cases}$$
(7.8)

Here the interphase map is a symmetrical lefthand Z-shape analogous to the initially concave S-shape of Case 2 analysed earlier. The slope of the stroke of the Z, and hence the deviation from the diagonal depends on the *ratio* of the widths of the development functions. The width of the one-lock region is determined by the same *ratio*.

I observe that interphase maps resulting from this second special case only differ from SLIM (for which $S = \frac{T_{WA}}{T_{WB}}$) by a modulo 1 translation parallel to the x axis by an amount $\frac{1}{2}\left(1 - \frac{T_{WB}}{T_{WA}}\right)$ (seen by replacing θ_A with $\theta_A' + \frac{1}{2}\left(1 - \frac{T_{WB}}{T_{WA}}\right)$ in expressions (7.8)). I would thus anticipate from Theorem 5.1 that the class of circle maps composed from them are dynamically equivalent to the SLIM model, with identical companion behaviour portraits. Empirical studies show this to be so and I am overjoyed to find that the one-lock region given by inequality (5.4) in Theorem 5.7 is

$$\left(\frac{T_{WA}}{T_{WB}}\right)\left(1-\alpha^*\right) > \beta^* > 1 - \left(\frac{T_{WA}}{T_{WB}}\right)\alpha^* \tag{7.9}$$

identical to that obtained earlier for SLIM (inequality 6.10).

Empirical studies have also confirmed the accuracy of equations (7.6) and (7.9) and show that all the theorems derived in section 5.1 also hold (at least to graphical accuracy) for the above zero-background cases (that is, when $\gamma_{Back}=0$). The efficacy of inequality (7.6) as a predictor of the extent of the one-lock region when γ_{Back} is small may be gauged by comparison with the results shown in Portraits 8 (lower right frame).

When lines go to curves

I show the effect of moving away from 'lineness' (absence of curvature) by featuring a curved corner version of THLIM whose plot has both corners 'rounded off' by tangential circular arcs. I define the imposed curvature in terms of a single parameter P which represents the distance of the tangential circle's centre from the original corner. Thus, curvature is defined simply as an increasing function of P. Diagram 7.4 shows 4 superimposed plots of curved corner THLIM interphase maps for increasing curvature parameter P. The associated behaviour portraits are shown in Portraits 7.

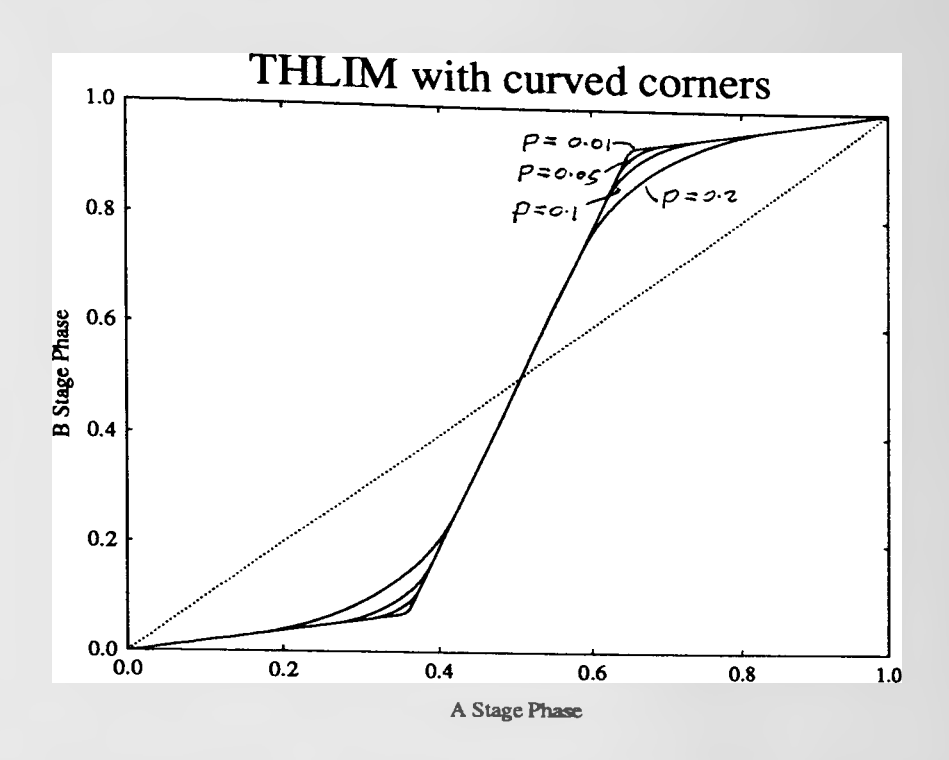
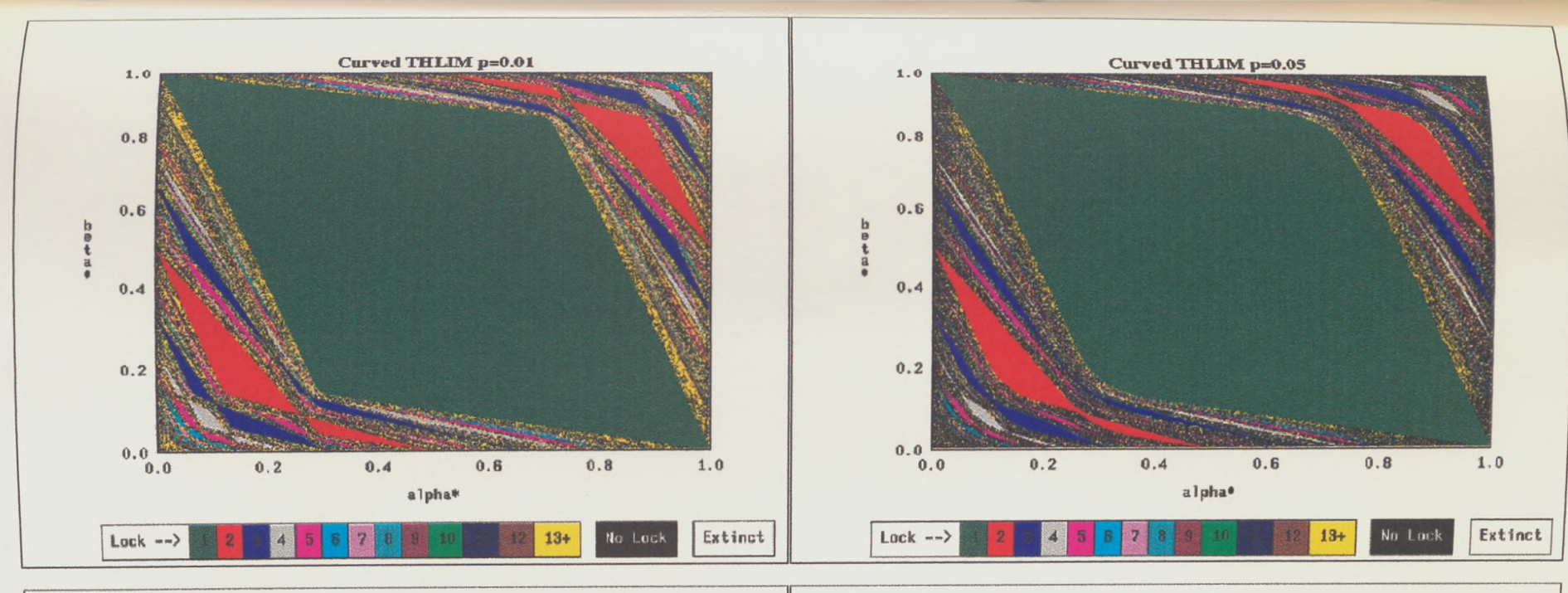


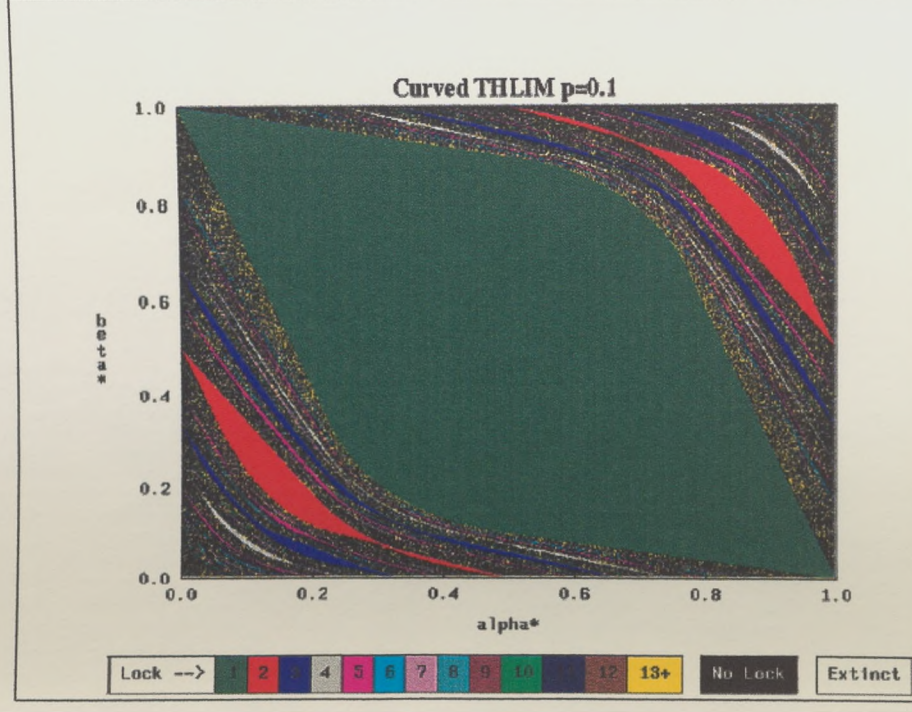
DIAGRAM 7.4 THLIM with curved corners for increasing curvature parameter P

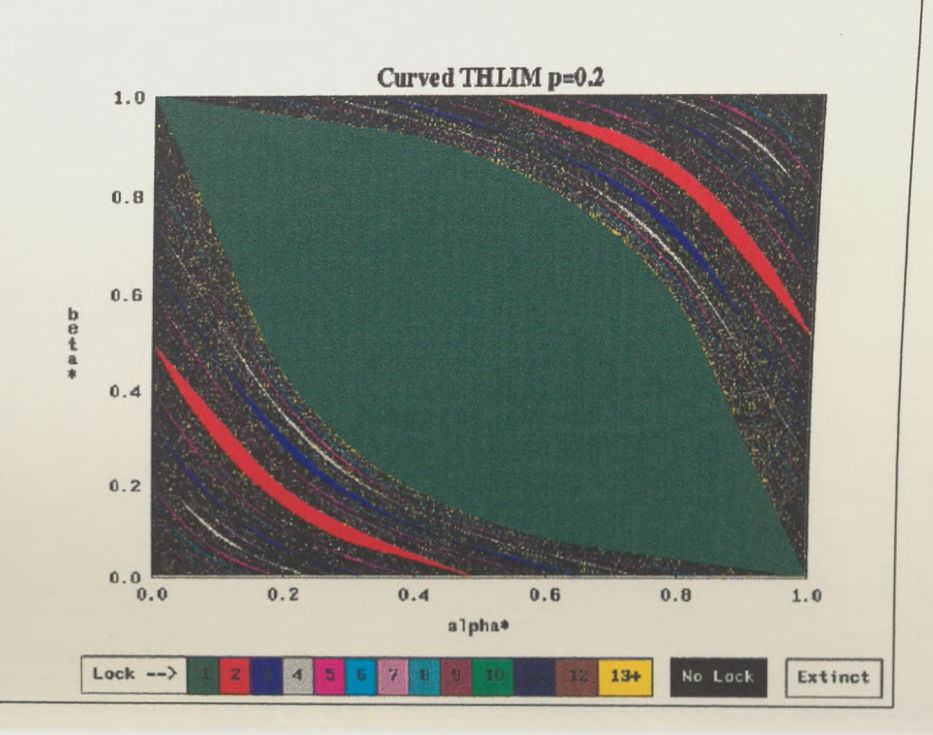
I observe that as P increases and the interphase map smoothly curves away from lineness, the same effect is carried through to the separate lock regions of the behaviour portrait (sequence from top left to lower right frame). Interestingly, I also see that the previously diffuse no-lock blackness prevails over regions of higher locking. When P reaches the value of 0.2 (lower right frame), there are virtually no lock regions beyond lock number 4. I observe that increasing curvature simultaneously imposes a flattening of the overall interphase map shape. This leads me to conjecture that the closeness of portions of the interphase map to the leading 45° diagonal interferes with higher locking behaviour.

In passing, I note that because the curved corner THLIM is a diffeomorphism, by Theorem 5.5 its associated behaviour portrait must have twofold rotational symmetry about its centre. I see that as $P\rightarrow 0$, the above limiting approach can serve as an alternative method (to using the corollary to Theorem 5.4 on THLIM in section 7.1 above) for establishing that the THLIM (and TLIM) behaviour portrait must have rotational symmetry of 2 about the centre point $(\frac{1}{2}, \frac{1}{2})$.

Portraits 7 Behaviour portraits associated with the curved corner THLIM plots of Diagram 7.4







7.3 CLOSENESS TO THE LEADING 45° DIAGONAL

In order to carefully examine the influence of closeness of portions of the interphase map to the leading 45° diagonal and hence on the system dynamics I explored a two stage model in which both stages had development functions shaped like Cauchy distributions.

Cauchy development distributions

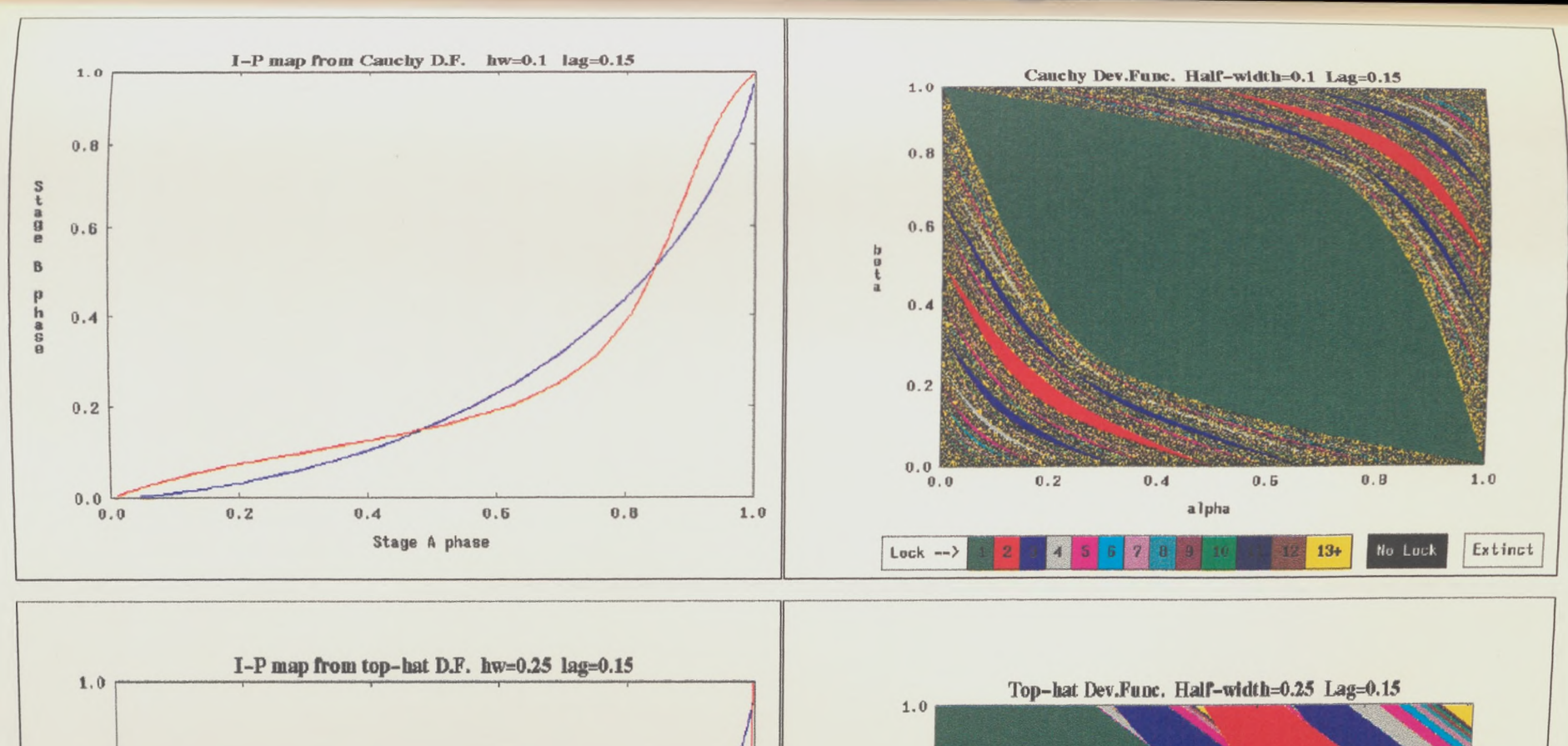
These are defined by

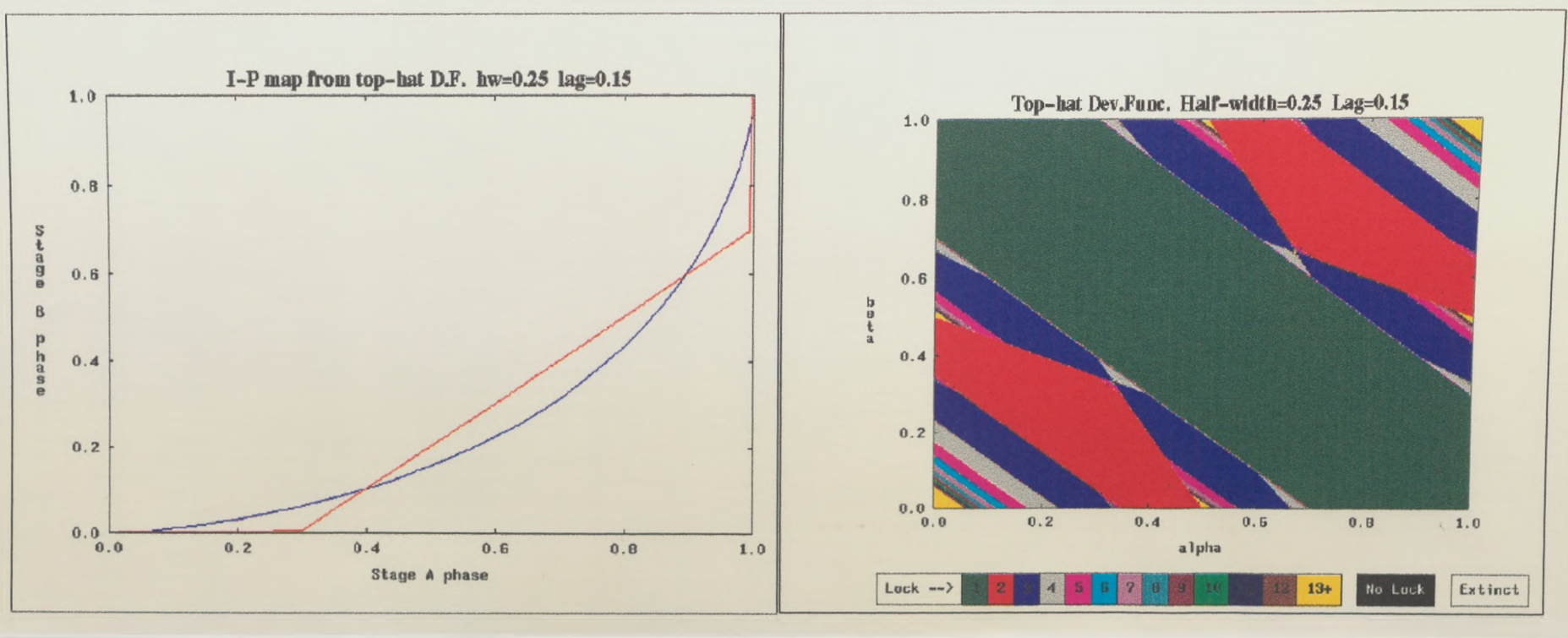
$$g_{i}(t) = \frac{1}{1 + \left(\frac{t - T_{Mi}}{T_{Wi}}\right)^{2}}$$
 $i \in \{A, B\}$ (7.10)

with peaks at T_{MA} and T_{MB} respectively and half-widths T_{WA} and T_{WB} respectively. The Cauchy distribution looks superficially similar to a Gaussian, but is more strongly peaked and has much longer tails. For the parameters used in this work, the appearance within the finite domain [0,1) is similar to that of a Gaussian distribution sitting on a non-zero background. Although it is possible to write down a closed form expression for the interphase map the result is both bulky and unilluminating and I shall not reproduce it here. Instead I show a typical example in Portraits 8 (top left frame-red line), in this case resulting from a simple lag (with a lag/width ratio of 1.5.) between two otherwise identical Cauchy development functions. The right frame shows the resulting behaviour portrait. Parameters are chosen so as to give an approximately equal "average" deviation from the leading 45° diagonal as the plot of the interphase map derived earlier in Diagram 5.2(a) from a lagged pair of Gaussians (blue line). Comparison of the two shows that the extended tails of the Cauchy distribution lead to an interphase map which has the desired closeness towards the leading 45° diagonal at the two ends (i.e. non-strictly concave shape).

Comparison of the Cauchy associated behaviour portrait with that associated with the strictly concave (Gaussian) Case 1 interphase map (Portraits 2 top right frame), shows that while the region of one-lock is larger in the Cauchy case than for the Gaussian,

Portraits 8 Closeness to the leading 45° diagonal. The left hand frame shows the interphase map (red line) used to construct the behaviour portrait shown in the right hand frame. Comparison is made with the Case 1 interphase map (left hand frames, blue line) shown earlier in Diagram 5.2(a).





the regions of higher lock-number are much reduced in size and the density of points of neutral or near-neutral stability is much increased.

I am thus led to fervently hypothesise that the size of the one-lock region reflects the maximum deviation of the interphase map from the leading 45° diagonal, whereas the size of the higher lock-number regions (in agreement with the curved corner THLIM model) is heavily influenced by the presence of portions of the interphase map lying close to the leading 45° diagonal.

To emphasise this hypothesis even further I returned to the top hat family and examined the dynamics of a number of classes of two-stage circle maps composed from the resulting interphase maps.

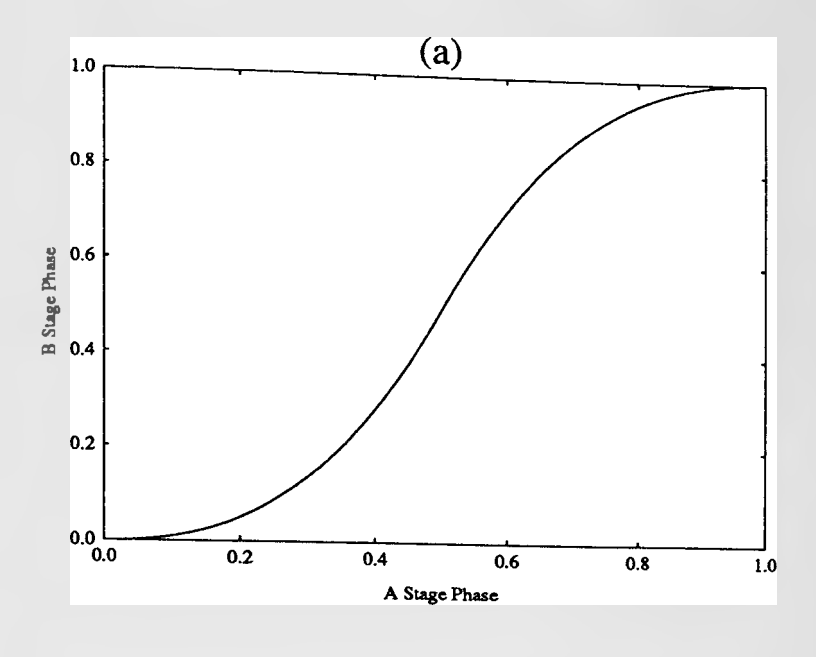
For the case γ_{Back} =0.005, the resulting interphase map is shown in Portraits 8 (lower left frame (red line)). This map may be compared with the Gaussian case interphase map with a similar average deviation from the leading 45° diagonal, (again shown by the blue line) in the same figure. I see that the interphase map from the top-hat case has a smaller maximum deviation from the diagonal than the Gaussian case, but diverges more rapidly near the origin and (1,1). I would expect this to produce a smaller one-lock region than the Gaussian case surrounded by larger regions of higher lock number and fewer neutrally stable points. Comparison of Portraits 8 (lower right frame) and Portraits 2 (top right frame) confirms that this is the case.

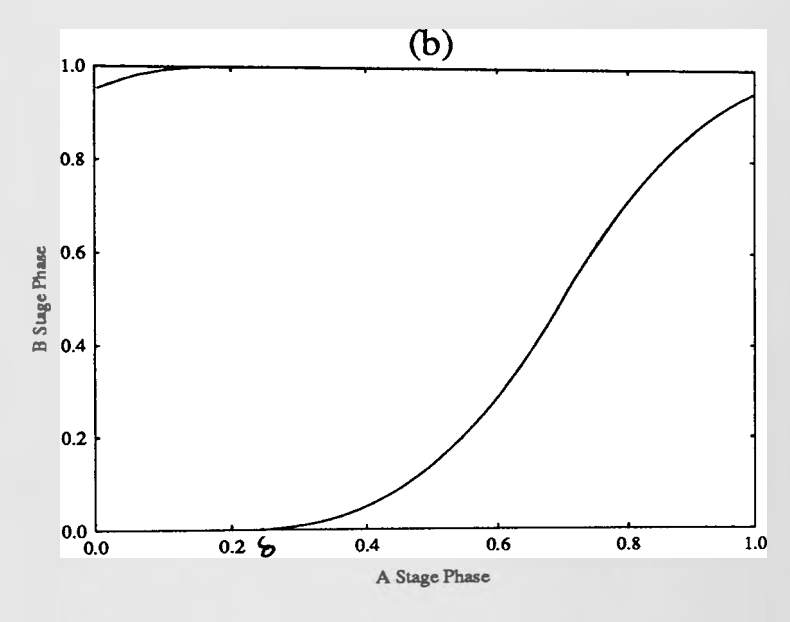
A comparison between Case 1 and Case 2

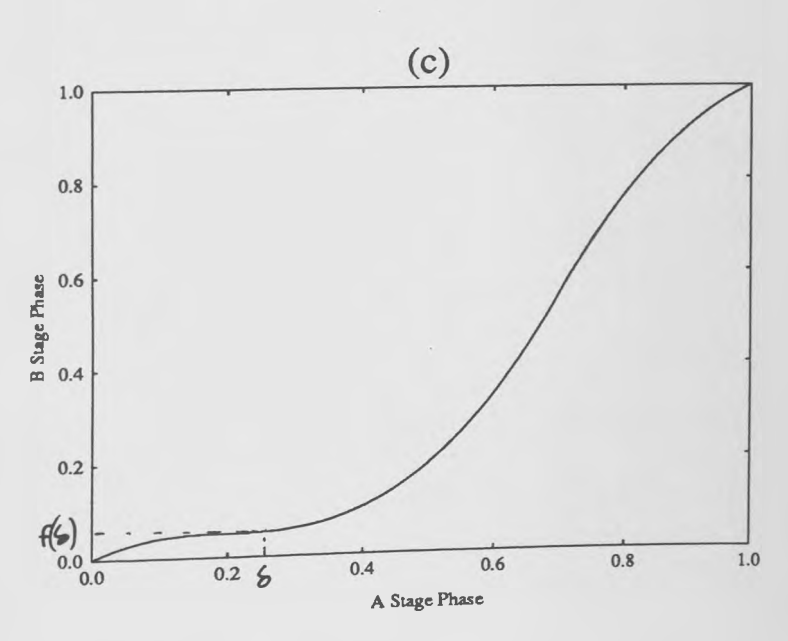
A somewhat baffling property of the earlier Case 1 and Case 2 models, is that the contrastingly different shape of their associated interphase maps seems to be inadequately represented in their associated behaviour portraits. I shall employ a purposeful translation modulo 1 to demonstrate why they turn out to be more similar than I might expect. In this context, I find it helpful to think of Case 1 and Case 2 interphase maps as the respective curved analogues of TLIM and THLIM.

I first observe that Theorems 5.1 and 5.2 together tell us that the behaviour portrait associated with the two stage circle map $F_{\alpha\beta}$ is unaffected by any translation (modulo1) applied to the interphase map f from which $F_{\alpha\beta}$ is composed. For any f, this species of transformation thus gives rise to an associated 'equivalence class' of interphase maps, each member of which (when incorporated within $F_{\alpha\beta}$) gives rise to the same behaviour portrait. I helpfully visualise the entire infinite set of such

Diagram 7.5







interphase map plots as those curves which appear within the unit square as it is shifted about the graph of the lift f(x) of the original interphase map f. I see that under such translations modulo 1, the complete set consists of all such plots obtained by confining the displacement of the unit square so that the line y=x must pass through its interior.

Realising this, I apply a modulo 1 translation to the Case 2 interphase map by a positive amount δ <1 parallel to the x-axis and an amount $f(\delta)$ parallel to the y-axis as shown in Diagram 7.5. I now see that $F_{\alpha\beta}$ composed from the Case 2 interphase map has the same dynamic behaviour as $F_{\alpha\beta}$ composed from an interphase map whose shape is no longer *strictly* concave rather like the Cauchy interphase map above. I spot that the overall quality of the behaviour portrait associated with the Case 2 interphase map (seen in Portraits 3) is closer to the above Cauchy case (e.g Portraits 8 top right frame) than any derived from the Case 1 interphase map (Portraits 2). In line with the above hypotheses, this is particularly true in terms of both general blackness and low lock region shape.

7.4 PRACTICAL BIOLOGICAL IMPLICATIONS

In this final section I give two diverse examples which illustrate the biological scope of the current model formulation.

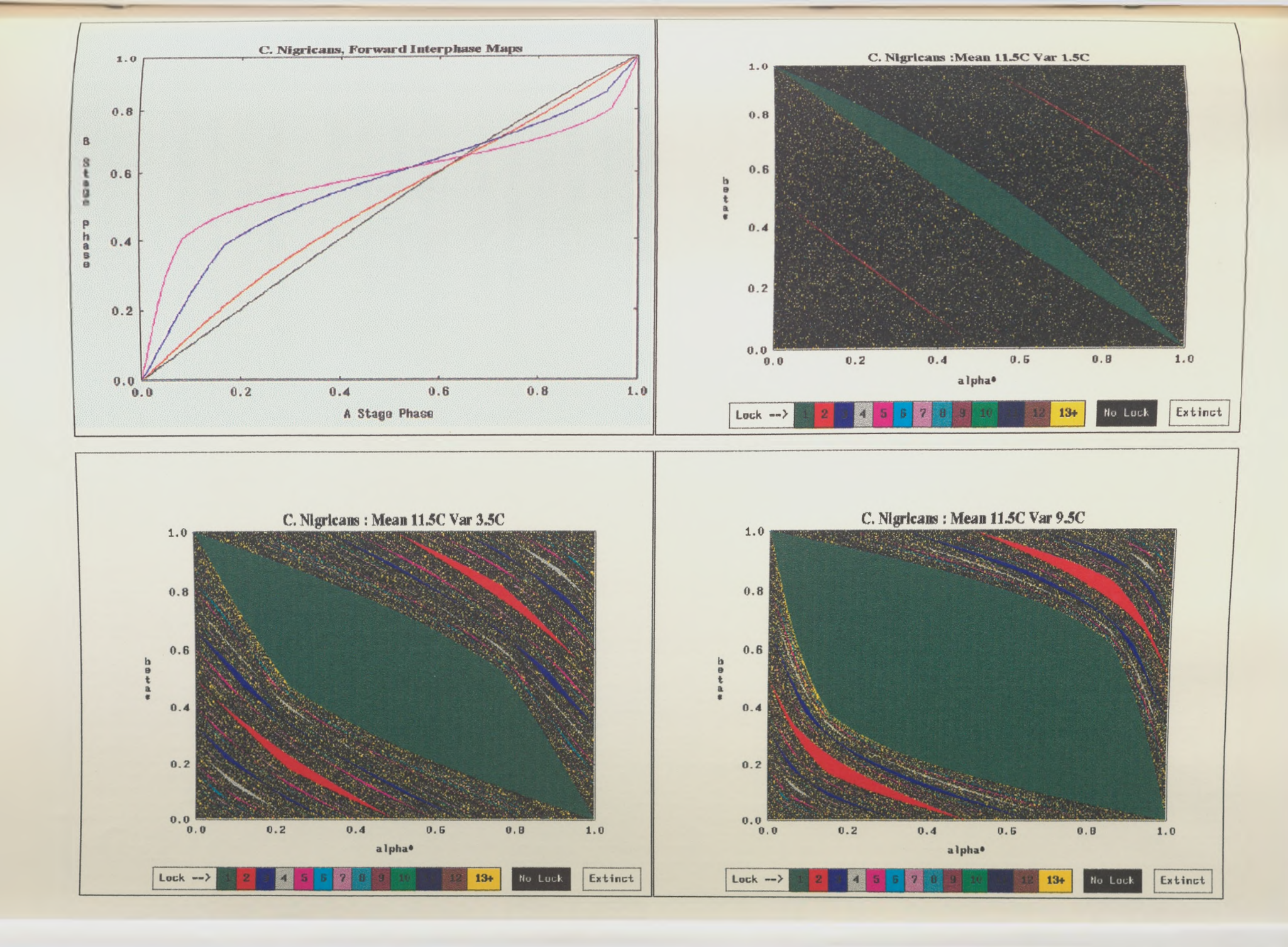
(a) Catops Nigricans revisited

I return to the two stage *Catops* model of Chapter 1. How does the preceding analysis help us to understand the observed dynamic behaviour of this model and thus gain insight into the biological context? Portraits 9 (top left frame) shows plots of interphase maps between the Pre-adult and Immature Adult stages obtained under 3 consecutively wider ranges of annual temperature variation, together with the respective behaviour portrait (top right, lower left, and lower right frames).

None of the interphase map plots have rotational symmetry because the 1 month time lag in temperature (the constant Tshift in equation 1.1) buckles their curves away from the centre point $(\frac{1}{2}, \frac{1}{2})$. Because the stage specific phase of the Immature Adult (B stage) initially leads the stage specific phase of the pre-adult (A stage), all the plots have the shape of an (albeit distorted) *lefthand* S, in other words an (initially) strictly convex rather than an (initially) strictly concave curve. I observe that the main effect of widening the range of annual temperature variation (and thus accentuating the difference between the development response exhibited by each stage) is to amplify the maximum deflection of the interphase map away from the leading 45° diagonal and (at the same time) to reduce the closeness of portions to it. In turn, this governs the design of the corresponding behaviour portrait.

I first see that in all cases (as I would expect) the associated behaviour portrait has the required generic twofold rotational symmetry property about the centre point $(\frac{1}{2}, \frac{1}{2})$. When the range of variation about the Koln mean of 11.5C is very narrow (10-13C), I see that the interphase map (orange line) deviates only very slightly from the leading 45° diagonal and the majority of it remains very close to it. Thus (in support of the 'closeness' hypothesis) I find that the associated behaviour portrait (top right frame) is almost completely made up of black no-lock regions with surfacing speckles of yellow high order (13+) lock. Only a narrow window region of (green) 1 lock together with fine strips of (red) 2 lock occur.

Portraits 9 Interphase maps and associated behaviour portraits for the Catops two stage model at 3 different ranges of annual temperature variation. The top left hand frame shows the 3 interphase maps (orange, blue, red lines) used to construct the respective behaviour portraits (top right, lower left, lower right frame).



In the next frame in the sequence (lower left) the annual range of variation is expanded to 8-15C and the interphase map (blue line) deviates further from the leading 45° diagonal. The associated behaviour portrait now takes on the more familiar appearance of a green central diagonal zone surrounded by satellite regions whose separate area diminishes as the lock number increases. In the final frame when the temperature range is the Koln average of 2-21C, the 1 lock zone takes up approximately 50% of the total behaviour portrait. Using the numerically precalculated look up table (as in Appendix A1.2), I find that the physiological time durations of each stage in the (1 lock) synchronised life cycle are then $\alpha = 0.169$, and $\beta = 0.395$. Recalling that a 1 lock was only just achievable when the *Catops* Default Model was exposed to this range of temperature variation (see Table 2, Chapter 1), I am therefore unsurprised to find that the corresponding point in the related behaviour portrait is to be found located only just within the 1 lock zone (at the lower left hand corner).

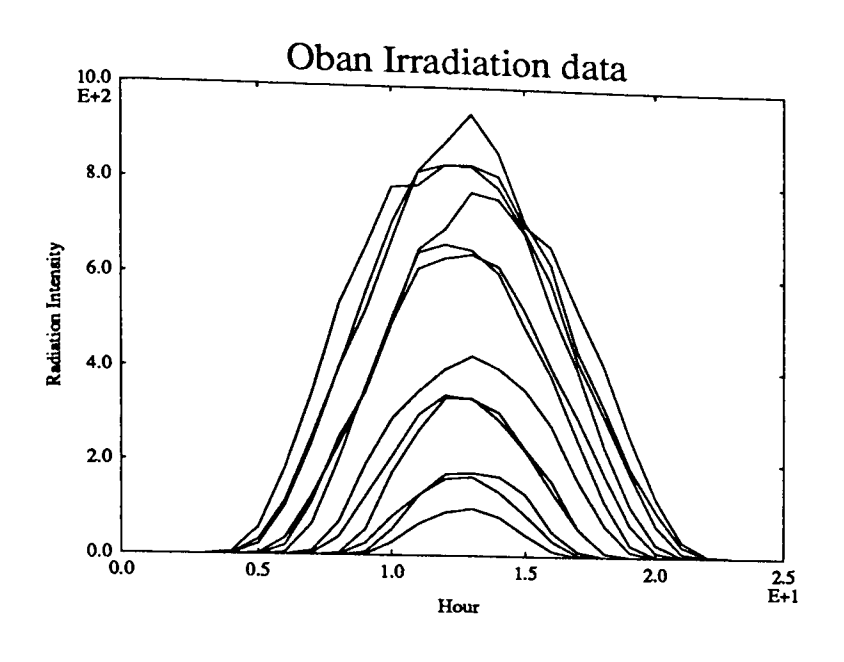
(b) Phytoplankton

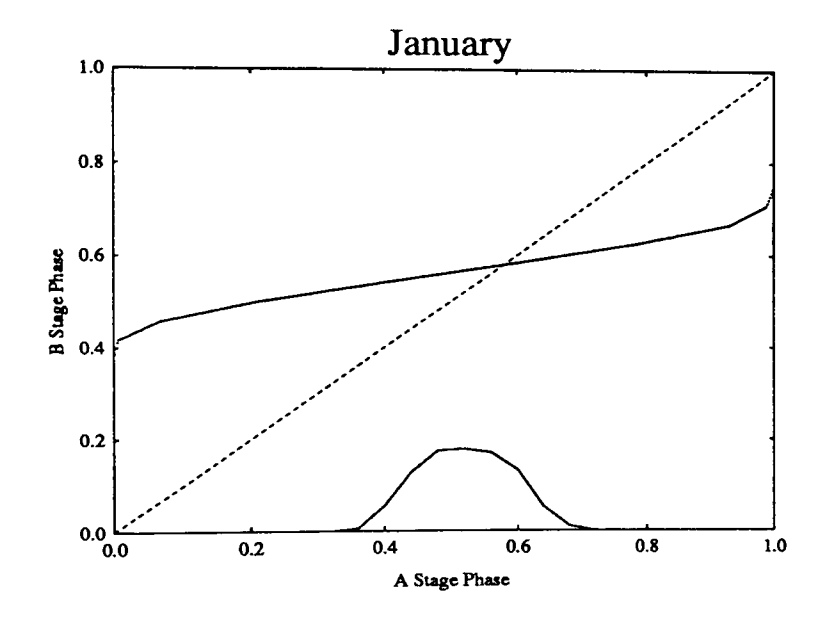
It is well established that some components of the cell cycles of both freshwater and marine phytoplankton require an incident flux of photons whilst others proceed at a rate which depends only on nutrients and temperature (e.g. Spudich & Sager 1980). Heath & Spencer (1985) have constructed a simulation model of marine phytoplankton based on the differentiation between light sensitive and light insensitive stages and have demonstrated synchronisation to an imposed light-dark cycle. The effects of stage specificity are thus implicated in the synchronisation of the life-cycles of such photosynthetic cells to the daily cycle in irradiance. Heath & Spencer (1985) demonstrated that the life cycle may be thought of as consisting of two successive stages:

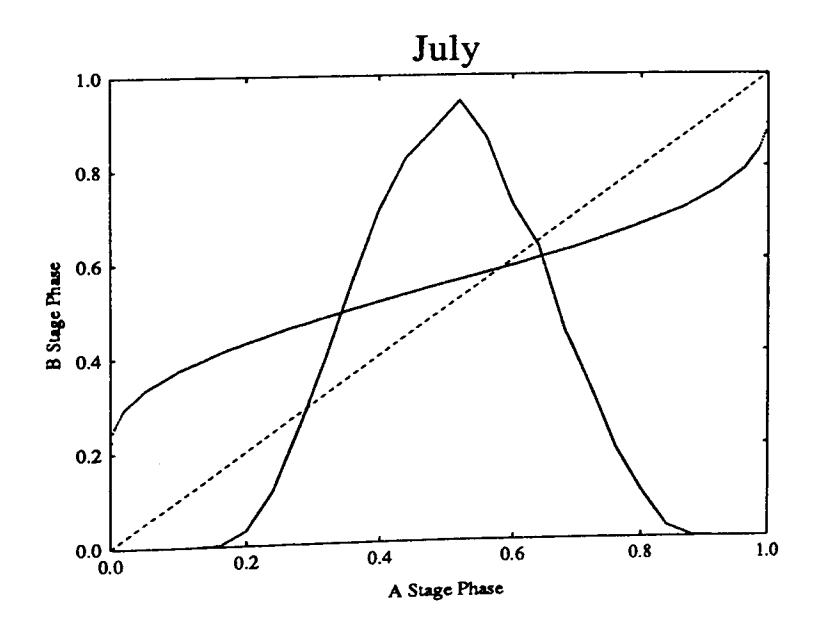
- (i) A stage- light dependent where duration at constant temperature in constant illumination is inversely proportional to the light intensity,
- (ii) B stage- light independent but (possibly) dependent on temperature and nutrient status.

Using the general two stage model, I shall now construct an alternative representation. I make the assumption that the effects of temperature variation and nutrient status on development are negligible in comparison to the effects of light intensity.

Diagram 7.6







Because the A stage is light dependent, I set up a development index which measures development in terms of the photon dosage absorbed by the organism during this stage of the life cycle. Development rate is then proportional to the rate of absorption of photons, which I assume to be directly proportional to the light intensity at the surface (sea level). This enables me to define an A stage phase $\theta_A(t)$ directly in terms of the proportion of daily photon dose delivered by (normalised) time of day t.

I assume that B stage development proceeds independently, at a constant development velocity measured in an (other) appropriate index. It immediately follows that the stage specific plot of B stage phase θ_B vs (normalised) real time t is the leading 45° degree diagonal.

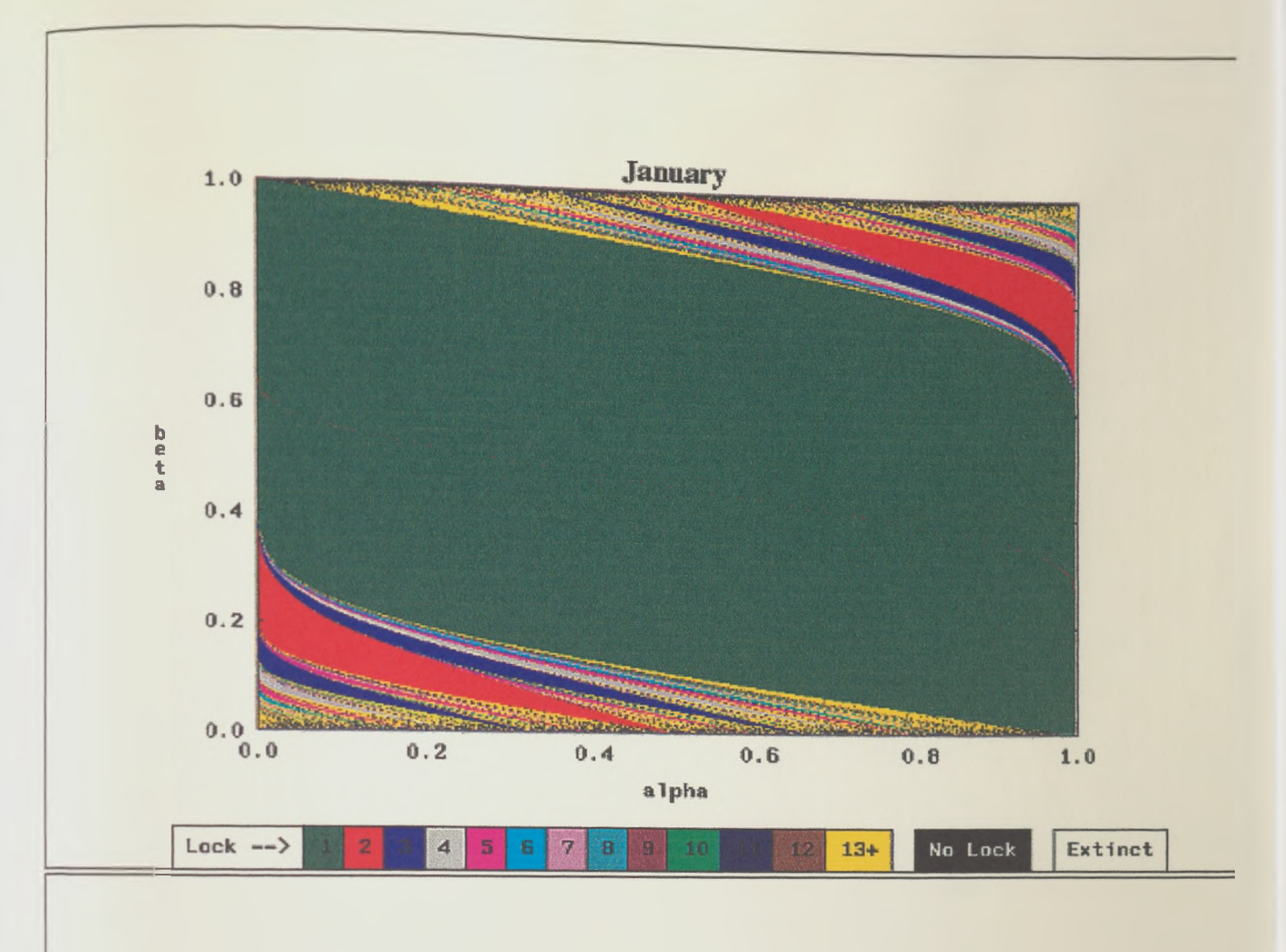
Hence the separate physiological time durations of each stage in this model are:

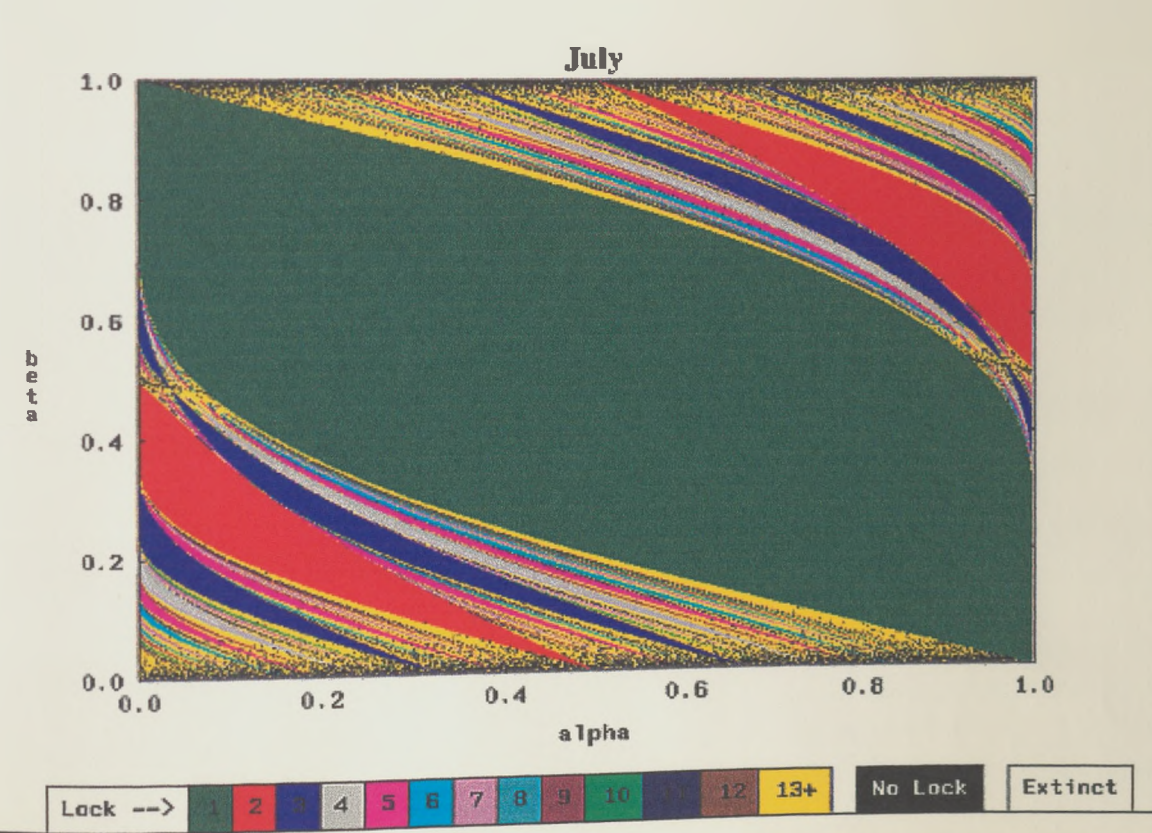
α≡quantity of 'daily photon doses' required to traverse the A stage, β≡quantity of daily development increments required to traverse the B stage.

Diagram 7.6 (top frame) shows monthly graphs, with linear interpolations between hourly placed data points, of the mean daily irradiation intensities recorded in the coastal town of Oban (west Scotland) for the calendar year 1991 (data from Heath). By the above assumptions, these graphs depict the mean daily development rate of the A stage for each month of the year.

For the most extreme months of January and July I used numerical integration to obtain the A stage phase $\theta_A(t)$ and the respective forward $(A \rightarrow B)$ interphase map f associated with each month. Diagram 7.6 (middle and lower frames) shows the plots of f for each month together with the monthly irradiation data (superimposed plot) from which it is derived. In this model because B stage phase $\theta_B(t)$ =t, the interphase map plot $\theta_B(=f(\theta_A))$ vs θ_A is simply the mirror image (in the leading 45° diagonal) of the stage specific plot of the A stage phase: $\theta_B = f(\theta_A) \Leftrightarrow \theta_A(t) = f^{-1}(\theta_B(t)) = f^{-1}(t)$ As with *Catops* each interphase map plot is thus a *lefthand* S.

Portraits 10 Behaviour portraits associated with the January and July interphase maps





Because of the virtual zero background troughs occurring between the peaks, the development rate functions have an innate top hat quality which (in turn) produces the strongly lineated appearance of the resulting interphase map plots. In particular, the January interphase map plot is almost the mirror image (in the leading 45° diagonal) of an interphase map which results from the second special case of top hat systems outlined above (expressions 7.8). Also as with *Catops*, both plots buckle away from the centre point $(\frac{1}{2}, \frac{1}{2})$. Although this again is the resultant effect of a slight rightward shift of the underlying development rate peaks, the shift is really an artefact produced by the statistical method employed in calculating the hourly mean irradiation intensities. (For example, the data point reading at 1300 hrs represents the mean value of the irradiation intensity taken over the hour *interval* 1200 hrs to 1300hrs averaged over the entire month).

Portraits 10 show the respective behaviour portraits for both chosen months. I see that they have a similar overall texture to that of a SLIM behaviour portrait. The January portrait is almost a reflection (as Theorem 5.3 would lead me to predict from its interphase map) of the SLIM behaviour portrait in the leading 45° diagonal.

I see that the two behaviour portraits differ most visibly in the comparative size of their (green) 1 lock region. Thinking of the A stage development rate function as an approximate top hat from the zero background subfamily (second special case) again would lead me to predict this. It follows that because the B stage top hat width is 1, the *ratio* of the A and B stage widths is directly governed by the width of the A stage. In January, the A stage width is much narrower than in July so that by the 1 lock conditions given in inequality (7.9) the converse would be expected of the respective regions in the January and July behaviour portraits. This is indeed the case.

For a given species of phytoplankton I now need only calculate the physiological time durations α and β for each stage to find what the synchronisation behaviour of a population of such individuals will be. A rough estimatory calculation is helpful to get a feel for the approach.

Example

Utilising the January behaviour portrait, I shall estimate the synchronisation behaviour of the phytoplankton species *Thalassiorira pseudonana* in January, by approximating the development function shown in Diagram 7.5 (middle frame) with a zero background top hat of altitude 150 $\mu Em^{-2}s^{-1}$ (vertical scale, micro-Einsteins, per square metre, per second) and a base width of 0.25 days (6 hours). This implies that α is given by the simple ratio;

α=duration of the A stage /duration of the daily illumination period

where durations are measured as proportions of 1 day.

Heath obtained that for the above species:

- (i) At a constant light intensity of 150 $\mu Em^{-2}s^{-1}$ the real time duration of the (light dependent) A stage is 1.85 hours=0.077 days. Thus I calculate $\alpha = 0.077/0.25 = 0.31$.
- (ii) For the (light independent) B stage the real time duration is 5.5 hours=0.23 days and therefore β =0.23.

Viewing the January behaviour portrait, I see that the parameter pair (0.31, 0.23) lies within the green 1 lock region and thus I estimate that during the winter this species will exhibit a synchronised life cycle, with one division occurring each day.

7.5 DISCUSSION

The key result which comes out of the foregoing analysis is that stage-specificity of developmental response is a powerful mechanism for synchronising life-cycles to periodic environmental forcing. The determinant of the power of the synchronising force, and hence its capacity for maintaining synchrony in the face of cycle-on-cycle variability in both environment and organism, depends on the extent of the stage-specificity. In a nutshell, the essence of synchronization behaviour in the general two stage model is determined by the amount of discontinuity (in a broad 'fuzzy' sense) present within the exhibited development response to the environment.

The shape of the interphase map gives an immediate visual measure of the amount of such discontinuity present. It serves to foresee (by the extent of the maximum deviation of its plot away from the leading 45° diagonal) the expected robustness and dominance of low lock behaviour. It can also indicate the likelihood of a sparsity of high lock behaviour, by the presence of plot portions close to the leading 45° diagonal. My investigations have also shown that (in any event) high lock regions become decreasingly smaller in *separate* area as the lock number increases and therefore, because of the inevitable presence of real world 'noise', biologically less significant.

The examples included in the final section give weight to the argument (previously outlined in section 4.1) that development dormancy, that is a period of the environmental repeat cycle when some life history-stages exhibit reduced development rates, is important in the maintenance of life cycle synchrony (e.g. Lacey 1986, Tauber et al 1986, Danks 1987). They powerfully re-enforce the strategic observation that relatively small differences in either the timing or the width of the growing season for the two stages can result in an interphase map sufficiently perturbed from the leading diagonal to imply that a majority of possible life-cycle lengths will result in observable (as opposed to formal) synchronisation.

CHAPTER 8 DISCUSSION

'Studies including more than one life stage are rare and those where the life history of the species studied is also reasonably well known are rarer still'. (Wolda 1988)

That stage specificity can lead to life cycle synchronisation would probably pass unnoticed in many quarters were it not for motivational data sets such as those obtained by Topp (1990). Perhaps the more exciting evolutionary aspects of the influence of periodic environments on life cycle phenomena have yet to be realised. I believe that simple models such as the general two stage model of this thesis have a key role to play in accumulating evidence about the dynamic properties of widely occurring biological systems. To ensure continual progress however, such models must be tested against real world data (Logan & Allen 1992). Sadly and in line with many other authors (e.g. Wolda 1988, Gilbert 1990), I report shortage of data in the life cycle context. Wolda (1988) has urged practical researchers in temperate areas "to concentrate on gathering data on all life stages together with the appropriate life history information". In the seasonal context, comparison of future investigations will need to rely upon data obtained from populations located at a variety of different latitudes.

A key message to emerge from Chapter 1 is that a relative modicum of behavioural data can go a long way towards promoting understanding of powerful underlying mechanisms. Stage specificity is the key synchronisational mechanism in the Catops default model. As well as having major generic implications, such a description has the quintessential robustness demanded of any model that purports to describe a biological process (Usher 1976). Equally impressive is the innate general property that a greater amplification of stage specificity implies a greater robustness of low ordered locking behaviour (visible in the revealing behaviour portraits of Catops in Portraits 9).

The introduction of the concept of physiological time in Chapter 2 provides the building block formulation from which the interphase map description later emerges in Chapter 4. This fundamental component provides a tangible instrument by which stage specificity can be gauged, both visually through the shape of its plot and analytically as a homeomorphism in the realm of dynamical systems theory. The phase description is powerful because it permits synchronisation behaviour to be analysed directly in terms of a dynamic outcome. I point out however, that there are some inevitable limitations of carrying out such an analysis in isolation.

Essentially the phase formulation tells us about types of dynamic behaviour that occur over the complete range of separate stage phase durations α^* and β^* . Because the values of these durations are (by definition) modulo 1, no information can be gleaned on the absolute durations of the component stages of the life cycle and therefore on the life cycle total duration. Consequently, although the model encompasses species with sub-annual life-cycle lengths as well as species with multi-annual life-cycles it does not distinguish results between them.

Whereas the behaviour portrait tells us for what values of α^* and β^* synchronisation occurs (and what the lock numbers are), it does not show the actual emergence (or recruitment) phases to which the life cycle locks. Hence (for example) the formulation cannot tells us anything about cohort splitting. This is exemplified in the simulation with the *Catops* default model where the model was found to synchronise to a 1 lock, lineages for an arbitrary cohort being shown in Diagram 1.7. Although the total life cycle duration is equal to 1 year, the initial cohort splits in two. In an extreme case, many cohorts could arise which, though synchronised in terms of emergence time of year, may actually emerge in different years.

The physiological time description has an innate robustness which stems from the fact that changes in the shape of development response graph vs environmental driving parameter result in a *lesser* change in the shape of the interphase map plot. Despite the multitude of subtly different graphs of development velocity vs temperature function reported in the literature, it turns out that their finer details bear little influence on the current model's synchronisation behaviour. The work of Chapter 7 goes some way to unifying the results of investigations into lineate and curved interphase maps by developing the (expected) robust theme that curves (as in elementary calculus) can be thought of as the limiting case of a 'staircase' of adjacent horizontal lines.

There is scope for investigation into important related areas. Computationally easy explorations into the selection pressures exerted by adverse conditions could be carried out by incorporating appropriate stage threshold criteria such as those suggested by Watt (1968) (see section 1.5). These would produce periods in the year termed 'holes' (as in the investigations of Gurney et al 1992), any lineages emerging into which would terminate. Prospects for a population surviving extinction in a given environment could thus be explored. To be fully productive such investigations would greatly benefit from diverse sources of data.

Attempts at constructing rigid proofs of some of the empirically verified results could be rewarding. In particular, I would anticipate the statement and proof of Theorem 5.5 (on twofold rotational symmetry of the behaviour portrait) to extend to the situation in which the interphase map need only be a homeomorphism. I have shown that this is fully supported by the results of empirical investigations.

As it now stands, the model addresses the fundamental question of the influence of stage specificity on life cycle synchronisation. The current description could be profitably extended to the more general n-stage life cycle scenario by adopting a parallel approach through the use of n-1 appropriate interphase maps. Such a model would become conceptually more difficult to handle because the associated behaviour portrait would move beyond a 3 dimensional representation. An interesting open question would be what influence the location of maximum stage specificity within the life cycle exerts on overall synchronisation behaviour. The idea of an optimal life cycle for a given organism in a given environment is an evolutionary interesting one, but derivation of optimal conditions is frequently not trivial, even for relatively straightforward biological models (e.g. Grist & Maghsoodi 1995). Is there an optimal stage specific strategy in terms of achieving greatest robustness of synchronisational outcome?

The current formulation could be extended to allow further exploration of the influences of a variety of diapause responses or forms of dormancy on life cycle synchronisation. Phil Crowley has suggested an interesting alternative diapause which may occur in some organisms. The speculative distinguishing feature is a 'switch' type mechanism invoked at the start of diapause whereby development rate becomes set by environmental conditions prevailing at that point in the repeat cycle. In the Catops model the mechanism could be implanted in the Immature Adult stage so that an individual's diapause development rate remains fixed at the associated start value (instead of being continually dependent on temperature and photoperiod). The plot of seasonal development rate vs time would thus be a horizontal straight line whose altitude would vary according to the temperature and photoperiod conditions present at the point of eclosion. By this mechanism, before the peak in the growing season, those individuals commencing their development at a later date become committed to a faster development rate than those commencing before them. Since the initial rate is maintained throughout the entire stage, they would have a greater opportunity to complete development and so reproduce before seasonally earlier individuals than in

the current model set up. The great potential for cohort overlap in this situation is self evident. Inclusion of the Crowleyesque mechanism can thus easily produce the 'kink' in the associated circle map plot (between the emergences of successive generations) required for non-invertibility and iterative chaotic behaviour.

In fact, chaos is conspicious by its absence in the current model dynamics. I have observed intriguingly (in Chapter 4) that chaotic behaviour could occur in the description, but only if development is permitted to proceed backwards. Because it would contravene the laws of entropy, such (hypothetical) reverse development never occurs in nature. For example, no creature has been found which 'undevelops' back into the egg from whence it came. Does the model have inadvertent potential to contribute to the lively philosophical debate on the role of chaos in evolutionary ecology (Logan & Allen 1992)?

In nature there will be a degree of blurring of the physiological characteristics of the individual through heterogeneity in terms of its development response to the environment. Further, the environment itself will generally be 'noisy' and therefore subject to a degree of unpredictability. In an effort to make the current description more realistic, a stochastic element could be introduced into the model by making the assumption that the physiological durations α and β of each stage are random variables drawn from some probability distribution. These stochastic parameters could be incorporated into the computational statement of the two stage circle map, investigations with which would then centre on the time evolution of an emergence phase distribution rather than on the dynamic behaviour of orbits. In their investigations with the Corbet model, Gurney et al (1994) found that inclusion of a narrow range (5-10%) of random variability in the individual development rate and duration of reproductive period did not alter their previously held deterministic conclusions. Encouragingly, they found that the emergence phase (probability) distribution of a lineage ultimately tended towards sharp stationary peaks that centred on the stationary phases of the deterministic model.

A reasonable operational definition of observable synchrony is that in the presence of realistic individual and environmental variability, an observer should be able to detect a finite number of distinguishable abundance peaks (of individuals at the key life-history stage) within a single environmental repeat cycle. My simulation studies suggest that locks with repeat lengths greater than ten or so generations, and hence with more than ten peaks of abundance within an environmental repeat cycle, do not

represent observable synchrony. This suggests that the (small) region of very high lock-numbers and near neutral stability shown in some of my investigations should be regarded as predicting effectively unsynchronised behaviour. However, even discounting all regions with lock numbers greater than twelve (shown in yellow on my plots) as well as all neutrally stable points (shown in black) I still conclude that quite subtle differences in developmental response to environmental forcing will imply low lock-number (and hence observable) synchrony for most life-cycle lengths.

As well as establishing the answer to the strategic question about the relation between stage specificity and synchronisation, the present work has also established a number of clear empirical relations between synchronisation behaviour and interphase-map shape. I suggest that experimental investigations of these questions can now proceed directly from developmental response measurements to (approximate) determination of synchronisation behaviour by visual analysis of the interphase map. Simple graphical techniques will suffice to construct the first few iterates of the two-stage circle map and hence to determine the stationary phases for observable locks.

REFERENCES

Agrell I. (1956) A mitotic gradient as the cause of the early differentiation in sea urchin embryo in Bertil Hanstrom Zoological Papers (Ed. Wingstrand K.G.), Zoological Institute, Lund, Sweden.

Agrell I. (1964) Natural division synchrony and mitotic gradients in metazoan tissues in Synchrony in Cell Division and Growth, Interscience Publishers Inc., New York.

Akin E. (1993) The General Topology of Dynamical Systems, American Mathematical Society.

Andrewartha H.G. and Birch L.C. (1954) The Distribution and Abundance of Animals, Methuen, London.

Angerer C.A. (1936) The effects of mechanical agitation on the relative viscosity of amoeba protoplasm, Journal of Cellular and Comparative Physiology 8, 329-336.

Arnold V.I. (1973) Ordinary Differential Equations, MIT Press.

Arnold V.I. (1988) Geometrical Methods in the Theory of Ordinary Differential Equations, 2nd edition, Springer Verlag, Berlin.

Arrowsmith D.K. and Place C.M. (1990) An Introduction to Dynamical Systems, Cambridge University Press, Cambridge.

Arrowsmith D.K. and Place C.M. (1992) Dynamical Systems, Chapman & Hall, London.

Bak P. (1986) The Devil's Staircase, Physics Today 39(12), 38-45.

Baker G.L. and Gollub J.P. (1990) Chaotic Dynamics, an Introduction, Cambridge University Press, Cambridge.

Barton-Wright H. (1933) Recent Advances in Plant Physiology, Methuen, London.

Beck S. D. (1980) Insect Photoperiodism, 2nd edition, Academic Press, New York.

Bernstein E. (1960) Synchronous division in Chlamydomonas Moewusii, Science 131, 1528-1529.

Berry LL., Kunz S.E. and Foerster K.W. (1977) A dynamic model of the Physiological Development of immature stable flies, Annals of the Entomological Society of America. 70(2), 173-176.

Blunck H.(1914) Die entwicklung des Dytiscus marginalis L. vom ei bis zur imago, Z. Wiss. Zool. 111, 76-157.

Braarud T. and Pappas I. (1951) Experimental studies on the dinoflagellate Peridinium triquetrum (Ehrb.) lebour, Avhandl Norskevidensakap-akad, Oslo I. Mat. naturr. Kl. 2, 1-23.

Brown F. (1976) in An Introduction to Biological Rhythms, (Ed. Palmer J.D.) Academic Press, New York.

Brown V.K., Hodek I. (Eds.) (1983) Diapause and Life Cycle Strategies in Insects, Dr. W. Junk, The Hague.

Brust R.A. (1991) Environmental Regulation of Autogeny in Culex tarsalis (Diptera: Culicidae) from Manitoba, Canada, Journal of Medical Entomolology 28(6): 847-853.

Carleton A. (1934) A rhythmic periodicity in the mitotic division of animal cells, Journal of Anatomy 68, 251-263.

Casale A. (1975) Ciclo biologico e morfologia preimaginale di coleoptera Staphilinoidea delle famiglie Leptinidae Catopidae, Redia 56, 199-230.

Chillingworth D.R.J. (1976) Differential Topology with a View to Applications, Pitman.

Clarke K.U. (1967) The growth responses of Locusta migratoria migratorioides to fluctuating temperature regimes, Bulletin of Entomological Research 57, 259-270.

Cloudsley-Thompson J.L. (1953) The significance of fluctuating temperatures on the physiology and ecology of insects, The Entomologist 86(8), 183-189.

Collet P. and Eckman J.P. (1980) Iterated Maps on the Interval as Dynamical Systems, Birkhauser, Boston.

Common I.F.B. (1954) A study of the ecology of the adult Bogong Moth Agrotis infusa (Boisd.) (Lepidoptera: Noctuidae), with special reference to its behaviour during migration and aestivation, Australian Journal of Entomology 2: 223-263.

Conover D.O. and Present T.M.C. (1990) Countergradient variation in growth rate: compensation for length of the growing season among Atlantic silversides from different latitudes, Oecologia 83, 316-324.

Cook J.R. and James T.W. (1960) Light induced division synchrony in Euglena gracilis var. bacillaris, Experimental Cell Research 21, 583-589.

Corbet P.S. (1957) The life histories of two summer species of dragonfly (Odonata: coenagriidae), Proceedings of the Zoological Society of London 128, 403-418.

Corbet P.S. (1980) Biology of Odonata, Annual review of Entomology 25,189-217.

Corbet P.S., Harvey I.F., Abisgold J., and Morris F. (1989) Seasonal regulation in pyrrhosoma nymphulla (sulzer) (zygoptera: coenagrionidae) 2. Effect of photoperiod on larval development in spring and summer, Odonatologica 18, 333-348.

Courtemanche M., Glass L., Belair J., Scagliotti D. and Gordon D. (1989) A Circle map In a Human Heart, Physica D 40, 299-310.

Courtney A.D. (1968) Seed dormancy and field emergence in Polygonum Aviculare, Journal of Applied Ecology 5, 675-684.

Crowley P.H., Nisbet R.M., Gurney W.S.C. and Lawton J.H. (1987) Population regulation in animals with complex life histories: formulation and analysis of a damselfly model, Advances in Ecological Research 17, 1-59.

Crowson R.A. (1981) Biology of the Coleoptera, Academic Press, London.

Crozier W.J. (1926) On curves of growth especially in relation to temperature, Journal of General Physiology 10, 53-73.

Danilevskii A. S. (1965) Photoperiodism and Seasonal Development of Insects, Oliver and Boyd, Edinburg and London.

Danks H.V. (1987) Insect dormancy: an ecological perspective, Biological Survey of Canada (Terestr. Arthoropods).

Danks H.V. (1991) Life cycle pathways and the analysis of complex life cycles in insects, The Canadian Entomologist 123(1), 23-40.

Danks H.V. and Oliver D.R. (1972) Seasonal emergence of some high arctic chironomidae (Diptera), The Canadian Entomologist 104, 661-686.

Davidson J. (1942) On the speed of development of insect eggs at constant temperatures, Australian Journal of Experimental Biology and Medical Science 20, 233-39.

de Candolle A. (1855) Geographie Botanique Raisonee, Masson, Paris.

de Melo W. and van Strien S. (1992) One Dimensional Dynamics, Springer Verlag, Berlin.

Deleurance-Glacon S. (1963) Contribution a l'etude des coleopteres cavernicoles de la Sous-Famille des trechinae, Anales de Speleologie 18, 227-265.

Denlinger D.L. (1986) Dormancy in tropical insects, Annual Review of Entomology 311, 239-264.

Denlinger D.L. (1991) Does lack of diapause result in less insect seasonality? Oecologia 87, 152-154.

Devaney R. L. (1986) An Introduction to Chaotic dynamics, Benjamin, New York.

Devaney R. L. (1990) Chaos, Fractals and Dynamics: computer experiments in mathematics, Addison Wesley, New York.

Downes M. F. (1988) Hatching and early postembryonic development in three spiders, at four temperatures, Bulletin of the British Arachnological Society 7(7) 204-208.

Dugundji J. (1965) Topology, Allyn and Bacon, London.

Engler I. (1982) Comparative Studies on the Seasonal Accommodation of Catopidae (Coleoptera) Zool. Jb. Syst. 109, 399-432.

Eubank W.P. (1973) The significance and thermodynamics of fluctuating versus static thermal environment on Heliothis zea egg developmental rates, Environmental Entomology 2, 491-496.

Evans G. (1975) The Life of Beetles, Allen & Unwin, London.

Eyring H. and Stern I. (1939) The Application of the theory of absolute reaction rates to proteins, Chemical Review 24, 253-270.

Fowler D.H. (1990) The Mathematics of Plato's Academy: A New Reconstruction, Clarendon, Oxford.

Gilbert F. (Ed.) (1990) Insect Life Cycles: Genetics, Evolution, and Coordination, Berlin:Springer Verlag.

Gordon S.C., Barrie I.A., and Woodford J.A.T. (1989) Predicting spring oviposition by raspberry cane midges from accumulated derived soil temperatures, Annals of Applied Biology 114, 419-427.

Gough L.H. (1905) Report of the plankton in the English Channel in 1903, Marine Biology Association of the U.K. International Fishery Investigation (Southern area), 1902-1903, London 325-377.

Grist E.P.M. (1994) Climatic factors affecting the activity of Natterjacks (Bufo calamita) and Common toads (Bufo bufo) outside the breeding season: Mathias revisited, The Herpetological Journal 4(4), (in press)

Grist E.P.M. and Gurney W.S.C. (1994) Stage specificity and the synchronisation of life cycles to periodic environmental variations, Journal of Mathematical Biology (submitted)

Grist E.P.M. and Maghsoodi Y. (1995) Optimal population stabilization and control using the Leslie matrix model, Bulletin of Mathematical Biology 57, (in press)

Gruner C. and Sauer K.P. (1988) Aestival dormancy in the cabbage moth Mamestra brassicae L. (Lepidoptera: Noctuidae), Oecologia 87, 152-154.

Gurney W.S.C. Crowley P.H. and Nisbet R.M. (1992) Locking Life-Cycles Onto Seasons: Circle-Map Models of Population Dynamics and Local Adaptation, Journal of Mathematical Biology 30, 251-279.

Gurney W.S.C. Crowley P.H. and Nisbet R.M. (1994) Stage Specific Quiescence as a mechanism for Synchronizing Life Cycles to Seasons, Theoretical Population Biology (in print).

Halberg F. J. (1959) Physiologic 24 hour periodicity: general and procedural conditions with reference to the adrenal cycle, Z. Vitam Horm Fermentforsch 10, 225-296.

Halberg F. J., Bittner J. and Smith D. (1958) Mitotic rhythm in mice, mammary tumour milk agent and breast cancer, Proceedings of the American Association of Cancer Research 2, 305.

Harper J.L. (1977) Population Biology of Plants, Academic Press, London.

Headlee T.J. (1914) Some data on the effect of temperature and moisture on the rate of insect development, Journal of Economic Entomology 7, 413-417.

Heath M.R (1986) The relationship between electron transport capacity and cell cycle stage in a marine diatom, Journal of Plankton Research 8(6), 1163-1175.

Heath M.R (1988) Interpretation of in vivo fluorescence and cell division rates of natural phytoplankton using a cell cycle model, Journal of Plankton Research 10(6), 1251-1272.

Heath M.R. and Spencer C.P. (1985) A model of the cell cycle and cell division phasing in a Marine Diatom, Journal of General Microbiology 131, 411-425.

Hellmers H. and Sundahl W.P. (1959) Response of Sequoia sepervirens (D. Don.) Endl. and Pseudotsuga menzieslii (Mirb.) Franco seedlings to temperature, Nature 184,1247-1248.

Hodek I. (1983) Mechanisms regulating seasonal adaptation in Diapause and Life Cycle Strategies in Insects, Brown V.K./Hodek I. (eds), Dr. W. Junk, The Hague.

Hoppensteadt F.C., and Keller J.B. (1976) Synchronization of periodical cicada emergences, Science 15, 335-337.

Hughes R.D. (1970) The seasonal distribution of bushfly (Musca vetustissima walker) in south-east Australia, Journal of Animal Ecology 39, 691-706.

Hultin E. (1955) The influence of temperature on the rate of enzymatic processes, Acta Chemica Scandinavica 9, 1700-1710.

Huryn A.D. and Wallace J.B. (1986) A method for obtaining in situ growth rates of larval Chironomidae (Diptera) and its application to studies of secondary production, Limnology and Oceanography 31(1), 216-222.

Hussein M.A. and Ahmad T. (1936) Studies on Schistocerca gregaria, the biology of a desert locust with special reference to temperature, Indian Journal of Agricultural Science VI(2), 188-282.

Ingersoll L.R., Zobel O.J., and Ingersoll A.C. (1948) Heat Conduction: With Engineering and Geological Applications, McGraw Hill, New York.

Israelson G. (1971) On the coleopterous fauna of the subterranean tunnel systems of small mammals with particular reference to burrows of small voles in Finland, Noctulae Entomologicae L1, 113-123.

James T.W. (1959) Synchronisation of cell division in amoebae, Annals of the New York Academy of Science 78, 501-511.

James T.W. (1964) Induced division synchrony in the flagellates, in *Synchrony in Cell Division and Growth*, (Ed. Zeuthen E.) Interscience Publishers Inc., New York.

Janisch E. (1938) Influence of temperature on the life history of insects, Trans. Ent. Soc. (London) 80,137-168.

Jeannel R. (1936) Monographie des Catopidae. Memoires de museum nationale d'histoire naturelle 1, Paris.

Johnson C.G. (1940) Development, hatching and mortality of the eggs of Cimex lectularius L. (hemiptera) in relation to climate, with observations on the effects of preconditioning to temperature, Parasitology 32, 127-173.

Johnson C.G. (1942) The ecology of the bed-bug, Cimex lectularius L in Britain, report on research, 1935-1940, Journal of Hygiene 41, 345-461.

Johnson H. and Lewin I. (1946) The growth rate of E. Coli in relation to temperature, quinine and coenzyme, Journal of Cellular and Comparative Physiology 28, 47-75.

Kamke E. (1950) Theory of Sets, Dover publications inc. New York.

Khan M.F. (1965) Some notes on Acanthocyclops, Proceedings of the Irish Academy of Biology 64,117-130.

Kim S. and Ostlund S. (1989) Universal scaling in circle maps, Physica D 39, 365-392.

Kramer P.J. (1958) in *The Physiology of Forest Trees* (Kramer P.J. and Trimann K.V. Eds.), Ronald press Company, New York.

Krogh A. (1914) On the influence of temperature on the rate of embryonic development, Z. Allg. Physiol. 16, 163-177.

Kudo R.R. (1947) Pelomyxa carolinensis Wilson. II Nuclear division and plasmotomy, Journal of Morphology **80**, 93-102.

Kunz S.E., Berry I.L. and Foerster K.W. (1977) The development of the immature forms of Stomoxys cacitrans, Annals of the Entomological Society of America. 70(2), 169-172.

Lacey E.P. (1986) The genetic and environmental control of reproductive timing in a short lived monocarpic species Daucus carota (Umbelliferaceae), Journal of Ecology 74,73-86.

Larsen E.B. and Thomsen M. (1940) The influence of temperature on the development of some species of Diptera, Vidensk. Medd. Dansk. Naturh. Koren. 104, 1-75.

Leedale G.F. (1959) Periodicity of mitosis and cell division in the Euglenineae, Archives of Microbiology 32, 32-38.

Leitch I. (1916) Some experiments on the influence of temperature on the rate of growth in Pisum sativum, Annals of Botany 30, 25-42.

Lin S.P. and Segel L.A. (1974) Drag force on a deforming sphere and circular cylinder, Journal of Fluid Mechanics 63, 417-429.

Lister A. and Lister G. (1925) Mycetezoa (3rd edition), Oliver and Boyd, Edinburgh.

Logan J.A. and Allen J.C. (1992) Nonlinear dynamics and chaos in insect populations, Annual Review of Entomolology 37, 455-77.

Logan J.A., Wollkind S.C., Hoyt S. and Tanigoshi C. (1976) An analytic model for the description of temperature dependent rate phenomena in arthropods, Environmental Entomology 5, 1133-1140.

Ludwig D. and Cable R.M. (1933) The effect of alternating temperatures on the pupal development of Drosophilia melanogaster Meigen, Physiological Zoology 6,493-508.

Lutz P.E. (1968) Effects of temperature and photoperiod on larval development in Lestes eurinus (Odonata:Lestidae), Ecology 49, 637-644.

Matsushima Y. (1972) Differentiable Manifolds, Marcel Dekker, New York.

Messenger P.S. (1964) The influence of rhythmically fluctuating temperatures on the development and reproduction of the spotted alfalfa aphid Therioaphis maculata, Journal of Economic Entomology 57, 71-76.

Messenger P.S. and Flitters N.E. (1959) Effect of variable temperature environments on egg development of three species of fruit fly, Annals of the Entomological Society of America 52, 191-204.

Mitchison J.M. (1971) The Biology of the Cell Cycle, Cambridge University Press, Cambridge.

Moon R.D. (1983) Simulating Developmental Time of Preadult face Flies (Diptera: Muscidae) from air temperature records, Environmental Entomology 12, 943-948.

Mordue W., Goldsworthy G.J., Brady J. and Blaney W.M. (1980) Insect Physiology, Blackwell Scientific Publications, Oxford.

Muller H.J. (1970) Formen der dormanz bei insekten, Nova Acta Leopodina 35, 7-27.

Nagase A. and Masaki S. (1991) Thermal and photoperiodic responses in aestivating pupae of Dictyoploca japonica (Lepidoptera: Saturniidae), Appl. Ent. Zool. 26(3), 387-396.

Nelson D.M. and Brand L.E. (1979) Cell division periodicity in 13 species of marine phytoplankton on a light:dark cycle, Journal of Phycology 15, 67-75.

Neugebauer O. (1969) The Exact Sciences in Antiquity, Dover, New York.

Neugebauer O. (1975) A History of Ancient Mathematical Astronomy, Vol(ii) Springer, Berlin.

Nielsen E.T. and Evans D.G.(1960) Temperature and pupal development in Aedes taeniorhynchus, Oikos 11, 200-222.

Norling U. (1984a) Life history patterns in the northern expansion of dragonflies, Advances in Odonatology 2, 127-156.

Norling U. (1984b) Photoperiodic control of larval development in Leucorrhinia dubia (vander linden): A comparison between populations from northern and southern sweden (anisoptera:libellulidae), Odonatologica 13, 529-550.

Norling U. (1984c) The life cycle and larval photoperiodic responses of Coenagrion hastulatum (charp) in two climatically different areas (odonata: zygoptera), Odonatologica 13, 429-449.

Overcash J.P. and Campbell J.A. (1955) Proceedings of the American Society of Horticultural Science 66, 87-92.

Palmer J.D. (Ed.) (1976) An Introduction to Biological Rhythms, Academic Press, New York.

Palmer W.A., Bay D.E. and Sharpe P.J.H. (1981) Influence of temperature on the development and survival of the immature stages of horn fly Haematobia irritans irritans (L.), Protection Ecology 3, 299-309.

Parker J.R. (1928) Some effects of temperature and moisture upon the activities of grasshoppers and their relation to grasshopper abundance and control, Trans. IV Int. Congr. Ent. Ithaca. 2, 322-332.

Parker J.R. (1930) Some Effects of temperatureand moisture upon Melanopus mexicanus and Camnula pellucida Bulletin of the University of Montana Agricultural Exp. Sta. No. 223, 1-132.

Parker R.A. and Pardue H.L.(1974) Empirical functions relating metabolic processes in aquatic systems to environmental variables, Journal of the Fisheries Research Board of Canada 31, 1550-1552.

Parker T.S. and Chua L.O. (1987) Chaos: a tutorial for engineers, Proceedings of IEEE 75, 982-1008.

Peairs L. M. (1927) Some phases of the relation of Temperature to the development of insects, West Virginia University Agricultural Agri. Exp. Sta. Bull. No. 208, 1-62.

Pener M.P. & Orshan L. (1983) in Diapause and Life Cycle Strategies in Insects, Brown V.K./Hodek I. (eds), Dr. W. Junk, The Hague.

Powsner L. (1935) Temperature and rate of development:Drosophilia, Physiological Zoology 8, 474-520.

Pradhan S. (1946) Insect population studies IV. Dynamics of temperature effect on insect development, Proceedings of the National Institute of Sciences of India 12, 385-404.

Precht H., Christophersen J., Hensel H. and Larcher W. (1973) Temperature and Life, Berlin, Springer-Verlag.

Preston C. (1983) Iterates of Maps on an Interval, Library of mathematics Volume 999, Springer, Berlin.

Remmert H. and Wunderling K. (1970) Temperature differences between arctic and alpine meadows and their ecological significance, Oecologia 4(2), 208-210.

Roff D. (1980) Optimizing Development Time in a seasonal environment: The 'ups and downs' of clinal variation, Oecologia 45, 202-208.

Sandefur J.T. (1990) Discrete Dynamical Systems, Clarendon press, Oxford.

Sanderson (1910) The relationship of temperature to the growth of insects, Journal of Economic Entomology 3,113-140.

Saunders D.S. (1981) Insect Photoperiodism- the clock and the counter: a review, Physiological Entomology 6(1), 99-116.

Schaffer W.M. (1988) Perceiving Order in the Chaos of Nature in Evolution of Life Histories of Mammals (Ed. Boyce M.S.), Yale University Press.

Sharpe J.H. and de Michele D.W. (1977) Reaction Kinetics of Poikilotherm Development, Journal of Theoretical Biology 64, 649-670.

Shelford V.E. (1929) Laboratory and Field Ecology, Williams and Wilkins, Baltimore.

Simon C. (1979) Debut of the Seventeen-Year-old-Cicada, Natural History Magazine, (May), 38-44.

Smale (1965) Diffeomorphisms with Many Periodic Points in Differential and Combinatorial Topology (Ed. Cairns S.), Princeton University Press.

Smale S. (1967) Differentiable Dynamical Systems, Bulletin of the American Mathematical Society, 73, 747-817.

Spoerl T. and Looney D. (1959) Synchronised budding of yeast cells following X-irradiation, Experimental Cell Research 17, 320-327.

Spudich J.L. and Sager R. (1980) Regulation of the Chlamydomonas cell cycle by light and dark, Journal of Cell Biology 85, 136-145.

Stinner R.E., Gutierrez A.P., and Butler G.D. (Jr.) (1974) An algorithm for temperature-dependent growth rate simulation, Canadian Entomologist 106, 519-524.

Sweeney B.M. and Hastings J.W. (1958) Rhythmic cell division in populations of Gonyaulux polyedra, Journal of Protozoology 5, 217-224.

Sweeney B.M. and Hastings J.W. (1962) Diurnal, tidal and lunar rhythms in the algae in Physiology and Biochemistry of the Algae (Ed. Lewin R.), Academic Press, New York.

Sylven B., Tobias C.A., Malmgren H., Ottoson R., and Thorell B. (1959) Cyclic variations in the peptidase and cathetic activities of yeast cultures synchronised with respect to cell multiplication, Experimental Cell Research 16, 75-87.

Tamiya H., Iwamura T., Shibata K., Hase E. and Nihei T. (1953) Correlation between photosynthesis and light independent metabolism in the growth of Chlorella, Biochemistry and Biophysics Acta 12, 23.

Tanaka K. (1992) Photoperiodic control of diapause and climatic adaptation of the house spider Achaearanea Tepidariorum (Araneaea, Theridiidae), Functional Ecology 6, 545-552.

Tasch P. and Topp W. (1991) Survival with insectivores. The life history tactics of the rove beetle Quedius Ochrepennis (Col. Staphylinidae), Zool. Jb. Syst. 118, 359-375.

Tauber M.J., Tauber C.A. and Masaki S. (1986) Seasonal Adaptations of Insects, Oxford University Press, Oxford.

Topp W. (1984) Synchronisation and polymorphic termination of the diapause response of Qxytelus rugosus (Grav) Col. Staphylinidae, Zool. Jb. Syst 111, 521-542.

Topp W. (1990) Selection for an optimal monovoltine life cycle in an unpredictable environment. Studies on the beetle Catops nigricans Spence, Oecologia 84, 134-141.

Topp W. and Engler I. (1980) Species packing in Catopidae (Col.) of a Beech stand, Zoologischer Anzeiger 205, 39-42.

Topp W. and Kirsten K. (1991) Synchronisation of pre-imaginal development and reproductive success in the winter moth Operata Brumata, Journal of Applied Entomology 111(2), 137-146.

Usher M.B. (1976) Extensions to models used in renewable resource management which incorporate an arbritrary structure, Journal of Environmental Management 4, 123-140.

van Strien S.J. (1991) Interval Maps in Structures in Dynamics, (Eds). Broer H.W., Dumortier F., Van Strien S.J. and Takens F., North Holland Publishing Co., Amsterdam.

van Wijk W.R. and de Vries D. A. (1963) Periodic Temperature Variations in *Physics of Plant Environments* van Wijk W.R. (ed), North Holland Publishing Co. Amsterdam.

Vogt W.G., Walker J.M., and Runko S. (1990) Estimation of development times for immature stages of the bush fly, musca vetustissima Walker (Diptera:Muscidae), and their simulation from air temperature and solar radiation records, Bulletin of Entomological Research 80, 73-78.

Watt K.E.F., (1968) Ecology and Resource management, Mc Graw Hill, New York.

Wigglesworth V.B. (1972) The Principles of Insect Physiology (7th edition), Chapman and Hall, London.

Williams C.T. and Wratten S.D. (1987) The winter development, reproduction and lifespan of viviparae of Sitobion avenae (F.) (Hemiptera: Aphididae) on wheat in England, Bulletin of Entomological Research 77, 19-34.

Winfree A. (1986) The Geometry of Biological Time, series in mathematical biology, Springer, Berlin.

Wipking W. (1988) Repeated larval diapause and diapause-free development in geographic strains of the burnet moth Zygaena trifolii Esp. (Insecta, Lepidoptera), Oecologia. 77, 557-564.

Wolda H. (1988) Insect seasonality: why?, Annual Review of Ecological Systems 19, 1-18.

Zaslavski V.A. (1988) Insect Development, Springer, Berlin.

Zeuthen E. (1964) Temperature induced division synchrony in *Tetrahymena*, in *Synchrony in Cell Division and Growth*, (Ed. Zeuthen E.) Interscience Publishers Inc., New York.

Zheng W.M. (1989) The w sequence for circle maps and misbehaved itineraries, Journal of Physics A: Maths General 22, 3647-3652.

Zheng W.M. (1991) Symbolic dynamics for the circle map, International Journal of Modern Physics B 5,481-495.

Zwolfer W. (1934) Die temperaturabhangigkleit der entwicklung der nonne (Lymantria monach L.) und ihre bevolkerlungswissenschaftliche answertung, Z.Ang. Ent. Berlin 21, 333-84.

APPENDICES

APPENDIX A1 (to Chapter 1)

A1.1 Construction of Photoperiod-compensated L3 Stage Development Rate I define functions $w_{L3}(P)$ and $z_{L3}(P)$ whose graph coincides with L3 stage SD and LD loglinear regression lines for P=Pmin and P=Pmax respectively. Thus when P=Pmin

$$\mathbf{w}_{L3} \text{ (Pmin)} = \mathbf{w}_{L3SD} \tag{A1.1a}$$

$$z_{L3} (Pmin) = z_{L3SD}$$
 (A1.1b)

where w_{L3SD} , z_{L3SD} were obtained from the SD loglinear regression line $y_{L3}(T) = \text{Ln} \left[g_{L3} \left(T, Pmin \right) \right] = \text{Ln} \left(w_{L3SD} \right) + z_{L3SD} T$, and when P=Pmax

$$\mathbf{w}_{L3} (Pmax) = \mathbf{w}_{L3LD} \tag{A1.2a}$$

$$z_{L3} (Pmax) = z_{L3LD}$$
 (A1.2b)

where w_{L3LD} , z_{L3LD} were obtained from the LD loglinear regression line $y_{L3}(T) = \text{Ln} [g_{L3}(T,Pmax)] = \text{Ln} (w_{L3LD}) + z_{L3LD} T$.

For intermediate photophases Pmin < P < Pmax , w_i (P) then takes values between w_{L3SD} and w_{L3LD} and z_i (P) takes values between z_{L3SD} and z_{L3LD} . The photophase function in equation (1.2) (pg. 127) then 'pushes' the w_{L3} and z_{L3} coefficients obtained from regression of SD data to respective coefficients obtained from regression of LD data in a periodic manner. In Diagram 1.2(a) the effect would be to continuously oscillate the L3 stage development curve between the outermost SD and LD regression curves. The SD and LD curves would be 'reached' at the desired photophases of Pmin and Pmax respectively.

A1.2 The Fast 'Look Up Table' Method

This numerical technique exploits the periodic nature of the seasonal development rate functions. S_i is calculated in terms of time of year i.e. for a period of one year only. Use is then made of the fact that Time of year = (Time in years) Modulo 1 year, in order to evaluate S_i for all stages i for any time t in years.

- (a) Divide the year into n evenly-spaced intervals.
- (b) Using a numerical integration technique such as Simpson's Rule, evaluate the integrals

$$G_i(k) = \int_0^k S_i(t)dt$$
 for k=0 to n. (A1.3)

The set of ordered pairs (k, G_i (k)) for k=0 to n is referred to as the Look Up Table' for the stage i. Clearly,the larger the value for n the greater the accuracy of the following interpolations.*

(c) The function G_i has now been calculated at discrete times of year t_k for k=0 to n. For more general *intermediate* times t_{k} falling between discrete times t_k and t_{k+1}

$$G_i(t_{R_i}) \equiv \text{InterpolationX}(t_k, t_{k+1}, G(t_k), G(t_{k+1}))$$
 (A1.4)

The stage i then completes development at time t_{Mi} where t_{Mi} is given by

$$G_i(t_{MS}) = G_i(t_{Ri}) + 1$$
 (A1.5)

by definition of development index.

(d) In general, $G_i(t_{Mi})$ will lie between $G_i(t_s)$ and $G_i(t_{s+1})$, so provided that $G_i(t_{Mi}) < G_i(1)$

$$t_{Mi} \equiv \text{InterpolationY}(t_s, t_{s+1}, G_i(t_s), G_i(t_{s+1}))$$
 (A1.6)

(e) If $G_i(t_{Mi}) > G_i(1)$ Interpolationy would 'go off the end' of the Look-Up Table. Full use is then made of the periodic nature of S_i so that $G_i(t_{Mi})$ can be replaced by $G_i(t_{zi}) = G_i(t_{Mi}) - G_i(1)$ in (A1.5) above, so that instead

$$t_{z_i} \equiv \text{InterpolationY}(t_s, t_{s+1}, G_i(t_s), G_i(t_{s+1}))$$
(A1.7)

t_{Mi} is then given by

$$t_{Mi} \equiv t_{zi} + N \tag{A1.8}$$

where N is the non-zero integer number of years required for G_i to achieve an increase of at least 1.

Since all stages here (for all temperature ranges under consideration) complete their development in under a year, G_i always attains a higher value then 1 in one year so that it turned out that N=1 for all stages of development.

*I found that n=100 gave indistinguishable results from n=1000 for all simulations. In order to gauge the accuracy of the Look Up Table Method employed, simulations for other, analytically integrable S_i [e.g obtained by defining linear g_i] were compared with results obtained by the Look Up Table technique. No detectable differences could be found after 100 years of run time. This gave a good indication of the high accuracy of the simulation results obtained even with n=100.

APPENDIX A5 (to Chapter 5)

Proofs of Theorem 5.6 (Case 1) and Theorem 5.7 (Case 2)

I seek necessary and sufficient conditions on α and β such that the map $F_{\alpha,\beta}$ has a stable fixed point. That is, as established in the proof of Theorem 5.5, I seek necessary and sufficient conditions for there to be at least two solutions to

$$\theta = F_{\alpha,\beta}(\theta)$$
 i.e. $f(\theta) = R_{\beta} f R_{\alpha}(\theta)$ (A5.1)

The interphase map f from which the map $F_{\alpha,\beta}$ is composed is continuous, everywhere differentiable, and strictly increasing so

$$f(0)=0; \quad x\to 1^- \Rightarrow f(x)\to 1^-$$
(A5.2)

$$Df(x)>0 0 \le x \le 1$$
 (A5.2)

I write (A5.1) as

$$f(\theta) = (\beta^* + f[(\theta + \alpha^*)^*])^*$$
(A5.4)

which can be re-expressed as

$$f(\theta) = \beta^* + f(\theta + \alpha^*) \qquad \text{for} \qquad 0 \le \theta < f^{-1}(1 - \beta^*) - \alpha^* \qquad (A5.5)$$

$$= \beta^* + f(\theta + \alpha^*) - 1 \qquad \text{for} \qquad f^{-1}(1 - \beta^*) - \alpha^* \le \theta < 1 - \alpha^* \qquad (A5.6)$$

$$= \beta^* + f(\theta + \alpha^* - 1) \qquad \text{for} \qquad 1 - \alpha^* \le \theta < 1 - \alpha^* + f^{-1}(1 - \beta^*) \quad (A5.7)$$

$$= \beta^* + f(\theta + \alpha^* - 1) - 1 \qquad \text{for} \qquad 1 - \alpha^* + f^{-1}(1 - \beta^*) \le \theta < 1 \qquad (A5.8)$$

$$= \beta^* + f(\theta + \alpha^*) - 1 \quad \text{for } f^{-1}(1 - \beta^*) - \alpha^* \le \theta < 1 - \alpha^*$$
 (A5.6)

$$= \beta^* + f(\theta + \alpha^* - 1) \quad \text{for} \quad 1 - \alpha^* \le \theta < 1 - \alpha^* + f^{-1}(1 - \beta^*) \text{ (A5.7)}$$

$$= \beta^* + f(\theta + \alpha^* - 1) - 1 \text{ for } 1 - \alpha^* + f^{-1}(1 - \beta^*) \le \theta < 1$$
(A5.8)

and re-arranged to give β* as

$$\beta^{*}(\theta) = \begin{cases} Y_{0}(\theta) \equiv f(\theta) - f(\theta + \alpha^{*}) & 0 \leq \theta < \theta_{L} \\ Y_{1}(\theta) \equiv f(\theta) - f(\theta + \alpha^{*}) + 1 & \theta_{L} \leq \theta < 1 - \alpha^{*} \\ Y_{2}(\theta) \equiv f(\theta) - f(\theta - (1 - \alpha^{*})) & 1 - \alpha^{*} \leq \theta < \theta_{R} \\ Y_{3}(\theta) \equiv f(\theta) - f(\theta - (1 - \alpha^{*})) + 1 & \theta_{R} \leq \theta < 1 \end{cases}$$
(A5.9)

where

$$\theta_{1} \equiv f^{-1} (1 - \beta^{*}) - \alpha^{*}; \qquad \theta_{R} \equiv f^{-1} (1 - \beta^{*}) - \alpha^{*} + 1$$
(A5.10)

The monotone increasing property of f implies that

$$Y_0(\theta) < 0$$
 $0 < \theta < 1 - \alpha^*$ (A5.11)

so, given that β^* must lie in [0,1), I need only investigate the functions Y_1 and Y_2 .

For functions Y₁ and Y₂ the following general properties hold:

$$Y_1(0)=Y_2(1)=1-f(\alpha^*)$$
 (A5.13)
 $Y_1(1-\alpha^*)=Y_2(1-\alpha^*)=f(1-\alpha^*)$ (A5.14)

$$Y_{1}(\theta_{L}) = \beta^{*} + f(\theta_{L}) > \beta^{*}$$

$$Y_{2}(\theta_{R}) = \beta^{*} + f(\theta_{R}) - 1 < \beta^{*}$$

$$0 < \theta_{R} < 1$$

$$(A5.15)$$

$$(A5.16)$$

$$\beta^* < 1 - f(\alpha^*) \Rightarrow \theta_L > 0, \theta_R > 1$$
 (A5.17)

A5.1 Proof of Theorem 5.6 (Case 1 conditions for a one Lock for a general concave (or convex) interphase map)

By strict concavity of f (that is $D^2f(x) > 0$), $x_2 > x_1 \Rightarrow D(x_2) > D(x_1) \forall x_1, x_2 \in S^1$ so that

$$DY_{1}(\theta) = Df(\theta) - Df(\theta + \alpha^{*})$$

$$DY_{2}(\theta) = Df(\theta) - Df(\theta - (1 - \alpha^{*}))$$

$$> 0$$

$$1 - \alpha^{*} < \theta < 1$$
(A5.18)

and hence $Y_1(\theta)$ is a monotone decreasing function for $0 < \theta < 1 - \alpha^*$ and $Y_2(\theta)$ is a monotone increasing function for $1 - \alpha^* < \theta < 1$.

However, my interest lies in

$$Y_1(\theta) \quad (0 <) \theta_L \le \theta < 1 - \alpha^*$$
 (A5.19a)
 $Y_2(\theta) \quad 1 - \alpha^* \le \theta < \theta_R (< 1)$ (A5.19b)

that is, the continuous bowl shaped function $Z(\theta)$ with dip (minimum) at $\theta=1-\alpha^*$

$$\beta^{*}(\theta) = Z(\theta) = \begin{cases} Y_{1}(\theta) & \theta_{L} \leq \theta < 1 - \alpha^{*} \\ Y_{2}(\theta) & 1 - \alpha^{*} \leq \theta < \theta_{R} \end{cases}$$
(A5.20)

By inequalities (A5.15), (A5.14) and (A5.16) respectively the altitude of the bowl

at the left 'rim'
$$\theta_L$$
 is $Z(\theta_L)=Y_1(\theta_L)=\beta^*+f(\theta_L)$ $>\beta^*$ by (A5.15) at the minimum $1-\alpha^*$ is $Z(1-\alpha^*)=Y_1(1-\alpha^*)=Y_2(1-\alpha^*)=f(1-\alpha^*)$ at the right 'rim' θ_R is $Z(\theta_R)=Y_2(\theta_R)=\beta^*+f(\theta_R)-1$ $<\beta^*$ by (A5.16) and hence

$$f(1-\alpha^*) < \beta^* < Z(\theta_L) < 1-f(\alpha^*)$$

$$f(1-\alpha^*) < Z(\theta_R) < \beta^* < 1-f(\alpha^*)$$
(A5.21a)
$$(A5.22b)$$

The horizontal line $Z=\beta^*$ 'cuts across' this curve at two points and thus $F_{\alpha,\beta}$ has two fixed points iff $f(1-\alpha^*)<\beta^*<1-f(\alpha^*)$, a single fixed point iff $\beta^*=f(1-\alpha^*)$ or $\beta^*=1-f(\alpha^*)$ and none otherwise. Since $F_{\alpha,\beta}$ is a strictly increasing homeomorphism a single fixed point must be neutrally stable and each pair of fixed points must contain one stable and one unstable member. This completes the proof of Theorem 5.6.

A5.2 Proof of Theorem 5.7 (Case 2 conditions for a one lock for an initially strictly concave (or convex) general 'S' shaped interphase map)

I now have

$$D^2f(x)>0 \ x<\frac{1}{2}; \ D^2f(\frac{1}{2})=0; \ D^2f(x)<0 \ x>\frac{1}{2}$$
 (A5.23)

$$f(1-x)=1-f(x)$$

$$f^{-1}(1-x)=1-f^{-1}(x)$$
(A5.24a)
(A5.24b)

Also now

$$Y_1(0)=Y_1(1-\alpha^*)=Y_2(1-\alpha^*)=Y_2(1)$$
 (A5.25)

I see that

$$DY_1(\theta) = f'(\theta) - f'(\theta + \alpha^*)$$
(A5.26)

SO

$$DY_1(0) = f'(0) - f'(\alpha^*)$$
 <0 (A5.27a)

$$DY_1(1-\alpha^*) = f'(1-\alpha^*) - f'(1)$$
 >0 (A5.27b)

and therefore $Y_1(\theta)$ has one turning point (minimum) in $0 < \theta < 1 - \alpha^*$ at $\theta = \theta_{T1} = (1 - \alpha^*)/2$ [by (A5.26), $f'(\theta_{T1}) = f'(\theta_{T1} + \alpha^*) \Rightarrow 1 - \theta_{T1} + \alpha^* = \theta_{T1} \Rightarrow \theta_{T1} = \frac{1 - \alpha^*}{2}$ ($\theta + \alpha^* = \theta$ is not possible)]

By a parallel argument, $Y_2(\theta)$ has one turning point (maximum) in $1-\alpha^*<\theta<1$, namely at $\theta=\theta_{TD}=1-\alpha^*/2$.

The altitude of the minimum is

$$Y_{1}(\theta_{T1}) = Y_{1}\left(\frac{(1-\alpha^{*})}{2}\right) = f\left(\frac{(1-\alpha^{*})}{2}\right) - f\left(\frac{(1-\alpha^{*})}{2} + \alpha^{*}\right) + 1$$

$$= f\left(\frac{(1-\alpha^{*})}{2}\right) + f\left(1 - \left(\frac{(1+\alpha^{*})}{2}\right)\right) \text{ by (A5.24a)}$$

$$= 2f\left(\frac{(1-\alpha^{*})}{2}\right) \qquad (A5.28a)$$

By similar simple algebra the altitude of the maximum is

$$Y_2(\theta_{T2}) = Y_2\left(1 - \frac{\alpha^*}{2}\right) = 1 - 2f\left(\frac{(1 - \alpha^*)}{2}\right)$$
 (A5.28b)

My interest now lies in the continuous 'sideways S' shaped function $Z(\theta)$ defined by

$$\beta^*(\theta) = Z(\theta) = \begin{cases} Y_1(\theta) & \theta_L \le \theta < 1 - \alpha^* \\ Y_2(\theta) & 1 - \alpha^* \le \theta < \theta_R \end{cases}$$
(A5.29)

which has its point of inflection at $\theta=1-\alpha^*$, and respective minimum and maximum altitudes as in equations (A5.28a) and (A5.28b) above. Thus for the horizontal line $Z=\beta^*$ to 'cut across' this curve and hence for $F_{\alpha,\beta}$ to have two fixed points it is a necessary condition that

$$2f\left(\frac{(1-\alpha^*)}{2}\right) < \beta^* < 1 - 2f\left(\frac{\alpha^*}{2}\right) \tag{A5.30}$$

and for a single solution to exist it is necessary that

$$\beta^* = 2f\left(\frac{1-\alpha^*}{2}\right) \text{ or } \beta^* = 1 - 2f\left(\frac{\alpha^*}{2}\right)$$
(A5.31)

However, these conditions are not sufficient unless $\theta_L < \theta_{T1}$ and $\theta_{T2} < \theta_{R}$.

But I see that

$$\beta^* > 2f\left(\frac{(1-\alpha^*)}{2}\right) \Rightarrow \beta^* > f\left(\frac{(1-\alpha^*)}{2}\right)$$

$$\Rightarrow \theta_L = f^{-1}(1-\beta^*) - \alpha^* = 1 - f^{-1}(\beta^*) - \alpha^* \quad \text{by (A5.24b)}$$

$$< \frac{1-\alpha^*}{2} = \theta_{T1}$$

and

$$\beta^* < 1 - 2f\left(\frac{\alpha^*}{2}\right) \Rightarrow \beta^* < 1 - f\left(\frac{\alpha^*}{2}\right) = f\left(1 - \frac{\alpha^*}{2}\right) \text{by} \quad (A5.24a)$$

$$\Rightarrow \theta_R = f^{-1}(1 - \beta^*) - \alpha^* + 1 = 2 - f^{-1}(\beta^*) - \alpha^*$$

$$> 1 - \frac{\alpha^*}{2} = \theta_{T2}$$

Hence conditions (A5.30) and (A5.31) are also sufficient.

Since $F_{\alpha\beta}$ is a strictly increasing diffeomorphism, each pair of fixed points must contain one stable and one unstable member and a single fixed point must be neutrally stable. This completes the proof of Theorem 5.7.

APPENDIX A6 (to Chapter 6)

A6.1 The 3 FORMS (plot configurations) of the SLIM circle map

From equations 6.7, I have that the SLIM circle map $\theta_{A(n+1)} = \tilde{F}_{\alpha,\beta}(\theta_{An})$ is given by

$$\theta_{A(n+1)} = \frac{\beta^*}{S} + (\theta_{An} + \alpha)^* \qquad \text{for } 0 \le (\theta_{An} + \alpha^*)^* < \frac{1-\beta^*}{S} \quad (6.7a)$$

$$= \frac{\beta^* - 1}{S} + (\theta_{An} + \alpha)^* \qquad \text{for } \frac{1-\beta^*}{S} \le (\theta_{An} + \alpha^*)^* < \frac{1}{S} \quad (6.7b)$$

$$= \frac{\beta^*}{S} \qquad \text{for } \frac{1}{S} \le (\theta_{An} + \alpha^*)^* < 1 \quad (6.7c)$$

I shall express equations (6.7) as a circle map solely in terms of θ_{An} . I note first that

$$(\theta_{An} + \alpha^*)^* = \theta_{An} + \alpha^* \qquad \text{for} \quad \theta_{An} + \alpha^* < 1$$

$$(\theta_{An} + \alpha^*)^* = \theta_{An} + \alpha^* - 1 \qquad \text{for} \quad \theta_{An} + \alpha^* \ge 1$$

$$(A6.1a)$$

$$(A6.1b)$$

Hence when $0 \le (\theta_{An} + \alpha^*) < 1$ in equations (6.7)

$$\theta_{A(n+1)} = \theta_{An} + \alpha^* + \frac{\beta^*}{S} \qquad \text{for} \qquad 0 \le \theta_{An} < \frac{1-\beta^*}{S} - \alpha^* \qquad (A6.2a)$$

$$= \theta_{An} + \alpha^* + \frac{\beta^* - 1}{S} \qquad \text{for} \qquad \frac{1-\beta^*}{S} - \alpha^* \le \theta_{An} < \frac{1}{S} - \alpha^* \qquad (A6.2b)$$

$$= \frac{\beta^*}{S} \qquad \qquad \text{for} \qquad \frac{1}{S} - \alpha^* \le \theta_{An} < 1 - \alpha^* \qquad (A6.2c)$$

and when $1 \le (\theta_{An} + \alpha^*) < 2$

$$\theta_{A(n+1)} = \theta_{An} + \alpha^* + \frac{\beta^*}{S} - 1 \qquad \text{for} \qquad 1 - \alpha^* \le \theta_{An} < \frac{1 - \beta^*}{S} - \alpha^* + 1 \quad \text{(A6.2d)}$$

$$= \theta_{An} + \alpha^* + \frac{\beta^* - 1}{S} - 1 \quad \text{for} \quad \frac{1 - \beta^*}{S} - \alpha^* + 1 \le \theta_{An} < \frac{1}{S} - \alpha^* + 1 \quad \text{(A6.2e)}$$

$$= \frac{\beta^*}{S} \qquad \qquad \text{for} \qquad \frac{1}{S} - \alpha^* + 1 \le \theta_{An} < 2 - \alpha^* \quad \text{(A6.2f)}$$

I now define three possible generic configurations of the circle map plot, in terms of the value of the constant $d = \alpha^* + \frac{\beta^*}{S}$.

(a) Form 1:
$$0 < d < \frac{1}{s}$$

If $d < \frac{1}{s}$ then $\frac{1}{s} - \alpha^* - \frac{\beta^*}{s} > 0$

$$\frac{1-\beta^*}{s} - \alpha^* + 1 > 1$$

and since $\theta_{An} < 1$,

$$\theta_{An} < \frac{1-\beta^*}{S} - \alpha^* + 1$$

Hence the Form 1 configuration occurs when conditions (A6.2a) to (A6.2d) are

(b) Form
$$2: \frac{1}{S} < d < \frac{1+\beta^*}{S}$$

If $\frac{1}{s} < d$ then $\frac{1-\beta^*}{s} - \alpha^* < 0$ so condition (A6.2a) no longer applies (because $\theta_{An} \ge 0$). Also, $\frac{1-\beta^*}{s} - \alpha^* + 1 < 1$ so that condition (A6.2d) no longer suffices to 'cover' the rightmost segment.

Because $d < \frac{1+\beta^*}{s}$ it follows that $\frac{1}{s} - \alpha^* > 0$ and so condition (A6.2b) still applies.

$$\frac{1}{S} - \alpha^* + 1 > 1$$

$$\theta_{An} < \frac{1}{S} - \alpha^* + 1$$

so that condition (A6.2e) now holds. Hence the Form 2 configuration occurs when conditions (A6.2b) to (A6.2e) are satisfied.

(c) Form 3:
$$\frac{1+\beta^*}{S} < d < 1 + \frac{\beta^*}{S}$$

If $\frac{1+\beta^*}{s} < d$ then $\frac{1}{s} - \alpha^* < 0$ and so condition (A6.2b) no longer applies. Now however, $1-\alpha^* > 0$ so that condition (A6.2c) still applies, and $\frac{1}{s} - \alpha^* + 1 < 1$ so that condition (A6.2e) no longer suffices to cover the rightmost segment. Clearly $\theta_{An} < 2-\alpha^*$ in condition (A6.2f) holds, because $\alpha^* < 1$. Hence the Form 3 configuration occurs when conditions (A6.2c) to (A6.2f) are satisfied.

A6. 2 Conditions for a 2 lock: FORM 2 and FORM 3 configurations

FORM 2
$$(\frac{1}{s} < d < \frac{1+\beta^*}{s})$$

I label the rightmost segment with the letter E.

(a) Itinerary Hb: passage through segment b after H requires that

$$0 < \frac{\beta^*}{S} < \frac{1}{S} - \alpha^* \tag{A6.3a}$$

$$\Rightarrow d < \frac{1}{S} \tag{A6.3b}$$

which contradicts d > 1/S. Thus itinerary Hb is impossible.

(b) Itinerary Ha: passage through segment a after H requires that

$$1 - \alpha^* < \frac{\beta^*}{S} < 1 + \frac{1}{S} - d \tag{A6.4a}$$

$$\Rightarrow$$
 1

Also, phase duration of Ha must satisfy

$$\frac{1}{S} - \alpha^* < \left(\frac{\beta^*}{S} + (d - 1)\right) < 1 - \alpha^*$$
(A6.5a)

$$\Rightarrow$$
 d < 1 (A65b)

which contradicts (A6.4b) above. Thus itinerary Ha is impossible.

(c) Itinerary HE: passage through E requires that

$$1 + \frac{1}{S} - d < \frac{\beta^*}{S} < 1 \tag{A6.6a}$$

$$\Rightarrow 1 + \frac{1 - \beta^*}{S} < d \tag{A6.6b}$$

Phase duration must satisfy

$$\frac{1}{S} - \alpha^* < \left(\frac{\beta^*}{S} + (d - 1 - \frac{1}{S})\right) < 1 - \alpha^*$$
(A6.7a)

$$\Leftrightarrow \frac{1}{2} + \frac{1}{S} < d < 1 + \frac{1}{2S} \tag{A6.7b}$$

Hence a 2 lock occurs iff (A6.6b) and (A6.7b) are both satisfied that is

$$\frac{1}{2} + \frac{1}{S} < d < 1 + \frac{1}{2S}$$
 and $d > 1 + \frac{1 - \beta^*}{S}$ (A6.8)

FORM 3
$$\left(\frac{1+\beta^*}{S} < d < 1 + \frac{\beta^*}{S}\right)$$

The horizontal section is now split into two parts which I shall label as H_1 (leftmost) and H_2 (rightmost).

(a1) Itinerary H_1a : by the same argument as in Form 2(b) passage through segment a after H_1 implies that d>1. Phase duration must this time satisfy

$$0 < \left(\frac{\beta^*}{S} + (d-1)\right) < 1 - \alpha^* \tag{A6.9a}$$

$$\Rightarrow \qquad \qquad d < 1 \tag{A6.9b}$$

contradicting d>1 above. Thus itinerary H₁a is impossible.

(a2) Itinerary H₂a: passage through a requires that

$$1-\alpha^* < \frac{\beta^*}{S} < (1+\frac{1}{S}-d)$$
 (A6.10a)

$$\Rightarrow \qquad \alpha^* + \frac{2\beta^*}{S} < 1 + \frac{1}{S} \tag{A6.10b}$$

and phase duration must satisfy

$$1 + \frac{1}{S} - \alpha^* < \left(\frac{\beta^*}{S} + (d-1)\right) < 1$$
 (A6.11a)

$$\Rightarrow 1 + \frac{1}{2S} < d \tag{A6.11b}$$

$$\Rightarrow \frac{\beta^*}{S} > 1 - \alpha^* + \frac{1}{2S} > \frac{1}{2S}$$
 (A6.11c)

$$\Rightarrow \qquad \beta^* > \frac{1}{2} \tag{A6.11d}$$

But from (A6.10b)

$$\alpha^* + \frac{2\beta^*}{S} < 1 + \frac{1}{S}$$
 (A6.12a)

$$\Rightarrow \qquad d < 1 + \frac{1}{2S} + \frac{1}{2S} - \frac{\beta^*}{S} < 1 + \frac{1}{2S} \tag{A6.12b}$$

since $\beta^* > \frac{1}{2}$. This contradicts (A6.11b). Thus H_2 a is impossible.

(b1) Itinerary H₁E: passage through E requires that

$$1 + \frac{1}{S} - d < \frac{\beta^*}{S} < 1 + \frac{1}{S} - \alpha^*$$
 (A6.13a)

$$\Leftrightarrow 1 + \frac{1 - \beta^*}{S} < d < 1 + \frac{1}{S} \tag{A6.13b}$$

Phase duration must satisfy

$$0 < \left(\frac{\beta^*}{S} + (d - 1 - \frac{1}{S})\right) < 1 - \alpha^*$$
 (A6.14)

which re-arranges to condition (A6.12b) above.

(A6.13b) and (A6.14) together imply that a 2 lock occurs when the conditions

$$1 + \frac{1 - \beta^*}{S} < d < 1 + \frac{1}{2S} \tag{A6.15}$$

are satisfied.

(b2) Itinerary H₂E: passage through E requires that inequality (A6.13b) must be satisfied. Phase duration must now satisfy

$$1 + \frac{1}{S} - \alpha^* < \left(\frac{\beta^*}{S} + (d - 1 - \frac{1}{S})\right) < 1$$
 (A6.16a)

$$\Rightarrow 1 + \frac{1}{S} < d \tag{A6.16b}$$

which contradicts $d < 1 + \frac{\beta^*}{S}$ (by definition of *FORM 3*). Thus H₂E is impossible. Conditions (A6.8) and (A6.15) taken together imply that a 2 lock occurs iff

$$\frac{1}{2} + \frac{1}{S} < d < 1 + \frac{1}{2S}$$
 and $d > 1 + \frac{1 - \beta^*}{S}$

A6.3 Conditions for a 3 lock: two other FORM 1 itineraries

(ii) Itinerary HbU

Repeating the same logical argument, phase duration must now satisfy

$$\left(\frac{1}{s} - \alpha^*\right) < \left(\frac{\beta^*}{s} + (d - \frac{1}{s}) + d\right) < (1 - \alpha^*)$$
(A6.17a)

$$\Leftrightarrow \frac{2}{3S} < d < \frac{1}{3} + \frac{1}{3S} \tag{A6.17b}$$

To pass through b and then U successively after H respectively requires that

$$\left(\frac{1}{S} - d\right) < \frac{\beta^*}{S} < \left(\frac{1}{S} - \alpha^*\right) \tag{A6.18a}$$

$$\Rightarrow \frac{1-\beta^*}{S} < d \tag{A6.18b}$$

and

$$0 < \frac{\beta^*}{S} + \left(d - \frac{1}{S}\right) < \left(\frac{1}{S} - d\right) \tag{A6.19a}$$

$$\Rightarrow \qquad \qquad d < \frac{2 - \beta^*}{2S} \tag{A6.19b}$$

must be satisfied. Combining inequalities (A6.17b), (A6.18b) and (A6.19b) the conditions for a 3 lock are thus

$$\frac{2}{3S} < d < \frac{1}{3} + \frac{1}{3S}$$
 and $\frac{1 - \beta^*}{S} < d < \frac{2 - \beta^*}{2S}$ (A6.20)

(iii) Itinerary HUa

Phase duration must satisfy

$$\left(\frac{1}{s} - \alpha^{\star}\right) < \left(\frac{\beta^{\star}}{S} + d + (d - 1)\right) < (1 - \alpha^{\star}) \tag{A6.21a}$$

$$\Leftrightarrow \qquad \frac{1}{3} + \frac{1}{3S} < d < \frac{2}{3} \tag{A6.21b}$$

To pass through U immediately after H requires that $d < \frac{1-\beta^*}{S}$ (by earlier inequality (6.13)), and then to continue passage through segment a requires that

$$(1-\alpha^*) < \left(\frac{\beta^*}{S} + d\right) < 1$$

$$(A6.22a)$$

$$\Leftrightarrow \frac{1}{2} < d < 1 - \frac{\beta^*}{S}$$
(A6.22b)

must be satisfied. The RHS of condition (A6.22b) is redundant, because $d < \frac{1-\beta^*}{S} < 1 - \frac{\beta^*}{S}$, since S>1. The LHS of (A6.22b) is also redundant, because if d < 1/2 a 2 lock occurs (by earlier inequality (6.12)). The conditions for a 3 lock are thus inequality (A6.21b) and earlier inequality (6.13) together, namely

$$\frac{1}{3} + \frac{1}{3S} < d < \frac{2}{3}$$
 and $d < \frac{1 - \beta^*}{S}$ (A6.23)

Appendix A7 (to Chapter 7)

A7.1 Derivation of the TLIM circle map

The two line interphase map TLIM is defined by

$$\theta_{B} \equiv \tilde{f}(\theta_{A}) = \begin{cases} S_{1}\theta_{A} & 0 \leq \theta_{A} < P \\ 1 - S_{2}(1 - \theta_{A}) & P \leq \theta_{A} < 1 \end{cases}$$
(A7.1)

where $\theta_A = P$ is the phase where segments L and R meet.

Observe that at the point (P,Q) where the two corresponding lines of the plot meet,

$$\begin{cases}
Q = S_1 P \\
Q = 1 - S_2 (1 - P)
\end{cases}$$
(A7.2)

which together imply that

$$P = \frac{1 - S_2}{S_1 - S_2} \tag{A7.3}$$

Clearly, this interphase map is a homeomorphism, with its inverse defined by

$$\theta_{A} = \vec{f}^{-1}(\theta_{B}) = \begin{cases} \frac{1}{S_{1}} \theta_{B} & 0 \le \theta_{B} < S_{1}P \\ 1 - \frac{1}{S_{2}} (1 - \theta_{B}) & S_{1}P \le \theta_{B} < 1 \end{cases}$$
(A7.4)

The TLIM Circle map $\tilde{F}_{\alpha,\beta} = \tilde{f}^{-1} R_{\beta} \tilde{f} R_{\alpha}$ is thus

$$\theta_{A(n+1)} = \tilde{F}_{\alpha,\beta}(\theta_{An}) = \begin{cases} \tilde{f}^{-1} R_{\beta} [S_1(\theta_{An} + \alpha)^*] & 0 \le (\theta_n + \alpha^*) < P \\ \tilde{f}^{-1} R_{\beta} (1 - S_2 [1 - (\theta_{An} + \alpha)^*]) & P \le (\theta_n + \alpha)^* < 1 \end{cases}$$
(A7.5b)

Dropping the A-stage suffix for clarity (so that $\theta_{An} \equiv \theta_n$), I observe that

$$R_{\beta}[S_{1}(\theta_{n} + \alpha)^{*}] = \begin{cases} \beta^{*} + S_{1}(\theta_{n} + \alpha)^{*} & \text{for } \beta^{*} + S_{1}(\theta_{n} + \alpha)^{*} < 1\\ \beta^{*} - 1 + S_{1}(\theta_{n} + \alpha)^{*} & \text{for } \beta^{*} + S_{1}(\theta_{n} + \alpha)^{*} > 1 \end{cases}$$
(A7.6)

$$0 \le (\theta_n + \alpha)^* < P$$

Equation (A7.5a) thus becomes

$$\beta^* + S_1(\theta_n + \alpha)^* < 1$$

$$\theta_{n+1} = \begin{cases} \frac{\beta'}{S_1} + (\theta_n + \alpha)^* & 0 \le \beta^* + S_1(\theta_n + \alpha)^* < S_1 P \\ 1 + \frac{\beta^* - 1}{S_2} + \frac{S_1}{S_2}(\theta_n + \alpha)^* & S_1 P \le \beta^* + S_1(\theta_n + \alpha)^* < 1 \end{cases}$$
(A7.7a)

$\beta^* + S_1(\theta_n + \alpha)^* > 1$

$$= \begin{cases} \frac{\beta^* - 1}{S_1} + (\theta_n + \alpha)^* & 0 \le \beta^* - 1 + S_1(\theta_n + \alpha)^* < S_1 P \\ 1 + \frac{\beta^* - 2}{S_2} + \frac{S_1}{S_2}(\theta_n + \alpha)^* & S_1 P \le \beta^* - 1 + S_1(\theta_n + \alpha)^* < 1 \end{cases}$$
(A7.8a)

$P \le (\theta_n + \alpha)^* < 1$

By a similar (though more protracted) argument, Equation (A7.5b) becomes

$$\frac{\beta^* + 1 - S_2 (1 - (\theta_n + \alpha)^*) < 1}{\theta_{n+1}} = \begin{cases}
\frac{\beta^* + 1 - S_2}{S_1} + \frac{S_2}{S_1} (\theta_n + \alpha)^* & 0 \le \beta^* + 1 - S_2 (1 - (\theta_n + \alpha)^*) < S_1 P & (A7.9a) \\
\frac{\beta^*}{S_2} + (\theta_n + \alpha)^* & S_1 P \le \beta^* + 1 - S_2 (1 - (\theta_n + \alpha)^*) < 1
\end{cases} (A7.9b)$$

$$\underline{\beta^* + 1 - S_2(1 - (\theta_n + \alpha)^*) > 1}$$

$$= \begin{cases} \frac{\beta^* - S_2}{S_1} + \frac{S_2}{S_1} (\theta_n + \alpha)^* & 0 \le \beta^* - S_2 (1 - (\theta_n + \alpha)^*) < S_1 P \\ \frac{\beta^* - 1}{S_2} + (\theta_n + \alpha)^* & S_1 P \le \beta^* - S_2 (1 - (\theta_n + \alpha)^*) < 1 \end{cases}$$
(A7.10a)

I must finally express the right-hand inequalities in equations (A7.7) to (A7.10) in terms strictly of $(\theta_n + \alpha)^*$. So (for example) in equation (A7.7a),

$$0 \le \beta^* + S_1(\theta_n + \alpha)^* < S_1 P$$

$$\Leftrightarrow \frac{-\beta^*}{S_1} \le (\theta_n + \alpha)^* < P - \frac{\beta^*}{S_1}$$

$$\Leftrightarrow 0 \le (\theta_n + \alpha)^* < P - \frac{\beta^*}{S_1} \text{ since } (\theta_n + \alpha)^* \ge 0$$

This gives an expression consisting of 8 terms:

$$\frac{\beta^{*}}{S_{1}} + (\theta_{n} + \alpha)^{*} \qquad 0 \leq (\theta_{n} + \alpha)^{*} < P - \frac{\beta^{*}}{S_{1}} \qquad (A7.11a)$$

$$1 + \frac{\beta^{*} - 1}{S_{2}} + \frac{S_{1}}{S_{2}} (\theta_{n} + \alpha)^{*} \qquad P - \frac{\beta^{*}}{S_{1}} \leq (\theta_{n} + \alpha)^{*} < \frac{1 - \beta^{*}}{S_{1}} \qquad (A7.11b)$$

$$\frac{\beta^{*} - 1}{S_{1}} + (\theta_{n} + \alpha)^{*} \qquad \frac{1 - \beta^{*}}{S_{1}} \leq (\theta_{n} + \alpha)^{*} < P + \frac{1 - \beta^{*}}{S_{1}} \qquad (A7.11c)$$

$$1 + \frac{\beta^{*} - 2}{S_{2}} + \frac{S_{1}}{S_{2}} (\theta_{n} + \alpha)^{*} \qquad P + \frac{1 - \beta^{*}}{S_{1}} \leq (\theta_{n} + \alpha)^{*} < P \qquad (A7.11d)$$

$$\frac{\beta^{*} + 1 - S_{2}}{S_{1}} + \frac{S_{1}}{S_{2}} (\theta_{n} + \alpha)^{*} \qquad P \leq (\theta_{n} + \alpha)^{*} < 1 - \left(\frac{\beta^{*} + 1}{S_{2}}\right) + \frac{S_{1}}{S_{2}} P \qquad (A7.11e)$$

$$\frac{\beta^{*} - S_{2}}{S_{1}} + \frac{S_{2}}{S_{1}} (\theta_{n} + \alpha)^{*} \qquad 1 - \frac{\beta^{*}}{S_{2}} \leq (\theta_{n} + \alpha)^{*} < 1 - \frac{\beta^{*}}{S_{2}} + \frac{S_{1}}{S_{2}} P \qquad (A7.11g)$$

$$\frac{\beta^{*} - 1}{S_{2}} + (\theta_{n} + \alpha)^{*} \qquad 1 - \frac{\beta^{*}}{S_{2}} + \frac{S_{1}}{S_{2}} P \leq (\theta_{n} + \alpha)^{*} < 1 - \frac{\beta^{*}}{S_{2}} + \frac{S_{1}}{S_{2}} P \qquad (A7.11b)$$

However, not all of these terms can exist given the constraints on S_1, S_2 and P [namely $S_1 > S_2$, $S_1, S_2 > 0$, $S_1 > 1$, $S_2 < 1$, $P = \frac{1 - S_2}{S_1 - S_2}$].

(A7.11d) Since $\frac{1-\beta^{\bullet}}{S_1} > 0$, the RHS inequality is impossible. Hence the left hand term does not exist.

(A7.11e) The RHS inequality, right limit

$$1 - \left(\frac{\beta^* + 1}{S_2}\right) + \frac{S_1}{S_2}P = \left(1 - \frac{1}{S_2} + \frac{S_1}{S_2}P\right) - \frac{\beta^*}{S_2}$$
$$= \left(\frac{1 - S_2}{S_1 - S_2}\right) - \frac{\beta^*}{S_2}$$
$$= P - \frac{\beta^*}{S_2} < P.$$

Hence the left hand term does not exist.

This leaves terms (A7.11a) to (A7.11c) and (A7.11f) to (A7.11h).

The TLIM circle map is therefore

$$\theta_{n+1} = \begin{cases} \frac{\beta^{*}}{S_{1}} + (\theta_{n} + \alpha)^{*} & 0 \leq (\theta_{n} + \alpha)^{*} < P - \frac{\beta^{*}}{S_{1}} \\ 1 + \frac{\beta^{*} - 1}{S_{2}} + \frac{S_{1}}{S_{2}} (\theta_{n} + \alpha)^{*} & P - \frac{\beta^{*}}{S_{1}} \leq (\theta_{n} + \alpha)^{*} < \frac{1 - \beta^{*}}{S_{1}} \\ \frac{\beta^{*} - 1}{S_{1}} + (\theta_{n} + \alpha)^{*} & \frac{1 - \beta^{*}}{S_{1}} \leq (\theta_{n} + \alpha)^{*} < P \\ \frac{\beta^{*}}{S_{2}} + (\theta_{n} + \alpha)^{*} & P \leq (\theta_{n} + \alpha)^{*} < 1 - \frac{\beta^{*}}{S_{2}} \\ \frac{\beta^{*} - S_{2}}{S_{1}} + \frac{S_{2}}{S_{1}} (\theta_{n} + \alpha)^{*} & 1 - \frac{\beta^{*}}{S_{2}} \leq (\theta_{n} + \alpha)^{*} < 1 - \frac{\beta^{*}}{S_{2}} + \frac{S_{1}}{S_{2}} P \\ \frac{\beta^{*} - 1}{S_{2}} + (\theta_{n} + \alpha)^{*} & 1 - \frac{\beta^{*}}{S_{2}} + \frac{S_{1}}{S_{2}} P \leq (\theta_{n} + \alpha)^{*} < 1 \end{cases}$$